

Utah State University

DigitalCommons@USU

All Graduate Theses and Dissertations

Graduate Studies

5-2013

Oxidative Aliphatic Carbon-Carbon Bond Cleavage Reactions

Caleb J. Allpress
Utah State University

Follow this and additional works at: <https://digitalcommons.usu.edu/etd>

 Part of the [Chemistry Commons](#)

Recommended Citation

Allpress, Caleb J., "Oxidative Aliphatic Carbon-Carbon Bond Cleavage Reactions" (2013). *All Graduate Theses and Dissertations*. 2003.

<https://digitalcommons.usu.edu/etd/2003>

This Dissertation is brought to you for free and open access by the Graduate Studies at DigitalCommons@USU. It has been accepted for inclusion in All Graduate Theses and Dissertations by an authorized administrator of DigitalCommons@USU. For more information, please contact digitalcommons@usu.edu.



OXIDATIVE ALIPHATIC CARBON-CARBON BOND CLEAVAGE REACTIONS

by

Caleb J. Allpress

A dissertation submitted in partial fulfillment

of the requirements for the degree

of

DOCTOR OF PHILOSOPHY

in

Chemistry

Approved:

Lisa M. Berreau, Ph.D.
Major Professor

Alvan C. Hengge, Ph.D.
Committee Member

John L. Hubbard, Ph.D.
Committee Member

Paul R. Grossl, Ph.D.
Committee Member

Bradley S. Davidson, Ph.D.
Committee Member

Mark R. McLellan, Ph.D.
Vice President for Research and
Dean of the School of Graduate
Studies

UTAH STATE UNIVERSITY
Logan, Utah

2013

Copyright © Caleb Allpress 2013

All Rights Reserved

ABSTRACT

Oxidative Aliphatic Carbon-Carbon Bond Cleavage Reactions

by

Caleb J. Allpress, Doctor of Philosophy

Utah State University, 2013

Major Professor: Dr. Lisa M. Berreau
Department: Chemistry and Biochemistry

The work presented in this dissertation has focused on synthesizing complexes of relevance to dioxygenase enzymes that oxidatively cleave aliphatic carbon-carbon bonds. The goal of this research was to elucidate mechanistic aspects of the activation of aliphatic carbon-carbon bonds towards cleavage by reaction with oxygen, and also investigate the regioselectivity of these reactions. The oxidative cleavage of a variety of enolizable substrates has been explored by utilizing several transition metal complexes supported by an aryl-appended tris(pyridylmethyl)amine ligand.

In order to probe the widely-accepted “chelate hypothesis” for how changes in regioselectivity are achieved as a function of metal ion, we synthesized the compound $[(6\text{-Ph}_2\text{TPA})\text{Fe}(\text{PhC}(\text{O})\text{COHC}(\text{O})\text{Ph})]\text{OTf}$. Based on UV-vis and IR spectroscopy, the acireductone enolate was found to bind via a six-membered chelate ring. By comparison with the reactivity of $[(6\text{-Ph}_2\text{TPA})\text{Ni}(\text{PhC}(\text{O})\text{COHC}(\text{O})\text{Ph})]\text{ClO}_4$, we determined that the chelate hypothesis was an insufficient explanation of the observed regioselectivity.

Rather, ferrous ion-mediated hydration of a vicinal triketone intermediate was the key factor in determining the regioselectivity of the C-C cleavage reaction.

We have developed a high-yielding synthetic route to protected precursors of C(1)H acireductones. Preparation of the complexes [(6-Ph₂TPA)M(PhC(O)COCHOC(O)CH₃)]ClO₄ (M = Fe, Ni) followed by judicious choice of deprotecting conditions allowed us to investigate the oxygen reactivity of a mono-nuclear complex with a dianionic acireductone substrate for the first time. This provides a promising strategy to continue investigations of complexes of relevance to the enzyme-substrate adduct of the acireductone dioxygenases.

Divalent late first-row transition metal complexes have been used to investigate some new strategies for the activation of dioxygen and subsequent cleavage of C-C bonds. We have utilized photoreduction of a Ni(II) center to generate a highly O₂-reactive Ni(I) fragment that leads to cleavage of a chloro-diketonate substrate. Additionally, we have found a Cu(II)-mediated thermal cleavage of chloro-diketonate substrates at room temperature. This reaction is interestingly accelerated by the addition of a catalytic amount of chloride ion.

PUBLIC ABSTRACT

Oxidative Aliphatic Carbon-Carbon Bond Cleavage Reactions

by

Caleb J. Allpress, Doctor of Philosophy

Utah State University, 2013

Major Professor: Dr. Lisa M. Berreau
Department: Chemistry and Biochemistry

The work presented in this dissertation has focused on the activation and cleavage of chemical bonds between two carbon atoms. The selective oxidative activation of carbon-carbon bonds is important due to potential applications in the utilization of biomass for fuel production, applications in wastewater treatment and bioremediation, and in developing new reactions for organic synthesis of fine chemicals including pharmaceuticals. Ideally these reactions would be carried out with high atom economy at low temperatures and pressures, and using earth-abundant elements as reagents and catalysts. With these points in mind, nature provides an ideal model framework, carrying out its chemistry at ambient temperature and pressure. Enzymes that cleave C-C bonds by a dioxygenolytic pathway have been our focus as they utilize dioxygen as a terminal oxidant and also do not require any coreductants, maximizing atom economy.

Our strategy has been to use small molecular models to study complex biological systems or, conversely, to take inspiration from highly active biological systems to design new ways to activate small molecules. We have focused on exploring the reaction

pathways of several dioxygenase enzymes that cleave aliphatic C-C bonds, with the goal of understanding fundamental factors involved in the activation and direction of cleavage of these bonds. These efforts have led to several important advances in understanding of the cleavage of C-C bonds. Additionally, the work presented here has thus far led to five peer-reviewed publications and five presentations at scientific conferences across the country.

ACKNOWLEDGMENTS

I would firstly like to extend special thanks to my doctoral advisor and mentor, Dr. Lisa Berreau, for her continued advice and support, and for putting up with me telling her she was wrong (even when she was right). I'm especially grateful for the freedom she has given me in pursuing chemistry that is inherently interesting, even if it was not always the chemistry we had originally intended to investigate.

I also thank the other members of my doctoral supervisory committee, Dr. John Hubbard, Dr. Alvan Hengge, Dr. Bradley Davidson, and Dr. Paul Grossl, as well as other faculty in the Department of Chemistry, for their support and allowing me to sound ideas off them throughout the years.

I would also like to thank all the members of the Berreau group during my time here for their mentorship, support and friendship, with special thanks to fellow grad students from the Berreau lab, Kasia, James, Stacey and Sushma, as well as honorary members Danyal and Angeline.

I am grateful to the various coauthors and collaborators: Dr. Ewa Szajna-Fuller and Dr. Katarzyna Grubel for providing characterization of two ferrous compounds, Dr. Atta Arif for performing all the X-ray crystallography, Dr. Dylan Houghton for performing electrochemistry, Dr. Dale Gardner for assistance with LC-MS experiments, Dr. Mark Mehn for providing the initial supply of $\text{Fe}(\text{OTf})_2 \cdot 2\text{CH}_3\text{CN}$, Jami Bennett and Dr. David Tierney for their EPR expertise, and Ana Miłaczewska and Dr. Tomasz Borowski for all the computations. Without their support and expertise, much of the work presented here would not have been possible.

Finally, I would like to thank my family for their support, especially my wonderful wife, Teresa. Without her support I would have been unable to accomplish all that I have. And, although she is late to the picture, I would like to thank my beautiful daughter Nova for her small contribution to typing up the final chapter of this dissertation.

Caleb J. Allpress

CONTENTS

	Page
ABSTRACT	iii
PUBLIC ABSTRACT	v
ACKNOWLEDGMENTS	vii
LIST OF TABLES	x
LIST OF FIGURES	xi
LIST OF SCHEMES	xv
CHAPTER	
1. OXIDATIVE ALIPHATIC CARBON-CARBON BOND CLEAVAGE REACTIONS IN ENZYMATIC SYSTEMS AND RELATED MODEL SYSTEMS	1
2. REGIOSELECTIVE ALIPHATIC CARBON-CARBON BOND CLEAVAGE BY A MODEL SYSTEM OF RELEVANCE TO IRON- CONTAINING ACIREDUCTONE DIOXYGENASE	73
3. IRON- AND NICKEL-CONTAINING MODEL SYSTEMS OF ACIREDUCTONE DIOXYGENASE THAT UTILIZE A C(1)H ACIREDUCTONE SUBSTRATE	120
4. PHOTOCHEMICALLY-INITIATED OXIDATIVE CARBON- CARBON BOND CLEAVAGE REACTIVITY IN CHLORO- DIKETONATE DIVALENT NICKEL COMPLEXES	163
5. DIOXYGENASE-TYPE CARBON-CARBON BOND CLEAVAGE IN A MONONUCLEAR COPPER(II) CHLORO-DIKETONATE COMPLEX	208
6. CONCLUSIONS	255
APPENDIX ...	278
CURRICULUM VITAE	292

LIST OF TABLES

Table		Page
1-1.	Aliphatic carbon-carbon bond cleaving dioxygenase enzymes, active site metal ions, and metal coordination environment	4
1-2.	Structural, spectroscopic, and redox properties of Fe(II) diketonate complexes of relevance to the enzyme/substrate adduct in Dke1	15
1-3.	UV-vis spectroscopic properties of acireductone monoanion complexes	50
1-4.	Level of ^{18}O incorporation in benzoic acid/benzoate products	51
2-1.	Summary of X-ray data collection and refinement	89
2-2.	Selected bond distances (\AA) and angles ($^\circ$) for 2 - ClO_4 and 4 · 0.5CH₃CN ...	90
2-3.	^1H NMR shifts for selected paramagnetic compounds (ppm)	92
2-4.	Summary of production of benzoylformic acid	103
4-1.	Crystallographic data for 5 , 6 , and 8	179
4-2.	Selected bond lengths (\AA) and angles ($^\circ$)	180
4-3.	Selected spectroscopic features for 4-9	181
5-1.	Summary of X-ray data collection and refinement	223
5-2.	Selected bond distances (\AA) and angles ($^\circ$) for 1 and 2 · CH_2Cl_2	224

LIST OF FIGURES

Figure	Page
1-1. Proposed structures for resting state and substrate-bound forms of Dke1 ...	7
1-2. β -diketone substrates for Dke1	9
1-3. Synthetic complexes of relevance to the ES adduct in Dke1	13
1-4. Methionine salvage pathway in <i>K. pneumonia</i>	37
1-5. (a) Metal coordination environment found in the resting state for Ni(II)-ARD and Fe(II)-ARD'. (b) and (c) Possible coordination motifs for the ES complexes of Ni(II)-ARD and Fe(II)-ARD'	39
1-6. (a) Proposed structure of acireductones. (b) X-ray crystallographically determined structures of the protonated form and rubidium salt of triose reductone. (c) X-ray crystallographically characterized structure of $[(\text{Ru}(\text{bipy})_2)_2(\mu\text{-C}_4\text{H}_4\text{O}_3)](\text{PF}_6)_2$	42
1-7. Native and alternative substrate for Ni(II)-ARD and Fe(II)-ARD'	43
1-8. Synthetic routes for the preparation of 1-4	49
1-9. Structural features of the hexanickel cluster 5 . (a) A view of the entire $\{\text{Ni}(\text{PhC}(\text{O})\text{C}(\text{O})\text{C}(\text{O})\text{Ph})(\text{CH}_3\text{OH})\}_6$ cluster. (b) View of a single layer ...	54
2-1. Thermal ellipsoid representation of the cationic portions of 2-ClO₄ (left) and 4 (right)	88
2-2. Comparison of selected paramagnetically shifted features in the ¹ H NMR spectra of 2-4	92
2-3. UV-vis spectra for 1-4 in CH ₃ CN	93
2-4. UV-vis spectra of 3-ClO₄ in CH ₃ CN before (solid line) and after (dashed line) the addition of O ₂	96
2-5. LC-MS data showing the chromatogram of a 1:1 benzoic acid: benzoylformic acid standard (top), and these products generated from the reaction of 3-ClO₄ with O ₂ (middle), and reaction of 1 with O ₂ (bottom)	98

2-6.	UV-vis spectra following the decay of 3-OTf in the presence of O ₂ at selected time intervals	100
2-7.	Plot of k _{obs} (s ⁻¹) versus [O ₂] (M) for the reaction of 3-OTf (0.47mM) in CH ₃ CN at 20°C	100
2-8.	[(6-Ph ₂ TPA)Fe(sol) _x](ClO ₄) ₃ before (top) and after (bottom) the addition of [Me ₄ N][PhC(O)C(OH)C(O)Ph]	106
3-1.	Selected portion of the paramagnetically-shifted ¹ H NMR spectrum of the previously reported compound 3 (top), and our <i>in situ</i> generated compound, assigned as 3 (bottom)	138
3-2.	Selected portion of the paramagnetically-shifted ¹ H NMR spectra of 7 (top) and 8 (bottom)	140
3-3.	UV-vis spectra showing the effects of adding excess NaOMe to MeOH solutions of 7 (left) and 8 (right)	141
3-4.	UV-vis spectra during the reactions of various species with O ₂ in MeOH ...	143
3-5.	Selected regions of the ¹ H NMR spectra collected during the reaction of 7 with 5 equivalents of NaOMe in CD ₃ OD under a nitrogen atmosphere	146
3-6.	Plot of the relative intensities of selected features in the ¹ H NMR during the reaction of 7 with 5 equivalents of NaOMe in CD ₃ OD under a nitrogen atmosphere (top) and under an oxygen atmosphere (bottom)	147
3-7.	¹ H NMR spectra of the 6-Ph ₂ TPA ligand (bottom) and the product mixture of the reaction of 7 with 5 equivalents of NaOMe under a nitrogen atmosphere (top)	148
3-8.	Selected regions of the ¹ H NMR spectra collected during the reaction of 7 with 5 equivalents of NaOMe in CD ₃ OD under an oxygen atmosphere	151
4-1.	Structures of a synthetic complex studied as a model system for Ni ^{II} -containing acireductone dioxygenase 1 and analogues 6 and 9 that are O ₂ -stable under ambient conditions	168
4-2.	Thermal ellipsoid representations of the cationic portions of 5 (top), 6 (middle) and 8 (bottom)	178
4-3.	Labeling scheme for the 6-Ph ₂ TPA ligand	182

4-4.	Absorption changes over time observed for the aerobic photochemical reaction of 4	183
4-5.	Selected features of the paramagnetic region of the ¹ H NMR spectra of analytically pure 4 and 10-13 and the reaction mixture produced upon irradiation of 4 under aerobic conditions at 350 nm for 20 hours in CH ₃ CN	184
4-6.	Selected features of the paramagnetic region of the ¹ H NMR spectra of analytically pure 5 and 10 and the reaction mixture produced upon irradiation of 5 under aerobic conditions at 350 nm for 20 hours in CH ₃ CN	186
4-7.	Selected features of the paramagnetic region of the ¹ H NMR spectra of analytically pure 6 and 10 and the reaction mixture produced upon irradiation of 6 under aerobic conditions at 350 nm for 20 hours in CH ₃ CN	187
4-8.	Structures of the organic products generated in photochemical reactions of 4-6 under aerobic or anaerobic conditions with irradiation at 350nm for 20 hours in CH ₃ CN	189
4-9.	Relative amounts of the organic products generated during the 350 nm irradiation of 4-6 in CH ₃ CN for 20 hours under aerobic (top) and anerobic conditions (bottom)	190
4-10.	Cyclic voltammograms of 4 (top) and 7 (bottom) obtained in freshly distilled CH ₃ CN (0.1 M [Me ₄ N][ClO ₄]) with an analyte concentration of 1.0 mM (4 ; 1.3 mM for 7) under an atmosphere of N ₂	195
4-11.	¹⁸ O labeling studies for the photochemical reactions of 4 and 6	199
4-12.	First-order plot for the photoreaction of 4-6 in aerobic CH ₃ CN at 29(1)°C, irradiating at 350 nm	200
4-13.	Representative first order plots of side-by-side studies of the photochemical reaction of 4 under O ₂ and N ₂ at ~29°C	200
5-1.	A subset of Cu/O ₂ adducts that have been investigated for their spectroscopic features and reactivity to provide insight into a variety of copper-containing enzymatic systems	211
5-2.	Thermal ellipsoid representation of the cationic portion of 1	225
5-3.	X-band EPR spectrum (top) and representative simulation (bottom) of	

1 at 20 K	226
5-4. X-band EPR of 1 and representative simulations, (top) at elevated temperature and low power, and (bottom) at low temperature and high power	227
5-5. Selected UV-vis spectra during the decay of the 363 nm absorption feature of 1 upon exposure to O ₂	228
5-6. Thermal ellipsoid representation of the cationic portion of 2	229
5-7. X-band EPR of 2 and the product mixture from the reaction of 1 with O ₂ ...	232
5-8. Organic species formed in the reaction of 1 with O ₂ in CH ₃ CN (top) and identification of their corresponding aromatic signals in the ¹ H NMR of the organic products (bottom)	233
5-9. ¹ H NMR spectrum (CD ₃ CN) of the recovered ligand	236
5-10. Time trace of the decay of 1 in the presence of O ₂ (blue line), or in the presence of O ₂ and Cl ⁻ (red line) (top). A natural log plot shows that after the induction period, the reaction of 1 with O ₂ is first order in 1 in either the presence of absence of Cl ⁻ (bottom)	239
5-11. UV-vis spectra showing the appearance of characteristic peaks associated with anthracene during the loss of the 363 nm feature of 1 when a solution of 1 is exposed to O ₂ in the presence of dihydroanthracene	242
5-12. Linear dependence of k _{obs} on the concentration of added Cl ⁻ salt	244
6-1. A selection of complexes investigated in this dissertation of relevance to C-C cleaving dioxygenases	255

LIST OF SCHEMES

Scheme	Page
1-1. Oxidative aliphatic carbon-carbon bond cleavage reactions discussed in this chapter	3
1-2. Proposed mechanistic pathways for Dke1	11
1-3. Acetoacetate cleavage reactivity of $\text{Tp}^{\text{iPr}_2}\text{Fe}(\text{acac})$ and $\text{Tp}^{\text{Me}_2}\text{Fe}(\text{acac})$...	16
1-4. O_2 -dependent aliphatic carbon-carbon bond cleavage reactivity of $\text{Fe}(\text{Xanthmal})_2$	17
1-5. O_2 -dependent aliphatic carbon-carbon bond cleavage reactivity of $\text{Tp}^{\text{Me}_2}\text{Fe}(\text{Phmal})$	18
1-6. (top) O_2 reactivity of $\text{Tp}^{\text{R}^2}\text{Fe}(\text{acac}^{\text{X}})$ ($\text{R} = \text{Me}, \text{iPr}$) complexes. (bottom) O_2 reactivity of $\text{Tp}^{\text{Ph}_2}\text{Fe}(\text{acac}^{\text{X}})$ complexes	19
1-7. Oxidative aliphatic carbon-carbon bond cleavage reaction of $\text{Ni}(\text{acac})_2(\text{H}_2\text{O})_2$ in the presence of ethylenediamine in water	21
1-8. Dke1-type reactivity in an Fe(III)-containing system	22
1-9. Proposed mechanistic pathways for aliphatic carbon-carbon bond cleavage reactivity in hydroxyethylphosphonate dioxygenase (HEPD)	25
1-10. Proposed mechanistic pathway for aliphatic carbon-carbon bond cleavage in 2,4'-Dihydroxyacetophenone dioxygenase (DAD)	29
1-11. (a) Proposed reaction pathway in fungal quercetinases. (b) Possible sites for O_2 activation in copper-containing fungal quercetinases. (c) Proposed outer sphere electron transfer reactivity of metal-coordinated flavonol with O_2 in bacterial quercetinases	31
1-12. Proposed structures of ES complexes for Ni(II)-ARD and Fe(II)-ARD' and reactions with O_2	40
1-13. Reaction pathway for uncatalyzed reaction of acireductone monoanion with O_2	44
1-14. Two alternative mechanisms for reactivity of an acireductone monoanion with O_2	45

1-15.	Computationally determined reaction pathway for aliphatic carbon-carbon bond cleavage upon reaction of IV ⁻ with O ₂	48
1-16.	O ₂ reactivity of divalent metal complexes of IV ⁻	52
1-17.	Reaction pathway of 1 with O ₂ via the formation of a 1,3-diphenyltriketone as an intermediate	52
1-18.	O ₂ reactivity of the hexanickel enediolate cluster compound 5	55
1-19.	O ₂ reactivity of the trinuclear bis-enediolate complex 7	55
1-20.	Reaction pathways for the cleavage of 4-hydroxyphenylpyruvate by O ₂ catalyzed by HMS or HPPD	59
1-21.	O ₂ reactivity of phenylpyruvate compounds	61
2-1.	Regiospecificity of aliphatic carbon-carbon bond cleavage of 1,2-dihydroxy-3-oxo-(<i>S</i>)-methylthiopentene by acireductone dioxygenases in the methionine salvage pathway	76
2-2.	Reaction of 1 with O ₂ to form Ni-ARD-type products via the formation of an intermediate triketone species and hydroperoxide (top). Decarbonylation of 1,3-diphenylpropantrione to form benzil via a Lewis acid-mediated benzoyl migration (bottom)	78
2-3.	Synthesis of 2-4	88
2-4.	Proposed mechanism for the Lewis acid-mediated isomerization of 2-hydroxy-1,3-diphenylpropan-1,3-dione in the presence of a base to form 2-oxo-2-phenylethylbenzoate	95
2-5.	Organic products detected in the reaction of 3-X with O ₂ in CH ₃ CN	97
2-6.	Proposed reaction pathway for the formation of benzoylformic acid from 2-oxo-2-phenylethylbenzoate	99
2-7.	¹⁸ O labeling studies in the reaction of 3-ClO₄ with O ₂	102
2-8.	Summary of the detection of benzoylformic acid in control reactions	105
2-9.	Attempted synthesis of [(6-Ph ₂ TPA)Fe(PhC(O)C(OH)C(O)Ph)](ClO ₄) ₂ , and the resulting products including oxidized organic species	107

2-10.	A possible pathway for the reaction of 3-X leading to the formation of benzoylformic acid via a Baeyer-Villiger oxidation	110
2-11.	Proposed reaction pathway involving triketone hydration as a means to generate Fe-ARD'-type products containing oxygen atoms derived from both O ₂ and H ₂ O	112
2-12.	Proposed sequence for hydrated triketone aliphatic carbon-carbon bond cleavage promoted by ferric iron species	114
3-1.	An overview of the methionine salvage pathway in <i>K. pneumonia</i>	122
3-2.	The proposed reaction pathways for Ni-ARD (top) and Fe-ARD' (bottom), wherein a change in the binding mode of the acireductone activates different carbon atoms to attack by dioxygen	123
3-3.	Reaction pathways of 1 and 2 with O ₂ via the formation of 1,3-diphenylpropantrione as an intermediate	125
3-4.	A combined chemical-enzymatic route for the synthesis of a C(1)H acireductone mono-anion that utilizes the E1 enolase/phosphatase enzyme from the methionine salvage pathway to generate a mono-anion <i>in situ</i> , with ~90% purity	127
3-5.	A solely chemical synthetic route for the synthesis of a C(1)H acireductone has been used to generate the Ba ²⁺ salt of the mono-anion	128
3-6.	A possible structure of an <i>in situ</i> generated phenyl reductone complex (3), and the product of its reaction with O ₂ in CH ₃ CN	128
3-7.	Strategy for generating a well-defined C(1)H acireductone complex and subsequently deprotecting it to investigate the dianionic acireductone's reactivity with O ₂	130
3-8.	Synthesis of 1-acetoxy-3-phenylpropan-2,3-dione (5), a protected acireductone, from 3-phenyl-2-propyn-1-ol	137
3-9.	Route to the <i>in situ</i> synthesis of 3 from 5 via the formation of a phenyl reductone tautomer (6)	138
3-10.	Synthesis of complexes 7 and 8	139
3-11.	Proposed reaction pathways for the reactions of 7 and 8 with a nucleophilic base (NaOMe) in the presence and absence of O ₂	144

3-12.	Previous attempts to generate a mononuclear nickel acireductone dianionic complex have resulted in displacement of the ancillary chelate ligand	149
3-13.	A summary of the various routes to oxidation of the C(1)H acireductone-derived species presented in this work	152
3-14.	Metal-dependent products of the oxidative enolate cleavage reactivity in the reactions of 7 and 8 with NaOMe in the presence of O ₂	154
3-15.	A proposed radical propagation pathway to give Fe-ARD'-type products...	156
3-16.	A proposed Baeyer-Villager reaction to give Fe-ARD'-type products	156
3-17.	Pathways proposed by QM/DMD simulations for the reactions catalyzed by the acireductone dioxygenases	157
4-1.	Proposed reaction pathways for the aliphatic carbon-carbon bond cleavage reactions catalyzed by Ni-ARD (top) and Dke1	165
4-2.	Proposed mechanism by which a Ni ^{II} -β-diketonate unit may be photochemically activated to generate a superoxo-diketonyl radical pair ...	169
4-3.	Synthesis of 2-chloro-1,3-diones (top) and Ni ^{II} 2-chloro-1,3-diketonate complexes supported by the 6-Ph ₂ TPA ligand (bottom)	177
4-4.	Ni ^{II} complexes generated upon irradiation of 4 at 350 nm for 20 hours in an aerobic solution of CH ₃ CN	185
4-5.	α-Cleavage products formed from the photoirradiation of 3a at 352 nm in aerobic CH ₃ CN for 2 hours	191
4-6.	Proposed reaction sequence for photoreduction of Ni(acac) ₂	193
4-7.	Proposed photochemical reaction pathways for 4-6 leading to the formation of I-IV	194
4-8.	Possible triketone formation and subsequent degradation pathways to form either diketone or carboxylate products	197
5-1.	Selected examples of copper oxygen chemistry including examples from enzymatic systems (top), catalytic reactions for synthesis (middle), and reactions that lead to C-C bond cleavage (bottom)	210

5-2.	Proposed reaction mechanisms for the copper-catalyzed oxidative cleavage of cyclic ketones (top) and of acyclic β -diketones (bottom)	213
5-3.	A proposed oxygen activation step in the dioxygenase reaction of quercetin dioxygenase	215
5-4.	Photo-induced dioxygenase cleavage of a chloro-diketonate substrate utilizing a Ni(II) center	216
5-5.	Synthesis of 1	222
5-6.	Products of the dioxygenolytic photoreactivity of a nickel chlorodiketonate include both chloride and carboxylate species	231
5-7.	Reaction of 1 with O ₂ in CH ₃ CN to form the chloride complex 2	234
5-8.	¹⁸ O incorporation into benzoic acid during the reaction of 1 with O ₂ in CH ₃ CN/H ₂ O	235
5-9.	Reactions of diphenylpropantrione in the presence of hydroperoxide and a Lewis acid	236
5-10.	Proposed reaction pathways for O ₂ with the diketonate anion of α -chloro-1,3-diphenylpropan-1,3-dione	237
5-11.	A proposed radical propagation pathway for the reaction of 1 with O ₂	240
5-12.	A possible reaction pathway for the auto-catalytic reaction of 1 with O ₂ ...	243
5-13.	Preliminary computational results for the reaction of 1 with O ₂ to form 1-Peroxo	245
6-1.	O ₂ reactivity of the acireductone dioxygenase model systems 1 and 2 in the presence and absence of water	257
6-2.	<i>In situ</i> generation of mono-nuclear di-anionic C(1)H acireductone complexes from 3 and 4 allowed investigation of their O ₂ cleavage reactivity	259
6-3.	Reaction pathway for the oxidative photo-cleavage of a Ni(II)-supported α -chloro diketonate	260
6-4.	A proposed role of chloride in accelerating the thermal oxidative cleavage of an α -chloro diketonate by complex 7	262

6-5.	Oxidative cleavage of an acireductone by ferric species in a regioselective manner	264
6-6.	The most common current strategy for the activation of O ₂ by a nickel system involves the initial reduction of a Ni(II) precursor by an external electron source to generate an O ₂ -reactive Ni(I) species	265
6-7.	Proposed synthetic scheme for investigating the role of ligand bulkiness, coordination number and metal ion identity in determining the regioselectivity of the dioxygenolytic reaction of a bulky acireductone	268
6-8.	The nitroxygenase reaction catalyzed by the manganese-containing form of QDO proceeds in a regiospecific manner (top). A proposed reaction of acireductone complexes with the nitroxyl donor Piloty's acid (bottom)	270
6-9.	Proposed variations of substituents of the diketonate moiety from 7 to investigate the scope of substrate cleavage by O ₂	272

CHAPTER 1

OXIDATIVE ALIPHATIC CARBON-CARBON BOND CLEAVAGE REACTIONS IN ENZYMATIC SYSTEMS AND RELATED MODEL SYSTEMS[†]

Abstract

Over the past decade, several metalloenzymes have been characterized that catalyze dioxygenase-type aliphatic carbon-carbon bond cleavage reactions. The substrates for these enzymes vary from species that are stable with respect to O₂ under ambient conditions, to examples that in anionic form exhibit O₂ reactivity in the absence of enzyme. Described herein are advances from studies of the enzymes themselves and model systems. These combined investigations provide insight into novel mechanistic pathways leading to aliphatic carbon-carbon bond cleavage and/or the factors that influence regioselectivity in the oxidative carbon-carbon bond cleavage reactions.

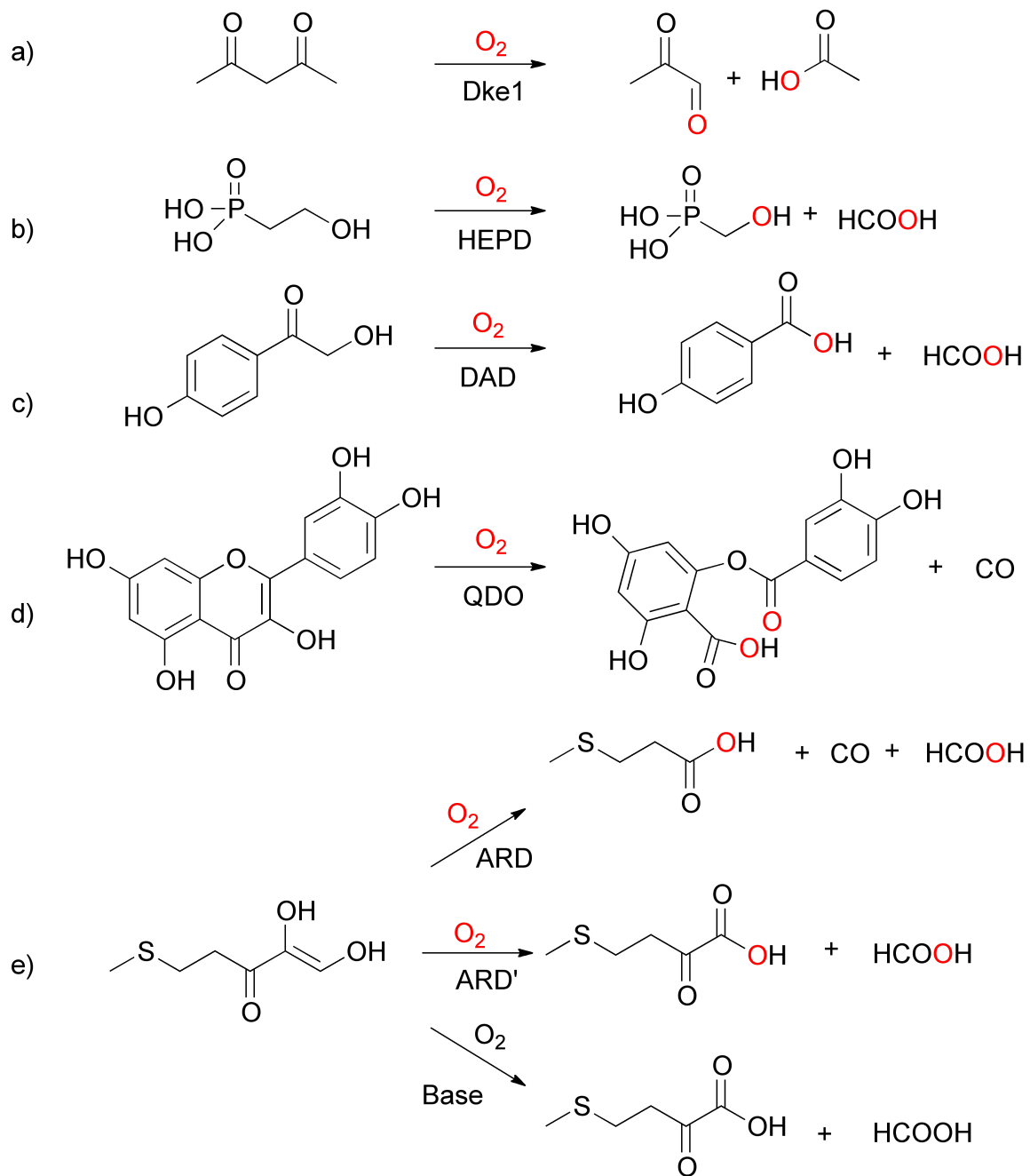
1. Introduction

One of the most challenging reactions in chemistry and biology is the selective oxidative cleavage of aliphatic carbon-carbon bonds. Despite the prevalence of such reactions in biological systems, there is currently little known regarding the mechanistic details of such processes. These types of reactions are of considerable current interest due to their potential for a broad array of applications, including the utilization of biomass in fuel production, the removal of otherwise intractable organic contaminants during wastewater treatment and other bioremediation, and for improving understanding of the treatment of human disease [1, 2].

[†] Coauthored by Caleb J. Allpress and Lisa M. Berreau. Reproduced in a modified format with permission from *Coord. Chem. Rev.* **2013**, 257, 3005-3029.

In nature several types of oxidative carbon-carbon cleavage reactions are catalyzed by metalloenzymes and involve the incorporation of both atoms of dioxygen into their products. These reactions may be divided into two sets, those that result in the cleavage of carbon-carbon bonds within an aromatic π -system (aromatic carbon-carbon bonds), and those that result in the cleavage of other carbon-carbon bonds (aliphatic carbon-carbon bonds). The former, which includes reactions catalyzed by intradiol and extradiol catechol dioxygenases, as well as other ring-cleaving dioxygenases, have been extensively investigated in studies of both enzymes and synthetic model systems [3-5]. Important themes in these investigations included the elucidation of novel mechanistic pathways and the discovery of how the metal oxidation state and ligand environment influence the regioselectivity of the oxidative reaction.

In contrast to systems that catalyze oxidative aromatic carbon-carbon bond cleavage, the metalloenzymes that cleave aliphatic carbon-carbon bonds have received much less attention until recently (with the exception of the quercetin dioxygenases), and are notable for their diversity in structure and substrate (Scheme 1-1). Most of the enzymes that catalyze these reactions are cupin-type proteins. The metal cofactor is most commonly iron, but other first-row transition metals, such as nickel and copper, are also found (Table 1-1). Metal binding residues at the active sites of these enzymes vary from the common 2-His, 1-carboxylate facial triad (hydroxyethylphosphonate dioxygenase, (HEPD)), to the 3-His (acetylacetonate 2,3-dioxygenase (Dke1)) and 3-His, 1-carboxylate (quercetin dioxygenase (QDO), acireductone dioxygenases (ARD and ARD')) binding motifs. The carbon-carbon bonds cleaved in these systems all have an accessible enol



Scheme 1-1. Oxidative aliphatic carbon-carbon bond cleavage reactions discussed in this chapter.

Table 1-1. Aliphatic carbon-carbon bond cleaving dioxygenase enzymes, active site metal ions, and metal coordination environment

Enzyme	Metal ion	Protein-derived ligands
Dke1	Fe(II)	3-His
HEPD	Fe(II)	2-His-1-carboxylate
DAD	Fe(II)	<i>a</i>
QDO	Cu(II) ^b	3-His-1-carboxylate
ARD/ARD'	Ni(II), Fe(II)	3-His-1-carboxylate

^aActive site ligand environment not yet determined. ^bFungal quercetinases contain Cu(II). Bacterial quercetinases exhibit activity with a variety of metal ions including Mn(II), Fe(II), Ni(II) and Co(II).

form, with the notable exception of hydroxyethylphosphonate. The relatively easily oxidizable quercetin and acireductone substrates are both oxygen-rich and are reminiscent of the common biological reductant ascorbic acid.

Two of the systems that have received the most attention recently, acetylacetone 2,3-dioxygenase and the acireductone dioxygenases, highlight the diversity of substrate oxidation in these enzymes and attendant mechanistic questions. In the former system the oxidation of the substrate is a difficult reaction with no synthetic model systems yet devised that can oxidatively cleave the native acetylacetone substrate in a biomimetic reaction. Thus, investigations have focused on the unique coordination motif and the role of charge at the enzyme active site. By contrast, the substrate for acireductone dioxygenases is readily oxidatively cleaved by O₂ in the absence of catalyst by simply

raising the pH. In studies of relevance to this system, efforts have focused on understanding the role that metal center may play in directing the regioselectivity of carbon-carbon bond cleavage.

Summarized herein are recent developments in understanding of metalloenzymes that catalyze oxidative aliphatic carbon-carbon bond cleavage via a dioxygenase-type reaction. Additionally, model systems of relevance to these enzymes are examined. Emphasis is placed on studies that have revealed mechanistic insight into overcoming the barrier to the spin-forbidden reaction between the organic substrate and O₂, and factors that influence regioselectivity in aliphatic carbon-carbon bond cleavage. We have limited the scope of this review to aliphatic carbon-carbon bond cleaving dioxygenases for which either mechanistic studies have been reported for the enzyme, or model systems have been reported. With this limitation, we have excluded systems such as carotenoid oxygenases, for which biochemical and computational studies have been summarized recently elsewhere [6]. Additionally, although the decarboxylation of 2-oxo acids such as α -ketoglutarate is a type of aliphatic carbon-carbon bond cleavage reaction that occurs in metalloenzymes, it is a chemically distinct process that is not included in this review. This is because it does not represent aliphatic carbon-carbon bond cleavage resulting from incorporation of both atoms of dioxygen into a single substrate [7]. Two exceptions that are included in this review are 4-hydroxyphenylpyruvate dioxygenase (HPPD) and hydroxymandelate synthase (HMS), which are functionally similar to α -ketoglutarate-dependent oxygenases but are formally dioxygenases.

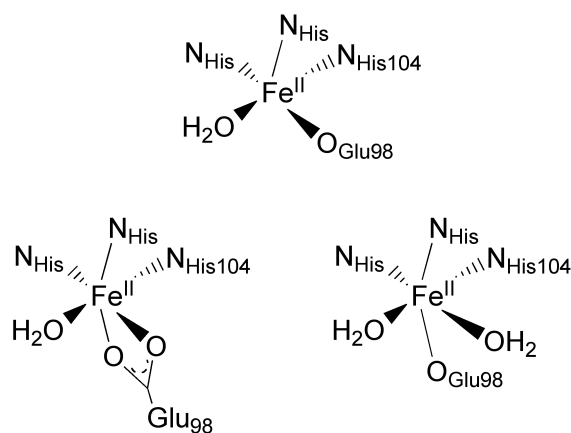
2. Metalloenzymes that oxidatively cleave aliphatic C-C bonds and their model systems

2.1 Acetylacetone 2,3-Dioxygenase (Dke1)

Acetylacetone is used industrially in the production of anti-corrosion agents, pharmaceutical compounds, and pesticides. It is also a precursor to several heterocyclic compounds (pyrazoles, diketamines) via condensation reactions. Simple metal acetylacetonate complexes are useful as catalysts. With its wide array of uses, it is important to note that acetylacetone is toxic to mammals [8], as well as to aquatic species [9] and microorganisms [10]. Therefore, bioremediation approaches toward the degradation of acetylacetone to less toxic byproducts are of current interest. In 2002, Straganz, *et al.* reported the identification of a bacterium (*A. johnsonii*) that can grow with acetylacetone as its only carbon source [11, 12]. This bacterium degrades acetylacetone to produce acetate and methyl glyoxal (Scheme 1-1(a)), the latter of which is converted to pyruvate. The enzyme that catalyzes this oxidative cleavage reaction is termed acetylacetone 2,3-dioxygenase, or diketone-cleaving enzyme (Dke1) [11, 12]. It is a tetrameric cytosolic protein with each 16.6 kDa subunit containing a single non-heme Fe(II) center. Structural studies of the Zn(II)-containing form of the enzyme (PDB: 3bal) revealed Dke1 to be a member of the cupin superfamily [13] of proteins. The Fe(II) center is ligated facially by three histidine residues (His62, His64, His104). The coordination of these residues makes the active site of Dke1 distinct from the more typical two histidine, one carboxylate facial triad found in an array of mononuclear non-heme iron enzymes that utilize O₂ to oxidize organic substrates (e.g. alpha-ketoglutarate (α -KG) dependent dioxygenases) [3, 14]. X-ray absorption spectroscopic studies of an

Fe(II)-dependent cupin oxygenase protein (*Bxe_A2876*) from *Burkholderia xenovorans*, which similarly to Dke1 oxidatively cleaves β -diketones, revealed a five or six coordinate metal center in the resting state. Specifically, the Fe(II) center has three coordinated histidine residues at 1.98 Å, a carboxylate ligand (perhaps Glu98) at \sim 2.08 Å, and one or two coordinated water molecules at 2.04 Å [15]. CD, MCD and VTVH MCD spectroscopic studies of Dke1 are consistent with a six-coordinate metal center in the resting state [14]. Drawings of possible five- and six coordinate resting state structures are shown in the top portion of Figure 1-1.

Resting State:



Substrate-bound:

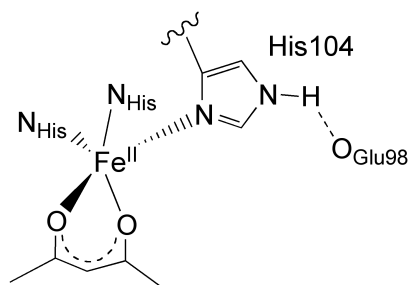


Figure 1-1. Proposed structures for resting state and substrate-bound forms of Dke1.

Bidentate coordination of the acetylacetonate substrate to the Fe(II) center in Dke1 results in the loss of glutamate as a ligand to the Fe(II) ion, and a reduction in the affinity of the Fe(II) center for a sixth water ligand (Figure 1-1(bottom)) [14]. Notably, computational studies suggest that the free Glu98 residue can act as a hydrogen bond acceptor for N ϵ -H of His104 (Figure 1-1(bottom)) [16]. This increases the electron density within His104 thus making it a better donor to the iron center, which may assist in stabilizing a higher oxidation state iron center during catalysis (*vide infra*). The importance of this interaction is suggested by the fact that mutation of Glu98 results in a 100-fold decrease in the rate-determining step of O₂ reduction [17].

The substrate-bound form of Dke1 is characterized by a new absorption feature, assigned as d π →acac π^* MLCT transition, in the visible region at ~415 nm ($\epsilon \sim 1000 \text{ M}^{-1} \text{ cm}^{-1}$). The increased charge within the active site of Dke1, versus 2-His-1-carboxylated ligated Fe(II) sites, decreases the energy of the *d* orbitals, which results in a shift to higher energy of the Fe(II)→acetylacetonate MLCT transition in the enzyme-substrate complex relative to that found in a typical α -KG dependent enzyme [14]. The Fe(II) center in the enzyme-substrate (ES) complex is proposed to be five-coordinate, thereby having an available coordination position for reaction with O₂.

O₂ consumption studies, combined with NMR experiments, showed that for each equivalent of acetylacetonate that is oxidatively cleaved by Dke1, one equivalent of O₂ is consumed [11]. Use of ¹⁸O₂ in the reaction revealed incorporation of a single labeled oxygen atom into methylglyoxal (70%) and acetate (97%), thus demonstrating a dioxygenase-type reaction [18]. Additionally, use of H₂¹⁸O and unlabeled O₂ resulted in

no ^{18}O incorporation into acetate, providing evidence that the reactive species formed are not susceptible to oxygen atom exchange from water.

Dke1 catalyzes the oxidative cleavage of a variety of β -diketones [11, 19]. In general, β -diketones wherein a terminal methyl group of acetylacetone has been replaced with homo-alkyls or non-ionizable rings are reasonable substrates, whereas analogs containing a charged substituent (e.g. a carboxylate) are not [11, 12]. Studies of the oxidative cleavage specificity of a series of β -diketone substrates in which the electronic properties of the R_1/R_2 substituents (Figure 1-2) were systematically varied revealed a strong preference for oxidative cleavage at the carbon-carbon bond adjacent to the most electron-deficient carbonyl carbon.

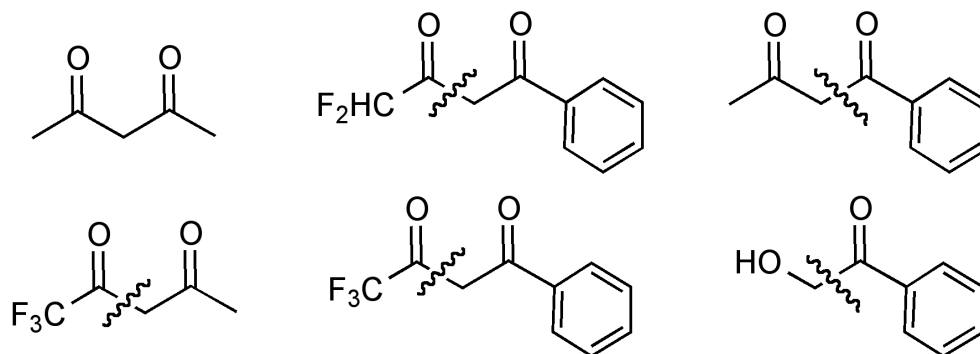


Figure 1-2. β -diketone substrates for Dke1.

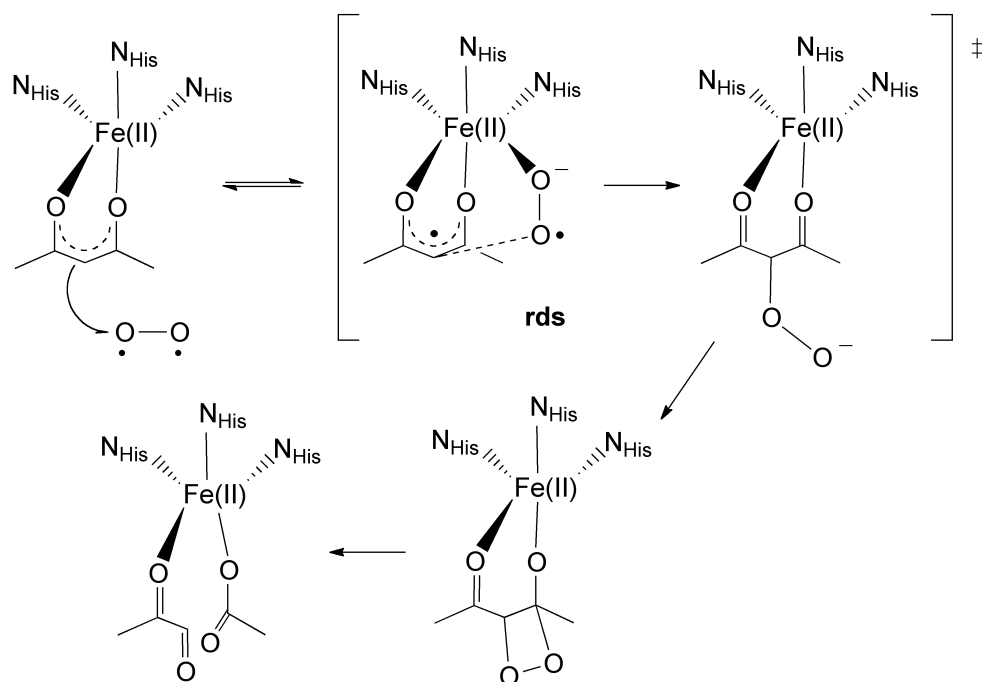
Single turnover kinetic studies of the reaction catalyzed by Dke 1 were performed by monitoring the loss of the MLCT band associated with the Fe(II)-diketonate enzyme-substrate complex [19]. Overall the reaction was found to be second order, $d[\text{ES}]/dt = -k_2[\text{ES}][\text{O}_2]$. Kinetic studies as a function of substrate structure revealed a correlation between the energy of the substrate HOMO and the rate of the reaction, with a higher

energy substrate HOMO corresponding to a faster reaction. These studies provide evidence for a rate-determining step that involves oxidation of the enzyme-substrate complex by O₂.

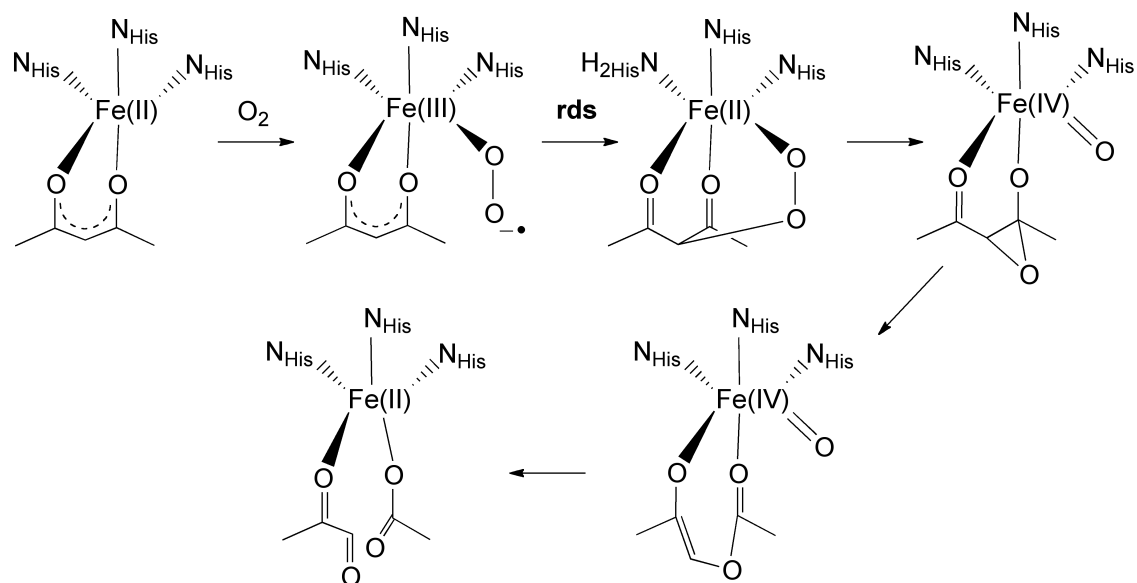
The results of the mechanistic experiments described above are consistent with a reaction pathway wherein the coordinated enolate acts as a two-electron reductant toward dioxygen. This results in the formation of a C(3)-peroxidate species wherein the terminal oxygen can nucleophilically attack the most electron deficient adjacent carbon center leading to a dioxetane intermediate which subsequently undergoes O-O and C-C bond cleavage to give the observed products (Scheme 1-2(top)). Alternatively, recent computational studies provide evidence that a lower energy pathway involves Fe(II)-mediated O₂ activation to form a Fe(III)-superoxo species, which subsequently electrophilically attacks the HOMO of the coordinated enolate to form a C3-bridged peroxy species in the rate-determining step (Scheme 1-2(bottom)). Cleavage of the O-O bond leads to the formation of an Fe(IV)=O species and an epoxide. Opening of the epoxide, followed by attack of the Fe(IV)=O on the resultant C=C bond would give the observed products [20].

Features of the active site chemistry of Dke1 have been recently investigated using a synthetic analog approach. These include an evaluation of the influence of the atypical neutral three-histidine coordination motif on the electronic properties of the iron center, evaluation of spectroscopic features associated with the coordination of acetylacetonate and analogs to an N₃-ligated Fe(II) center, and evaluation of the O₂ reactivity of five-coordinate compounds of relevance to ES adducts. The results of these studies are summarized below.

Reaction of coordinated enolate with O₂:



Metal-centered activation of O₂:



Scheme 1-2. Proposed mechanistic pathways for Dke1.

2.1.1. Structural and Spectroscopic Models. Synthetic complexes of structural relevance to the enzyme/substrate adduct of Dke1 have all utilized a tripodal supporting chelate ligand with three heterocyclic nitrogen donors in order to mimic the facial arrangement of three histidines at the active site of the enzyme [21-25]. The most commonly used ligands have been hydro(trispyrazolyl)borate (Tp) ligands, which are widely used in model systems of non-heme iron systems [3]. Tp ligands have been successfully used to mimic the 2-His-1-carboxylate facial triad donor set due to their inherent negative charge [3, 26]. However, an important distinction between three histidine ligands and the 2-His-1-carboxylate facial triad as Fe(II) binding motifs is the absence of negative charge in the former. For this reason, Fiedler has additionally utilized neutral tris(imidazolyl)phosphine ligands, which have the added advantage of containing imidazole rings, potentially making them better mimics of histidine ligands than pyrazole-based ligands [22, 23]. This variety of ligands has allowed the properties of $[(L)Fe(acac^x)]$ ($acac^x$ = a variety of acac-derived diketonates) complexes to be probed as a function of ligand electronics and sterics, including coordination number and geometry, redox potentials and electronic structure [22-24].

$Tp^{R^2}Fe(acac^x)$ (Figure 1-3(a)) complexes have consistently been found to be six-coordinate by X-ray crystallography, with a bound solvent molecule, although when the crushed solid is dried in vacuo, elemental analysis is consistent with the removal of solvent [22]. By contrast, complexes with a bulkier supporting chelate ligand such as $Tp^{Ph^2}Fe(acac^x)$ (Figure 1-3(b)) are consistently found to be five-coordinate in the solid state, with the geometry changing from distorted square-based pyramidal to distorted trigonal bipyramidal as the bulkiness of the substituents on the $acac^x$ ligand are increased

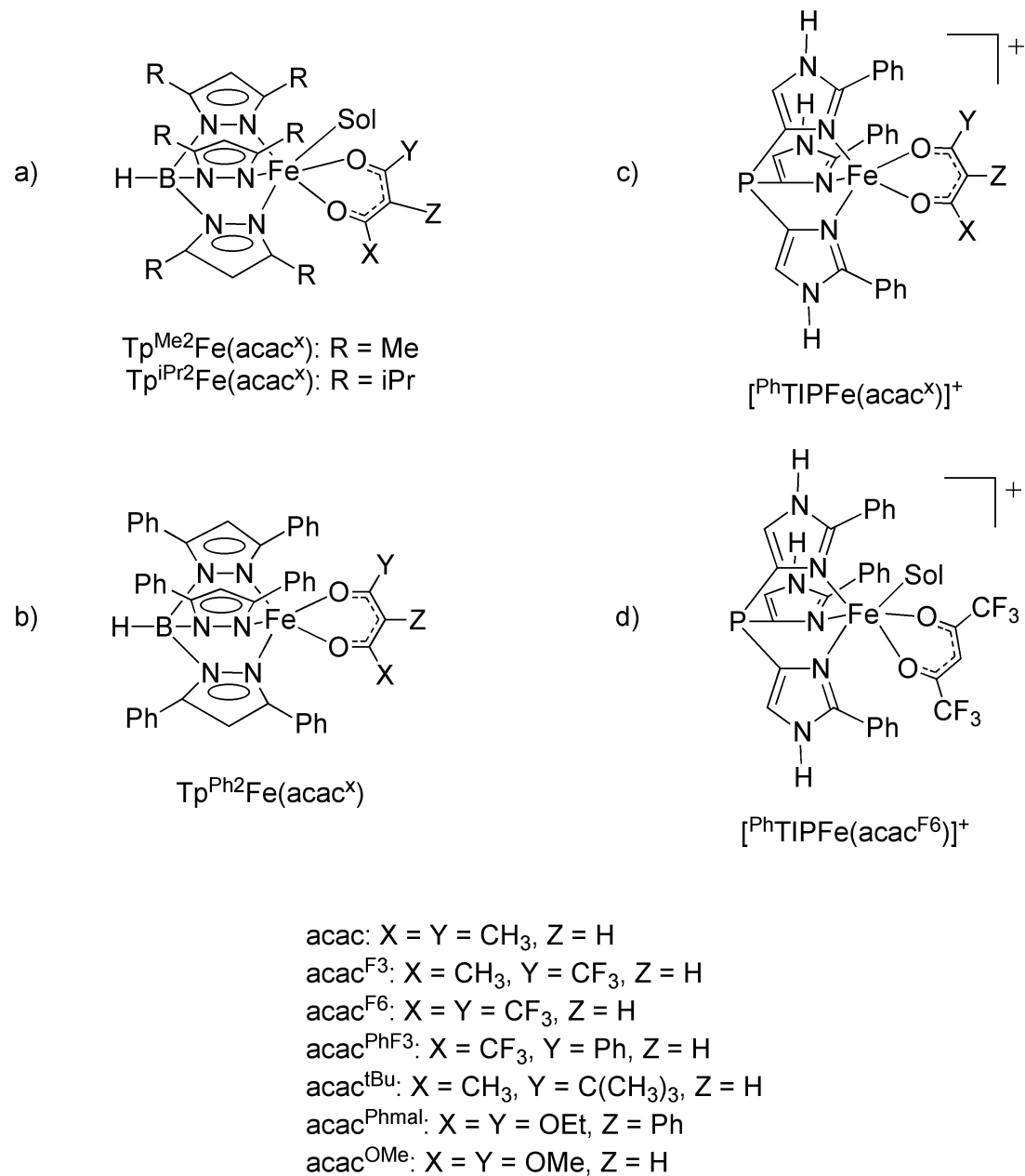


Figure 1-3. Synthetic complexes of relevance to the ES adduct in Dke1.

[22]. The tris(imidazole)phosphine-ligated $[\text{TIP}^{\text{Ph}}\text{Fe}(\text{acac}^{\text{x}})]^+$ complexes (Figure 1-3(c)) are all five-coordinate in the solid state, except for the case where both diketonate substituents are trifluoromethyl groups (Figure 1-3(d)), which is a six-coordinate complex [22, 23].

Similar to the acetylacetonate-bound form of Dke1, the electronic absorption features of the Fe(II) diketonate complexes shown in Figure 1-3 contain two features that have been assigned by DFT to a MLCT and a primarily diketonate-based transition, respectively (Table 1-2) [22, 23]. There is a notable blue-shifting of the MLCT absorption feature between the complexes $\text{Tp}^{\text{Me}_2}\text{Fe}(\text{acac}^{\text{x}})$ and $\text{Tp}^{\text{Ph}_2}\text{Fe}(\text{acac}^{\text{x}})$, despite similarities in the electron donating ability of the supporting ligands, consistent with the transition from a six- to a five-coordinate complex lowering the d orbital energies [22]. Importantly, there is also a blue-shifting of the MLCT absorption feature between the five-coordinate complexes $\text{Tp}^{\text{Ph}_2}\text{Fe}(\text{acac}^{\text{x}})$ and $[\text{TIP}^{\text{Ph}_2}\text{Fe}(\text{acac}^{\text{x}})]^+$ [22, 23]. A similar shift was observed between the acetylacetonate-bound forms of HPPD (4-hydroxyphenylpyruvate dioxygenase), an iron-containing enzyme with a facial triad and Dke1, highlighting the important role of the more positive charge in a 3-His binding motif in lowering the energy of the d orbitals [14]. Within these series of complexes, for a given supporting ligand set, the absorption features move to lower energy as the electron-withdrawing ability of the substituents on the acac^{x} ligand increases, with the notable exception of $[\text{TIP}^{\text{Ph}}\text{Fe}(\text{acac}^{\text{F}_6})]^+$, suggesting that this complex retains a six-coordinate geometry in solution, consistent with the poorer electron donating ability of the acac^{F_6} π orbitals.

Table 1-2. Structural, spectroscopic, and redox properties of Fe(II) diketonate complexes of relevance to the enzyme/substrate adduct in Dke1.

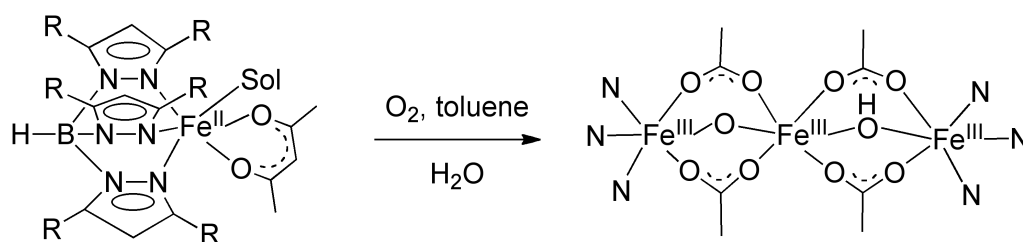
Diketonate Complex	C.N.	Ancillary ligand charge	τ^a	Wavelength (nm)	E (mV)	Ref
^{Me2} TpFe(acac)	6	-1	-	348, 438	-303	[22]
^{Me2} TpFe(acac ^{F3})	6	-1	-	377, 479	-34	[22]
^{Ph2} TpFe(acac)	5	-1	0.0	356, 420	-58	[22]
^{Ph2} TpFe(acac ^{F3})	5	-1	0.3	363, 462	158	[22]
[^{Ph} TIPFe(acac)] ⁺	5	0	0.5	351, 415	E _{p,a} = 120	[23]
[^{Ph} TIPFe(acac ^{F3})	5	0	0.64	373, 461	E _{p,a} = 360	[23]
[^{Ph} TIPFe(acac ^{F6})	6	0		382, 509	N/A	[23]
Dke1-acac	5	0	n.d.	357, 417	n.d.	[14]
Dke1-acac ^{F3}	n.d.	0		382, 450	n.d.	[19]
HPPD-acac	5	-1	n.d.	364, 435	n.d.	[14]

n. d. = Not determined. ^a $\tau = 1.0$ for a purely trigonal bipyramidal geometry and $\tau = 0$ for a purely square pyramidal geometry [27].

Electrochemical studies have shown a redox wave for the Fe(II/III) couple that is reversible for Tp^{Ph2}Fe(acac^x) and Tp^{Me2}Fe(acac^x), but irreversible for [TIP^{Ph}Fe(acac^x)]⁺ complexes (Table 1-2) [22, 23]. As expected, the complexes become more difficult to oxidize with greater electron-withdrawing substituents on the acetylacetonate derived ligands, with a lower coordination number, and with an increase in positive charge in the complex.

2.1.2 Functional Models. The study of functional model systems of Dke1 began inadvertently in 1993 when Kitajima *et al.* synthesized Tp^{iPr2}Fe(acac) while studying the reaction of ferrous complexes with dioxygen to form peroxo-bridged diferric compounds [25]. This compound has some relevance to Dke1, having a facial arrangement of three

heterocyclic nitrogen donors and the acetylacetonate substrate bound, and also exhibits cleavage reactivity of the diketonate ligand. Specifically, exposure of a toluene solution of $\text{Tp}^{\text{iPr}_2}\text{Fe}(\text{acac})$ to air at -78°C led to the formation of a bluish green species (assigned as a μ -peroxo adduct), followed by subsequent decay to a reddish brown complex that was found by X-ray crystallography to be a trimeric Fe(III) complex with bridging acetate, oxo and hydroxo moieties (Scheme 1-3). Labeling studies confirmed that the source of the acetate ligand was acetylacetonate, although, unfortunately, ^{18}O -labeling studies were not reported, which would have confirmed whether the acetate ligand was formed via a hydrolytic or oxidative process. In a subsequent study by Siewert *et al.*, it was found that exposure of the related compound $\text{Tp}^{\text{Me}_2}\text{Fe}(\text{acac})$ to dry O_2 led to oxidation of the iron center, although no cleavage products were detected [21]. However, when the reaction was repeated in the presence of H_2O , iron complexes containing acetate ligands were detected by MS (Scheme 1-3), suggesting that in the Kitajima system, the observed products were due to hydrolytic chemistry rather than oxidative chemistry.

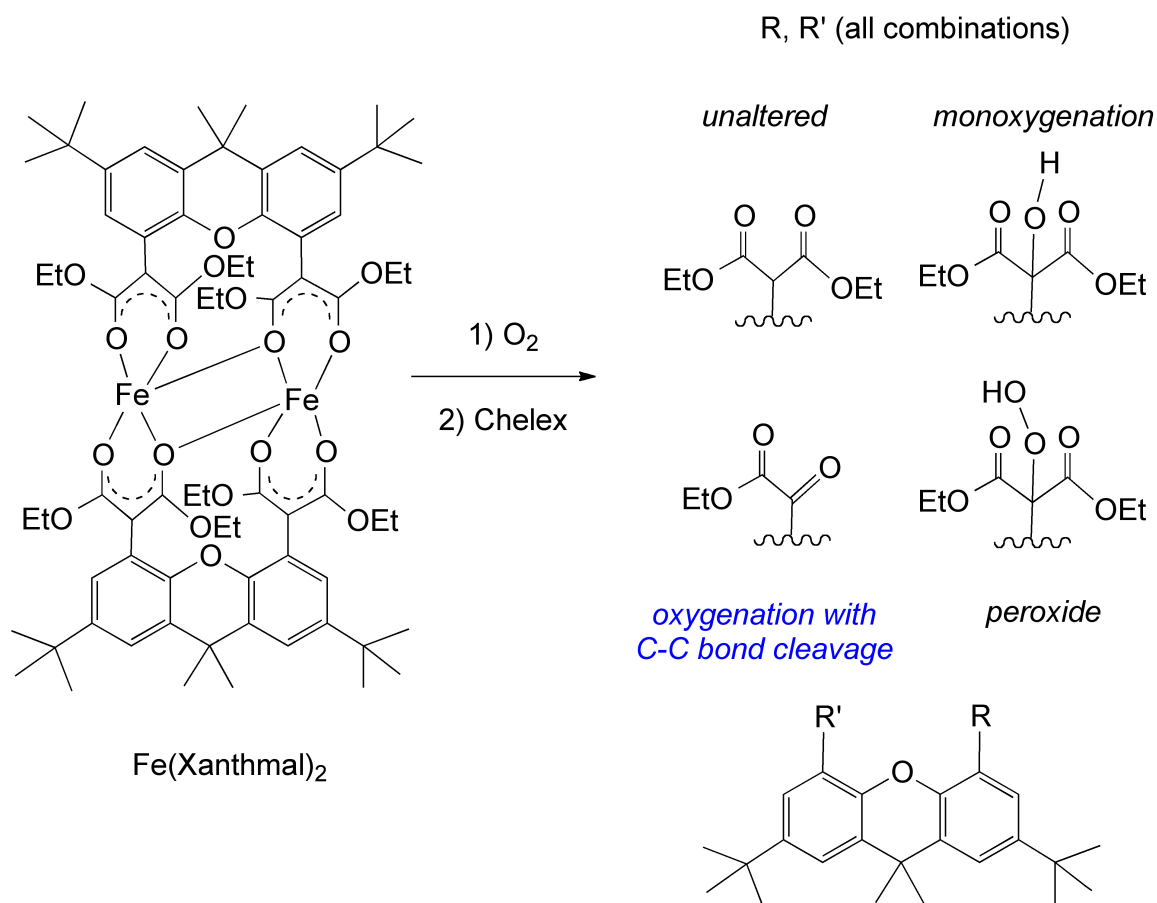


$\text{Tp}^{\text{Me}_2}\text{Fe}(\text{acac})$: R = Me

$\text{Tp}^{\text{iPr}_2}\text{Fe}(\text{acac})$: R = iPr

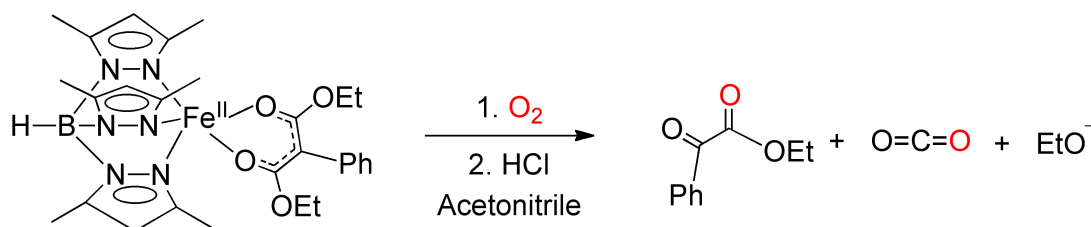
Scheme 1-3. Acetoacetonate cleavage reactivity of $\text{Tp}^{\text{iPr}_2}\text{Fe}(\text{acac})$ and $\text{Tp}^{\text{Me}_2}\text{Fe}(\text{acac})$.

In 2008, Siewert, *et al.* reported studies of $\text{Fe}(\text{Xanthmal})_2$ (Scheme 1-4) which undergoes O_2 -dependent reactivity at the malonate portion of the ligand to give an α -keto ester product resulting from oxidative aliphatic C-C bond cleavage [28]. This compound is notable for being the inspiration for the use of a malonate diketonate ligand in future systems of relevance to Dke1 [21, 24], and is proposed to react via the initial formation of a ferric-superoxo species. Interestingly, a monooxygenation of the ligand is also observed, proposed to occur via the initial formation of a μ -peroxo species between two iron centers, which cleaves to form $\text{Fe}(\text{IV})=\text{O}$ units which in turn oxidize the ligand.



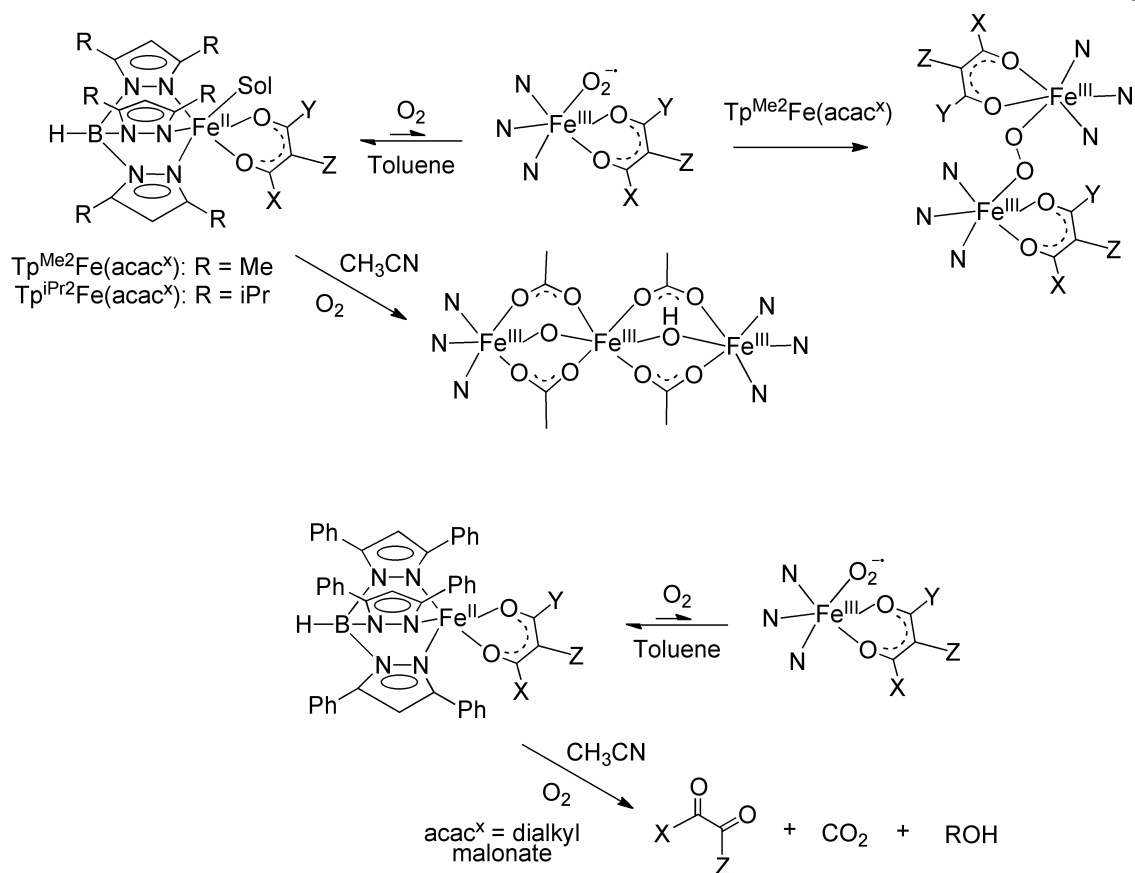
Scheme 1-4. O_2 -dependent aliphatic carbon-carbon bond cleavage reactivity of $\text{Fe}(\text{Xanthmal})_2$.

Siewert et al. also reported the oxygen reactivity of $\text{Tp}^{\text{Me}_2}\text{Fe}(\text{Phmal})$ ($\text{Phmal} = 3$ -phenylmalonate) with dry O_2 , leading to the identification of ethyl benzoylformate and ethylcarbonate (which subsequently decomposes to CO_2 and EtO^-), the expected products of Dke1-type cleavage (Scheme 1-5) [21]. The system was found to be catalytic with regard to substrate oxidation with a TOF of 55 h^{-1} . The lack of reactivity of an analogous ferric complex or a LiPhmal salt led to the proposal of iron-centered activation of O_2 via the formation of a ferric superoxo species as the likely first step in the reaction mechanism of the Dke1 enzyme.



Scheme 1-5. O_2 -dependent aliphatic carbon-carbon bond cleavage reactivity of $\text{Tp}^{\text{Me}_2}\text{Fe}(\text{Phmal})$.

The series of $\text{Tp}^{\text{R}_2}\text{Fe}(\text{acac}^x)$ complexes reported by Fiedler exhibit O_2 reactivity that is relatable to the complexes of Kitajima and Limberg. Specifically, reaction of $\text{Tp}^{\text{Me}_2}\text{Fe}(\text{acac}^x)$ (except $X = \text{F}_6$ (Figure 1-3)) with O_2 leads to the formation of a green intermediate, followed by decay to a new species. Similar to the reactivity observed by Kitajima, the intermediate is assigned as a μ -peroxo species based on EPR, MCD and DFT calculations, and the product is assigned as a trinuclear ferric species with bridging acetato-derived ligands based on EPR and a crystal structure in the case of $\text{Tp}^{\text{Me}_2}\text{Fe}(\text{acac}^x)$ (Scheme 1-6(top)) [24]. It is worth noting that the mechanism of the



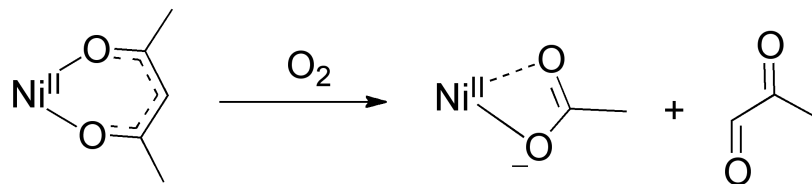
Scheme 1-6. (top) O_2 reactivity of $\text{Tp}^{\text{R}_2}\text{Fe}(\text{acac}^{\text{X}})$ (R = Me, iPr) complexes. (bottom) O_2 reactivity of $\text{Tp}^{\text{Ph}_2}\text{Fe}(\text{acac}^{\text{X}})$ complexes. Substituents X, Y, and Z defined as in Figure 1-3.

cleavage of acetylacetonate derivatives to form acetate products has not yet been investigated and the results of ^{18}O -labeling studies have not been reported.

By contrast, the complexes $\text{Tp}^{\text{Ph}_2}\text{Fe}(\text{acac}^{\text{X}})$ (Scheme 1-6 (bottom)) and $\text{TIP}^{\text{Ph}}\text{Fe}(\text{acac}^{\text{X}})^+$ do not rapidly react with O_2 to form the same μ -peroxo species, due to the increased steric bulk preventing dimer formation in solution. The lower reactivity of these complexes with dioxygen suggests that the formation of a ferric superoxo species is endergonic, and without the thermodynamic driving force provided by the formation of a μ -peroxo species, any equilibrium that forms lies far toward reactants. It is likely that the

increased steric bulk does not significantly impede dioxygen access to the metal center, as when NO was added to solutions of $\text{Tp}^{\text{Ph}_2}\text{Fe}(\text{acac}^x)$ and $\text{TIP}^{\text{Ph}}\text{Fe}(\text{acac}^x)^+$ binding was observed, giving the first spectroscopic and structural analogues of a superoxo adduct of relevance to Dke1. Interestingly, in the complexes $\text{Tp}^{\text{Ph}_2}\text{Fe}(\text{acac}^{\text{Phmal}})$ and $\text{Tp}^{\text{Ph}_2}\text{Fe}(\text{acac}^{\text{OMe}})$ (Figure 1-3), oxidative cleavage similar to that found by Siewert et al. was observed (Scheme 1-6(bottom)) [21]. Thus, in model systems without secondary structural interactions to stabilize intermediates, only activated, electron-rich substrates (malonates) can be cleaved (Schemes 1-5 and 1-6(bottom)), thus indicating the important role such secondary interactions may play in the enzymatic reaction mechanism. This is also consistent with the proposed reaction mechanism for Dke1 wherein the rate-determining step is the electrophilic attack of an oxygen species on the central carbon of the diketonate, and thus substrates with a higher energy π system will react significantly faster. At present, the oxygen reactivity of $\text{TIP}^{\text{Ph}}\text{Fe}(\text{malonate})$ species has not been reported, and thus the influence of increased positive charge on Dke1-like cleavage chemistry has not been investigated in model systems.

2.1.3 Dke1-type reactivity in Ni(II) complexes. There has also been a nickel-containing system reported that has some relevance to the diketonate-cleaving reactivity of Dke1. It was found that the combination of $\text{Ni}(\text{acac})_2(\text{H}_2\text{O})_2$ with ethylenediamine in water, in the presence of dioxygen, leads to the formation of $[\text{Ni}(\text{en})_2(\text{OAc})]^+$ over the course of 18 days (Scheme 1-7) [29]. An anaerobic control resulted in no cleavage, leading the study's authors to propose direct reaction of the $\text{Ni}^{\text{II}}(\text{acac})$ unit with dioxygen, without any redox changes occurring at the metal center. Such a reaction pathway would

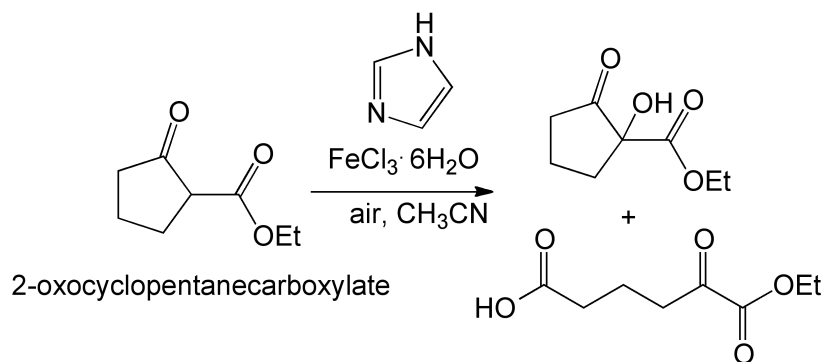


Scheme 1-7. Oxidative aliphatic carbon-carbon bond cleavage reaction of Ni(acac)₂(H₂O)₂ in the presence of ethylenediamine in water.

be akin to that shown in Scheme 1-2(top) wherein the coordinated enolate reacts directly with O₂ [30].

2.1.4 Dke1-type reactivity in an Fe(III)-containing system. An interesting recently reported system involves an *in situ* generated ferric complex containing both imidazole and 2-oxocyclopentanecarboxylate (a diketone) as ligands [31]. In the presence of O₂, reaction occurs leading to either a single oxygen or dioxygen being incorporated into the diketone (Scheme 1-8). Notably, the substrate in this system also has an ester moiety akin to the electron-rich malonate substrates described above. While the direct relevance of this system to Dke1 is unclear, due to the higher oxidation state of the iron center, the dioxygenase-like aliphatic carbon-carbon bond cleavage chemistry is interesting in that it is regioselective, leading to exclusive opening of the pentanone ring, suggesting that steric strain is an alternative means for activating ligands towards Dke1-type chemistry.

2.1.5 Perspective. Following the discovery of the Dke1 enzyme, interest quickly became focused on the elucidation of the relationship between structure and spectroscopic features, as well as



Scheme 1-8. Dke1-type reactivity in an Fe(III)-containing system.

the reaction pathway by which oxidative cleavage of the strong aliphatic carbon-carbon bond of a metal-coordinated diketonate is achieved. The His₃ ligand donor set for the Fe(II) center of Dke1 is notably different from many non-heme iron enzymes that are involved in the oxidation of organic substrates using O₂. To date, studies of Dke1 and synthetic model complexes have provided considerable insight into how the electronic environment of the Fe(II) center relates to the observed physical properties of Fe(II)-diketonate species. However, considerably less information is currently available with regard to the factors that govern carbon-carbon bond cleavage within the diketonate. For example, thus far only model systems that contain an electron-rich diketonate ligand (e.g. malonate) have been shown to undergo reaction with O₂ to give *oxidative* carbon-carbon bond cleavage. Reactions involving less electron-rich Fe(II)-diketonate species (e.g. acetoacetonate) have been found to instead exhibit *hydrolytic* cleavage. The chemical factors that determine which reaction pathway is operable remain to be elucidated. In terms of oxidative reactivity, a clear target for future model studies are systems that stabilize the formation of a mononuclear Fe(III)-superoxo species in the presence of a coordinated diketonate ligand. Importantly, the ligand environments employed in such

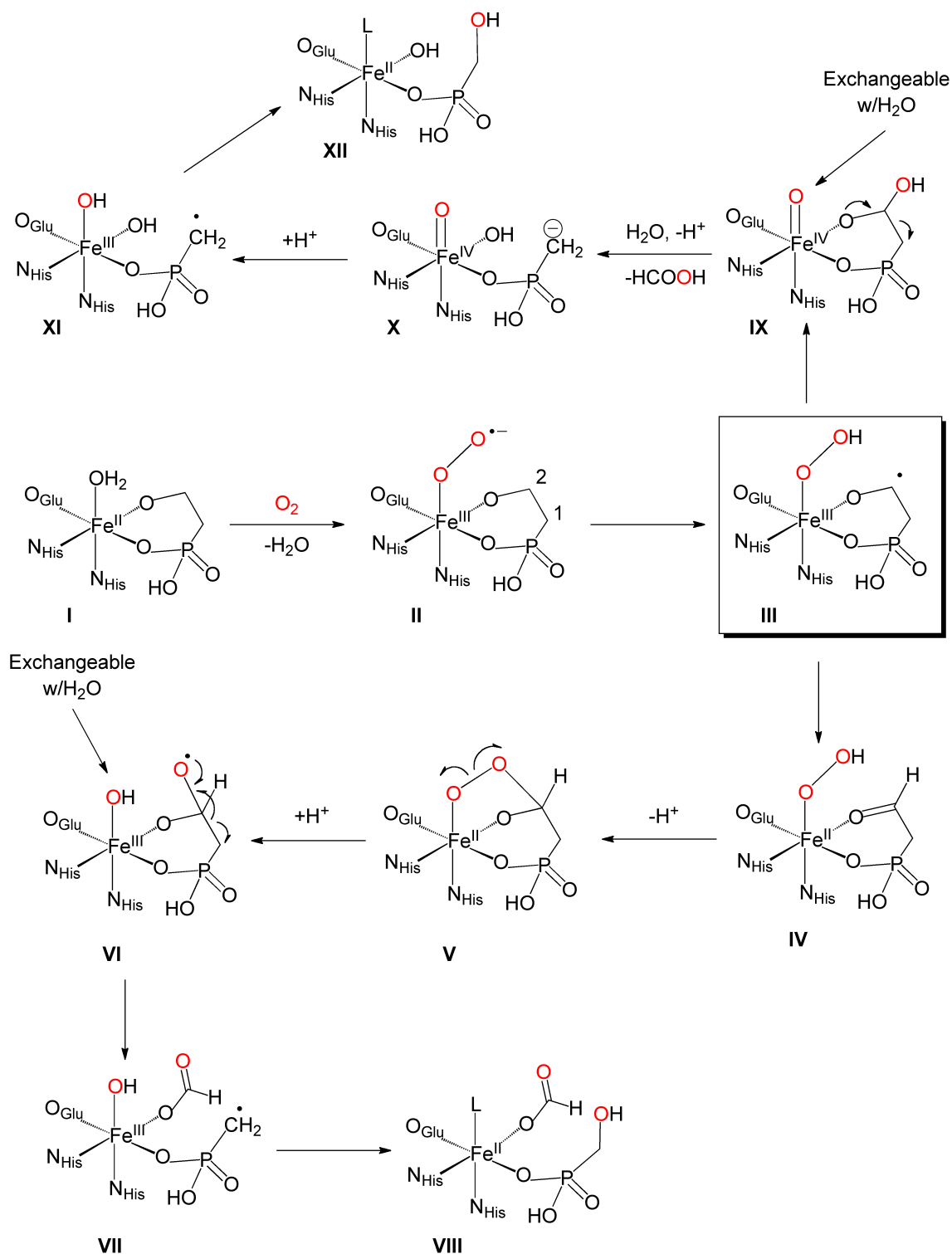
complexes should prevent the subsequent formation of diiron(III)- μ -peroxo species, perhaps via secondary interactions. Additionally, future studies should also address how the charge of the supporting ligand environment influences aliphatic carbon-carbon bond cleavage reactivity. Finally, an alternative approach to studying oxidative carbon-carbon bond cleavage reactions of relevance to Dke1 are investigations of diketonate complexes of other metal ions capable of generating $M(II)-O_2^-$ species. Such systems may provide insight into the feasibility of carbon-carbon bond cleavage without the need to generate high-valent Fe(IV) species, such as is shown in Scheme 1-2.

2.2 Hydroxyethylphosphonate dioxygenase (HEPD)

Organic compounds containing phosphorous-carbon bonds play important roles in agriculture and medicine. For example, phosphinothricin is a component of the herbicides Bast, Liberty, and Ignite, whereas fosfomycin is a naturally occurring antibiotic. Notably, the biosynthetic pathways for phosphinothricin tripeptide and fosfomycin both involve oxidation reactions catalyzed by non-heme iron dependent enzymes. However, whereas the reaction sequence leading to the formation of fosfomycin involves the formation of an epoxide [32-41], the reaction sequence leading to the formation of phosphinothricin tripeptide involves the oxidative cleavage of a $C(sp^3)-C(sp^3)$ bond in the conversion of 2-hydroxyethylphosphonate (HEP) to hydroxymethylphosphonate (HMP) and formate (Scheme 1-1(b)) [42-49]. This reaction is catalyzed by 2-hydroxyethylphosphonate dioxygenase (HEPD), a cupin-type protein with an active site that contains a mononuclear non-heme Fe(II) center ligated by a 2-His-1-carboxylate facial triad along with three molecules of water in the resting state. The HEP substrate coordinates in a

bidentate fashion, leaving one position on the Fe(II) center available for subsequent oxygen activation reactivity (Scheme 1-9) [42, 46].

Labeling studies involving the use of $^{18}\text{O}_2$ showed that HEPD is a dioxygenase enzyme, albeit complementary studies using H_2^{18}O provided evidence for an exchangeable oxygen atom in the reaction pathway [42]. Hydrogen atom abstraction occurs stereospecifically at C(2) [45], with the *pro-S* hydrogen atom being abstracted to generate a substrate radical. Notably, while the hydrogen atoms at the C(1) position of the substrate are not removed during the oxidative C(1)-C(2) carbon-carbon bond cleavage reaction, it has been found that the C(1) hydrogen substituents are racemized during the reaction [45]. Two possible mechanisms that account for the observed experimental outcomes during HEP oxidation are shown in Scheme 1-9 [44, 46, 47]. In one pathway (**I-VII**), an initially formed Fe(III)-superoxo species abstracts a hydrogen atom from the C(2) center in the rate determining step, giving a Fe(III) hydroperoxo complex and a substrate radical (**III**, Scheme 1-9). One-electron transfer to the iron center results in the formation of a coordinated aldehyde (**IV**). C-O bond formation between the distal oxygen and C(2), followed by homolytic cleavage of the O-O bond, gives a gemdiol radical and a ferric hydroxide species (**VI**), the latter of which is exchangeable with water. This radical species can undergo homolytic C-C bond cleavage to give coordinated formate and a methyl phosphonate radical (**VII**). Attack of the substrate radical on the axial hydroxide gives the final products. Alternatively, the radical species **III** (Scheme 1-9) could undergo homolytic O-O bond cleavage resulting in hydroxylation of the substrate and the formation of an Fe(IV)=O moiety (**IX**, Scheme 1-9). Aliphatic carbon-carbon bond cleavage results in the extrusion of formic acid and the formation of an anion that is



Scheme 1-9. Proposed mechanistic pathways for aliphatic carbon-carbon bond cleavage reactivity in hydroxyethylphosphonate dioxygenase (HEPD).

oxidized to radical **XI**, at which point stereochemical information at C(1) could be lost. Rebound with the ferric hydroxide species would provide the HMP product. Recently, the roles of water, the active site environment and proton transfer processes in the aliphatic carbon-carbon bond cleavage portion of this pathway have been examined computationally [48, 49].

To date, there have been no model systems reported for HEPD.

2.3 2,4'-Dihydroxyacetophenone dioxygenase (DAD)

The degradation of bisphenol A, a xenobiotic with endocrine-disrupting activity, is carried out by various bacteria. A minor dead-end product in this degradation pathway is 2,4'-dihydroxyacetophenone (DHAP) [50]. In 1984, Hopper *et al.* discovered an enzyme from *Alcaligenes* sp. 4HAP capable of degrading 2,4'-dihydroxyacetophenone by a dioxygenase reaction to yield formate and 4-hydroxybenzoic acid (Scheme 1-1(c)) [51, 52]. Purification and characterization of 2,4'-dihydroxyacetophenone dioxygenase (DAD), induced by growth of *Alcaligenes* sp. using 4-hydroxyacetophenone as the sole carbon source, showed the enzyme was a homotetramer that contained 0.95 equivalents of iron per tetramer, as determined colorimetrically using ferrozine [53]. A comparison of its sequence with other oxygenase enzymes showed no significant similarity. The structure of the enzyme has not yet been solved, although collection of a diffraction data set to 3.1 Å resolution has been reported [54].

Recently, a DAD from *Burkholderia* sp. strain AZ11 was isolated, purified and cloned [55]. This enzyme was found to oxidatively cleave 2,4'-dihydroxyacetophenone to form 4-hydroxybenzoic acid and formate, with concomitant consumption of one equivalent of dioxygen, with K_m and V_{max} determined to be 1.60 μM and 6.28 $\mu\text{M min}^{-1}$

$^1\text{mg}^{-1}$, respectively, in air-saturated solvent. This enzyme is also a homotetramer, but was found to contain 1.63-1.69 equivalents of iron per enzyme. Based on the electronic absorption features of the protein (350 nm ($5.8 \text{ mM}^{-1}\text{cm}^{-1}$) and 560 nm ($1.4 \text{ mM}^{-1}\text{cm}^{-1}$)), the iron center has preliminarily been assigned as a ferric oxidation state, although it must be noted that EPR measurements to confirm this assignment have not yet been performed. It was also found that upon addition of substrate to the enzyme, there is growth of an absorption feature at 400 nm, strongly suggesting that the substrate is involved in direct binding to iron at the active site. Substrate specificity assays have shown the importance of the α -hydroxyketone unit, as total loss of activity was observed when DHAP was replaced with acetophenone or 2-phenylethanol derivatives. The only other molecule found to be a substrate for this enzyme was the less electron rich α -hydroxyketone 2-hydroxyacetophenone, which exhibited an activity only 4.4% of that of the native substrate.

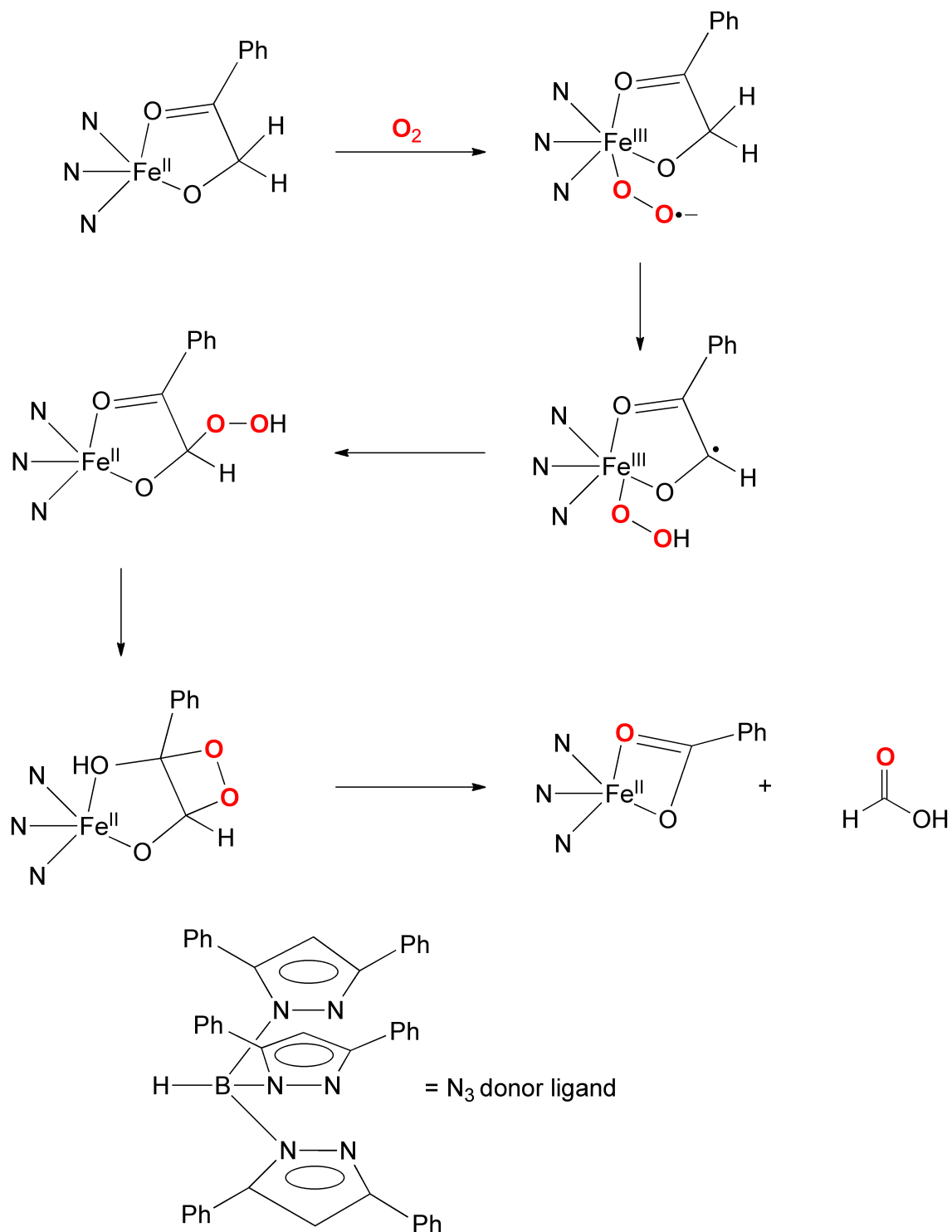
The α -hydroxy ketone unit, necessary for the enzyme activity, is related by tautomerization to an enediol. This has led to suggestions that the DAD may catalyze the oxidation of its substrate in a manner similar to that of catechol dioxygenases. While it is not yet clear whether DAD contains a ferric or ferrous center at the active site, either oxidation state could be expected to lead to the observed chemistry – by oxidative activation of the substrate, or by reduction of dioxygen to form a superoxo species [4].

2.3.1 Model studies. The production of model systems of relevance to DAD has been hindered by the absence of structural or definitive spectroscopic characterizations of the enzyme active site. Nonetheless, an important role of synthetic bioinorganic chemistry is the elucidation of structural motifs that may act as functional models of an

enzyme. In this regard, Paria et al. have synthesized a ferrous complex of 2-hydroxyacetophenone, supported by a hydrotris(3,5-diphenylpyrazolyl)borate ligand (Scheme 1-10) [56]. The use of trispyrazolylborate ligands has a long history in the study of non-heme iron enzymes, typically used for the modeling of the facial triad. Although it is unclear whether this facial triad exists in DAD, given the lack of homology with other dioxygenases. The 2-hydroxyacetophenone binds to the iron center via the keto and alkoxo oxygens to form a five-membered chelate. The complex is a distorted trigonal bipyramid ($\tau = 0.62$) [27], and exhibits absorption features at 505 and 560 nm, which are assigned to charge transfer bands by analogy to ferrous benzoylformate complexes.

Exposure of benzene solutions of this complex to O₂ leads to rapid decay of the charge transfer bands. Analysis of the organic products of the solution shows the production of benzoic acid and formate, the expected products of DAD-like cleavage; the inorganic product has been determined to remain in the ferrous oxidation state. ¹⁸O studies have shown low (~40%) incorporation of one label from dioxygen into the benzoic acid product, and the low level of incorporation has been attributed to water exchange with the product. However, this proposition is questionable, as the exchange of water into benzoic acid under acidic conditions has previously been found to occur only over prolonged reaction times [57].

Use of low temperature studies has not allowed the characterization of any intermediate in the reaction, however the use of intercepting reagents such as 2,4-di-*tert*-butylphenol (DTBP) and 2,4,6-tri-*tert*-butylphenol (TTBP) has provided evidence for a likely ferric superoxo intermediate. The lack of ligand oxidation, and progression of the reaction in the presence of radical scavengers, have been used to rule out the possibility

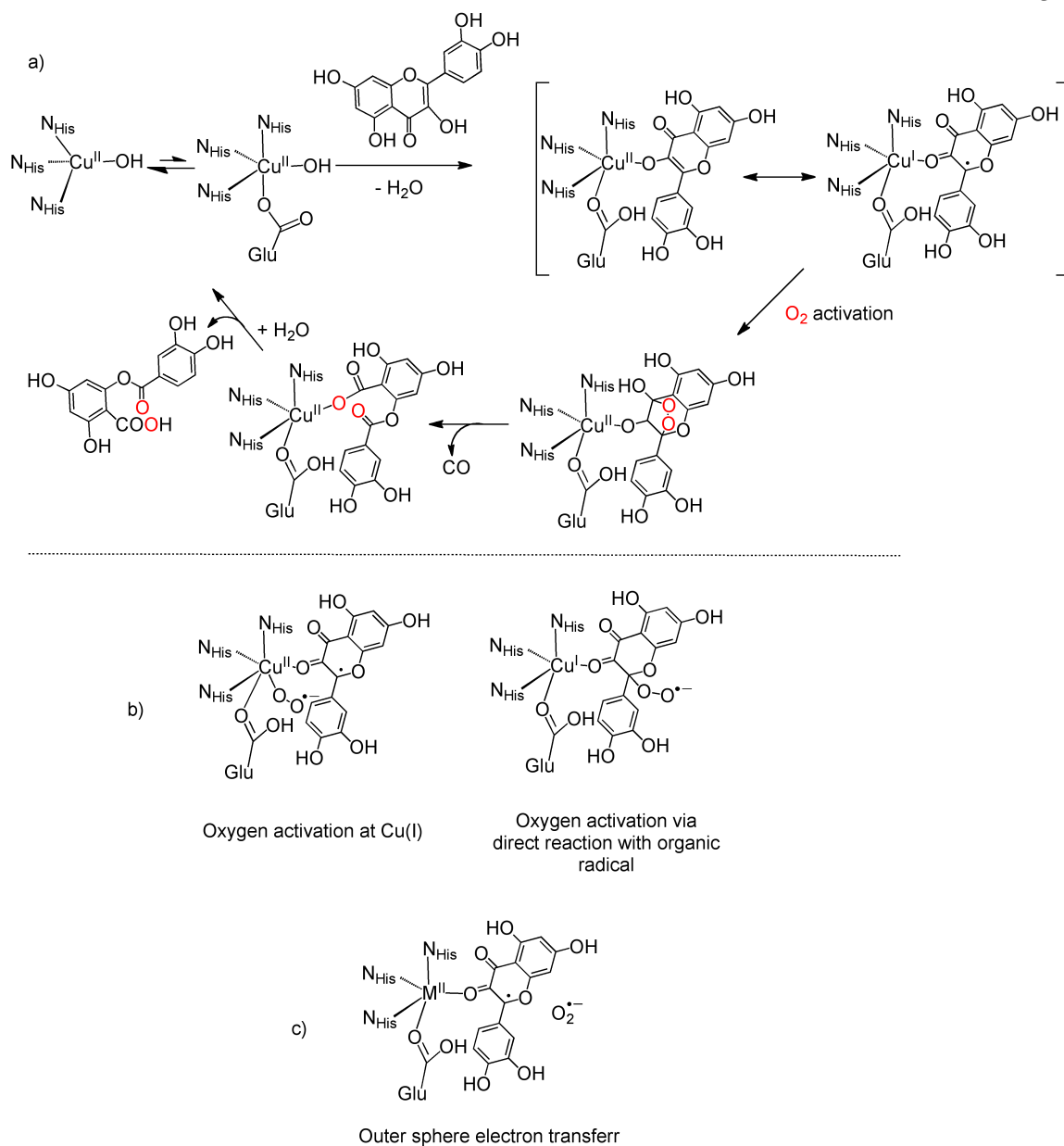


Scheme 1-10. Proposed mechanistic pathway for aliphatic carbon-carbon bond cleavage in 2,4'-dihydroxyacetophenone dioxygenase (DAD).

of a Fe(IV)=O intermediate and a free radical mechanism, respectively. The proposed overall mechanism is shown in Scheme 1-10. Interestingly, it is distinct from the catechol dioxygenase-like mechanism proposed in studies of the enzyme, in that rather than involving an alkenyl/acyl migration, the formation of a dioxetane ring and subsequent collapse is proposed for the carbon-carbon cleaving step. However, the alkenyl/acyl migration may be relevant in this system, as hydrolysis of the resulting anhydride would lead to the observed low ~50% ^{18}O incorporation into the products.

2.4 Quercetin dioxygenases (QDOs)

Quercetin is a flavonol that is produced in numerous fruits and vegetables and is well known for its antioxidant and antimicrobial properties [58-60]. Degradation of plants results in the deposition of quercetin in the soil where bacteria and fungi degrade this flavonol in a 2,4-dioxygenolytic type oxidative carbon-carbon bond cleavage reaction (Scheme 1-1(d)) that also results in the formation of CO. Fungal quercetinases are known to contain a mononuclear Cu(II) center and have been extensively investigated [61-68]. The active site Cu(II) center is typically ligated by three histidine residues and a water molecule in a distorted tetrahedral geometry. However, a five-coordinate structure containing an additional coordinated glutamate ligand has also been identified. The ES complex exhibits monodentate coordination of quercetin via a deprotonated O-3 atom [68]. It is proposed that this coordination motif enables the formation of a bridging peroxo species from which dioxygenase-type oxidative aliphatic carbon-carbon bond cleavage occurs (Scheme 1-11) [65-69]. Notably, the oxygen activation step may involve electron transfer to generate a Cu(II) superoxide species, or an internal redox tautomer



Scheme 1-11. (a) Proposed reaction pathway in fungal quercetinsases. (b) Possible sites for O_2 activation in copper-containing fungal quercetinsases. (c) Proposed outer sphere electron transfer reactivity of metal-coordinated flavonol with O_2 in bacterial quercetinsases.

having Cu(I) flavonoxo radical character (Scheme 1-11(bottom)), with both enabling the subsequent formation of the required cyclic peroxide species.

Recent studies of a bacterial quercetinase from *B. subtilis* showed that when this enzyme is produced in *E. coli* it binds a variety of divalent metals, with the highest level of reactivity being found for Mn(II) [70-73]. The Fe(II)-containing form of this protein has been characterized by X-ray crystallography, with the Fe(II) coordination environment of this bicupin-type protein being comprised of three histidine donors, one glutamate ligand, and a water molecule [70]. Notably, EPR studies using NO suggest that substrate binding blocks access of O₂ to the Fe(II) center in this enzyme [70].

Interestingly, the quercetinase from *Streptomyces sp. strain FLA* is most active with Ni(II) as the cofactor, albeit incorporation of other divalent metal ions such as Co(II), Fe(II), and Mn(II) also produces active enzyme [74, 75].

The wide variety of divalent metal ions utilized by bacterial quercetinases, the M(II)/M(III) couples of which span more than 1.5 V, suggest that a reaction mechanism involving oxidation of the divalent metal center to form a M(III)-O₂⁻ species is not likely. Additionally, an internal redox processes leading to the formation of a M(I)-flavonoxo radical species akin to that proposed for Cu(II)-containing quercetinases also does not seem feasible for Mn(II), Fe(II), Ni(II), or Co(II) containing quercetinases due to the lack of accessibility of their M(I) oxidation state. An alternative mechanistic pathway that has been proposed for such systems involves outer sphere electron transfer from the substrate to dioxygen to form a M(II)-O₂⁻/flavonoxo radical species (Scheme 1-11(bottom)) [5]. Recombination of the radicals would subsequently allow for a reaction pathway involving a cyclic peroxide species and aliphatic carbon-carbon bond cleavage. The outer

sphere electron transfer hypothesis is consistent with the observed chemical reactivity of free flavonolate anions (*vide infra*), which undergo reaction with O₂ to generate 2,4-dioxygenolytic cleavage products [76-79]. Thus, the role of the divalent metal ion in quercetinases may be to stabilize the deprotonated flavonolate, transition states and intermediates, versus mediating electron transfer to overcome the spin-barrier with O₂.

2.4.1 Cu(II)-containing structural models. Several synthetic Cu(II) flavonolate complexes have been prepared as structural models for the ES adduct in fungal quercetinases. These complexes are supported by a variety of chelating nitrogen donor ligands and contain flavonol ligands that vary in terms of the presence of electron donating/withdrawing substituents. The structural and spectroscopic properties of the majority of these compounds are described in recent reviews [80, 81].

2.4.2 Functional models.

2.4.2.1 Flavonolate anion reactivity with O₂. Kinetic and mechanistic studies of the oxygenation of 3-hydroxyflavone and analogs under basic conditions, or in the form of alkali metal salts, have been previously reported [80, 82]. The products generated in reactions involving the anion of 3-hydroxyflavone (a carboxylate (*O*-benzoysalicylate or hydrolysis products thereof) and CO) mimic the enzymatic reaction and result from 2,4-dioxygenolytic type oxidative aliphatic carbon-carbon bond cleavage (Scheme 1-1(d)). Notably, increasing the electron density in the flavonolate anion through substitution at the 4'-position of the C(3)-aromatic substituent, increases the rate of reaction, which is consistent with a more electron rich flavonolate being a better reducing agent toward O₂. Evidence for the reaction of the flavonolate with O₂ involving single electron transfer was found in terms of a long-lived flavonoxy radical species that was identified by EPR

[78]. Overall, these studies provide evidence that an outer sphere single electron transfer pathway is feasible between the flavonolate anion and O₂ as an initial step toward 2,4-dioxygenolytic aliphatic carbon-carbon bond cleavage.

2.4.2.2 Reactivity of Cu(II)-flavonolate complexes with O₂. Upon heating, Cu(II)-coordinated flavonolate complexes also undergo reaction with O₂ to produce CO and a Cu(II)-coordinated carboxylate having two oxygen atoms derived from O₂. However, other reaction pathways that do not lead to CO release have also been identified [80]. For the systems that exhibit biomimetic reactivity, the reaction is slower than that of potassium flavonolate. This is consistent with the copper center withdrawing electron density from the bidentate-coordinated flavonolate. In terms of the mechanism of oxygen activation, the presence of the redox active metal ion enables a valence tautomerism between Cu(II)-flavonolate and Cu(I)-flavonoxy radical species, the latter of which may react with triplet O₂ at the metal center or at the organic radical (Scheme 1-11(b)). Kinetic studies have been performed for a variety of Cu(II) flavonolate complexes, with all of the reactions requiring temperatures of > 80 °C to proceed with a second order rate constant of at least $1.0 \times 10^{-3} \text{ M}^{-1}\text{s}^{-1}$ [80, 81]. Notably, oxygenation of [Cu(3-Hfl)(idpa)]ClO₄ in the presence of excess acetate or triphenylacetate dramatically increases the rate of reaction [83]. This rate enhancement has been suggested to be the result of competition between coordination of the flavonolate ketone moiety and acetate anion. A coordinated flavonolate ligand having enhanced monodentate coordination character is expected to be more electron-rich and therefore more reactive for electron transfer with O₂.

2.4.2.3 O₂ reactivity of metal flavonolate complexes of other 3d metals. Divalent metal flavonolate complexes of structural relevance to bacterial quercetinases are considerably fewer in number [84], and only a handful of synthetic metal flavonolate complexes for metals other than copper have been investigated in terms of their thermal O₂ reactivity. Examples of reactive model systems have thus far been reported containing Co(II) [77], Co(III) [85, 86], Mn(II) [87, 88], Fe(III) [87-90], and Zn(II) [91]. For the Co(III) complex [Co(III)(salen)(4'-MeOflaH)], reactivity between the flavonolate and O₂ is proposed to occur following dissociation of the flavonolate from the Co(III) center [85, 86]. O₂ reactivity studies of an Fe(III) flavonolate complex, [Fe(III)(salen)(3-Hfl)], demonstrated that the rate of reaction could be enhanced through the addition of bulky carboxylates (e.g. triphenylacetate) [89]. As noted previously for Cu(II)-containing systems, the rate enhancement is likely due to metal coordination of the carboxylate, which induces the formation of a more reactive monodentate flavonolate-ligated Fe(III) complex. Evidence for direct single electron transfer from the flavonolate to produce superoxide anion has been detected in reactions involving [Fe(III)(salen)(3-Hfl)] and [Zn(3-Hfl)(idpa)]ClO₄ [82][89].

2.4.3 Perspective. Studies of the Cu(II)-containing fungal quercetinases and relevant model compounds over the past decade have suggested that a Cu(II)-flavonolate species, or a Cu(I)-flavonoxy radical species, react with O₂ to initiate aliphatic carbon-carbon bond cleavage. The discovery of bacterial quercetinases that can utilize a variety of divalent metal ions of differing redox potentials to promote the same reaction suggests that in these systems it is the single electron transfer reactivity of the coordinated flavonolate moiety itself with O₂, not metal-based oxygen activation, that is likely a key

step in the reaction pathway. Overall, the studies described herein suggest that the metal center in quercetinases is responsible for stabilizing the deprotonated form of the substrate and tuning it in terms of electron density (via coordination effects) for subsequent reactivity with O₂.

2.5 Acireductone Dioxygenases (ARDs)

The methionine salvage pathway, which has been identified in mammals, yeast, bacteria, protozoa, and plants, is involved in several major cellular functions related to cell proliferation and differentiation. The most well-studied methionine salvage pathway is from the bacterium *K. pneumonia* [92]. Within this pathway (Figure 1-4), an acireductone intermediate has been identified at the only branch point. This intermediate is a substrate for two different acireductone dioxygenase enzymes whose only constitutive difference is the nature of the metal ion coordinated within the active site. A divalent iron-containing enzyme, Fe(II)-ARD', catalyzes oxidative C(1)-C(2) bond cleavage within the acireductone substrate and the production of 4-methylthio-2-oxobutanoic acid (MTOB) and formate in an "on-pathway" reaction (Figure 1-4(inset)). MTOB is a precursor for the regeneration of methionine via a transaminase-catalyzed reaction. A nickel-containing dioxygenase, Ni(II)-ARD, catalyzes a reaction that is a shunt out of the methionine salvage pathway wherein the cleavage of the C(1)-C(2) and C(2)-C(3) bonds of the substrate results in the formation of 2-methylthiopropionic acid, formate, and CO (Figure 1-4(inset)).

The Fe(II)-ARD' and Ni(II)-ARD-catalyzed reactions are of interest for several reasons. First, while several metalloenzymes exhibit varying degrees of activity as a function of the metal ion present, the ARD/ARD' system is the only demonstrated

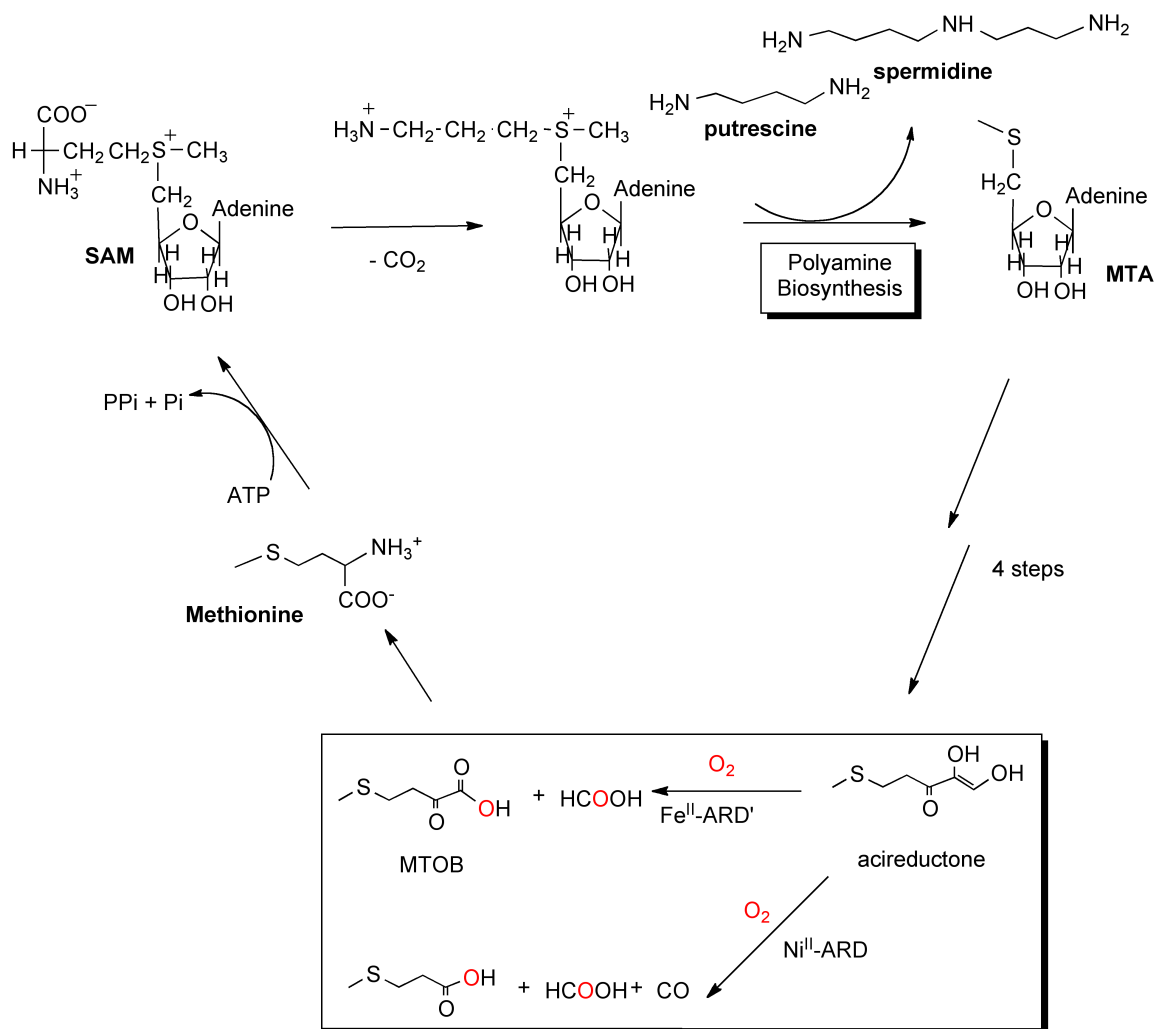


Figure 1-4. Methionine salvage pathway in *K. pneumoniae*.

example of different chemical reactions resulting from a change of the metal ion bound within the same protein component [92]. Second, the reaction catalyzed by Ni(II)-ARD results in the generation of CO, a biological signaling molecule. Third, the role of the divalent metal ion in these dioxygenases is proposed to be that of a Lewis acid which stabilizes a dianionic form of the acireductone substrate for reaction with O₂. This notion is supported by the fact that Mg(II)-containing ARD' catalyzes MTOB formation. For Fe(II)-ARD', the role of the divalent iron center thus contrasts from that found in other

Fe(II)-containing dioxygenases wherein the metal center is directly involved in oxygen activation via redox reactivity. Fourth, the observed regioselectivity of aliphatic carbon-carbon cleavage promoted by Fe(II)-ARD' and Ni(II)-ARD is proposed to be the result of differing coordination modes for the acireductone dianion (an enediolate) in the ES complexes. This proposed coordination chemistry-driven regioselectivity for carbon-carbon cleavage is distinct from that proposed for the iron-containing catechol dioxygenases wherein the oxidation state of metal center (Fe(II) vs. Fe(III)) impacts substrate activation and the site of reactivity with O₂.

The “chelate-hypothesis” for ARDs was proposed on the basis of comparative spectroscopic investigations of Ni(II)-ARD and Fe(II)-ARD' [93-98]. The combined results of NMR and XAS studies, as well as evaluation of X-ray crystallographic studies of a putative Ni(II)-ARD (*Mm*ARD, PDB 1VR3), provide evidence that the divalent metal center in the resting state form of Ni(II)-ARD and Fe(II)-ARD' is coordinated by three histidine residues (His96, His98, His 140), a glutamate (Glu102), and two water molecules (Figure 1-5(a)). For both metalloenzymes, the formation of the ES complex is proposed to result in displacement of at least one water ligand, and perhaps a histidine residue, to enable bidentate substrate coordination. Notably, Ni(II)-ARD and Fe(II)-ARD' appear to differ significantly in the structural features of the C-terminus, which results in differing secondary environments near the substrate coordination site. Specifically, NMR studies suggest that while in Ni(II)-ARD Trp162 is positioned within ~7 Å of the metal center, in Fe(II)-ARD' disorder within in the last 22 residues of the C-terminus (Asp157-Ala179) results in a more open coordination environment. Substrate docking studies suggest that bidentate coordination within the more sterically congested

Ni(II)-ARD binding site occurs via the O(1) and O(3) atoms whereas within the more open active site of Fe(II)-ARD the substrate coordinates via the adjacent O(1) and O(2) atoms (Figure 1-5(b and c)). The “chelate hypothesis” is that these differing coordination modes activate specific carbon centers within the coordinated acireductone for reactivity with O₂, leading to differences in the regiospecificity of aliphatic carbon-carbon bond cleavage.

On the basis of spectroscopic and kinetic studies of Ni(II)-ARD and Fe(II)-ARD', both enzymes exhibit an ordered sequential mechanism (Scheme 1-12), with the acireductone substrate initially coordinating to the metal center as a dianion in the

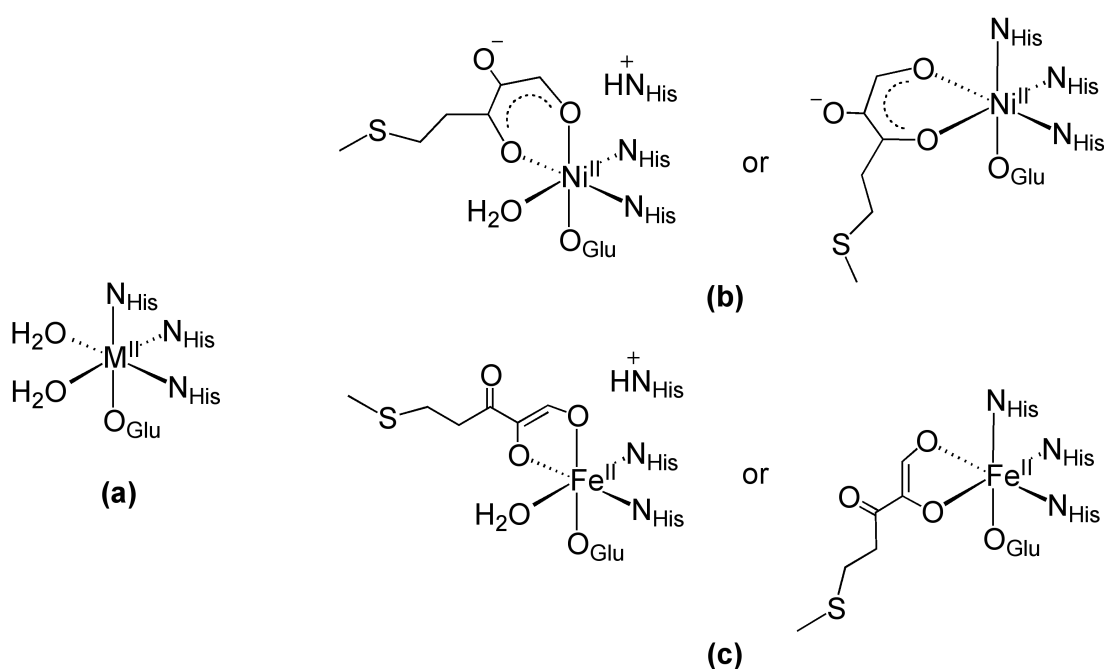
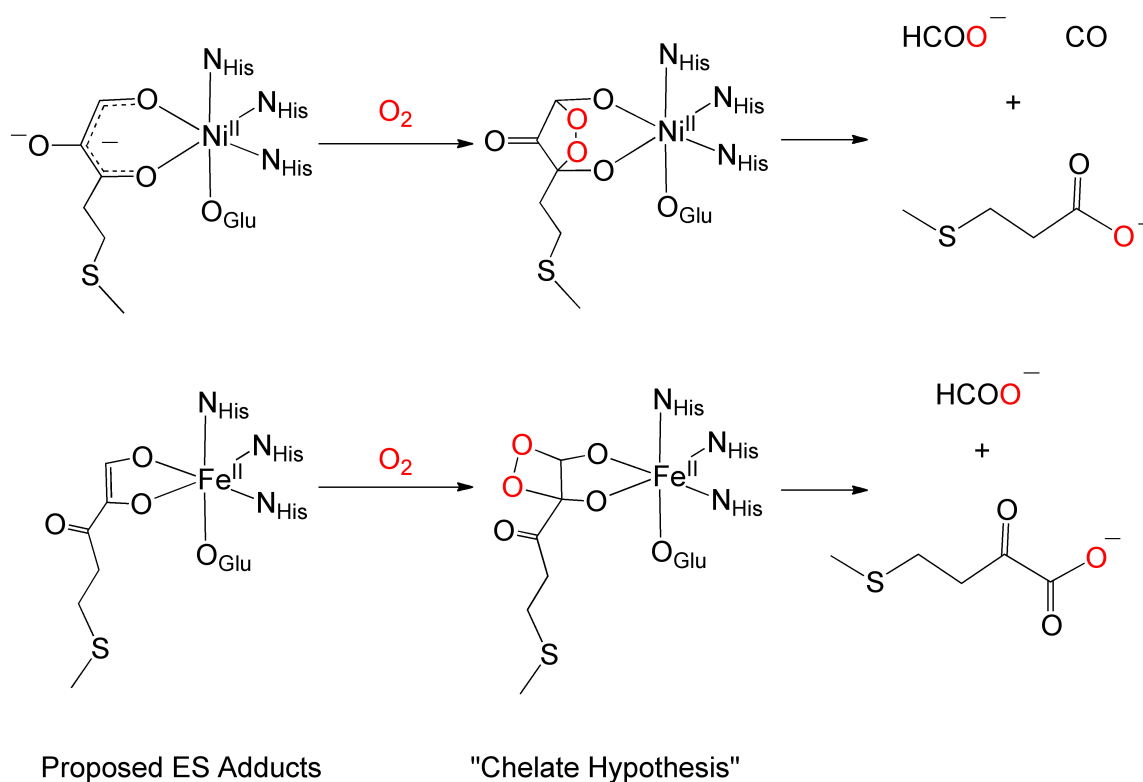


Figure 1-5. (a) Metal coordination environment found in the resting state for Ni(II)-ARD and Fe(II)-ARD'. (b) and (c) Possible coordination motifs for the ES complexes of Ni(II)-ARD and Fe(II)-ARD'.

anaerobic ES complex. The electron-rich coordinated substrate for each is then proposed to react directly with O_2 , likely via one-electron steps, to generate a C(1)-coordinated peroxy species which subsequently forms a six-membered cyclic peroxide species for Ni(II)-ARD, or a five-membered analog in Fe(II)-ARD'. Subsequent O-O and C-C bond cleavage leads to the observed products. These proposed reaction pathways fit with results of ^{18}O labeling experiments wherein one oxygen atom from $^{18}O_2$ is found in each carboxylate product (% ^{18}O label incorporation ~75% for alkyl carboxylates) [99]. We note that as oxygen atoms of aliphatic carboxylates/carboxylic acids (e.g. butyrate/butyric acid) do not exchange to any significant extent under standard conditions (25 °C, water,



Scheme 1-12. Proposed structures of ES complexes for Ni(II)-ARD and Fe(II)-ARD' and reactions with O_2 .

14 days) [57], the level of ^{18}O incorporation in the aliphatic product results from the ARD/ARD' reactions. A ^{14}C label incorporated at the C(2) position of the acireductone substrate was found in the CO product generated via the Ni(II)-ARD catalyzed reaction. Use of cyclopropyl analog substrate provided evidence for a radical pathway in the Ni(II)-ARD and Fe(II)-ARD'-catalyzed reactions [93]. Use of this analog substrate results in the irreversible inactivation of Ni(II)-ARD after ~ 100 turnovers and Fe(II)-ARD' after ~ 20 turnovers in the presence of O_2 .

2.5.1 Structural features, coordination chemistry, and O_2 reactivity of open-chain acireductones. As shown in Figure 1-6(a), protonated, neutral forms of acireductone have been suggested to form structures involving a six-membered ring. However, the X-ray structures of the rubidium salt and protonated neutral form of triose reductone ($\text{R} = \text{R}' = \text{H}$; Figure 1-6(b)) revealed that all three oxygen atoms are positioned on one side of the carbon chain [100, 101]. Prior to our studies outlined herein, only one transition metal compound having a coordinated acyclic acireductone ligand had been characterized by X-ray crystallography. This compound, $[(\text{Ru}(\text{bipy})_2)_2(\mu\text{-C}_4\text{H}_4\text{O}_3)](\text{PF}_6)_2$ (Figure 1-6(c)) was generated as a byproduct in reactions of $[\text{Ru}(\text{bipy})_2\text{Cl}_2 \cdot 2\text{H}_2\text{O}]$ in ethylene glycol in the presence of NH_4PF_6 . Similar to the triose reductone structures, the acireductone ligand in $[(\text{Ru}(\text{bipy})_2)_2(\mu\text{-C}_4\text{H}_4\text{O}_3)](\text{PF}_6)_2$ is coordinated with all three oxygen atoms on the same side of the carbon chain [102]. In this case, it is a dianion that bridges two Ru(II) centers. Similar backbone carbon-carbon bond distances, and C(1)-O and C(3)-O units (1.29 and 1.30 Å, respectively) that are shorter than the C(2)-O bond (1.39 Å), indicate a delocalized enolate anion along the three carbon backbone.

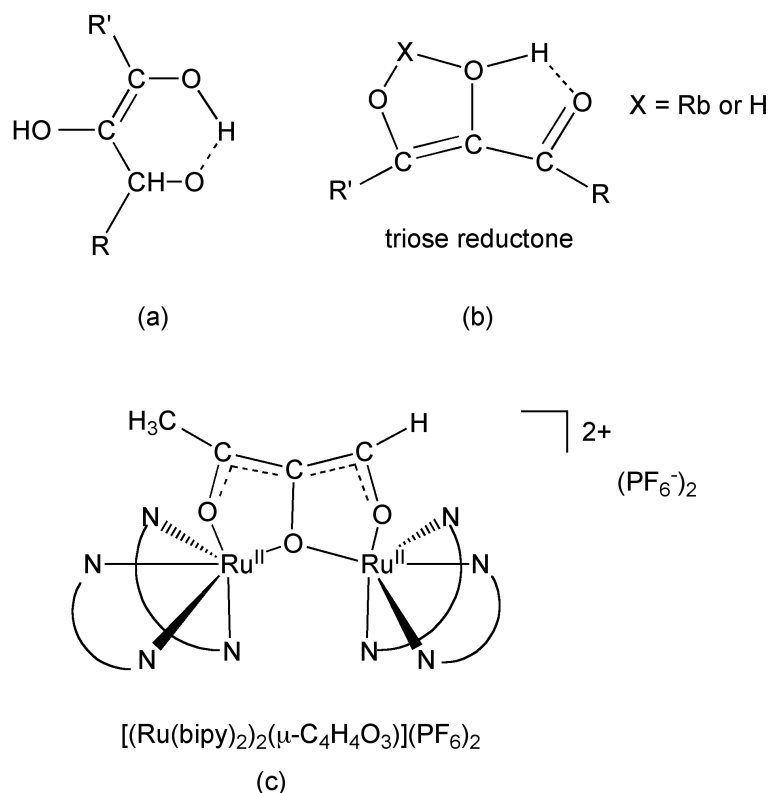


Figure 1-6. (a) Proposed structure of acireductones. (b) X-ray crystallographically determined structures of the protonated form and rubidium salt of triose reductone. (c) X-ray crystallographically characterized structure of $[(Ru(bipy)_2)_2(\mu-C_4H_4O_3)](PF_6)_2$.

Open chain acireductone anions exhibit a $\pi \rightarrow \pi^*$ transition with the wavelength of this absorption feature depending on the protonation level. For example, the monoanions **II**⁻ and **III**⁻ (Figure 1-7), which are analog substrates for ARD enzymes, exhibit intense absorption bands at 305 ($20,000 \text{ M}^{-1}\text{cm}^{-1}$) and 320 ($14,000 \text{ M}^{-1}\text{cm}^{-1}$) nm, respectively [93]. This feature red-shifts upon formation of the dianion, with **II**²⁻ and **III**²⁻ exhibiting features at 345 ($14,000 \text{ M}^{-1}\text{cm}^{-1}$) and 360 ($11,000 \text{ M}^{-1}\text{cm}^{-1}$) nm, respectively. These protonation level-dependent spectral features enabled the assignment of the coordinated acireductone substrate as a dianion in the anaerobic ES complexes of Ni(II)-ARD and Fe(II)-ARD' [93].

Acireductone anions are reactive with O_2 in the absence of enzyme catalysis [93]. For example, exposure of aqueous solutions of **II**⁻ and **III**⁻ to air results in the formation of Fe(II)-ARD'-type products (α -ketoacid and formate). The second-order rate constant for the non-enzymatic reaction of O_2 with **II**⁻ is 66-times slower than the same reaction with the dianion **II**²⁻ (0.12 vs. $8 \text{ M}^{-1}\text{s}^{-1}$) [93].

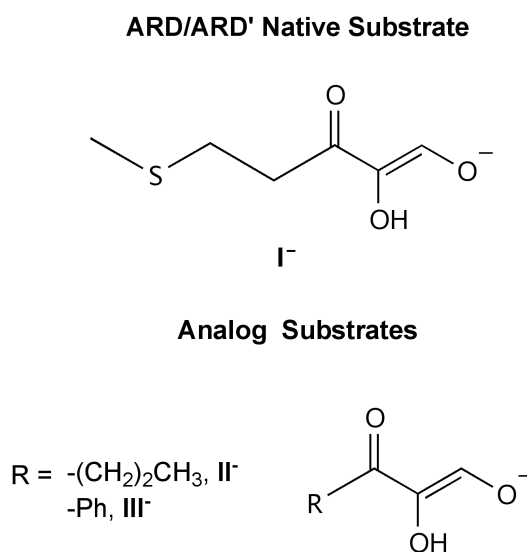
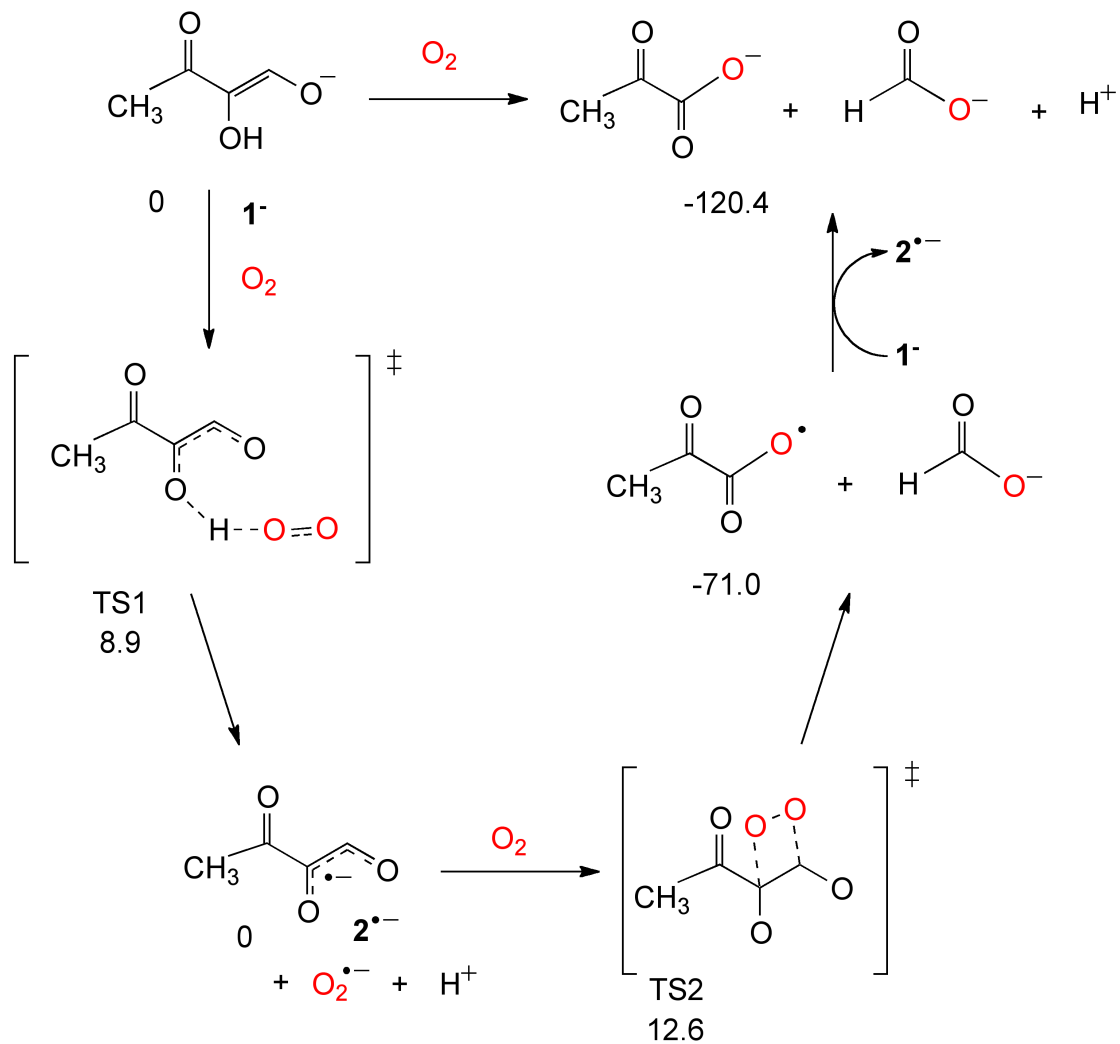


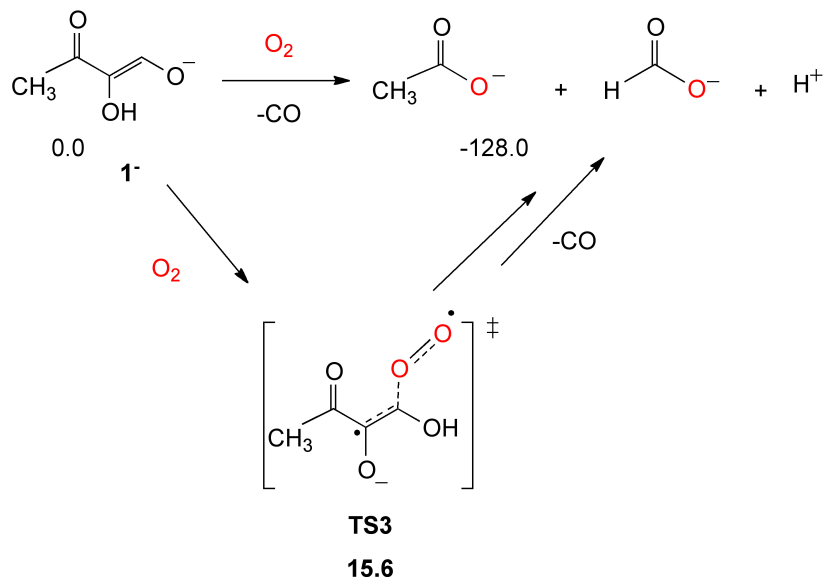
Figure 1-7. Native and alternative substrate for Ni(II)-ARD and Fe(II)-ARD'.

Borowski has computationally examined the uncatalyzed reaction of a acireductone monoanion with O_2 [103]. These DFT calculations provide a rationale for the observed formation of α -ketoacid and formate (Scheme 1-13). The initial step between the acireductone monoanion and 3O_2 involves a single electron transfer reaction, resulting in the formation of superoxide and a radical anion via a thermodynamically neutral process. This reaction is akin to that proposed for the Ni(II)-ARD and Fe(II)-

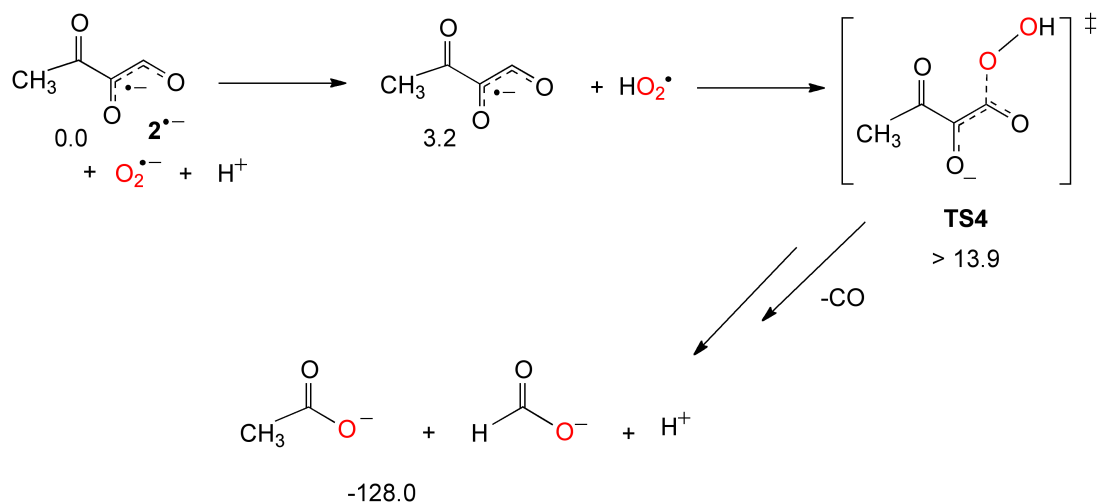


Scheme 1-13. Reaction pathway for uncatalyzed reaction of acireductone monoanion with O_2 . Energies given are in kcal/mol.

Direct reaction of acireductone anion with triplet O₂:



Recombination of radicals:



Scheme 1-14. Two alternative mechanisms for reactivity of an acireductone monoanion with O₂. These pathways, both of which involve formation of singlet peroxide species, produce two carboxylic acids and CO (Ni(II)-ARD-type products). Energies given are in kcal/mol.

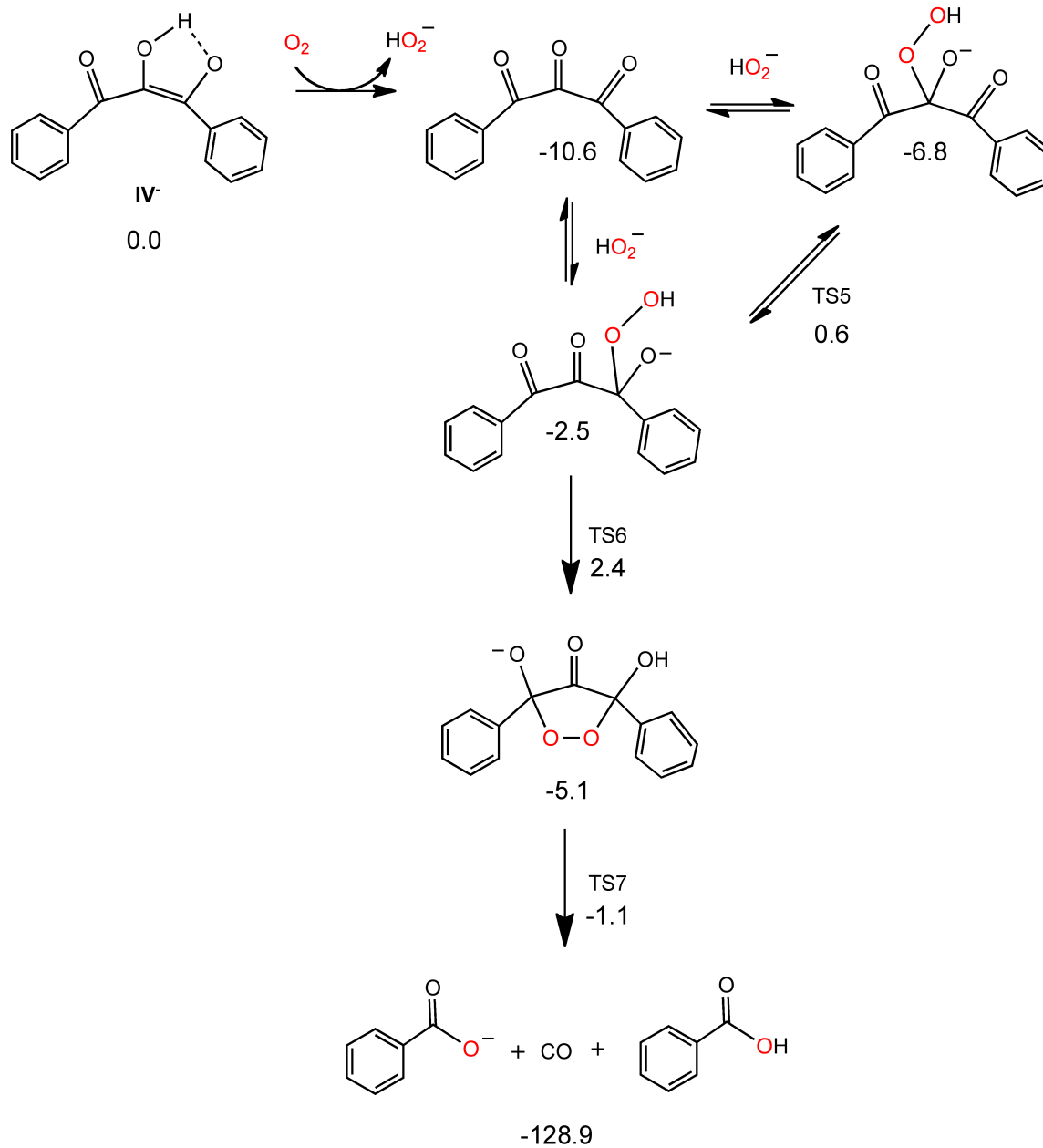
ARD' ES complexes with O₂. In the absence of the enzyme, the lowest energy subsequent reaction is that of the radical anion with ³O₂ to form a α-keto-acid radical and formate. A final radical propagation step involving the acireductone monoanion gives the α-ketoacid and formate products. The rate-determining step in this sequence involves the formation the four-membered cyclic peroxide transition state species that subsequently undergoes O-O and C(1)-C(2) bond cleavage. A five-membered ring TS species produced from the radical anion 2•- and ³O₂ leads to Ni(II)-ARD products but involves a significantly transition state barrier (19.8 kcal/mol). Notably, mechanisms that involve a singlet peroxide species (Scheme 1-14) favor Ni(II)-ARD type CO release reactivity. These pathways have transition states at higher energy than the pathway leading to α-ketoacid formation.

2.5.2 Model systems containing an acireductone monoanion. For initial synthetic model studies, we used the bulky acireductone monoanion [PhC(O)C(OH)C(O)Ph]⁻ (**IV**⁻, Scheme 1-15). While **IV**⁻ is not a substrate for Ni(II)-ARD or Fe(II)-ARD', it is convenient to use due to ease of synthesis relative to analogs of the native acireductone substrate [104]. Anion **IV**⁻ is akin to Fe(II)-ARD'/Ni(II)-ARD substrate **III**⁻ (Figure 1-7), but has an additional phenyl substituent at the C(1) position. The extended conjugation in **IV**⁻ results in an absorption maximum at 385 nm. The most stable form of **IV**⁻ has the terminal phenyl groups arranged *cis* with respect to each other and with the central oxygen protonated. The presence of the C(1)-phenyl group introduces important differences versus the C(1)-H enzyme substrates **I-III**. For example, reaction of the **IV**⁻ with O₂ results in C(1)-C(2) and C(2)-C(3) cleavage (Ni(II)-ARD-type

products), specifically, benzoic acid/benzoate and CO. The level of ^{18}O incorporation in the benzoic acid/benzoate is 65-72%.

To gain insight into the factors governing the O_2 reaction of IV^- versus the reactions of monoanion forms of **I-III**, computational studies were performed [105]. A radical mechanism akin to that described above for the C(1)-H type acireductones **I-III** was evaluated, along with a pathway leading to the formation peroxo species (termed a hydroperoxide mechanism). For IV^- , the latter was found to be more energetically feasible [105]. This mechanism (Scheme 1-15) involves an initial two-electron oxidation of IV^- with O_2 to give 1,3-diphenylpropanetrione and hydroperoxide anion. Subsequent reaction between the trione and HO_2^- gives a hydroperoxide group coordinated to the central carbon that can easily migrate to the terminal position. Attack of the terminally-bound hydroperoxide at the C(3) carbonyl yields a five-membered ring that can decompose to benzoate anion, benzoic acid and CO. The radical mechanism is less feasible due to high barriers associated with the formation of cyclic peroxide species [105].

In addition to the features of the primary coordination sphere of Ni(II)-ARD described above, the active site secondary environment of this metalloenzyme contains two phenylalanine residues that are proposed to help orient the coordinated substrate [96]. On the basis of these features, we used the aryl-appended N_4 -donor ligand 6- Ph_2TPA (*N,N*-bis((6-phenyl-2-pyridyl)methyl)-*N*-(2-pyridylmethyl)amine) [106] to prepare the first analytically pure complex of structural relevance to the proposed ES adduct in Ni(II)-ARD ($[(6\text{-Ph}_2\text{TPA})\text{Ni}(\text{PhC}(\text{O})\text{C}(\text{OH})\text{C}(\text{O})\text{Ph})]\text{ClO}_4$ (**1**), Figure 1-8)



Scheme 1-15. Computationally determined reaction pathway for aliphatic carbon-carbon bond cleavage upon reaction of **IV⁻** with O_2 . Energies given are in kcal/mol.

[107]. A structurally similar complex can be constructed under identical conditions using a supporting chelate ligand wherein the two aryl appendages have been replaced by two hydrogen bond donors (**3**, Figure 1-8(b)) [108]. However, we encountered difficulties when trying to prepare similar complexes wherein either the metal has been changed (e.g. Co(II)), or the ligand environment is less sterically hindered (e.g. 6-PhTPA) [109, 110]. The complicating issue in these syntheses is a water-dependent, Lewis acid promoted rearrangement of **IV** to give an ester. Synthetic procedures performed under water-free or trace water conditions enabled the preparation of [(6-Ph₂TPA)Co(PhC(O)C(OH)C(O)Ph)]OTf (**2**) and isolation of analytically pure [(6-PhTPA)Ni(PhC(O)C(OH)C(O)Ph)]ClO₄ (**4**, Figure 1-8), respectively [110].

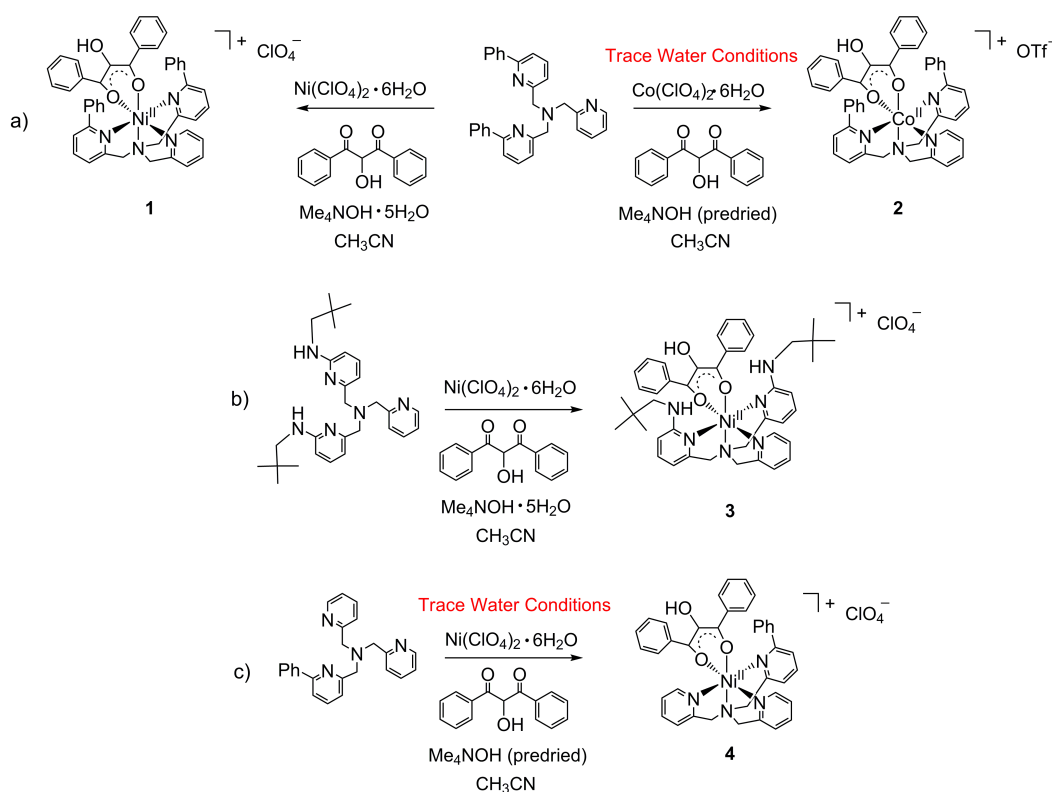


Figure 1-8. Synthetic routes for the preparation of **1-4**.

Complexes **1** and **4** were characterized by single crystal X-ray crystallography [107, 110]. Overall, the Ni(II) centers in **1** and **4** are structurally similar to the ES adduct of Ni(II)-ARD in terms of the overall coordination number [98]. These complexes exhibit similar structural features with C-C bond distances within the six-membered ring chelate enolate being consistent with a delocalized formulation for the bound anion. The average Ni-O/N distances are slightly longer in the synthetic complexes (2.16 Å) than those found by XAS for the enzyme ES adduct (2.04 Å) [94]. The proposed six-membered chelate ring for the coordinated bulky acireductone in **2** and **3** is proposed based on comparison of ¹H NMR spectroscopic comparisons to X-ray crystallographically characterized air stable acetylacetonate- or dibenzoylmethane-coordinated analogs [108, 110]. It should be noted that while each of complexes **1-4** are paramagnetic, sharp signals associated with the supporting chelate ligand are diagnostic for particular structural features [107-110]. Additionally, each complex exhibits a $\nu_{\text{O-H}}$ vibration in the solid state IR spectrum, consistent with the presence of the bulky acireductone monoanion C(2)-OH substituent. When dissolved in acetonitrile, each complex forms an orange solution due to an absorption band in the region of 385-399 nm (Table 1-3).

Table 1-3. UV-vis spectroscopic properties of acireductone monoanion complexes.^a

Complex	Absorption Maximum	Reference
1	399 (6800)	[111]
2	397 (n.d.)	[110]
3	393 (10000)	[108]
4	399 (10300)	[110]

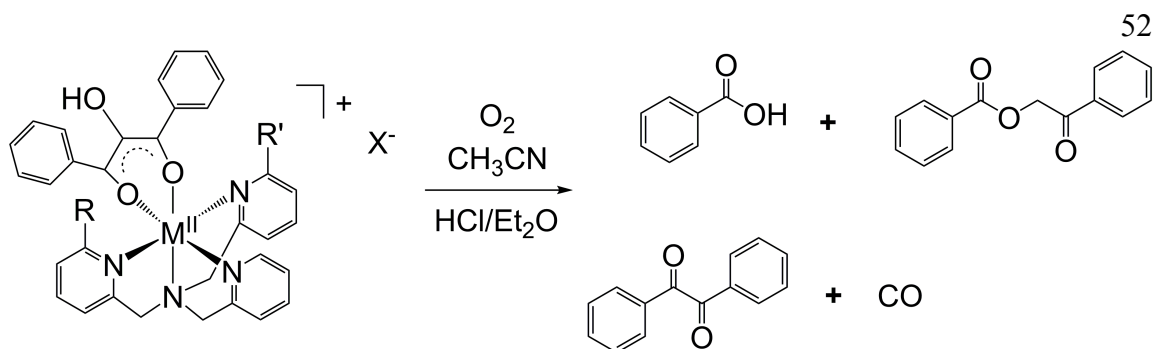
^aSpectra collected in CH₃CN at ambient temperature. n.d. = not determined.

The absorption feature in the visible region of **1-4**, which is comprised primarily of a $\pi \rightarrow \pi^*$ transition of the coordinated enolate, is lost upon the introduction of O₂. Kinetic studies of the reactions of **1** with O₂ show that this reaction is second-order overall with a rate of 1.7 M⁻¹s⁻¹ [105]. Analysis of the acireductone-derived products generated upon reaction of analytically pure **1-4** with O₂ revealed the formation of benzoic acid/benzoate, CO, the diketone benzil, and in some cases the acireductone isomerization product (Scheme 1-16). These products match those produced upon reaction of Me₄N[PhC(O)C(OH)C(O)Ph] with O₂, with the exception of benzil. The formation of benzil provides experimental evidence for the triketone pathway leading to aliphatic carbon-carbon bond cleavage as proposed computationally for the reaction of the bulky acireductone with O₂ [105]. Specifically, benzil can be generated via a Lewis acid-promoted benzoyl migration involving 1,3-diphenyltriketone. Alternatively, diphenylpropantrione and hydroperoxide may react to generate Ni(II)-ARD-type products (carboxylic acid/carboxylate and CO) (Scheme 1-17). Comparisons of the product mixtures obtained for the O₂ reactions of **1** and **3** revealed that the amount of benzil produced relative to benzoic acid/benzoate depends on the nature of the supporting chelate ligand [108]. The benzoic acid/benzoate products generated in the reactions of **1**

Table 1-4. Level of ¹⁸O incorporation in benzoic acid/benzoate products

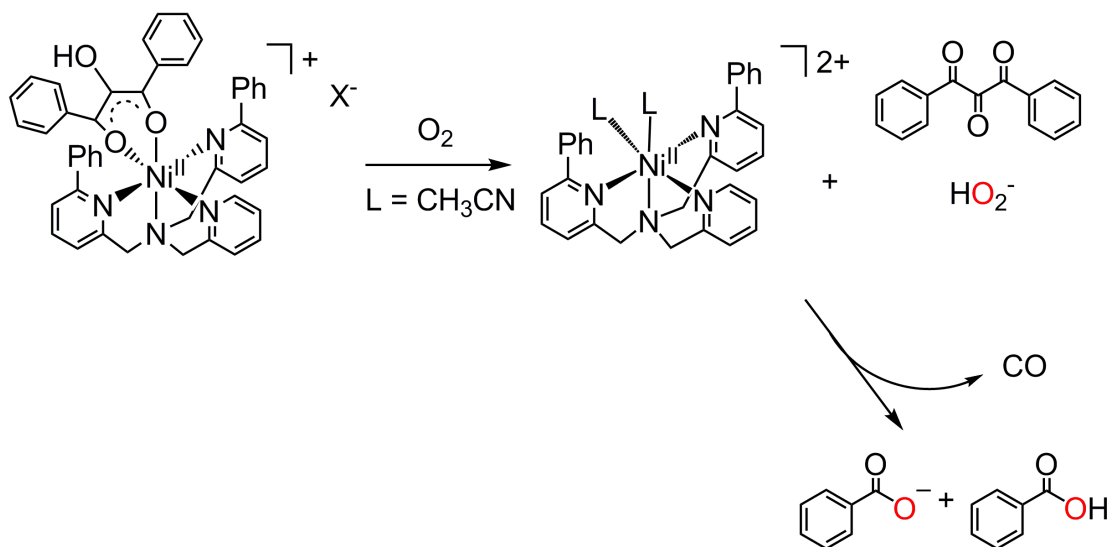
Complex	% ¹⁸ O incorporation	Reference
Me ₄ N[PhC(O)C(OH)C(O)Ph]	65	[105]
1	64 ^a , 59 ^b	[111]

^a[(6-Ph₂TPA)Ni(O₂CPh)]ClO₄; ^bbenzoic acid



- 1: M = Ni^{II}; R = R' = Ph (6-Ph₂TPA)
- 2: M = Co^{II}; R = R' = Ph (6-Ph₂TPA)
- 3: M = Ni^{II}; R = R' = NHCH₂C(CH₃)₃ (bnppapa)
- 4: M = Ni^{II}; R = Ph; R' = H (6-PhTPA)

Scheme 1-16. O₂ reactivity of divalent metal complexes of IV⁻.



Scheme 1-17. Reaction pathway of **1** with O₂ via the formation of a 1,3-diphenyltriketone as an intermediate.

contain an ^{18}O label when the reaction is performed using $^{18}\text{O}_2$. The level of ^{18}O isotope incorporation derived from $^{18}\text{O}_2$ for the reactions of $\text{Me}_4\text{N}[\text{PhC}(\text{O})\text{C}(\text{OH})\text{C}(\text{O})\text{Ph}]$, and **1** is given in Table 1-4. Notably, while the level of incorporation is similar.

2.5.3 Model systems containing an acireductone dianion. Our first attempt to generate an acireductone dianion complex of relevance to the proposed ES complex in Ni(II)-ARD involved treatment of **1** (Figure 1-8) with one equivalent of $\text{Me}_4\text{NOH}\cdot 5\text{H}_2\text{O}$ in CH_3CN under anaerobic conditions [107]. This resulted in a red-shift of the electronic absorption spectral feature to $\sim 420\text{ nm}$ ($\epsilon \sim 2500\text{ M}^{-1}\text{cm}^{-1}$), suggesting the formation of a new enediolate complex (**5**). This structure of this complex was later verified as a hexanickel enediolate cluster, $\{\text{Ni}(\text{PhC}(\text{O})\text{C}(\text{O})\text{C}(\text{O})\text{Ph})(\text{CH}_3\text{OH})\cdot 1.33\text{CH}_3\text{OH}\}_6$ (**5**, Figure 1-9(top)), via independent synthesis [112]. Within this cluster, the enediolate form of the bulky acireductone is coordinated in a bridging position between two Ni(II) centers, forming two five-membered chelate rings akin to the motif found in $[(\text{Ru}(\text{bipy})_2)_2(\mu\text{-C}_4\text{H}_4\text{O}_3)](\text{PF}_6)_2$ [102].

Addition of O_2 to an in-situ generated CH_3CN solution of **5** results in the rapid bleaching of the orange-red color and the formation of a Ni(II) dibenzoate complex, $[(6\text{-Ph}_2\text{TPA})\text{Ni}(\text{O}_2\text{CPh})_2(\text{H}_2\text{O})]$ (**6**) and carbon monoxide (Scheme 1-18) [112]. Use of ^{18}O in the reaction mixture resulted in $\sim 86\%$ incorporation of one labeled oxygen atom per benzoate ligand. It should be noted that benzil is also produced in this reaction providing evidence that the aliphatic carbon-carbon bond cleavage reaction occurs via the triketone pathway.

In an attempt to isolate a mononuclear Ni(II) enediolate complex of relevance to the ES adduct proposed for Ni(II)-ARD, we utilized a new ligand (6-NA-6- Ph_2TPA)

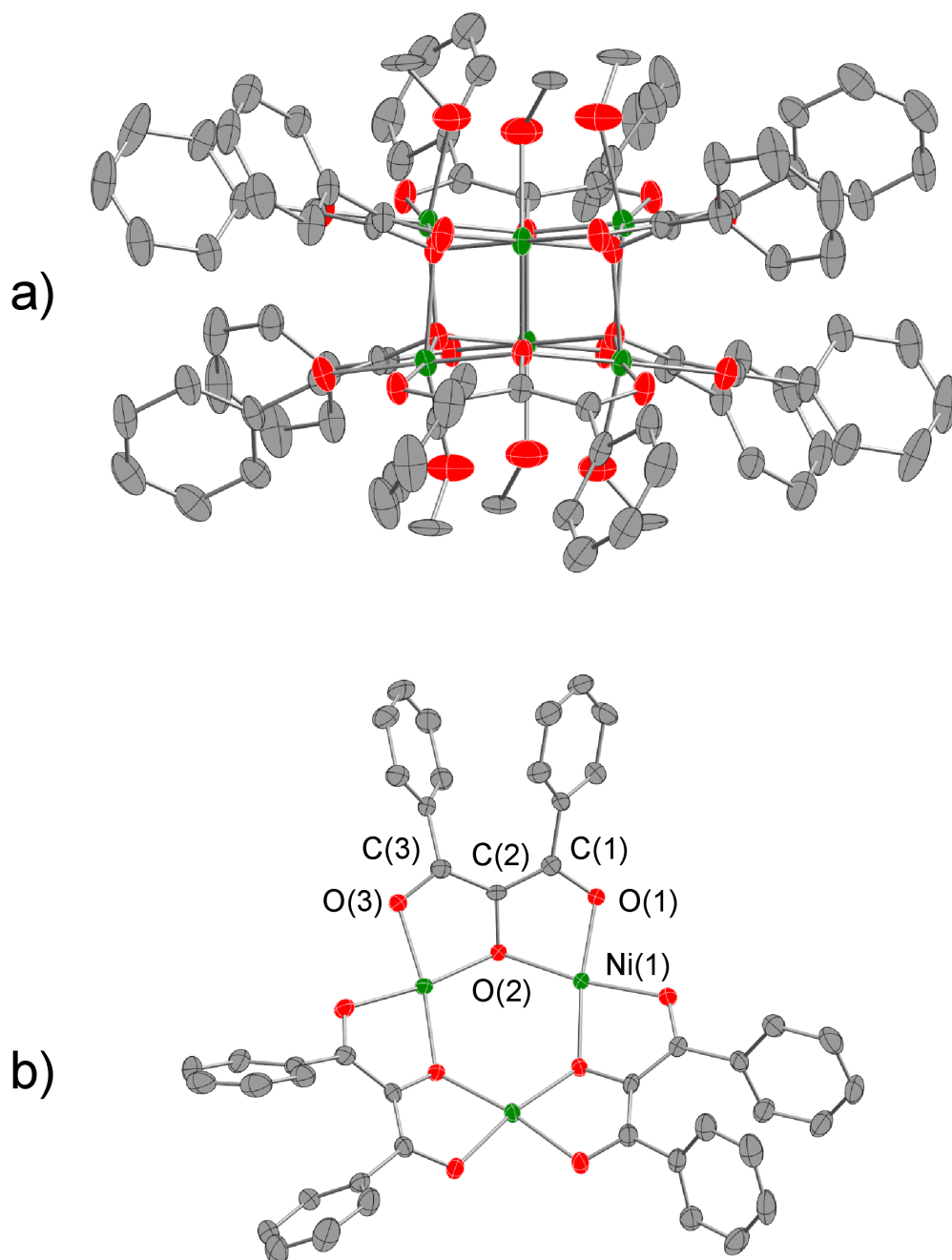
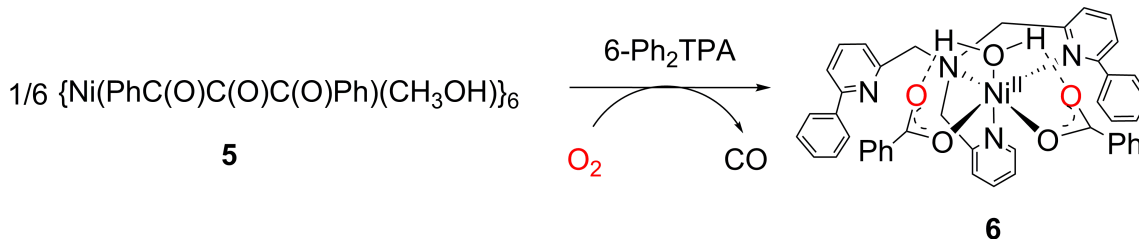
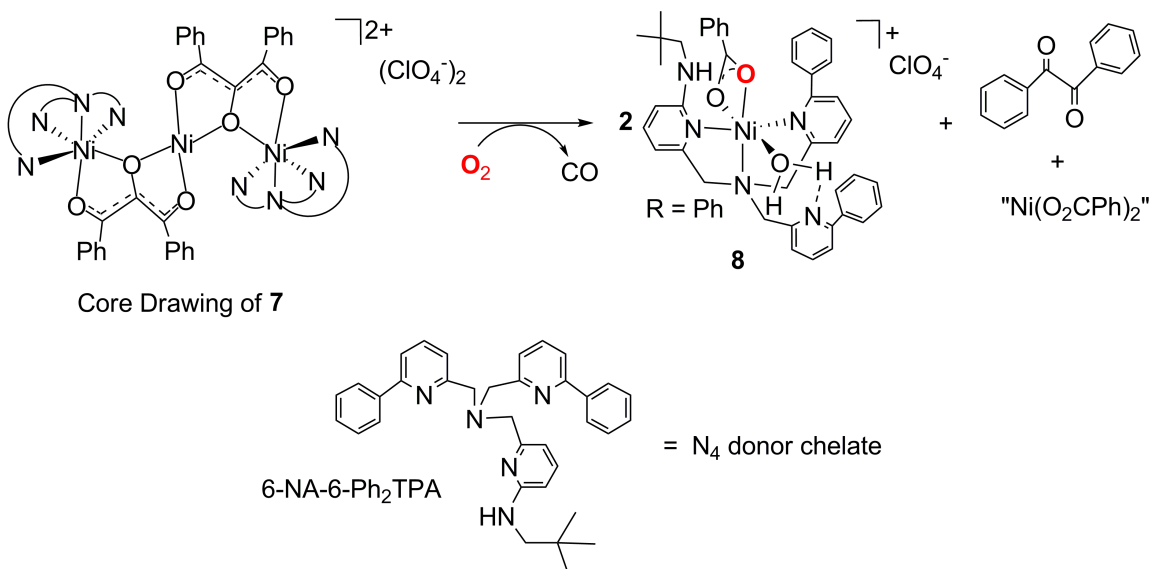


Figure 1-9. Structural features of the hexanickel cluster **5**. (a) A view of the entire $\{\text{Ni}(\text{PhC}(\text{O})\text{C}(\text{O})\text{C}(\text{O})\text{Ph})(\text{CH}_3\text{OH})\}_6$ cluster. (b) View of a single layer.



Scheme 1-18. O₂ reactivity of the hexanickel enediolate cluster compound 5.

wherein the features of the 6-Ph₂TPA ligand have been augmented with a hydrogen bond donor neopentyl group [113]. Using this ligand, repeated attempts to synthesize either a mononuclear diketonate monoanion complex, or an enediolate complex, resulted only the isolation of a trinuclear Ni(II) bis-enediolate complex (7, Scheme 1-19). Similar to the hexanickel cluster, each enediolate ligand in this trinuclear complex is positioned in a bridging motif between two Ni(II) centers and forms two five-membered chelate rings. In this case one Ni(II) center, the central metal ion within the trinuclear cation, is square planar. The two terminal pseudooctahedral Ni(II) centers are equivalent via a C₂ rotation.



Scheme 1-19. O₂ reactivity of the trinuclear bis-enediolate complex 7.

The absorption spectrum of **7** is notably different from that exhibited by the hexanickel cluster **5**, with an intense broad absorption band centered at 463 nm ($\epsilon \sim 16,000 \text{ M}^{-1} \text{ cm}^{-1}$). This feature is likely comprised of both a ligand-based $\pi \rightarrow \pi^*$ feature and a LMCT involving the square planar Ni(II) center.

Exposure of a CH₃CN solution of **7** to O₂ results in products akin to those generated from decomposition of the hexanickel cluster in the presence of a chelate ligand (e.g. 6-Ph₂TPA), specifically, [(6-NA-6-Ph₂TPA)Ni(O₂CPh)]ClO₄ (**8**) CO, and benzil [113]. The level of ¹⁸O incorporation in the benzoate product is similar to that found for the reaction of **5** with O₂ (~86%). One additional product, Ni(O₂CPh)₂·nCH₃OH, was identified and is proposed to be derived from the central Ni(II) center in the trinuclear compound.

2.5.4 Perspective. The chemistry of acireductone dioxygenases is important based on the fact that these enzymes are found at the only branch point of the biologically universal methionine salvage pathway. The reactivity of these enzymes may represent a possible regulatory shunt and/or a source of the signaling molecule CO. The key open question for acireductone dioxygenases concerns what factors govern the regioselectivity of aliphatic carbon-carbon bond cleavage. XAS and NMR spectroscopic studies of Ni(II)-ARD and Fe(II)-ARD' have been used as the primary basis for formulating the "chelate hypothesis" to explain the reaction regioselectivity. However, the results of the Fe(II)-ARD' NMR studies need to be viewed with some caution. Specifically, the proposed structure of Fe(II)-ARD', with its more open active site environment, is based on the spectroscopic similarity of this protein to a metal-free mutant (H98S). The assumption in this comparison is that the structural similarities of the proteins extend to the active site

and that any structural changes due to metal binding are minimal. As the chelate hypothesis is based on the fact that the active site secondary environments in Ni(II)-ARD and Fe(II)-ARD' differ, it is important to note that clear evidence for a difference in the chelation mode of the substrate in the ES complexes of Ni(II)-ARD and Fe(II)-ARD' cannot be discerned either from existing XAS or UV-vis data. Based on these issues, a significant advance in the field of acireductone dioxygenases would be the definitive structural characterization of ARD ES complexes of specific metal ion content.

To date, no iron-containing model systems have been used to investigate the Fe(II)-ARD'. Such a model system would allow the investigation of important questions such as whether the subtle differences in Lewis acidity of Fe(II) and Ni(II) is sufficient to change the binding mode of an acireductone substrate. Additionally, the ability of a Fe(II) center to modulate the regioselectivity of oxidative cleavage of an acireductone substrate could also be probed. The lack of model iron-containing model systems is presumably due to the anaerobic reactivity of acireductone substrates (to produce an ester via an isomerization reaction). The varying water-sensitivity of a model acireductone substrate as a function of both metal ion identity and chelate ligand structure imply that this challenge may be overcome by judicious choice of reaction conditions.

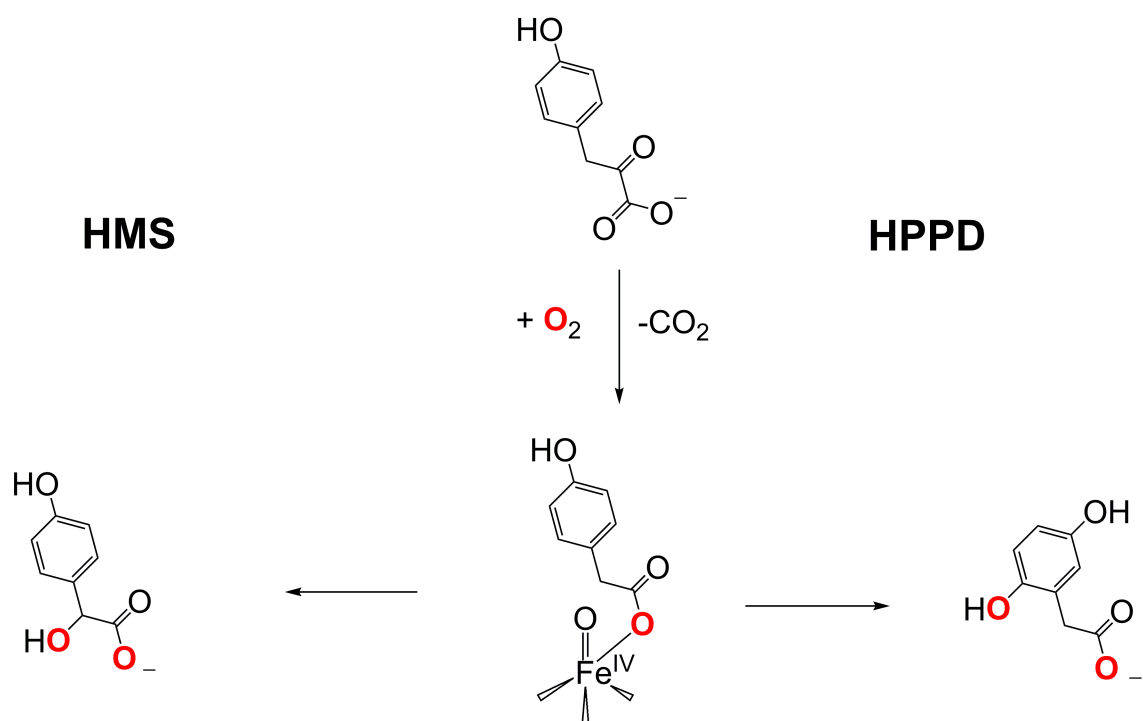
Additional investigations are also necessary to further define the mechanism leading to regioselective aliphatic carbon-carbon cleavage in C(1)-H type acireductones by ARDs. Specifically, as the only computational study reported to date for C(1)-H type acireductones is not directly relevant to enzyme catalysis, in that turnover depends on a radical propagation step, further mechanistic investigations are clearly warranted. The synthetic model complexes reported to date have been useful in terms of developing

model systems of structural and functional relevance to ARDs, but have involved an acireductone analog containing a C(1)-phenyl group that is not a substrate for the enzyme. Thus, an important advance in terms of synthetic chemistry would be the preparation and characterization of Ni(II) and Fe(II) complexes of a C(1)-H acireductone ligand that is a substrate for the enzyme. Additionally, as the vast majority of the mechanistic studies reported to date have involved acireductone monoanion species, it is important that future studies focus on acireductone dianion species to be of more relevance to the enzyme chemistry.

2.6 Dioxygenase-type reactivity of Fe(II) and Co(II) phenylpyruvate enolate complexes

Of general relevance to the enzymes noted above are recent enzymatic and model studies of aliphatic carbon-carbon bond cleavage reactions of phenylpyruvate. The cleavage of carbon-carbon bonds within a phenylpyruvate moiety by a dioxygenase-type reaction has been the subject of numerous studies, both in enzymatic and small molecular systems. These reactions interestingly exhibit variable regioselectivity, with cleavage of the C(1)-C(2) bond of a phenylpyruvate substrate to liberate CO₂ gas observed in the reactions catalyzed by 4-hydroxyphenylpyruvate dioxygenase (HPPD) or hydroxymandelate synthase (HMS), while reactions catalyzed by Dke1 lead to cleavage of the C(2)-C(3) bond to form oxalate. The reasons for this differing regioselectivity have not yet been evaluated.

The oxidation of 4-hydroxyphenylpyruvate, an important intermediate in tyrosine catabolism, has been extensively studied in enzymatic systems. In reactions with dioxygen, it is converted to 2,5-dihydroxyphenylacetate (homogentisate) by 4-

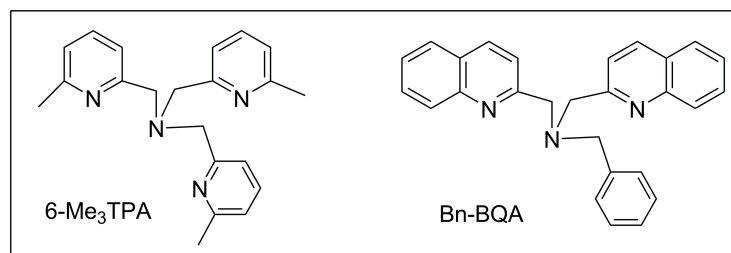
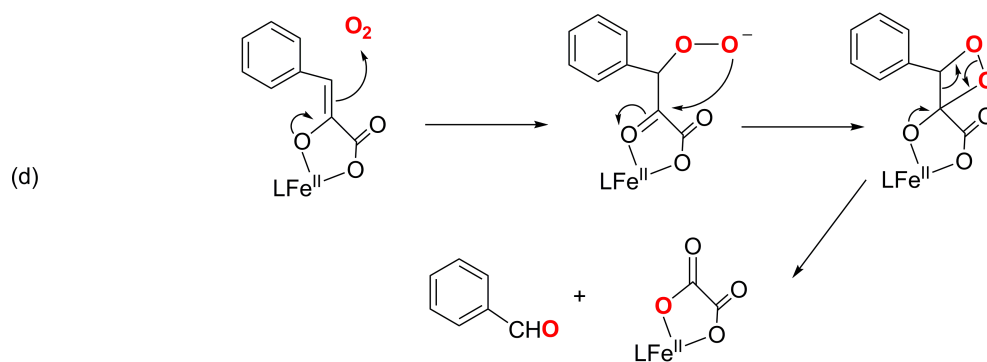
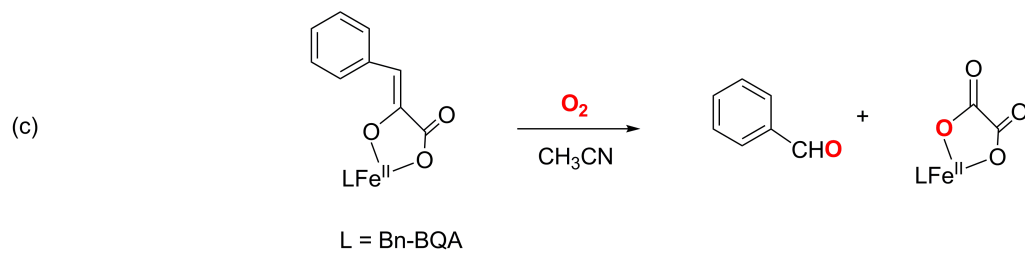
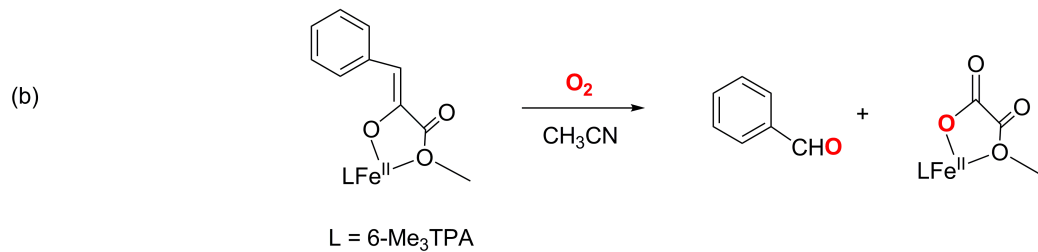
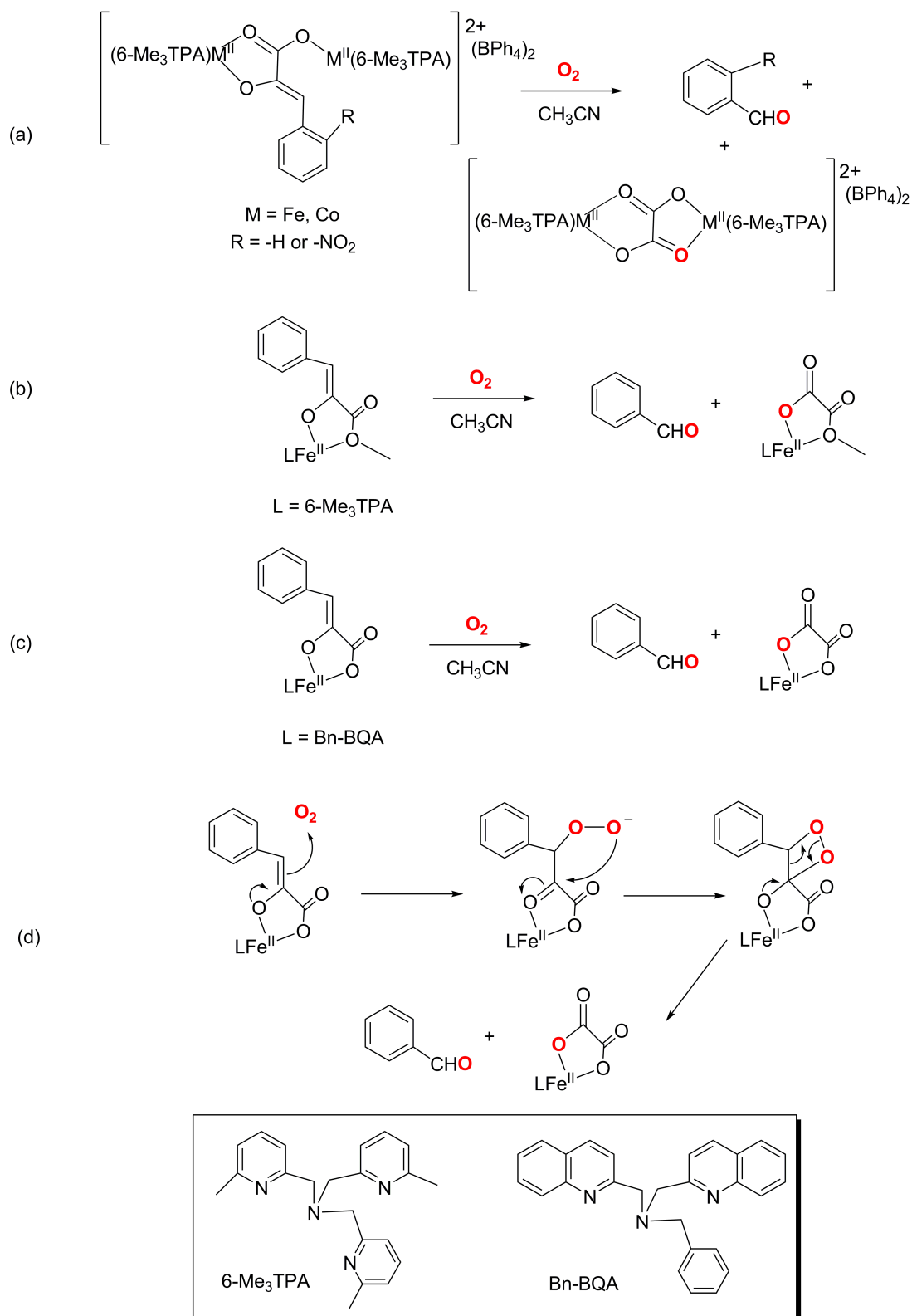


Scheme 1-20. Reaction pathways for the cleavage of 4-hydroxyphenylpyruvate by O_2 catalyzed by HMS or HPPD. Both reactions proceed by an initial oxidative decarboxylation to generate an $Fe(IV)=O$ species.

hydroxyphenylpyruvate dioxygenase (HPPD), or alternatively to homomandelate by hydroxymandelate synthase (HMS). These two enzymes share many characteristics with alpha-keto acid-dependent enzymes, in that they oxidatively decarboxylate an alpha-keto acid to generate a high-valent Fe(IV)=O species, and subsequently oxygenate a substrate (Scheme 1-20). However, HPPD and HMS are unique in that the oxidized substrate and the oxidized alpha-keto acid are the same molecule, leading to a net dioxygenolytic cleavage of an aliphatic carbon-carbon bond. At present, no model systems have been reported that mimic the chemistry of HPPD and HMS.

An atypical oxidative cleavage of the aliphatic C(2)-C(3) bond of phenylpyruvate by Dke1 to produce oxalate has also been recently reported [114]. The biological relevance of this reactivity has not yet been determined and mechanistic studies of this enzymatic reaction have not yet been reported. However, the reactivity of some Fe(II) and Co(II) complexes with a coordinated phenylpyruvate (pp) enolate ligand provide insight into how this reaction may take place [115, 116]. Importantly, these studies highlight the importance of an enolizable substrate, and the role a metal center can play in activating such a substrate towards reaction with dioxygen.

Exposure of the bridging phenylpyruvate complex $[(6\text{-Me}_3\text{TPA})_2\text{M}_2(\text{R-pp})]^{2+}$ (M = Fe(II) or Co(II)) to O₂ results in oxidative C(2)-C(3) bond cleavage within the phenylpyruvate ligand to give oxalate and benzaldehyde (or *p*-nitrobenzaldehyde) (Scheme 1-21(a)). Use of ¹⁸O₂ in the reactions revealed incorporation of a single labeled oxygen atom into benzaldehyde (80% (M = Fe(II))) and oxalate, thus demonstrating a dioxygenase-type reaction. It is suggested that the reaction with O₂ occurs at the enolate C(3) carbon atom and not at the metal center. In such a system, the role of the metal



Scheme 1-21. O₂ reactivity of phenylpyruvate compounds.

center is not to directly interact with dioxygen, but rather to stabilize the enolized form of the substrate. In this regard, these model systems are very similar to the acireductone dioxygenases, which also do not require metal-centered redox chemistry. Formation of C(3)-peroxo moiety (Scheme 1-21(d)) is proposed, which would enable subsequent C(2)-C(3) and O-O bond cleavage via a dioxetane ring and the generation of the final products.

Mononuclear Fe(II) analogs having either a coordinated phenylpyruvate ester, or a tridentate (Bn-BQA) supporting ligand, have been shown to exhibit similar reactivity upon exposure to O₂ (Scheme 1-21(b) and (c)). Notably, the binuclear phenylpyruvate compounds (Scheme 1-21(a)) are the most reactive, with the reaction with O₂ being significantly faster than the mononuclear counterparts (Scheme 1-21(b)), or even systems having an unsaturated Fe(II) center (Scheme 1-21(c)). In contrast to the iron-containing systems, mononuclear Co(II) analogs do not lead to cleavage of the phenylpyruvate substrate. Rather, oxidation of Co(II) to Co(III) occurs and the coordinated substrate remains intact, albeit deprotonated.

3.0 Conclusions

The studies outlined herein provide initial insight into the chemistry involved in metalloenzyme-catalyzed aliphatic carbon-carbon cleavage reactions. This is a field that is at an early stage of development and additional investigations are clearly needed to advance fundamental understanding of these reactions. Of particular interest will be the development of synthetic systems that exhibit reactivity of relevance to enzyme turnover and are amenable to detailed mechanistic investigations. Studies of reactive compounds of this type will provide insight into the pathways of the biological reactions, as well as

provide insight into strategies for the development of novel oxidation catalysts to address important issues in energy, bioremediation, and medicine in the future.

3.1 Dissertation Outline

The research presented henceforth details our studies in the area of oxidative carbon-carbon bond cleavage via a dioxygenase-type reaction pathway. The goal of this research is to provide insight into the reaction pathways of dioxygenase enzymes and thus develop new methodology for the activation and direction of carbon-carbon cleavage. To investigate the oxidative cleavage of various enolizable substrates we have utilized late first-row transition metal complexes supported by an aryl-appended tris(pyridylmethyl)amine ligand. In Chapter 2, we have generated the first-ever functional small molecular model of the enzyme-substrate adduct of iron-containing acireductone dioxygenase and investigated the role a metal center plays in the regioselectivity of its cleavage reaction. Chapter 3 extends this work to use a substrate with electronic structure and protonation levels that are more directly relevant to the native substrate of the acireductone dioxygenases. In Chapter 4, we have utilized a novel photo-initiated method to generate a superoxo-diketonyl radical pair to investigate one of the proposed reaction pathways for acetylacetone dioxygenases. Finally, in Chapter 5 we extend this work using a copper center, and have found a new route to facile oxygen activation for carbon-carbon bond cleavage. Overall, the complexes we have synthesized and studied have relevance to the enzymes acetylacetone dioxygenase, quercetin dioxygenase and the acireductone dioxygenases.

References

- [1] S.K. Hanson, R.T. Baker, J.C. Gordon, B.L. Scott, A.D. Sutton, D.L. Thorn, *J. Am. Chem. Soc.*, 131 (2009) 428-429.
- [2] *Biodegradation and Bioremediation, Soil Biology*, Vol. 2, A. Singh, O.P. Ward (Eds.), Springer, Berlin, Germany 2004.
- [3] M. Costas, M.P. Mehn, M.P. Jensen, L. Que, Jr., *Chem. Rev.*, 104 (2004) 939-986.
- [4] T.D.H. Bugg, S. Ramaswamy, *Curr. Opin. Chem. Biol.*, 12 (2008) 134-140.
- [5] S. Fetzner, *App. Environ. Microbiol.*, 78 (2012) 2505-2514.
- [6] D. Buongiorno, G. Straganz, *Coord. Chem. Rev.*, 257 (2013) 541-563.
- [7] K.S. Hewitson, N. Granatino, R.W.D. Welford, M.A. McDonough, C.J. Schofield, *Phil. Trans. R. Soc. A*, 363 (2005) 807-828.
- [8] G. Ballatyne, T.J. Crawley, *J. Appl. Toxicol.*, 21 (2001) 165-171.
- [9] R.V. Thurston, T.A. Gilfoil, E.L. Meyn, R.K. Zajdal, T.I. Aoki, G.D. Veith, *Water Res.*, 19 (1985) 1145-1155.
- [10] G. Bringmann, R. Kühn, *Water Res.*, 14 (1980) 231-241.
- [11] G.D. Straganz, A. Glieder, L. Brecker, D.W. Ribbons, W. Steiner, *Biochem. J.*, 369 (2003) 573-581.
- [12] G. Straganz, L. Brecker, H.J. Weber, W. Steiner, D.W. Ribbons, *Biochem. Biophys. Res. Commun.*, 297 (2002) 232-236.
- [13] J.M. Dunwell, A. Purvis, S. Khuri, *Phytochemistry*, 65 (2004) 7-17.
- [14] A.R. Diebold, M.L. Neidig, G.R. Moran, G.D. Straganz, E.I. Solomon, *Biochemistry*, 49 (2010) 6945-6952.
- [15] S. Leitgeb, G.D. Straganz, B. Nidetzky, *FEBS*, 276 (2009) 5983-5997.

- [16] H. Brkic, D. Buongiorno, M. Ramek, G. Straganz, S. Tomic, *J. Biol. Inorg. Chem.*, 17 (2012) 801-815.
- [17] S. Leitgeb, G.D. Straganz, B. Nidetzky, *Biochem. J.*, 418 (2009) 403-411.
- [18] G. Straganz, H. Hofer, W. Steiner, B. Nidetzky, *J. Am. Chem. Soc.*, 126 (2004) 12202-12203.
- [19] G.D. Straganz, B. Nidetzky, *J. Am. Chem. Soc.*, 127 (2005) 12306-12314.
- [20] A.R. Diebold, G.D. Straganz, E.I. Solomon, *J. Am. Chem. Soc.*, 133 (2011) 15979-15991.
- [21] I. Siewert, C. Limberg, *Angew. Chem. Int. Ed. Engl.*, 47 (2008) 7953-7956.
- [22] H. Park, J.S. Baus, S.V. Lindeman, A.T. Fiedler, *Inorg. Chem.*, 50 (2011) 11978-11989.
- [23] M.M. Bittner, J.S. Baus, S.V. Lindeman, A.T. Fiedler, *Eur. J. Inorg. Chem.*, (2012) 1848-1856.
- [24] H. Park, M.M. Bittner, J.S. Baus, S.V. Lindeman, A.T. Fiedler, *Inorg. Chem.*, 51 (2012) 10279-10289.
- [25] N. Kitajima, H. Amagi, N. Tamura, M. Ito, Y. Moro-oka, K. Heerwegh, A. Penicaud, R. Mathur, C. Reed, P.D.W. Boyd, *Inorg. Chem.*, 32 (1993) 3583-3584.
- [26] P.C. Bruijninx, G. van Koten, R.J. Klein Gebbink, *Chem. Soc. Rev.*, 37 (2008) 2716-2744.
- [27] A.W. Addison, T.N. Rao, J. Reedijk, J. van Rijn, G.C. Verschoor, *J. Chem. Soc., Dalton Trans.*, (1984) 1349-1356. .
- [28] I. Siewert, C. Limberg, S. Demeshko, E. Hoppe, *Chem. Eur. J.*, 14 (2008) 9377-9388.

- [29] M.G.M.B. Martin, M. Horner, M.B. Behm, F.S. Nunes, *Z. Anorg. Allg. Chem.*, 637 (2011) 1299-1233.
- [30] C.J. Allpress, A.M. Arif, D.T. Houghton, L.M. Berreau, *Chem. Eur. J.*, 17 (2011) 14962-14973.
- [31] K. Schroder, B. Join, A.J. Amali, K. Junge, X. Ribas, M. Costas, M. Beller, *Angew. Chem. Int. Ed. Engl.*, 50 (2011) 1425-1429.
- [32] P. Liu, A. Liu, F. Yan, M.D. Wolfe, J.D. Lipscomb, H.W. Liu, *Biochemistry*, 42 (2003) 11577-11586.
- [33] P. Liu, M.P. Mehn, F. Yan, Z. Zhao, L. Que, Jr., H.W. Liu, *J. Am. Chem. Soc.*, 126 (2004) 10306-10312.
- [34] L.J. Higgins, F. Yan, P. Liu, H.W. Liu, C.L. Drennan, *Nature*, 437 (2005) 838-844.
- [35] F. Yan, T. Li, J.D. Lipscomb, A. Liu, H.W. Liu, *Arch. Biochem. Biophys.*, 442 (2005) 82-91.
- [36] F. Yan, J.W. Munos, P. Liu, H.W. Liu, *Biochemistry*, 45 (2006) 11473-11481.
- [37] F. Yan, S.J. Moon, P. Liu, Z. Zhao, J.D. Lipscomb, A. Liu, H.W. Liu, *Biochemistry*, 46 (2007) 12628-12638.
- [38] J.W. Munos, S.J. Moon, S.O. Mansoorabadi, W. Chang, L. Hong, F. Yan, A. Liu, H.W. Liu, *Biochemistry*, 47 (2008) 8726-8735.
- [39] D. Yun, M. Dey, L.J. Higgins, F. Yan, H.W. Liu, C.L. Drennan, *J. Am. Chem. Soc.*, 133 (2011) 11262-11269.
- [40] H. Huang, W.C. Chang, P.J. Pai, A. Romo, S.O. Mansoorabadi, D.H. Russell, H.W. Liu, *J. Am. Chem. Soc.*, 134 (2012) 16171-16174.
- [41] A. Milaczewska, E. Broclawik, T. Borowski, *Chem. Eur. J.*, 19 (2013) 771-781.

- [42] R.M. Cicchillo, H. Zhang, J.A. Blodgett, J.T. Witteck, G. Li, S.K. Nair, W.A. van der Donk, W.W. Metcalf, *Nature*, 459 (2009) 871-874.
- [43] J.T. Witteck, R.M. Cicchillo, W.A. van der Donk, *J. Am. Chem. Soc.*, 131 (2009) 16225-16232.
- [44] H. Hirao, K. Morokuma, *J. Am. Chem. Soc.*, 132 (2010) 17901-17909.
- [45] J.T. Witteck, P. Malova, S.C. Peck, R.M. Cicchillo, F. Hammerschmidt, W.A. van der Donk, *J. Am. Chem. Soc.*, 133 (2011) 4236-4239.
- [46] S.C. Peck, H.A. Cooke, R.M. Cicchillo, P. Malova, F. Hammerschmidt, S.K. Nair, W.A. van der Donk, *Biochemistry*, 50 (2011) 6598-6605.
- [47] H. Hirao, K. Morokuma, *J. Am. Chem. Soc.*, 133 (2011) 14550-14553.
- [48] L. Du, J. Gao, Y. Liu, D. Zhang, C. Liu, *Org. Biomol. Chem.*, 10 (2012) 1014-1024.
- [49] L. Du, J. Gao, Y. Liu, C. Liu, *J. Phys. Chem. B*, 116 (2012) 11837-11844.
- [50] J. Spivack, T.K. Leib, J.H. Lobos, *J. Biol. Chem.*, 269 (1994) 7323-7329.
- [51] D.J. Hopper, E.A. Elmorsi, *Biochem. J.*, 218 (1984) 269-272.
- [52] D.J. Hopper, *Biochem. J.*, 239 (1986) 469-472.
- [53] D.J. Hopper, M.A. Kaderbhai, *Biochem. J.*, 344 Pt 2 (1999) 397-402.
- [54] A. Bower, School of Biological Science, University of Southampton, 2008. PhD Thesis.
- [55] M. Enya, K. Aoyagi, Y. Hishikawa, A. Yoshimura, K. Mitsukura, K. Maruyama, *Biosci. Biotechnol. Biochem.*, 76 (2012) 567-574.
- [56] S. Paria, P. Halder, T.K. Paine, *Angew. Chem. Int. Ed. Engl.*, 51 (2012) 6195-6199.
- [57] M.L. Bender, R.R. Stone, R.S. Dewey, *J. Am. Chem. Soc.*, 78 (1956) 319-321.
- [58] I. Erlund, *Nutr. Res.*, 24 (2004) 851-874.

- [59] P.G. Pietta, *J. Nat. Prod.*, 63 (2000) 1035-1042.
- [60] R.L. Prior, *Am. J. Clin. Nutr.*, 78 (2003) 570S-578S.
- [61] T. Oka, F.J. Simpson, *Biochem. Biophys. Res. Commun.*, 43 (1971) 1-5.
- [62] T. Oka, F.J. Simpson, H.G. Krishnamurty, *Can. J. Microbiol.*, 18 (1972) 493-508.
- [63] H.K. Hund, J. Breuer, F. Lingens, J. Huttermann, R. Kappl, S. Fetzner, *Eur. J. Biochem.*, 263 (1999) 871-878.
- [64] S. Tranchimand, G. Ertel, V. Gaydou, C. Gaudin, T. Tron, G. Iacazio, *Biochimie*, 90 (2008) 781-789.
- [65] I.M. Kooter, R.A. Steiner, B.W. Dijkstra, P.I. van Noort, M.R. Egmond, M. Huber, *Eur. J. Biochem.*, 269 (2002) 2971-2979.
- [66] R.A. Steiner, I.M. Kooter, B.W. Dijkstra, *Biochemistry*, 41 (2002) 7955-7962.
- [67] F. Fusetti, K.H. Schröter, R.A. Steiner, P.I. van Noort, T. Pijning, H.J. Rozeboom, K.H. Kalk, M.R. Egmond, B.W. Dijkstra, *Structure*, 10 (2002) 259-268.
- [68] R.A. Steiner, K.H. Kalk, B.W. Dijkstra, *Proc. Natl. Acad. Sci. U. S. A.*, 99 (2002) 16625-16630.
- [69] H. Merkens, R. Kappl, R.P. Jakob, F.X. Schmid, S. Fetzner, *Biochemistry*, 47 (2008) 12185-12196.
- [70] B. Gopal, L.L. Madan, S.F. Betz, A.A. Kossiakoff, *Biochemistry*, 44 (2005) 193-201.
- [71] M.R. Schaab, B.M. Barney, W.A. Francisco, *Biochemistry*, 45 (2006) 1009-1016.
- [72] B.M. Barney, M.R. Schaab, R. LoBrutto, W.A. Francisco, *Protein Expr. Purif.*, 35 (2004) 131-141.

- [73] L. Bowater, S.A. Fairhurst, V.J. Just, S. Bornemann, *FEBS Letters*, 557 (2004) 45-48.
- [74] H. Merkens, R. Kappl, R.P. Jakob, F.X. Schmid, S. Fetzner, *Biochemistry*, 47 (2008) 12185-12196.
- [75] H. Merkens, S. Fetzner, *FEMS Microbiol. Lett.*, 287 (2008) 100-107.
- [76] A. Nishinaga, T. Tojo, H. Tomita, T. Matsuura, *J. Chem. Soc., Perkin Trans. 1*, (1979) 2511-2516.
- [77] A. Nishinaga, T. Matsuura, *J. Chem. Soc., Chem. Commun.*, (1973) 9-10.
- [78] L. Barhács, J. Kaizer, G. Speier, *J. Org. Chem.*, 65 (2000) 3449-3452.
- [79] E. Balogh-Hergovich, G. Speier, *J. Org. Chem.*, 66 (2001) 7974-7978.
- [80] J.S. Pap, J. Kaizer, G. Speier, *Coord. Chem. Rev.*, 254 (2010) 781-793.
- [81] J. Kaizer, J.S. Pap, G. Speier, *Copper Dioxygenases*, in: K.D. Karlin, S. Itoh (Eds.) *Copper-Oxygen Chemistry; Wiley Series on Reactive Intermediates in Chemistry and Biology*, Wiley, New York, NY, 2011.
- [82] J. Kaizer, E. Balogh-Hergovich, M. Czaun, T. Csay, G. Speier, *Coord. Chem. Rev.*, 250 (2005) 2222-2233.
- [83] E. Balogh-Hergovich, J. Kaizer, G. Speier, *J. Mol. Catal. A: Chem*, 206 (2003) 83-87.
- [84] K. Grubel, K. Rudzka, A.M. Arif, K.L. Klotz, J.A. Halfen, L.M. Berreau, *Inorg. Chem.*, 49 (2010) 82-96.
- [85] A. Nishinaga, N. Numada, K. Maruyama, *Tetrahedron Lett.*, 30 (1989) 2257-2258.
- [86] A. Nishinaga, T. Kuwashige, T. Tusutsui, T. Mashino, K. Maruyama, *J. Chem. Soc., Dalton Trans.*, (1994) 805-810.

- [87] J. Kaizer, G. Baráth, J. Pap, G. Speier, *Chem. Commun.*, (2007) 5235-5237.
- [88] J. Kaizer, J.S. Pap, G. Speier, Iron and Manganese-containing Flavonol 2,4-Dioxygenase Mimics, in: *Biomimetics*, L.D. Pramatarova (Ed.), Intech, Bulgaria, 2011, 29-42.
- [89] G. Baráth, J. Kaizer, G. Speier, L. Párkányi, E. Kuzmann, A. Vértes, *Chem. Commun.*, (2009) 3630-3632.
- [90] J.S. Pap, A. Matuz, G. Baráth, B. Kripli, M. Giorgi, G. Speier, J. Kaizer, *J. Inorg. Biochem.*, 108 (2012) 15-21.
- [91] L. Barhács, J. Kaizer, G. Speier, *J. Mol. Catal. B: Chem*, 172 (2001) 117-125.
- [92] T.C. Pochapsky, T. Ju, M. Dang, R. Beaulieu, G.M. Pagani, B. OuYang, Nickel in Acireductone Dioxygenase, in: A. Sigel, H. Sigel, R.K.O. Sigel (Eds.) *Metal Ions in Life Sciences: Nickel and Its Surprising Impact in Nature*, John Wiley & Sons, Clichester West Sussex, England, 2007, 473-498.
- [93] Y. Dai, T.C. Pochapsky, R.H. Abeles, *Biochemistry*, 40 (2001) 6379-6387.
- [94] F. Al-Mjeni, T. Ju, T.C. Pochapsky, M.J. Maroney, *Biochemistry*, 41 (2002) 6761-6769.
- [95] T.C. Pochapsky, S.S. Pochapsky, T. Ju, H. Mo, F. Al-Mjeni, M.J. Maroney, *Nat. Struct. Biol.*, 9 (2002) 966-972.
- [96] T. Ju, R.B. Goldsmith, S.C. Chai, M.J. Maroney, S.S. Pochapsky, T.C. Pochapsky, *J. Mol. Biol.*, 363 (2006) 523-534.
- [97] T.C. Pochapsky, S.S. Pochapsky, T.T. Ju, C. Hoefler, J. Liang, *J. Biomol. NMR*, 34 (2006) 117-127.

- [98] S.C. Chai, T. Ju, M. Dang, R.B. Goldsmith, M.J. Maroney, T.C. Pochapsky, *Biochemistry*, 47 (2008) 2428-2438.
- [99] J.W. Wray, R.H. Abeles, *J. Biol. Chem.*, 270 (1995) 3147-3153.
- [100] D. Semmingsen, *Acta Chem. Scand.*, 28B (1974) 141-146.
- [101] B. Aurivillius, G. Lundgren, *Acta Chem. Scand.*, 9 (1955) 912-916.
- [102] J.C. Jeffrey, D.J. Liard, M.D. Ward, *Inorg. Chim. Acta*, 251 (1996) 9-12.
- [103] T. Borowski, *J. Mol. Structure: Theochem*, 772 (2006) 89-92.
- [104] Y. Zhang, M.H. Heinsen, M. Kostic, G.M. Pagani, T.V. Riera, I. Perovic, L. Hedstrom, B.B. Snider, T.C. Pochapsky, *Biorg. Med. Chem.*, 12 (2004) 3847-3855.
- [105] L.M. Berreau, T. Borowski, K. Grubel, C.J. Allpress, J.P. Wikstrom, M.E. Germain, E.V. Rybak-Akimova, D.L. Tierney, *Inorg. Chem.*, 50 (2011) 1047-1057.
- [106] M.M. Makowska-Grzyska, E. Szajna, C. Shipley, A.M. Arif, M.H. Mitchell, J.A. Halfen, L.M. Berreau, *Inorg. Chem.*, 42 (2003) 7472-7488.
- [107] E. Szajna, A.M. Arif, L.M. Berreau, *J. Am. Chem. Soc.*, 127 (2005) 17186-17187.
- [108] K. Grubel, A.L. Fuller, B.M. Chambers, A.M. Arif, L.M. Berreau, *Inorg. Chem.*, 49 (2010) 1071-1081.
- [109] C.J. Allpress, K. Grubel, E. Szajna-Fuller, A.M. Arif, L.M. Berreau, *J. Am. Chem. Soc.*, 135 (2013) 659-668.
- [110] K. Grubel, G.K. Ingle, A.L. Fuller, A.M. Arif, L.M. Berreau, *Dalton Trans.*, 40 (2011) 10609-10620.
- [111] E. Szajna-Fuller, B.M. Chambers, A.M. Arif, L.M. Berreau, *Inorg. Chem.*, 46 (2007) 5486-5498.

- [112] K. Rudzka, K. Grubel, A.M. Arif, L.M. Berreau, *Inorg. Chem.*, 49 (2010) 7623-7625.
- [113] K. Rudzka, A.M. Arif, L.M. Berreau, *Inorg. Chem.*, 47 (2008) 10832-10840.
- [114] C.M. Di Giuro, D. Buongiorno, E. Leitner, G.D. Straganz, *J. Inorg. Biochem.*, 105 (2011) 1204-1211.
- [115] T.K. Paine, J. England, L. Que, *Chem. Eur. J.*, 13 (2007) 6073-6081.
- [116] B. Chakraborty, P. Halder, P.R. Banerjee, T.K. Paine, *Eur. J. Inorg. Chem.*, (2013) 5843-5853.

CHAPTER 2

REGIOSELECTIVE ALIPHATIC CARBON-CARBON BOND CLEAVAGE BY A
MODEL SYSTEM OF RELEVANCE TO IRON-CONTAINING ACIREDUCTONE
DIOXYGENASE[†]**Abstract**

Mononuclear Fe(II) complexes ($[(6\text{-Ph}_2\text{TPA})\text{Fe}(\text{PhC}(\text{O})\text{C}(\text{R})\text{C}(\text{O})\text{Ph})]\text{X}$ (**3-X**: R = OH, X = ClO₄ or OTf; **4**: R = H, X = ClO₄)) supported by the 6-Ph₂TPA chelate ligand (6-Ph₂TPA = *N,N*-bis((6-phenyl-2-pyridyl)methyl)-*N*-(2-pyridylmethyl)amine) and containing a β-diketonate ligand bound via a six-membered chelate ring have been synthesized. The complexes have all been characterized by ¹H NMR, UV-vis, infrared spectroscopy, and variably by elemental analysis, mass spectrometry and X-ray crystallography. Treatment of dry CH₃CN solutions of **3-OTf** with O₂ leads to oxidative cleavage of the C(1)-C(2) and C(2)-C(3) bonds of the acireductone via a dioxygenase reaction, leading to formation of carbon monoxide and two equivalents of benzoic acid, as well as two other products not derived from dioxygenase reactivity: 2-oxo-2-phenylethylbenzoate and benzil. Treatment of CH₃CN/H₂O solutions of **3-X** with O₂ leads to the formation of an additional product, benzoylformic acid, indicative of the operation of a new reaction pathway in which only the C(1)-C(2) bond is cleaved. Mechanistic studies show that the change in regioselectivity is due to the hydration of a vicinal triketone intermediate in the presence of both an iron center and water. This is the first structural and functional model of relevance to iron-containing acireductone

[†] Coauthored by Caleb J. Allpress, Katarzyna Grubel, Ewa Szajna-Fuller, Atta M. Arif, and Lisa M. Berreau. Reproduced in a modified format with permission from *J. Am. Chem. Soc.* **2013**, *135*, 659-668.

dioxygenase (Fe-ARD'), an enzyme in the methionine salvage pathway that catalyzes the regiospecific oxidation of 1,2-dihydroxy-3-oxo-(*S*)-methylthiopentene to form 2-oxo-4-methylthiobutyrate. Importantly, this model system is found to control the regioselectivity of aliphatic carbon-carbon bond cleavage by changes involving an intermediate in the reaction pathway, rather than by the binding mode of the substrate, as had been proposed in studies of acireductone enzymes.

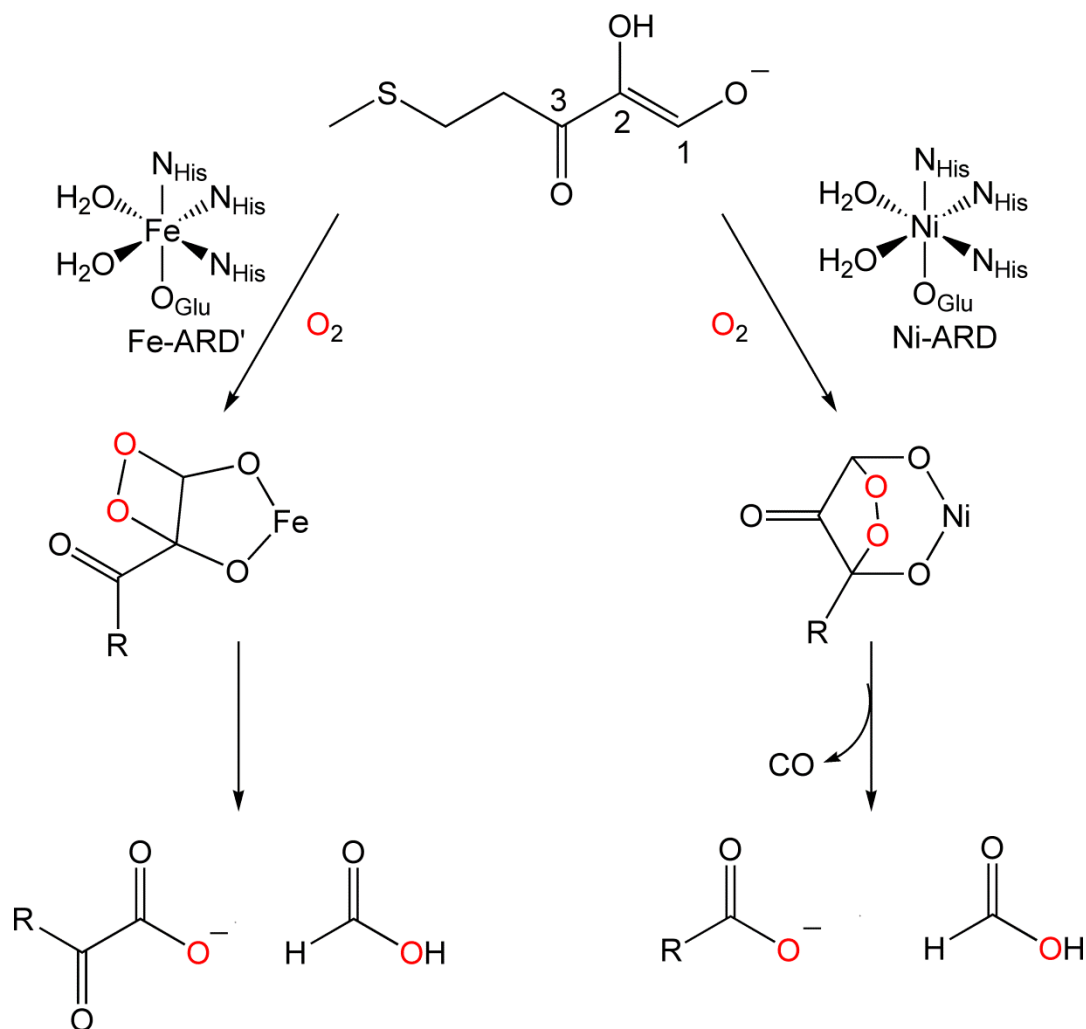
Introduction

One of the most challenging reactions in chemistry and biology is the selective oxidative cleavage of carbon-carbon bonds. The enzymes that carry out these reactions are typically dioxygenases, which incorporate two oxygen atoms into products via an oxidative mechanism, and often contain a metal co-factor (typically iron) in a non-heme binding pocket.¹ While the mechanism of enzymes that cleave aromatic carbon-carbon bonds such as the extradiol and intradiol catechol dioxygenases have been extensively studied,^{2,3} enzymes that cleave aliphatic carbon-carbon bonds have received much less attention until recently. These enzymes, which include acetylacetone-cleaving dioxygenase (Dke1)⁴, 2,4'-dihydroxyacetophenone dioxygenase,⁵ hydroxyethylphosphonate dioxygenase⁶ and the acireductone dioxygenases,⁷ are the subject of growing interest. The acireductone dioxygenases, found in the methionine salvage pathway, are of particular current interest due to the change in regiospecificity of the reaction as a function of metal ion bound at the active site. This differing reactivity within the enzymes as a function of metal ion identity is unique at present in biology.

The methionine salvage pathway is ubiquitous in biological systems and is responsible for recycling the methylthio-unit of 5'-methylthioadenosine to regenerate

methionine.⁸ 5'-Methylthioadenosine is generated during the consumption of S-adenosylmethionine in the synthesis of polyamines such as spermine and spermidine. These polyamines are associated with cell growth and apoptosis, and defects in polyamine regulation are associated with oncogenesis.⁹ In aerobic systems, the methionine salvage pathway contains a single branch point. The reaction at this branch point involves an acireductone intermediate (1,2-dihydroxy-3-oxo-(S)-methylthiopentene) that undergoes a reaction catalyzed by one of two different dioxygenase enzymes (Scheme 2-1).⁹ In the on-pathway reaction, iron-containing acireductone dioxygenase (Fe-ARD') catalyzes the oxidative cleavage of the C(1)-C(2) bond resulting in the formation of formic acid and an α -keto acid, the latter of which undergoes transamination in a subsequent step to regenerate methionine. In the off-pathway reaction, nickel-containing acireductone dioxygenase (Ni-ARD) catalyzes the oxidative cleavage of the C(1)-C(2) and C(2)-C(3) bonds of the acireductone to form formic acid, carbon monoxide (CO) and a carboxylic acid.¹⁰ The mechanism of Ni-ARD has been the focus of several recent studies, primarily through model systems, for two main reasons: (1) nickel-containing dioxygenases were hitherto unknown; and (2) the production of CO is of particular current interest due to its role in cellular signaling.¹¹ In this context, the branch point in the methionine salvage pathway at which the acireductone dioxygenases operate represents a combination of a potential regulatory shunt coupled with the production of a signaling molecule.

Despite catalyzing reactions with differing regioselectivity, Fe-ARD' and Ni-ARD contain identical peptide sequences, and bind the divalent metal cofactor with the same four amino acid residues (3His, 1Glu).⁹ Thus, the only constitutive difference for



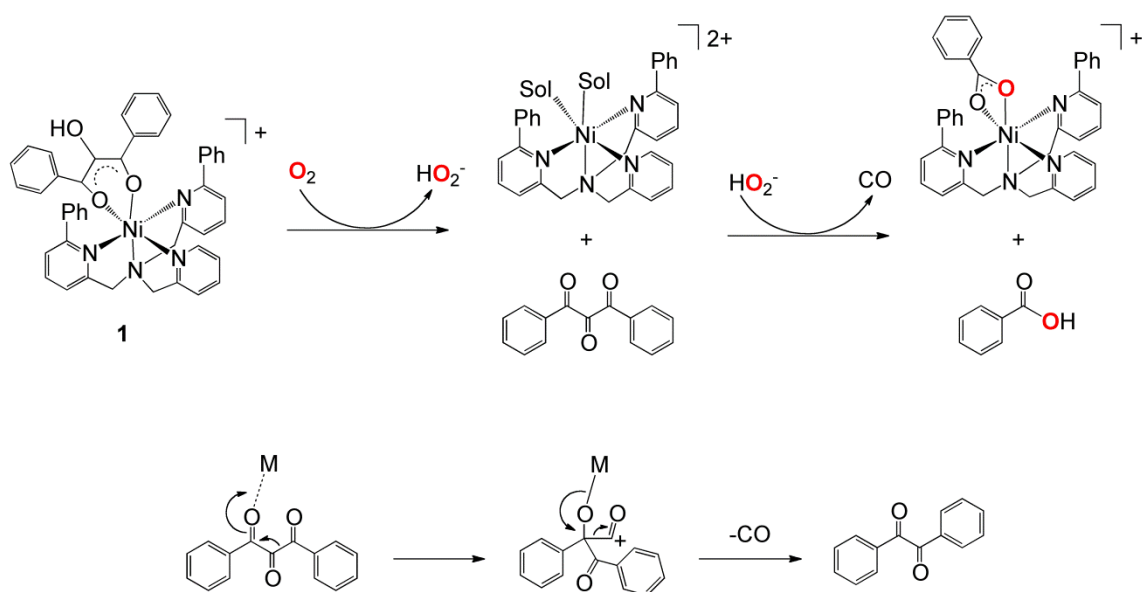
Scheme 2-1. Regiospecificity of aliphatic carbon-carbon bond cleavage of 1,2-dihydroxy-3-oxo-(*S*)-methylthiopentene by acireductone dioxygenases in the methionine salvage pathway. The on-pathway reaction (left) is catalyzed by the iron-containing enzyme Fe-ARD['], while the off-pathway reaction (right) is catalyzed by the nickel-containing enzyme Ni-ARD.

the two enzymes is the nature of the metal at the active site. To date, no model complexes have been synthesized to study the reaction pathway in Fe-ARD['].

The current hypothesis for the difference in regiospecificity is that a change in the coordination mode of the substrate from a six-membered chelate in Ni-ARD, to a five-membered chelate in Fe-ARD['] results in the observed differences in selectivity of bond

cleavage (Scheme 2-1).⁹ To probe this chelate ring hypothesis, we have previously prepared a Ni(II)-containing complex of a bulky acireductone (2-hydroxy-1,3-diphenylpropan-1,3-dione), [(6-Ph₂TPA)Ni(PhC(O)C(OH)C(O)Ph)]ClO₄ (**1**), that is supported by an aryl-appended TPA ligand (6-Ph₂TPA = *N,N*-bis((6-phenyl-2-pyridyl)methyl)-*N*-(2-pyridylmethyl)amine) in order to mimic the hydrophobic binding pocket found in ARDs.¹² X-ray crystallographic and ¹H NMR solution studies of **1** revealed that the acireductone moiety in this complex is coordinated as a six-membered chelate ring. Upon treatment of **1** with O₂, the C(1)-C(2) and C(2)-C(3) bonds of the acireductone were cleaved, and CO was generated, in a Ni-ARD-type reaction (Scheme 2-2 (top)). Mechanistic studies suggest this reaction proceeds by an initial net two-electron process to form 1,3-diphenylpropantrione (a vicinal triketone) and hydroperoxide anion, which may then combine to form a dioxetane ring and subsequently cleave the C-C bonds.¹³ The triketone intermediate was implicated by the detection of benzil, which is formed in the reaction mixture via a benzoyl migration and decarbonylation (Scheme 2-2 (bottom)).¹⁴ We note that the production of benzil was the only initial evidence for a reaction pathway involving a triketone intermediate. Benzoyl migration is not possible with the native ARD substrate, and so such a byproduct would not be produced in the enzyme, even if the reaction were to proceed via a triketone intermediate.

In the present work, we have investigated the role of the metal center in the O₂ reactivity of acireductones by utilizing an iron-containing analogue of **1**. While spectroscopic studies provide evidence for a six-membered chelate ring for the coordinated acireductone, we have found that the presence of iron and water in the reaction mixture opens up a new oxidative reaction pathway not accessible in our nickel-



Scheme 2-2. Reaction of **1** with O_2 to form Ni-ARD-type products via the formation of an intermediate triketone species and hydroperoxide (top). Decarbonylation of 1,3-diphenylpropantrione to form benzil via a Lewis acid-mediated benzoyl migration (bottom).

containing system. This new reaction pathway results in the formation of benzoylformic acid, the α -keto acid product that would be expected in a Fe-ARD' type reaction.

Experimental

General Methods. All reagents were obtained from commercial sources and were used without additional purification unless otherwise noted. 1,3-diphenylpropantrione was purchased from TCI America. Solvents were dried according to published procedures and were purified by distillation under N_2 prior to use.¹⁵ Air-sensitive reactions were performed in an MBraun Unilab glovebox under a N_2 atmosphere or by using standard Schlenk techniques. $Fe(OTf)_2 \cdot 2CH_3CN$ was prepared from Fe powder, and $FeCl_3$ was prepared from $FeCl_3 \cdot 6H_2O$ using known procedures.^{16, 17} The bulky

acireductone 2-hydroxy-1,3-diphenylpropan-1,3-dione was synthesized by modifying a literature procedure as described below.¹⁸ The 6-Ph₂TPA (*N,N*-bis((6-phenyl-2-pyridyl)methyl)-*N*-(2-pyridylmethyl)amine) ligand, [(6-Ph₂TPA)Ni(CH₃CN)(H₂O)](ClO₄)₂ and 2-oxo-2-phenylethylbenzoate were synthesized by following previously published procedures.¹⁹⁻²¹

Physical Methods. ¹H NMR spectra of organic compounds were obtained using a JEOL ECX-300 spectrometer; chemical shifts were referenced to the residual solvent peak in CD₂H₂CN (1.94 ppm, quintet). ¹H NMR spectra of paramagnetic complexes were obtained using a Bruker ARX-400 spectrometer and parameters, as previously described.²² UV-vis data was collected on a HP8453A spectrometer at ambient temperature. IR spectra were recorded on a Shimadzu FTIR-8400 spectrometer as KBr pellets. Room temperature magnetic susceptibilities were determined using the Evans method.²³ GC-MS data was obtained on a Shimadzu GCMS-QP5000 gas chromatograph/mass spectrometer with a GC-17A gas chromatograph, using an Alltech EC5 30 m × 25 mm × 25 μm thin film capillary column and temperature program: *T*_{initial}: 70 °C (5 min); temperature gradient: 23 °C min⁻¹; *T*_{Final}: 250 °C (10 min). LC-MS data was obtained using negative-ion APCI on a LCQ Thermo Finnigan MS via a HP1100 with a Betasil C18 10 × 2.1 mm column; solvent gradient from 5% aqueous methanol to 50% aqueous methanol. CO was detected using an Agilent 3000A Micro gas chromatograph. Mass spectral data for metal complexes was collected by the Mass Spectrometry Facility, University of California, Riverside. Elemental analysis was performed by Atlantic Microlabs Inc., Norcross, GA for all compounds except **3-OTf**, which was analyzed by Canadian Microanalytical Service, Ltd.

Kinetic Studies. Measurements were performed on a HP8453A spectrometer at 20 °C. All manipulations of **3-X** were performed under a nitrogen atmosphere. O₂-saturated solutions of CH₃CN (8.2 mM) were prepared by bubbling dry O₂ through a solution of dry CH₃CN.²⁴ Solutions containing lower O₂ concentrations were prepared by diluting the 8.2 mM solution with N₂-saturated CH₃CN using gas tight syringes.

Caution! *Perchlorate salts of metal complexes with organic ligands are potentially very explosive. Only small amounts of material should be prepared, and these should be handled with extreme caution.*²⁵

2-Hydroxy-1,3-diphenyl-propan-1,3-dione. NaHCO₃ (1.68 g, 20.0 mmol) was placed in a flask with 0.10 M RuCl₃ (800 μL, 0.080 mmol) and diluted with H₂O (7.2 mL), CH₃CN (48 mL) and EtOAc (48 mL). Oxone (24.4 g, 40.0 mmol) was added in one portion and stirred until a bright yellow suspension formed and effervescence ceased. Benzylidene acetophenone (1.66 g, 8.00 mmol) was added in one portion to initially form a brown solution that became yellow over time. The progress of reaction was carefully monitored by TLC (3:1 hexanes:EtOAc) and after 18 minutes the suspension was diluted with 50 mL EtOAc and the solid residue filtered off, washing with a further 30 mL EtOAc. The filtrate was washed with 40 mL saturated Na₂SO₃ and 40 mL H₂O. The organic layer was dried over Na₂SO₄, filtered and then the solvent was removed under reduced pressure to yield the crude product. Recrystallization from hot EtOH afforded white needle-like crystals that were collected by filtration and washed with cold EtOH followed by Et₂O (0.37 g, 20%). ¹H NMR (300 MHz, CD₃CN, 25 °C): δ = 7.99 (d, ³J(H,H) = 7.2 Hz, 4H; Ar-H), 7.66 (t, ³J(H,H) = 7.6 Hz, 2H; Ar-H), 7.52 (t, ³J(H,H) = 7.5

Hz, 4H; Ar-H), 6.34 (d, $^3J(\text{H,H}) = 7.2$ Hz, 1H; CH), 4.68 (d, $^3J(\text{H,H}) = 7.0$ Hz, 1H; OH) ppm.

[(6-Ph₂TPA)Fe(CH₃CN)](ClO₄)₂ (2-ClO₄). Fe(ClO₄)₂·6H₂O (0.040 g, 0.11 mmol) was dissolved in CH₃CN (~2 mL), added to 6-Ph₂TPA (0.049 g, 0.11 mmol), and the resulting solution was stirred for 24 hours under an N₂ atmosphere. The solution was then concentrated under reduced pressure and the metal complex was precipitated by introducing excess Et₂O. The solid was then dried under reduced pressure (0.059 g, 73%). Et₂O diffusion into a CH₃CN solution of **2-ClO₄ afforded yellow crystals suitable for X-ray crystallography. Anal. Calcd for C₃₄H₃₂Cl₂FeN₆O₈: C, 52.39; H, 4.14; N, 10.78. Found: C, 52.12; H, 4.25; N, 11.24. $\mu_{\text{eff}} = 5.21 \mu_{\text{B}}$; UV-vis, nm (ϵ , M⁻¹cm⁻¹): 285 (14800); FTIR (KBr, cm⁻¹): 1093 (ν_{ClO_4}), 623 (ν_{ClO_4}).**

[(6-Ph₂TPA)Fe(CH₃CN)](OTf)₂·0.5CH₂Cl₂ (2-OTf). Fe(OTf)₂·2CH₃CN (0.11 mmol) was dissolved in CH₃CN (~2 mL), added to 6-Ph₂TPA (0.11 mmol) and the resulting mixture was stirred for 24 hours under a N₂ atmosphere. The solvent was then removed under reduced pressure and the metal complex precipitated by addition of excess hexanes to a CH₂Cl₂ solution. Anal. Calcd for C₃₄H₂₉F₆FeN₄O₆S₂·0.5CH₂Cl₂: C, 47.07; H, 3.44; N, 7.96. Found: C, 47.04; H, 3.58; N, 7.89. The presence of 0.5 equivalents of CH₂Cl₂ in the EA sample was confirmed by integration of the signal of this solvent in the ¹H NMR spectrum of the sample. $\mu_{\text{eff}} = 5.03 \mu_{\text{B}}$; FTIR (KBr, cm⁻¹): 1248 (ν_{OTf}), 1225 (ν_{OTf}), 1167 (ν_{OTf}), 1030 (ν_{OTf}).

[(6-Ph₂TPA)Fe(PhC(O)C(OH)C(O)Ph)]ClO₄ (3-ClO₄). Me₄NOH·5H₂O (0.0049 g, 0.026 mmol) was dissolved in CH₃CN (2.0 mL) and stirred with 2-hydroxy-1,3-diphenyl-propan-1,3-dione (0.0063 g, 0.026 mmol) for 2 minutes under a N₂

atmosphere. This solution was then added to a CH₃CN (1.0 mL) solution of **2-ClO₄** (0.026 mmol) and stirred for 5 minutes. The solvent was then immediately removed under reduced pressure. UV-vis, nm (ϵ , M⁻¹cm⁻¹): 385 (5080). FTIR (KBr, cm⁻¹): 3430 (ν_{OH}), 1094 (ν_{ClO_4}), 623 (ν_{ClO_4}).

[(6-Ph₂TPA)Fe(PhC(O)C(OH)C(O)Ph)]OTf (3-OTf). LiHMDS (0.015 g, 0.091 mmol) was dissolved in Et₂O (~2 mL) and added to a CH₃CN solution of 2-hydroxy-1,3-diphenyl-propan-1,3-dione (0.022 g, 0.090 mmol) under a N₂ atmosphere to form an orange solution that became cloudy after 1 minute. To this solution was added a CH₃CN solution of **2-OTf** (0.090 mmol) and the resultant slurry was stirred for 12 hours and then filtered through a glass wool/Celite plug. The filtrate was then combined with a second slurry of LiHMDS (0.091 mmol) and 2-hydroxy-1,3-diphenyl-propan-1,3-dione (0.091 mmol) in Et₂O/CH₃CN and stirred for 2 days. The solvent was removed under reduced pressure and the crude material was redissolved in CH₂Cl₂ and filtered through a celite plug. The compound was then precipitated, first by vapour diffusion of Et₂O into a CH₃CN solution, and then by addition of hexanes to a CH₂Cl₂ solution, to yield a brown solid (0.062 g, 71%). Anal. Calcd for C₄₇H₃₇F₃FeN₄O₆S•CH₂Cl₂: C, 58.08; H, 4.05; N, 5.77. Found: C, 58.03; H, 4.29; N, 5.39. $\mu_{\text{eff}} = 5.13 \mu_{\text{B}}$; UV-vis, nm (ϵ , M⁻¹cm⁻¹): 385 (8090); FTIR (KBr, cm⁻¹): 3430 (ν_{OH}), 1256 (ν_{OTf}), 1227 (ν_{OTf}), 1169 (ν_{OTf}), 1032 (ν_{OTf}).

[(6-Ph₂TPA)Fe(PhC(O)CHC(O)Ph)]ClO₄ (4). Me₄NOH•5H₂O (0.0067 g, 0.037 mmol) was dissolved in CH₃CN (~2 mL) and stirred with dibenzoylmethane (0.0076 g, 0.034 mmol) for ~1 hour under a N₂ atmosphere. This solution was then added to a CH₃CN (~2 mL) solution of **2-ClO₄** (0.034 mmol) and stirred for 18 hours to produce a dark red solution. The solvent was then removed under reduced pressure and the residue

was dissolved in CH_2Cl_2 and filtered through a glass wool/Celite plug. The filtrate was condensed under reduced pressure and precipitation of the product was induced by the addition of excess hexanes. Recrystallization of the crude product from $\text{CH}_3\text{CN}/\text{Et}_2\text{O}$ yielded red-brown crystals suitable for X-ray crystallography (0.016 g, 57%). Anal. Calcd for $\text{C}_{45}\text{H}_{37}\text{ClFeN}_4\text{O}_6$: C, 65.81; H, 4.54; N, 6.83. Found: C, 65.46; H, 4.57; N, 7.27. HRMS (ESI): m/z calcd for $\text{C}_{45}\text{H}_{37}\text{FeN}_4\text{O}_2^+$: 721.2266 [$M\text{-ClO}_4$] $^+$; found: 721.2279. $\mu_{\text{eff}} = 5.12 \mu_{\text{B}}$; UV-vis, nm (ϵ , $\text{M}^{-1}\text{cm}^{-1}$): 357 (13400); FTIR (KBr, cm^{-1}): 1094 (ν_{ClO_4}), 623 (ν_{ClO_4}).

2,2-dihydroxy-1,3-diphenylpropan-1,3-dione. Initially this triketone hydrate was prepared by exposing 1,3-diphenylpropantrione to moist air for several weeks, during which time it changed color from yellow to white. The hydrate may also be synthesized by crystallization of 1,3-diphenylpropantrione from wet ethanol. Notably the hydration is reversible, and dehydration will occur over the course of several hours when the hydrate is dissolved in dry solvent. ^1H NMR (300 MHz, CD_3CN , 25°C): $\delta = 7.98$ (d, $^3J(\text{H,H}) = 7.2$ Hz, 4H; Ar-H), 7.58 (t, $^3J(\text{H,H}) = 7.4$ Hz, 2H; Ar-H), 7.44 (t, $^3J(\text{H,H}) = 7.5$ Hz, 4H; Ar-H), 6.03 (s, 2H; OH) ppm. ^{13}C NMR (100.6 MHz, CD_3CN , 25°C): $\delta = 196.3$, 135.6, 131.3, 130.7, 130.1, 96.8 ppm.

Isomerization of 2-hydroxy-1,3-diphenyl-propan-1,3-dione promoted by 2-ClO_4 . Complex **2-ClO₄** (0.010 mmol) was dissolved in ~ 1 mL CH_3CN and to this solution was added a CH_3CN solution of 2-hydroxy-1,3-diphenyl-propan-1,3-dione (0.010 mmol) and $\text{Me}_4\text{NOH}\cdot 5\text{H}_2\text{O}$ (0.010 mmol) under a N_2 atmosphere. The resulting solution was stirred for 48 hours and the solvent was then removed under reduced

pressure. Analysis of the organic products by GC-MS and ^1H NMR showed the major product was 2-oxo-2-phenylethylbenzoate.

Reaction of 3-X with O_2 . A 3.0 mL aliquot of **3-X** (4.8 mM) in CH_3CN or 95% $\text{CH}_3\text{CN}/\text{H}_2\text{O}$ was placed in a vial. This solution was then purged with O_2 for 15 seconds, sealed and stirred for 12 hours. The solvent was then removed under reduced pressure. The organic products were analyzed by LC-MS as described below.

Control reaction testing for benzoylformic acid production from 2-hydroxy-1,3-diphenyl-propan-1,3-dione. $\text{Me}_4\text{NOH}\cdot 5\text{H}_2\text{O}$ (0.026 mmol) was dissolved in CH_3CN or 85% $\text{CH}_3\text{CN}/\text{H}_2\text{O}$ (1 mL) and was added to 2-hydroxy-1,3-diphenyl-propan-1,3-dione (0.026 mmol). This solution was then either diluted with 2 mL CH_3CN , or was combined with 0.026 mmol of either $[(6\text{-Ph}_2\text{TPA})\text{Ni}(\text{CH}_3\text{CN})(\text{H}_2\text{O})](\text{ClO}_4)_2$ or **2- ClO_4** dissolved in CH_3CN (2 mL), and stirred for 5 minutes. These solutions were then purged with O_2 , sealed and stirred for 12 hours. The solvent was then removed under reduced pressure. The organic products were analyzed by LC-MS as described below. Benzoylformic acid was only detected in the reaction involving **2- ClO_4** .

Control reaction testing for benzoylformic production from 1,3-diphenylpropantrione. Either 1,3-diphenylpropantrione (0.026 mmol) was dissolved in CH_3CN (1 mL), or 2,2-dihydroxy-1,3-diphenylpropan-1,3-dione was dissolved in 85% $\text{CH}_3\text{CN}/\text{H}_2\text{O}$ (1 mL). This solution was then either diluted with 2 mL CH_3CN , or combined with 0.026 mmol of either $[(6\text{-Ph}_2\text{TPA})\text{Ni}(\text{CH}_3\text{CN})(\text{H}_2\text{O})](\text{ClO}_4)_2$ or **2- ClO_4** dissolved in CH_3CN (2 mL). To each solution was added 31% H_2O_2 (0.026 mmol) and NEt_3 (0.026 mmol). The solutions were then sealed and stirred for 12 hours. The solvent

was then removed under reduced pressure. The organic products were analyzed by LC-MS as described below.

Control reactions testing for benzoylformic production from 2-oxo-2-phenylethylbenzoate. $\text{Me}_4\text{NOH}\cdot 5\text{H}_2\text{O}$ (0.026 mmol) was dissolved in CH_3CN or 85% $\text{CH}_3\text{CN}/\text{H}_2\text{O}$ (1 mL) and added to 2-oxo-2-phenylethylbenzoate (0.026 mmol). This solution was then either diluted with 2 mL CH_3CN or combined with **2- ClO_4** (0.026 mmol) dissolved in CH_3CN (2 mL) and stirred for 5 minutes. These solutions were then purged with O_2 , sealed and stirred for 12 hours. The solvent was then removed under reduced pressure. The organic products were then analyzed by LC-MS as described below. Benzoylformic acid was not detected for either of these reactions.

Reaction of 1,3-diphenylpropantrione with ferric salts. Under a nitrogen atmosphere, diphenylpropantrione or 2,2-dihydroxy-1,3-diphenylpropan-1,3-dione (0.026 mmol) was dissolved in CH_3CN or 85% $\text{CH}_3\text{CN}/\text{H}_2\text{O}$ (1 mL), respectively, and to these solutions was added FeCl_3 or $\text{Fe}(\text{ClO}_4)_3\cdot 6\text{H}_2\text{O}$ (0.105 mmol) in CH_3CN (2 mL). The solutions were then sealed and stirred for 12 hours. The solvent was then removed under reduced pressure. The organic products were then analyzed by LC-MS as described below.

Reaction of 2-hydroxy-1,3-diphenylpropan-1,3-dione with $\text{Fe}(\text{ClO}_4)_3\cdot 6\text{H}_2\text{O}$. Under a nitrogen atmosphere, $\text{Me}_4\text{NOH}\cdot 5\text{H}_2\text{O}$ (0.026 mmol) was dissolved in 85% $\text{CH}_3\text{CN}/\text{H}_2\text{O}$ (1 mL) and was added to 2-hydroxy-1,3-diphenylpropan-1,3-dione (0.026 mmol). To this solution was added $\text{Fe}(\text{ClO}_4)_3\cdot 6\text{H}_2\text{O}$ (0.105 mmol) in CH_3CN (2 mL). The solution was sealed and stirred for 12 hours. The solvent was then removed under

reduced pressure. The organic products were then analyzed by LC-MS as described below.

General procedure for organic product recovery and analysis. To each crude product mixture, 1 mL of 10 mM HCl and 3 mL Et₂O was added and stirred for three hours. The organic layer was then decanted and the aqueous layer extracted with a further 3 mL Et₂O. The organic fractions were combined and solvent evaporated under reduced pressure. Recovery of the organic material, determined as percent mass of the acireductone starting material, was typically ~80%. For further analysis, the organic products were redissolved in either CH₃CN (GC-MS) or 1:1 MeOH:H₂O (LC-MS). Products were identified by comparison to the retention times and fragmentation patterns of authentic compounds. The ratio of benzoic acid to benzoylformic acid was determined from a calibration curve based on peak area in the LC-MS spectrum.

¹⁸O labeling studies. For H₂¹⁸O labeling, a 3.0 mL aliquot of 4.8 mM **3-CIO₄** in CH₃CN was combined with a 10 μL aliquot of H₂¹⁸O under a nitrogen atmosphere. This solution was then exposed to ¹⁶O₂, sealed and stirred for 12 hours. The solvent was then removed under reduced pressure.

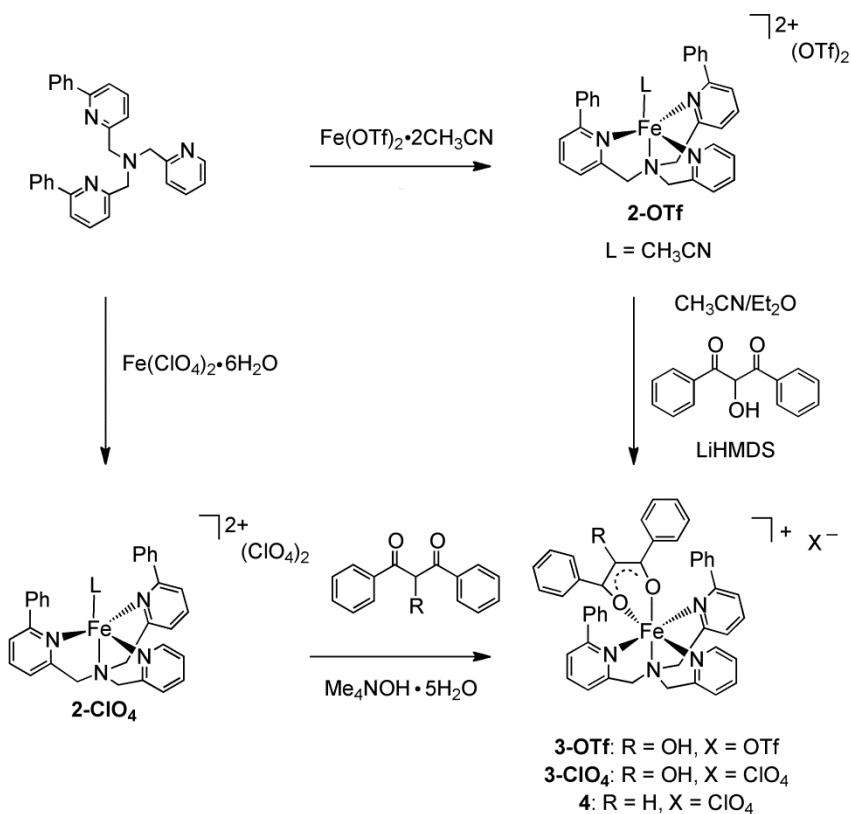
For ¹⁸O₂ labeling, a 3.0 mL aliquot of 4.8 mM **3-CIO₄** was placed in a solvent transfer flask from which the atmosphere was removed by three freeze-pump-thaw cycles. ¹⁸O₂ was then introduced into the flask, after which it was resealed and allowed to stir for 12 hours. The solvent was then removed under reduced pressure.

¹⁸O incorporation levels in benzoic acid and benzoylformic acid were determined from the relative intensities of the [M-1]⁻, [M+1]⁻ and [M+3]⁻ molecular ions in the LC-MS spectrum.

Results

Complex synthesis and characterization. In our initial attempts to generate an iron-containing analogue of **1**, admixture of equimolar amounts of $\text{Fe}(\text{ClO}_4)_2 \cdot 6\text{H}_2\text{O}$ and 6- Ph_2TPA in CH_3CN enabled the facile generation of $[(6\text{-Ph}_2\text{TPA})\text{Fe}(\text{CH}_3\text{CN})](\text{ClO}_4)_2$ (**2-ClO₄**) (Scheme 2-3). This compound has been isolated and comprehensively characterized (X-ray crystallography (Figure 2-1), elemental analysis, ^1H NMR, IR and a magnetic susceptibility measurement). When **2-ClO₄** is combined with the monoanion of the bulky acireductone in dry acetonitrile, a new complex, $[(6\text{-Ph}_2\text{TPA})\text{Fe}(\text{PhC}(\text{O})\text{C}(\text{OH})\text{C}(\text{O})\text{Ph})]\text{ClO}_4$ (**3-ClO₄**) is formed, however it has not been obtained in analytically pure form. Therefore, in an alternative synthetic approach, we combined the anhydrous salt $\text{Fe}(\text{OTf})_2 \cdot 2\text{CH}_3\text{CN}$ with 6- Ph_2TPA in dry CH_3CN , which led to the facile generation of $[(6\text{-Ph}_2\text{TPA})\text{Fe}(\text{CH}_3\text{CN})](\text{OTf})_2$ (**2-OTf**). Reaction of this complex with an excess of LiHMDS and acireductone under strictly anhydrous conditions allowed the generation and isolation of analytically pure $[(6\text{-Ph}_2\text{TPA})\text{Fe}(\text{PhC}(\text{O})\text{C}(\text{OH})\text{C}(\text{O})\text{Ph})]\text{OTf}$ (**3-OTf**). Thus far X-ray quality crystals of **3-X** (**X** = **ClO₄** or **OTf**) have not been obtained. Therefore, we have synthesized $[(6\text{-Ph}_2\text{TPA})\text{Fe}(\text{PhC}(\text{O})\text{CHC}(\text{O})\text{Ph})]\text{ClO}_4$ (**4**) by combining **2-ClO₄** with one equivalent of the anion of dibenzoylmethane, as outlined in Scheme 2-3, to use as a structural and ^1H NMR spectroscopic model to evaluate the coordination mode of the acireductone ligand in **3-X**. X-ray quality crystals of **4** were grown by diffusion of Et_2O into a CH_3CN solution of the complex.

X-ray crystallography. As shown in Figure 2-1, X-ray crystallographic studies of **2-ClO₄** revealed a cationic portion containing a single molecule of acetonitrile bound



Scheme 2-3. Synthesis of **2-4**. All reactions were performed under anaerobic conditions. CH_3CN was used as the solvent unless otherwise noted.

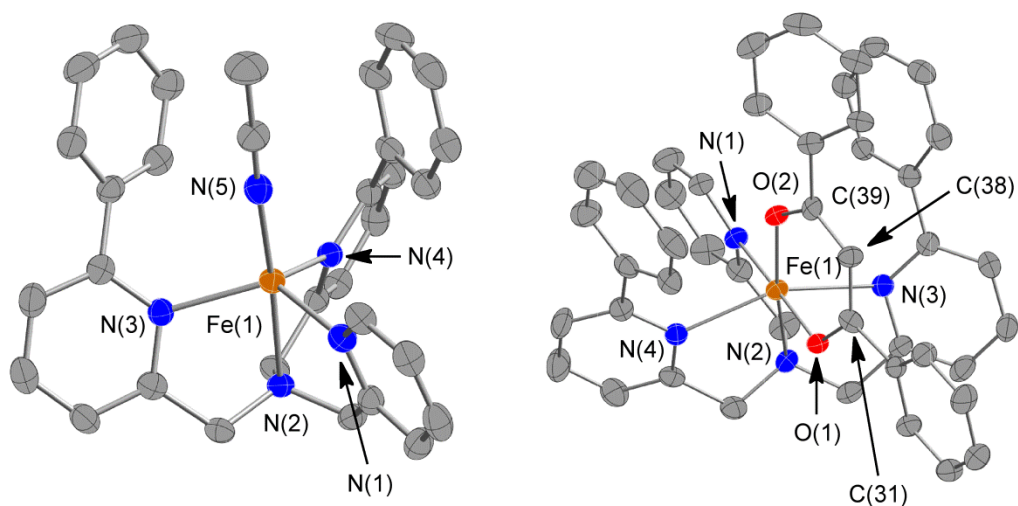


Figure 2-1. Thermal ellipsoid representation of the cationic portions of **2-ClO₄** (left) and **4** (right). Ellipsoids are drawn at 50% probability. Hydrogen atoms are omitted for clarity.

Table 2-1. Summary of X-ray Data Collection and Refinement.^a

	2-ClO₄	4•0.5CH₃CN
Formula	C ₃₆ H ₃₅ Cl ₂ FeN ₇ O ₈	C ₉₀ H ₇₄ Cl ₂ Fe ₂ N ₈ O ₁₂ •CH ₃ CN
<i>M_r</i>	820.46	1683.23
Crystal system	Monoclinic	Tetragonal
Space group	<i>P</i> 2 ₁ / <i>c</i>	<i>I</i> -4
<i>a</i> / Å	13.7317(3)	34.4839(4)
<i>b</i> / Å	19.1640(3)	34.4839(4)
<i>c</i> / Å	14.2994(4)	13.5578(2)
<i>α</i> / °	90	90
<i>β</i> / °	94.5399(10)	90
<i>γ</i> / °	90	90
<i>V</i> / Å ³	3751.14(15)	16122.1(4)
<i>Z</i>	4	8
<i>D_c</i> / Mg m ⁻³	1.453	1.387
<i>T</i> / K	150(1)	150(1)
Color	yellow	red-brown
Crystal shape	prism	plate
Crystal size / mm	0.28x0.23x0.15	0.35x0.35x0.05
<i>μ</i> / mm ⁻¹	0.606	0.497
F(000)	1696	6992
<i>θ</i> range / °	3.75-27.48	2.00-26.00
Completeness to <i>θ</i> / %	99.2	99.3
Reflections collected	15757	13636
Independent reflections	8519	13631
<i>R</i> _{int}	0.0365	0.0525
Data/restraints/ parameters	8519 / 0 / 595	13631/0/1057
GoF / <i>F</i> ²	1.022	1.012
<i>R</i> ₁ , w <i>R</i> ₂ / <i>I</i> > 2σ(<i>I</i>)	0.0542, 0.1379	0.0515, 0.0914
<i>R</i> ₁ , w <i>R</i> ₂ / all data	0.0811, 0.1569	0.0817, 0.1028
max./min. transmission	0.9146/0.8487	0.9756/0.8454
Δρ _{max/min} / eÅ ⁻³	0.696/-0.594	0.701/-0.395

^aRadiation used: Mo Kα (*λ* = 0.71073 Å); diffractometer: Nonius KappaCCD. Crystallographic files in CIF format for **2-ClO₄** and **4•0.5CH₃CN** have been deposited in The Cambridge Crystallographic Data Center (CCDC-954437). This data can be obtained free of charge via www.ccdc.cam.ac.uk/data_request/cif.

Table 2-2. Selected bond distances (Å) and angles (°) for **2-ClO₄** and **4·0.5CH₃CN**.**2-ClO₄**

Fe(1)-N(1)	2.090(2)	N(1)-Fe(1)-N(4)	108.19(9)
Fe(1)-N(2)	2.190(2)	N(1)-Fe(1)-N(5)	97.13(9)
Fe(1)-N(3)	2.149(2)	N(3)-Fe(1)-N(2)	76.11(9)
Fe(1)-N(4)	2.123(2)	N(1)-Fe(1)-N(2)	78.81(9)
Fe(1)-N(5)	2.096(2)	N(1)-Fe(1)-N(3)	123.11(9)
		N(5)-Fe(1)-N(2)	172.11(9)
		N(4)-Fe(1)-N(3)	113.93(9)
		N(5)-Fe(1)-N(3)	100.93(9)
		N(5)-Fe(1)-N(4)	111.60(9)
		N(4)-Fe(1)-N(2)	76.21(8)

4·0.5CH₃CN^a

Fe(1)-N(1)	2.156(3)	O(2)-Fe(1)-O(1)	88.82(12)
Fe(1)-N(2)	2.194(3)	O(2)-Fe(1)-N(1)	98.08(12)
Fe(1)-N(3)	2.371(4)	O(1)-Fe(1)-N(1)	172.73(13)
Fe(1)-N(4)	2.293(4)	O(2)-Fe(1)-N(2)	169.06(13)
Fe(1)-O(1)	2.012(3)	O(1)-Fe(1)-N(2)	94.92(12)
Fe(1)-O(2)	1.979(3)	N(1)-Fe(1)-N(2)	78.70(13)
O(1)-C(31)	1.278(5)	O(2)-Fe(1)-N(4)	111.32(13)
O(2)-C(39)	1.270(5)	O(1)-Fe(1)-N(4)	95.81(13)
C(31)-C(38)	1.408(6)	N(1)-Fe(1)-N(4)	79.61(13)
C(38)-C(39)	1.403(6)	N(2)-Fe(1)-N(4)	78.59(14)
		O(2)-Fe(1)-N(3)	96.72(12)
		O(1)-Fe(1)-N(3)	86.26(12)
		N(1)-Fe(1)-N(3)	95.13(12)
		N(2)-Fe(1)-N(3)	73.32(13)

^aData for one of two cations present in asymmetric unit.

to the iron center, resulting in a trigonal bipyramidal geometry ($\tau = 0.97$).²⁶ By contrast, **4**·**0.5CH₃CN** has a cationic portion containing a distorted octahedral Fe(II) center, with the dibenzoylmethane anion coordinated in a bidentate fashion via a six-membered chelate ring. A summary of the parameters of data collection, and selected bond distances and angles of **2** and **4**·**0.5CH₃CN** are presented in Table 2-1 and Table 2-2. As is expected for the fully delocalized diketonate anion, the C-O bond lengths (O(1)-C(31) 1.278(5)Å and O(2)-C(39) 1.270(5) Å) are similar, as are the C-C bond lengths within the chelate ring (C(31)-C(38) 1.408(6) Å and C(38)-C(39) 1.403(6) Å). The overall structural features of **4**·**0.5CH₃CN**, as well as the bond distances involving the coordinated diketonate anion, are highly similar to those found for the Ni(II)-containing acireductone complex **1**.¹²

¹H NMR Spectroscopy. A previous study on the paramagnetically-shifted features in the ¹H NMR spectra for a variety of nickel complexes with the same chelate ligand (6-Ph₂TPA) has demonstrated the sensitivity of the peak distribution pattern to the coordination of different anions.²² As shown in Figure 2-2, complex **3-CIO₄** exhibits signals in the paramagnetically-shifted region of the ¹H NMR spectrum that are very similar to those exhibited by the dibenzoylmethane complex **4**, albeit the signals for **3-CIO₄** are shifted slightly upfield.²⁷ By contrast, the solvate complex **2-CIO₄** has a distinctly different pattern of peaks in the paramagnetic region. It is also worth noting that **2-OTf** and **3-OTf** have the same peak distribution patterns as **2-CIO₄** and **3-CIO₄**, respectively. On the basis of these spectroscopic comparisons, we formulate the solution structure of **3-X** as [(6-Ph₂TPA)Fe(PhC(O)C(OH)C(O)Ph)]X wherein, similar to the

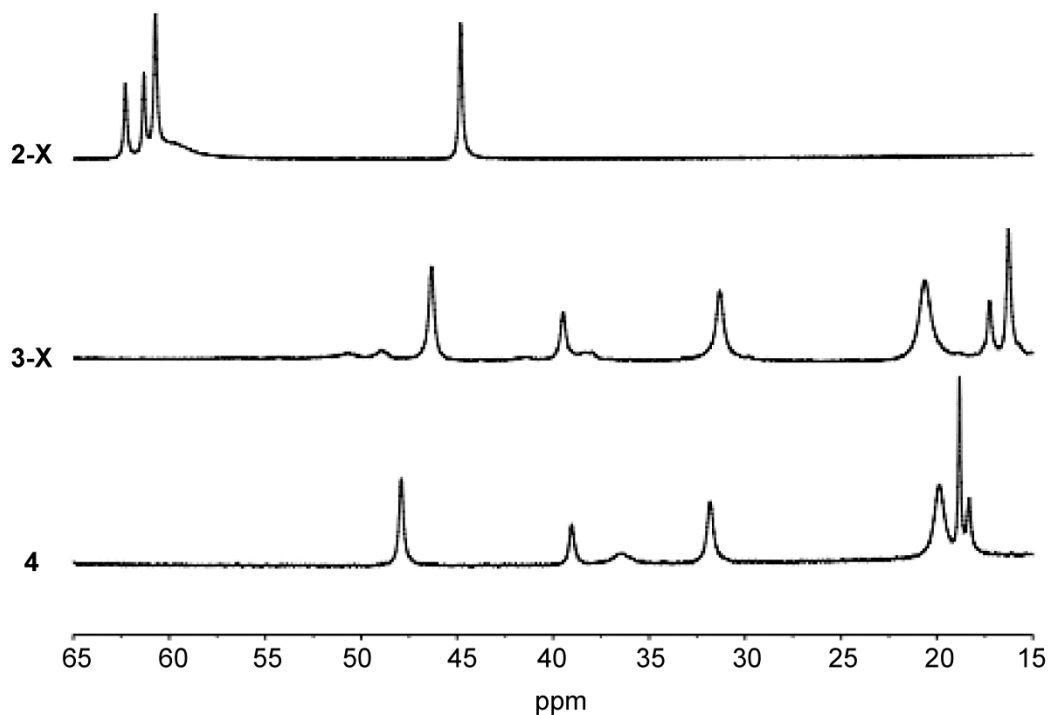


Figure 2-2. Comparison of selected paramagnetically shifted features in the ^1H NMR spectra of 2-4. Spectra were measured in CD_3CN using a 400 MHz spectrometer at 298 K.

Table 2-3. ^1H NMR shifts for selected paramagnetic compounds (ppm).

2-OTf	2-ClO ₄	3-OTf ^a	4 ^a
112.9	113.6	127.3	131.5
102.1	101.5	92.7	94.5
85.8	84.7	80.2	77.2
60.5	60.5	67.6	67.0
62.5	62.3	45.9	48.1
61.2	61.3	40.4	39.3
60.6	60.7	30.3	36.6
44.8	44.8	21.3	32.0
9.8	9.9	17.2	19.9
4.6	4.6	16.5	18.9
4.5	4.4	10.6	18.5
-8.8	-8.6		
-12.3	-12.3		

^a 3-OTf and 4 both contain additional overlapping peaks in the diamagnetic region, partially due to the diketone phenyl protons, that are not presented in this table.

Ni(II)-analog **1**, the bulky acireductone is bound via a six-membered chelate ring. A summary of the chemical shifts of ^1H NMR resonances of **2-OTf**, **2-CfO₄**, **3-OTf**, and **4** is presented in Table 2-3.

UV-vis and Infrared Spectroscopy. The absorption spectra of **3-CfO₄** and **3-OTf** exhibit features with $\lambda_{\text{max}} = 385$ nm, albeit with differing extinction coefficients depending on the counter ion (5080 and $8090 \text{ M}^{-1}\text{cm}^{-1}$ respectively). We attribute this absorption band primarily to a $\pi\text{-}\pi^*$ transition of the acireductone diketonate that is coordinated to the iron center, consistent with our structural proposal of the acireductone being bound via a six-membered chelate ring. Similar features are found for both **4** ($\lambda_{\text{max}} = 357$ nm; hypsochromically shifted, as expected in the absence of the hydroxyl group) and **1** ($\lambda_{\text{max}} = 399$ nm) when dissolved in acetonitrile (Figure 2-3).¹² We note that a shoulder feature on the longer wavelength side of the $\pi\text{-}\pi^*$ transition of **3-X** and **4** may be due to an MLCT transition as has been identified in spectroscopic studies of Dke1 and

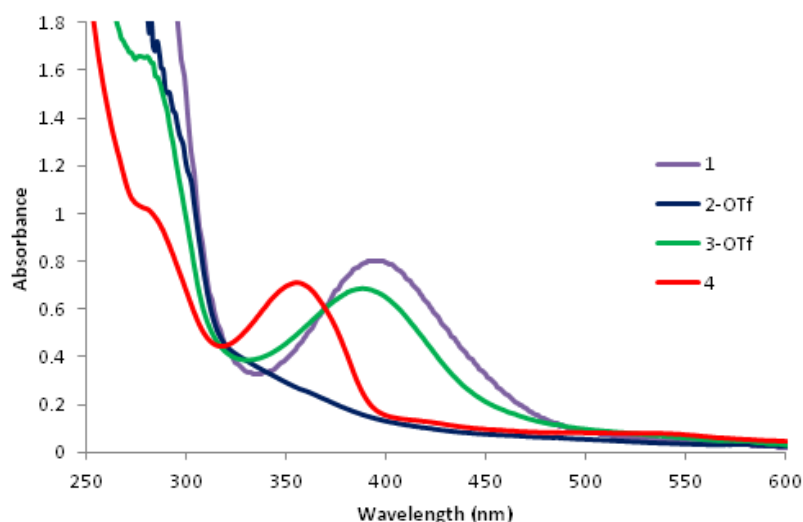


Figure 2-3. UV-vis spectra for **1-4** in CH_3CN .

relevant model compounds.^{28,29}

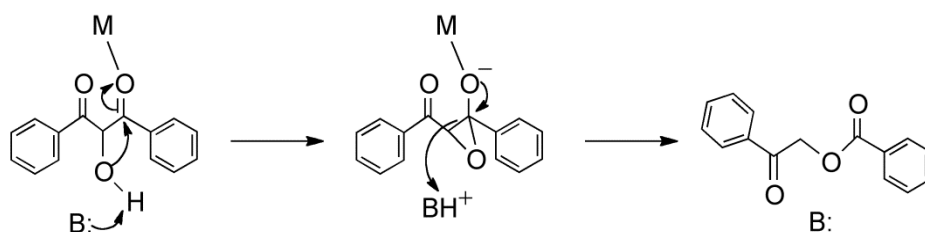
The proposed six-membered chelate is additionally supported by the IR spectral features of **3-X** wherein a O-H stretch is present at $\sim 3430\text{ cm}^{-1}$, and no free C=O stretch is found at $\sim 1700\text{ cm}^{-1}$. If the acireductone were coordinated as a five-membered ring, the hydroxyl group would instead likely be deprotonated and a free C=O moiety would be present.

Thus, in contrast to the proposed binding mode of the acireductone in the enzyme-substrate complex wherein changing the metal center from Ni to Fe changes the binding mode of the acireductone from a six-membered to a five-membered chelate ring, in our synthetic systems, our acireductone binds via a six-membered chelate when either metal ion is present. This is unsurprising, as the difference in Lewis acidity between Ni(II) and Fe(II) is modest, and is not proposed as the factor that differentiates the binding mode in the enzyme. It is, rather, changes in the tertiary structure of the enzyme, resulting in a more open binding pocket in Fe-ARD' that are proposed to direct the acireductone to bind via a five-membered chelate.³⁰ Our model systems have the same secondary structural features, as defined by having the same 6-Ph₂TPA chelate ligand, and thus exhibit the same binding mode for the acireductone. Therefore, our model system is an ideal case to test the chelate hypothesis for the differing reactivity of Fe-ARD' and Ni-ARD; if the proposal is correct, our iron-containing complexes **3-X** should exhibit the same dioxygenase reactivity as our previously reported nickel-containing system **1**.

Anaerobic Reactivity. Our inability to generate analytically pure **3-ClO₄** has been due to an anaerobic water-promoted isomerization reaction of the acireductone ligand. The exclusion of water in the synthesis of **3-OTf** was likely the factor that

allowed its generation in analytically pure form. Evidence for the formation of **3-ClO₄**, followed by its subsequent decay, was found by monitoring (UV-vis) of a reaction mixture wherein an acetonitrile solution of **2-ClO₄** was combined with the bulky acireductone anion under anaerobic conditions. Slow decay of the 385 nm absorption band was observed upon prolonged stirring, and analysis of the organic products by GC-MS showed that the ester 2-oxo-2-phenylethylbenzoate, an isomer of the bulky acireductone, had been produced. This same isomerization reactivity has been previously reported for the Co(II) analog [(6-Ph₂TPA)Co(PhC(O)C(OH)C(O)Ph)]ClO₄ (**5**), wherein a water and Lewis acid-mediated isomerization reaction of the acireductone ligand resulted in the formation of the same ester (2-oxo-2-phenylethylbenzoate, Scheme 2-4).²¹ By contrast, the nickel-containing complex **1** does not efficiently promote this isomerization chemistry under wet conditions. We also note that in the O₂ reactivity studies of **3-ClO₄** described below, the reaction to generate ester is always operative.

Aerobic reactivity. Exposure of acetonitrile solutions of **3-X** to O₂ at ambient temperature results in the rapid bleaching of the 385 nm absorption feature (Figure 2-4), indicating decomposition of the acireductone anion. Analysis of the headspace gas of the



Scheme 2-4. Proposed mechanism for the Lewis acid-mediated isomerization of 2-hydroxy-1,3-diphenylpropan-1,3-dione in the presence of a base to form 2-oxo-2-phenylethylbenzoate.

reaction vessel shows that CO has been produced qualitatively. After prolonged exposure to O₂, total loss of the well-defined paramagnetically-shifted features in the ¹H NMR spectrum is observed, consistent with a change in oxidation state from Fe(II) to Fe(III). Our attempts to isolate and characterize the iron-containing products of these oxygenation reactions have thus far been unsuccessful, presumably due to the poor affinity of Fe(III), a hard Lewis acid, for the aryl-appended TPA ligand. However, acidification of the crude reaction mixture followed by extraction with Et₂O has allowed us to analyze the organic compounds produced in the decomposition of the acireductone. In the reaction of **3-OTf** with O₂, the major products observed were benzoic acid and

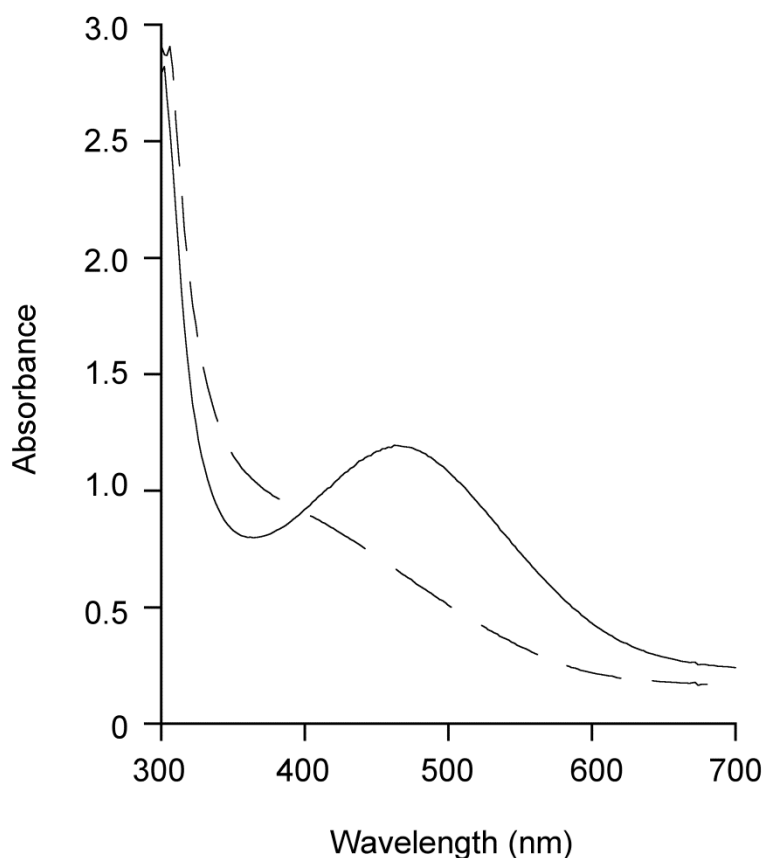
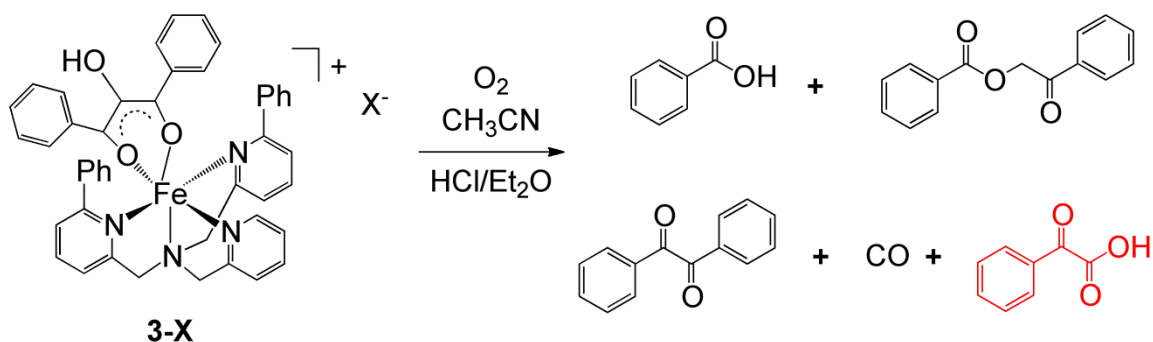


Figure 2-4. UV-vis spectra of **3-ClO₄** in CH₃CN before (solid line) and after (dashed line) the addition of O₂.

benzil, along with small amounts of the ester (Scheme 2-5). These products were the same as were observed in the reaction of the Ni analogue **1** with O₂²⁰, and thus are generally consistent with the chelate hypothesis, which predicts that **3-OTf** and **1**, having the same six-membered chelate ring for acireductone binding, should produce the same products in a dioxygenase reaction.



Scheme 2-5. Organic products detected in the reaction of **3-X** with O₂ in CH₃CN.

Benzoylformic acid (red) was only detected when X = ClO₄ or when the reaction of **3-OTf** was performed with the addition of H₂O.

It was therefore very surprising to discover that benzoylformic acid is produced in the reaction of **3-ClO₄** with O₂, in addition to the other products produced in the reaction of **3-OTf** (Scheme 2-5; Figure 2-5). Benzoylformic acid is an α -keto acid, and is the expected product in the oxidation of the bulky acireductone if it were undergoing Fe-ARD' type reactivity. Given that all our spectroscopy detailed above strongly suggests that **3-OTf** and **3-ClO₄** have the same solution structure, precluding a five-membered chelate, this change in reactivity was very interesting. Our initial hypothesis was that the ester initially formed by an isomerization reaction could undergo a separate oxygenation reaction to generate benzoyl-2-oxo-2-phenylethanoate. This anhydride would

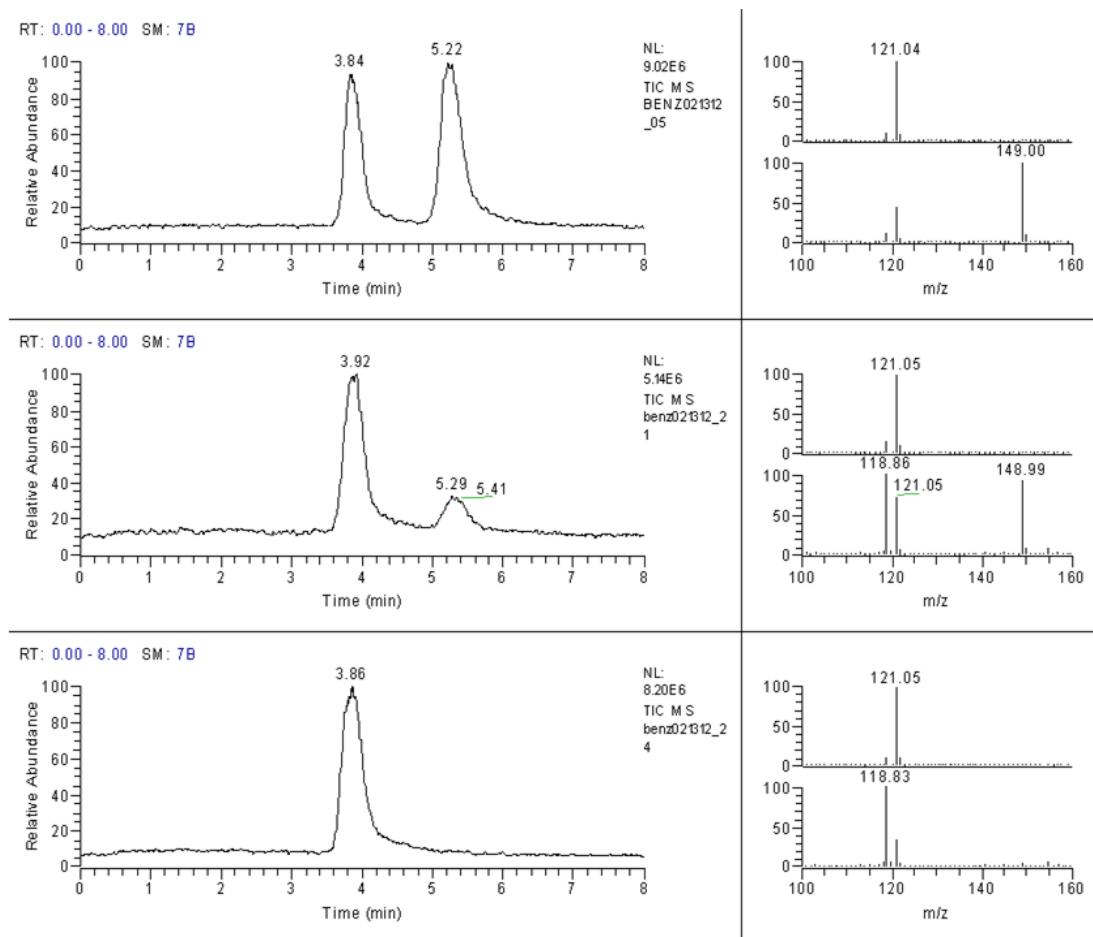
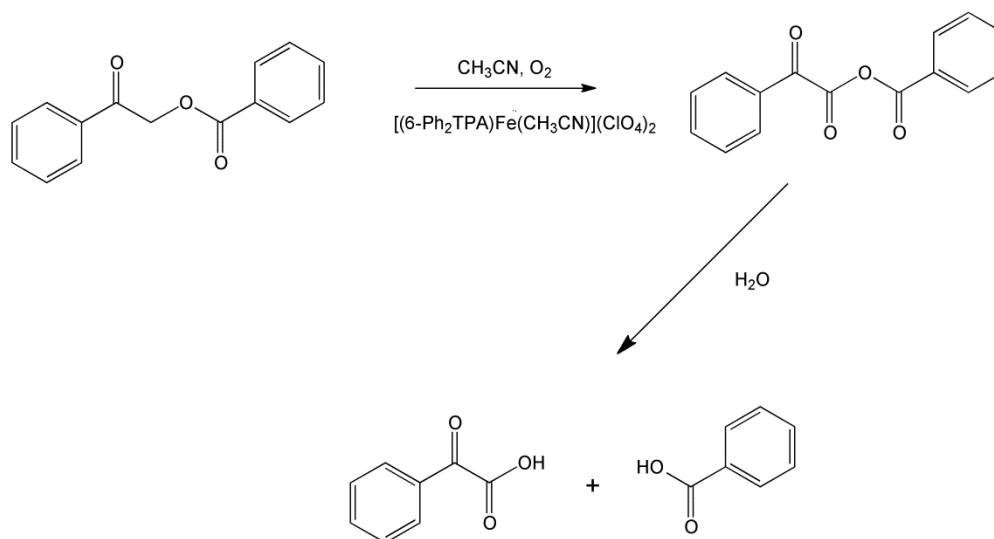


Figure 2-5. LC-MS data showing the chromatogram of a 1:1 benzoic acid:benzoylformic acid standard (top), and these products generated from the reaction of **3-ClO₄** with O₂ (middle), and reaction of **1** with O₂ (bottom). Mass spectra on the right show the relative abundance of molecular ions in each chromatogram from 3.5-4.5 min (upper) and 5-6 min (lower), corresponding to the presence of benzoic acid ($[M-1]^- = 121$ m/z) and benzoylformic acid ($[M-1]^- = 149$ m/z), respectively.

subsequently undergo hydrolysis to generate the observed benzoylformic acid (and an equivalent of benzoic acid, Scheme 2-6). However, a control reaction in which the ester was exposed to O₂ in the presence of **2-ClO₄** did not lead to the generation of benzoylformic acid. Rather only trace amounts of the hydrolytic products benzoic acid and 2-hydroxyacetophenone were detected in addition to unreacted ester.



Scheme 2-6. Proposed reaction pathway for the formation of benzoylformic acid from 2-oxo-2-phenylethylbenzoate. A control experiment showed that this reaction did not proceed.

Kinetics. In order to gain more insight into why **3-ClO₄** exhibits different regioselectivity in C-C bond cleavage than **1** and **3-OTf**, we undertook mechanistic studies. For both **3-ClO₄** and **3-OTf**, the reaction is found to be first order in each of **3-X** and O₂, with an overall rate constant, $k_2 = 0.40 \text{ M}^{-1}\text{s}^{-1}$ (Figures 2-6 and 2-7). The similarity of the rate in each case implies they have the same rate-determining step, and the differentiation in terms of reactivity likely occurs after the acireductone itself has

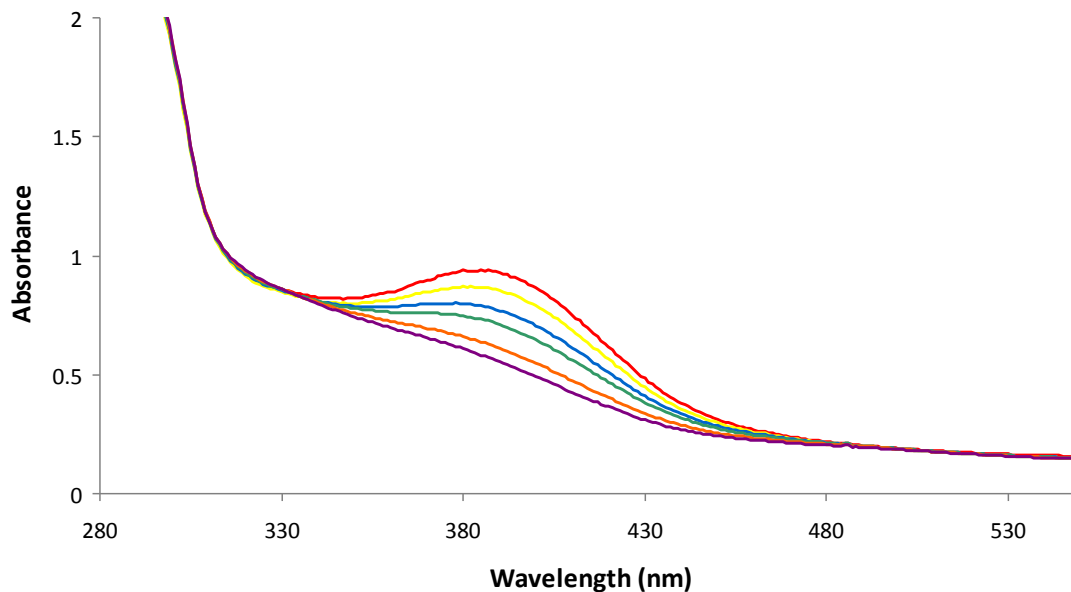


Figure 2-6. UV-vis spectra following the decay of **3-OTf** in the presence of O_2 at selected time intervals. An isosbestic point is observed at 332 nm.

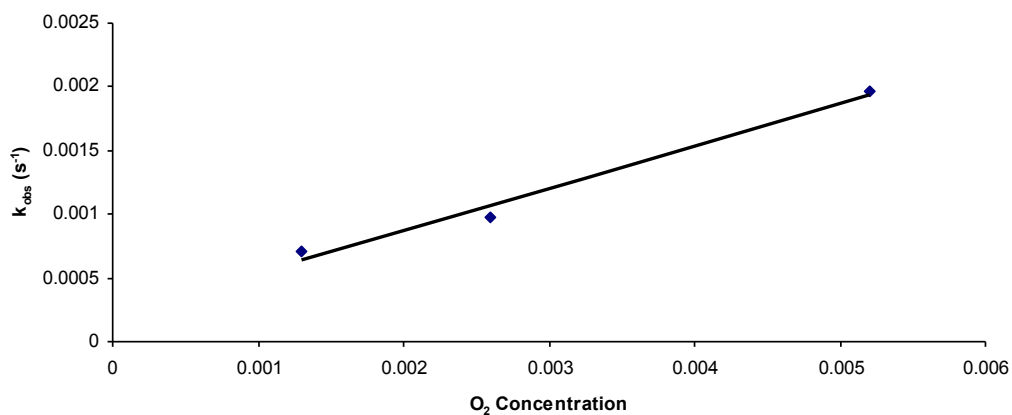
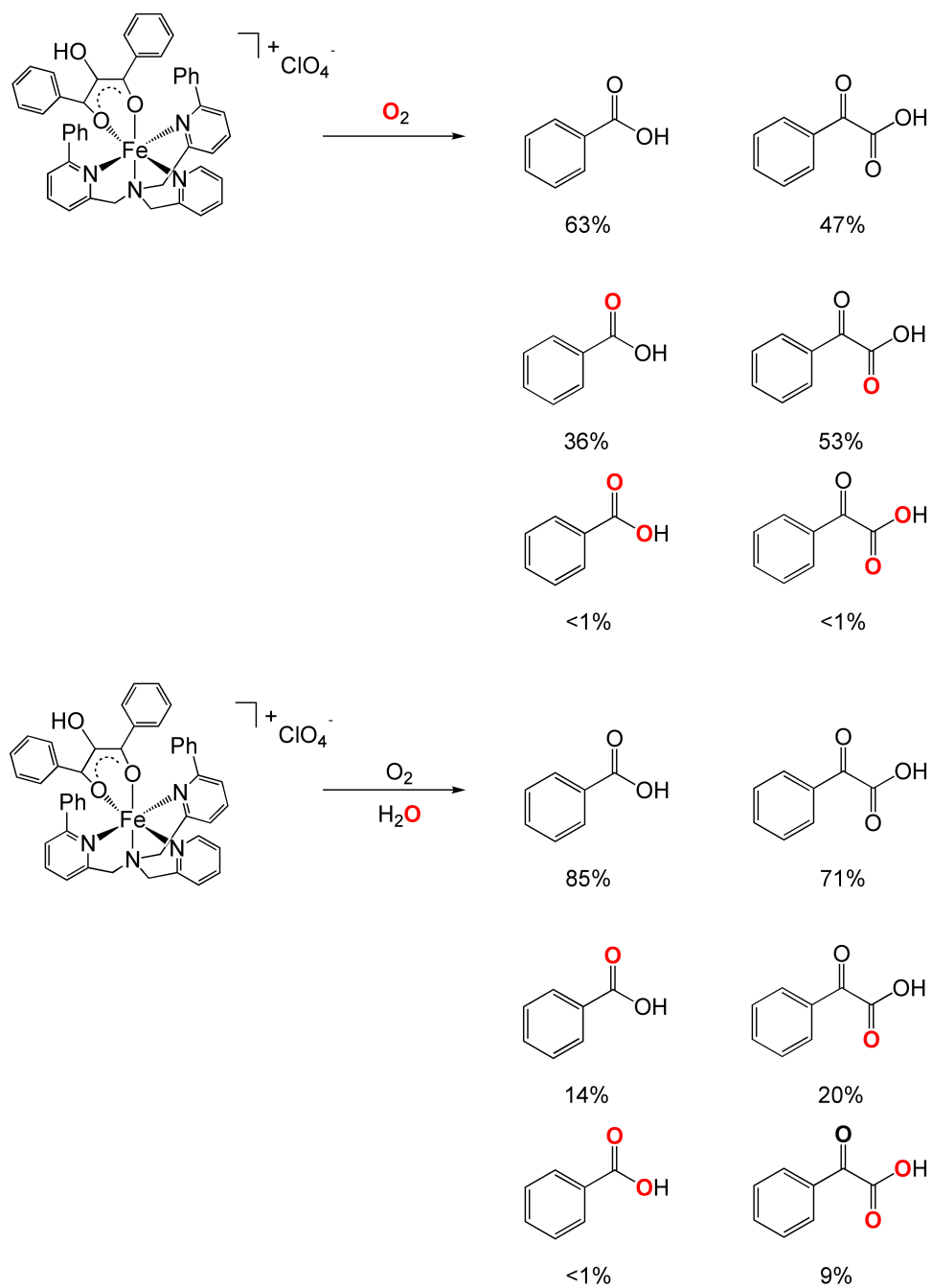


Figure 2-7. Plot of $k_{obs} (s^{-1})$ versus $[O_2]$ (M) for the reaction of **3-OTf** (0.47mM) in CH_3CN at $20^\circ C$. $[O_2]$ was changed by adding varying aliquots of O_2 - and N_2 -saturated CH_3CN to the reaction cell.

been consumed. It is also worth noting that these reactions are slightly slower than was observed in the analogous reaction of **1** ($k = 1.7 \text{ M}^{-1}\text{s}^{-1}$).¹³

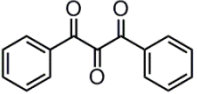
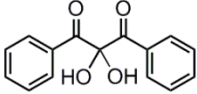
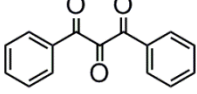
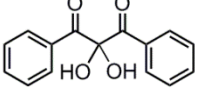
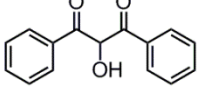
Investigations of Fe/O₂ Reactivity. A common paradigm in dioxygenase reactions involving a ferrous center is the direct metal-centered activation of O₂, forming a ferric-superoxo species. Speculating that such a species could be partially responsible for the differentiation in reactivity between **1** and **3-CIO₄**, we investigated its feasibility. The formation of such a species would require the dissociation of one of the phenyl-appended pyridyl arms of the chelate ligand to open up a coordination position. Low temperature ¹H NMR studies of **4** in CD₃CN (-40°C) and CD₃OD (-70°C) have shown no evidence of loss of the C_s symmetry of the complex, suggesting that dissociation of a chelate ligand arm is unlikely to be occurring. Additionally, in the reaction of **3-X** with O₂ in acetonitrile at -40°C, we have observed no intermediates consistent with the formation of a ferric-superoxo species by UV-vis. Attempts to intercept a superoxo intermediate by hydrogen atom abstraction from common probes such as dihydroanthracene, 2,4-di-^tbutylphenol and 2,4,6-tri-^tbutylphenol have all yielded a negative result.³¹ Based on these results we conclude that it is unlikely that the reaction proceeds via a ferric-superoxo intermediate.

Isotopic labeling. Labeling studies of the reaction of **3-CIO₄** with ¹⁸O₂ show a modest incorporation of a single label into both benzoic acid (36%) and benzoylformic acid (53%). We hypothesized that water in the reaction mixture (due to the use of the pentahydrate base Me₄NOH·5H₂O to generate **3-CIO₄**) was at least partially responsible for the loss of label, as addition of H₂¹⁸O to the ¹⁶O₂ reaction results in modest label incorporation (Scheme 2-7). To probe whether water could have a role in the reaction, we



Scheme 2-7. ¹⁸O labeling studies in the reaction of 3-ClO₄ with O₂. Relative abundance was determined by intensity of appropriate molecular ions in the relevant LC-MS spectrum.

Table 2-4. Summary of production of benzoylformic acid.

Reaction	Solvent	Benzoic acid ^a	Benzoylformic acid ^a
3-OTf $\xrightarrow{\text{O}_2}$	CH ₃ CN	100	0
3-CfO₄ $\xrightarrow{\text{O}_2}$	CH ₃ CN	82	18
3-OTf $\xrightarrow{\text{O}_2}$	95% CH ₃ CN/H ₂ O	81	19
3-OTf $\xrightarrow{\text{O}_2}$	50% CH ₃ CN/H ₂ O	64	36
 $\xrightarrow[\text{2-CfO}_4]{\text{HO}_2^{-b}}$	CH ₃ CN	83	17
 $\xrightarrow[\text{2-CfO}_4]{\text{HO}_2^{-b}}$	95% CH ₃ CN/H ₂ O	73	27
 $\xrightarrow{\text{2 FeCl}_3}$	CH ₃ CN	100	0
 $\xrightarrow{\text{2 Fe(CfO}_4)_3 \cdot 6\text{H}_2\text{O}}$	95% CH ₃ CN/H ₂ O	61	39
 $\xrightarrow[\text{4 Fe(CfO}_4)_3 \cdot 6\text{H}_2\text{O}]{\text{Me}_4\text{NOH} \cdot 5\text{H}_2\text{O}}$	95% CH ₃ CN/H ₂ O	67	33

^aRelative percentage of the total amount of benzoic acid and benzoylformic acid determined by LCMS peak area. Benzil and ester are additional products not presented in this table. ^bHO₂⁻ generated in situ by combining 1.1 equivalents of 30% H₂O₂ (aq) and NEt₃.

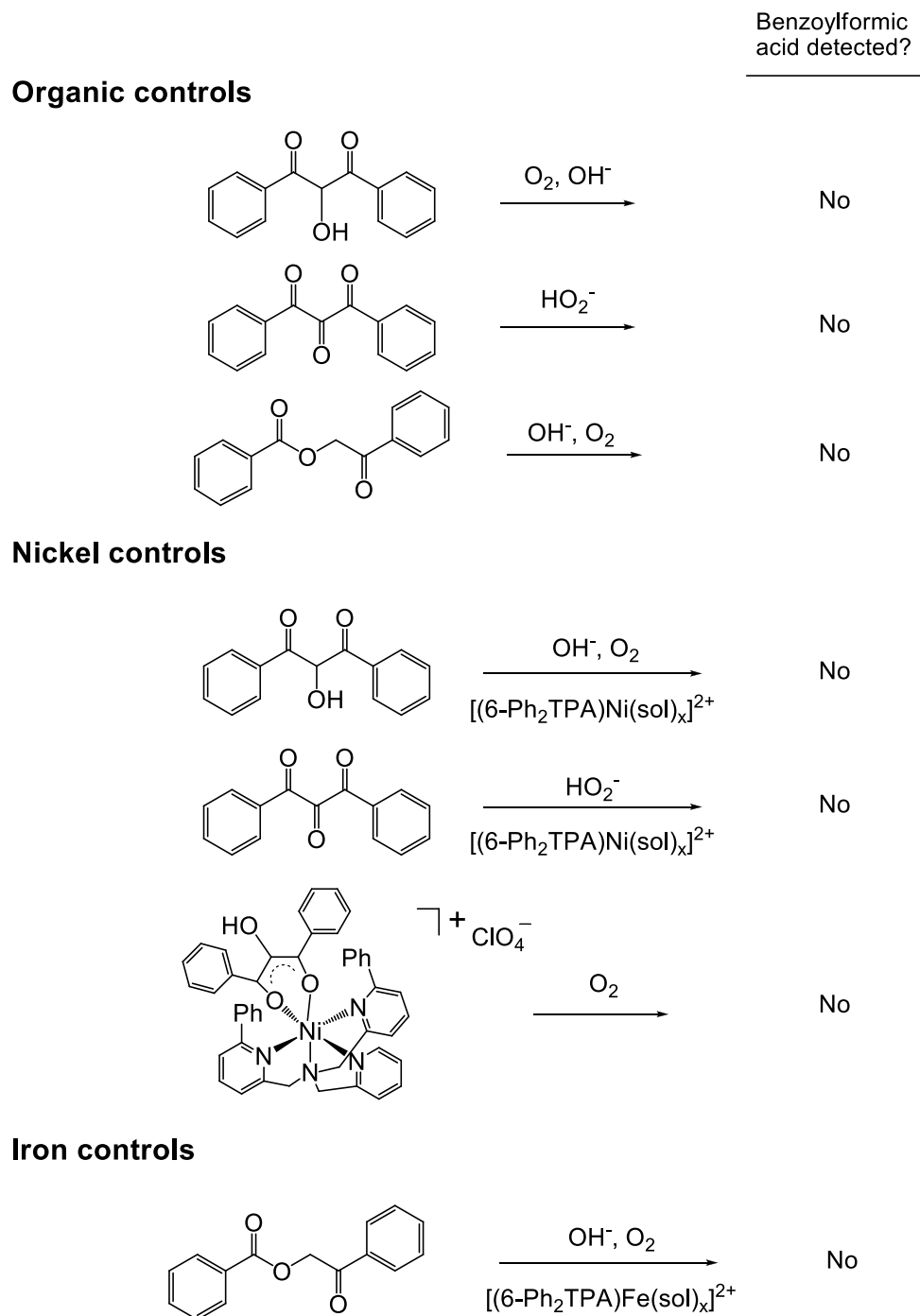
repeated the reaction of **3-OTf** with O₂ in the presence of 5% added water. Gratifyingly, we observed the production of benzoylformic acid (Table 2-4), therefore indicating that the presence of water had been the reason for the differing observed reactivities of **3-OTf** and **3-CfO₄**.

Scope of α -keto acid formation. Having established the importance of water in the generation of the α -keto acid, we conducted a series of control reactions specifically searching for benzoylformic acid formation. Most importantly, we have reinvestigated

the products generated in the reaction of the nickel complex **1** with O₂ in both pure CH₃CN and 95% CH₃CN/H₂O using the work-up procedure and analysis methods (GC-MS and LC-MS) employed for the O₂ reaction of **3-X**. Notably, no benzoylformic acid formation was detected starting from **1** (Scheme 2-8; Figure 2-5 (LC-MS)). Additionally, reaction of the triketone (1,3-diphenylpropantrione) in the presence of the hydroperoxide anion and [(6-Ph₂TPA)Ni(CH₃CN)(H₂O)](ClO₄)₂ resulted in no detectable benzoylformic acid formation (Scheme 2-8). Treatment of the tetramethylammonium salt of the bulky acireductone anion with O₂ also failed to yield any α-keto acid formation. Taken together, these results imply that both water and an iron center are required for α-keto acid formation.

Raising the amount of water present in the reaction of **3-OTf** with O₂ results in a marked increase in the amount of benzoylformic acid produced, as summarized in Table 2-4. However, we have been unable to generate equimolar amounts of benzoic acid and benzoylformic acid regardless of the amount of water present in the system. Interestingly, reaction of the triketone (the two-electron oxidized form of the acireductone) with HO₂⁻ in the presence of a ferrous complex also results in the generation of benzoylformic acid. When the same reaction is repeated, starting from the hydrated triketone (2,2-dihydroxy-1,3-diphenylpropan-1,3-dione) an increase in the amount of benzoylformic acid produced is observed (Table 2-4). These results suggest that the water-sensitivity of the oxidation chemistry is due to the hydration of a triketone intermediate.

We have also investigated the role of ferric species in the reaction chemistry. Attempts to isolate ferric complexes by the combination of Fe(ClO₄)₃·6H₂O, 6-Ph₂TPA, Me₄NOH·5H₂O and the bulky acireductone have been unsuccessful. Monitoring these



Scheme 2-8. Summary of the detection of benzoylformic acid in control reactions. Each reaction was carried out in CH₃CN, and also in 95% CH₃CN/H₂O. Regardless of solvent conditions, no benzoylformic acid was detected in any of these control reactions.

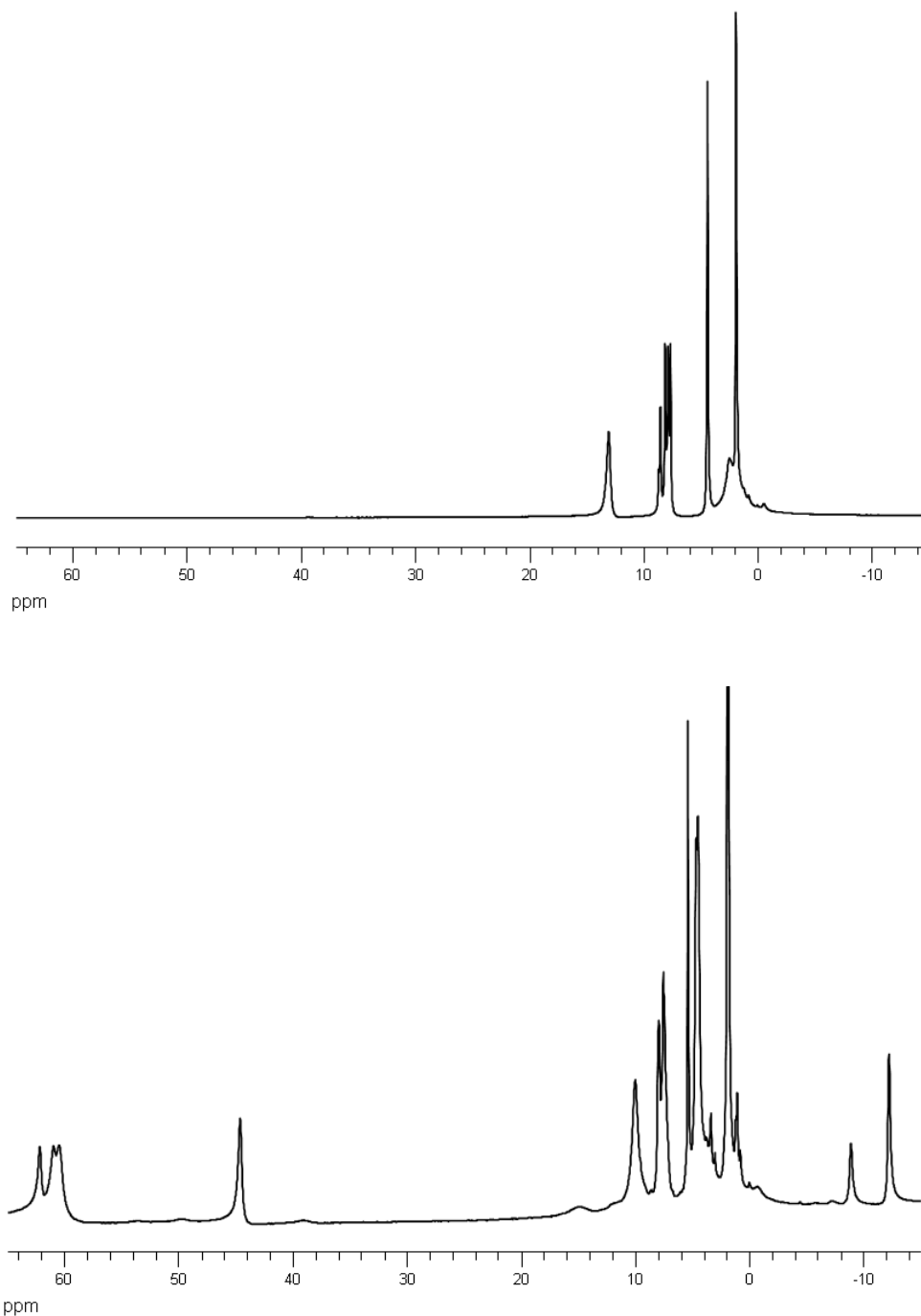
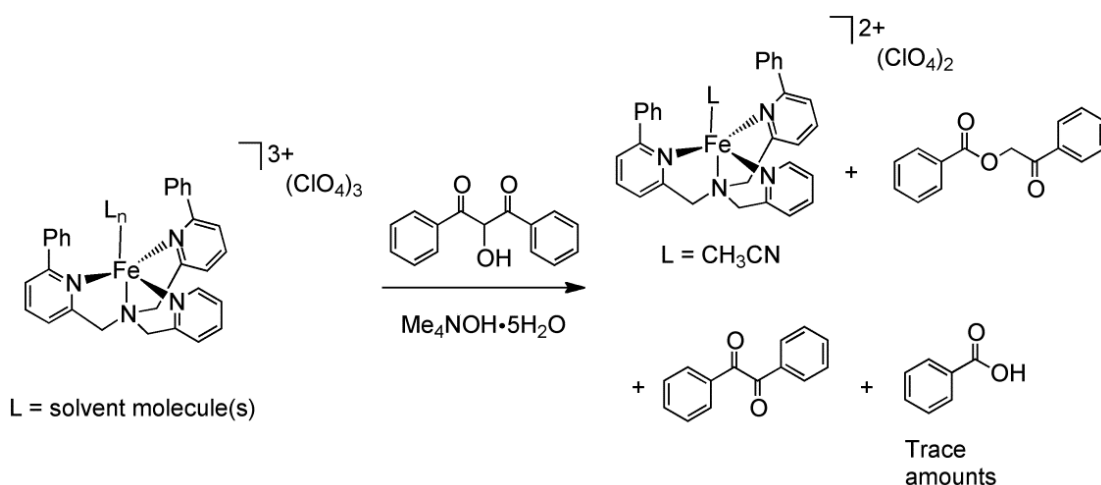


Figure 2-8. $[(6\text{-Ph}_2\text{TPA})\text{Fe}(\text{sol})_x](\text{ClO}_4)_3$ before (top) and after (bottom) the addition of $[\text{Me}_4\text{N}][\text{PhC}(\text{O})\text{C}(\text{OH})\text{C}(\text{O})\text{Ph}]$. The bottom spectrum is consistent with the formation of a ferrous species, and is likely $[(6\text{-Ph}_2\text{TPA})\text{Fe}(\text{CH}_3\text{CN})](\text{ClO}_4)_2$ (**2-ClO₄**); c.f. Figure 2-2.

reactions by ^1H NMR in the paramagnetic region shows the growth of peaks consistent with the reduction of Fe^{III} to form the ferrous species **2-ClO₄** (Figure 2-8). Subsequent analysis of the organic products of this reaction shows the production of the ester as a major species as well as triketone, and trace amounts of benzoic acid (Scheme 2-9). Given that ferric/ferrous couple is a one-electron process, we next combined four equivalents of a ferric salt with the acireductone anion, or two equivalents with the triketone. As shown in Table 2-4, these reactions also lead to carbon-carbon bond cleavage, with the regioselectivity influenced by the water content of the reaction mixture. We note that the ferric-mediated oxidative cleavage of vicinal triketones in water has previously been reported,³² and the oxidation of acireductone analogues, such as ascorbic acid by ferric ions, is well documented.^{33, 34} This oxidation of an acireductone in the absence of molecular oxygen is particularly interesting due to the recent discovery of the operation of a methionine salvage pathway under anaerobic conditions.³⁵



Scheme 2-9. Attempted synthesis of $[(6\text{-Ph}_2\text{TPA})\text{Fe}(\text{PhC}(\text{O})\text{C}(\text{OH})\text{C}(\text{O})\text{Ph})](\text{ClO}_4)_2$, and the resulting products including oxidized organic species.

Discussion

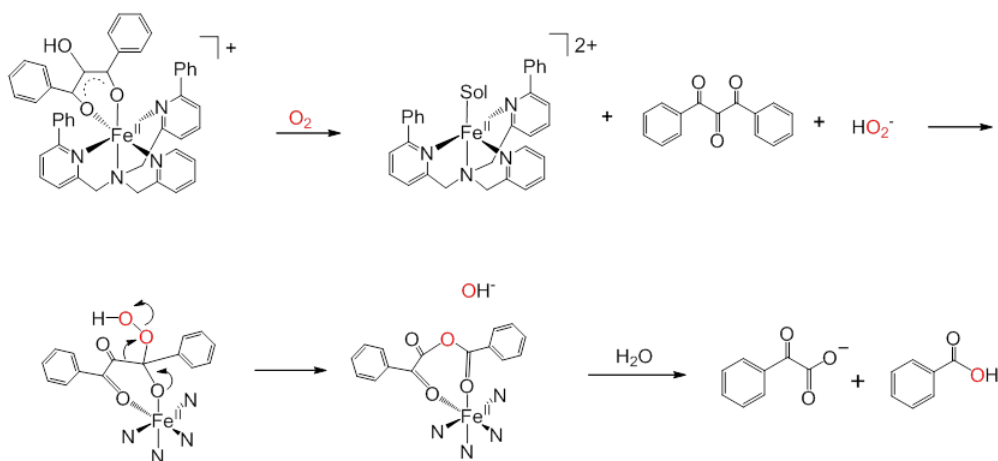
The chelate ring hypothesis was formulated on the basis of a number of observations in studies of Ni-ARD and Fe-ARD'.⁹ First, oxygen uptake studies, as well as spectroscopic studies performed in the presence of oxygen, provided no evidence for oxygen binding at the active site in either metal-containing form of the enzyme. Additionally, Fe-ARD'-type reactivity was found to occur when the enzyme is reconstituted with magnesium, implying that iron-centered redox activity may not be important in directing the regiospecificity of the reaction. Second, NMR studies provided evidence for a metal-dependent entropy switch that converts the active site tertiary structure between a closed (Ni-ARD) and open (Fe-ARD') form. Docking studies show that the acireductone would likely coordinate via a five-membered chelate in Fe-ARD', but in the more congested Ni-ARD active site, it would bind via a less sterically-demanding six-membered chelate.³⁰ These binding modes would activate the C(1)/C(2) or C(1)/C(3) positions, respectively for reaction with oxygen (Scheme 2-1), leading in turn to the proposed products for the Fe-ARD' and Ni-ARD catalyzed reactions. Notably, the structural data currently available for enzyme-substrate (ES) adducts of Fe-ARD' or Ni-ARD, respectively, is limited to XAS data, which does not provide definitive proof of the substrate coordination motif.⁹ Additionally, the UV-vis absorption features of the ES adducts are similar, which may actually indicate that there is no difference in binding mode.

Our previous studies of a nickel-containing complex (**1**) supported the chelate hypothesis in terms of the coordination mode of the bulky acireductone ligand, which is

akin to that proposed for the ES complex of Ni-ARD. The O₂ reactivity of **1**, while resulting in the formation of Ni-ARD type products, proceeded via a different pathway than that being proposed for the enzyme. Specifically, the initial reaction in the model system leads to the formation of triketone and hydroperoxide intermediates from which carbon-carbon bond cleavage was found to occur. In the enzyme, the coordinated acireductone is proposed to react directly with O₂ to give a coordinated cyclic peroxide species from which aliphatic C-C bond cleavage occurs. The results described herein show that a simple change in the metal ion from Ni(II) in **1** to Fe(II) in **3-X**, while maintaining the same supporting ligand coordination environment, has no effect on the coordination mode of the bulky acireductone. However, despite the congruence of the structure of **1** and **3-X**, α -keto acid formation was found to occur upon reaction of **3-X** with O₂ in the presence of water. Thus, an oxidative pathway is accessible, leading to a change in the regiospecificity of carbon-carbon bond cleavage that does not require distinct acireductone coordination motifs. This result is in contrast to the chelate hypothesis, and shows that this hypothesis is not sufficient to explain the chemistry encountered in our model system.

An alternative proposed mechanism for the cleavage of the C(1)-C(2) bond in Fe-ARD' is a Baeyer-Villiger type oxidation (Scheme 2-10).¹³ In this reaction, a carbonyl moiety migrates to the peroxo oxygen in the tetrahedral intermediate to form an anhydride with subsequent release of OH⁻. Subsequent hydrolysis of this species would generate the observed α -keto acid product. This is an attractive proposition, as differences in the electronic structure of Fe(II) and Ni(II) could be used to rationalize the ability of **3-X** to promote this reaction more efficiently than **1**. Fe(II) is a known catalyst for Baeyer-

Villiger oxidations,⁴² and a prior computational study has shown that in oxidative cleavage of the bulky acireductone the transition state for a Baeyer-Villiger reaction is only 3.5 kcal/mol, suggesting that subtle variations in reaction conditions (i.e. Ni(II) vs Fe(II)) would be sufficient to change the reaction selectivity.¹³ However, while this Baeyer-Villiger pathway does include a hydrolytic step, it may be ruled out as it makes no provision for the necessity of water in changing the reaction regioselectivity.



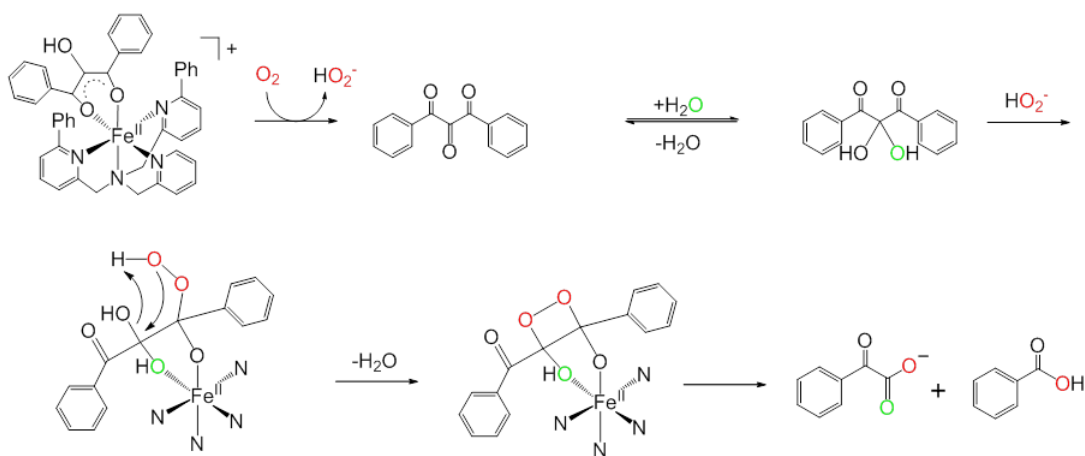
Scheme 2-10. A possible pathway for the reaction of **3-X** leading to the formation of benzoylformic acid via a Baeyer-Villiger oxidation. The regioselectivity of this reaction does not depend upon the presence of water.

In the reaction of **3-X** with O₂ in the presence of water we never observe the formation of benzoic acid and benzoylformic acid in an equimolar ratio (Table 2-4). Thus, there are always at least two oxidative pathways operative. Regardless of conditions, it appears that an O₂ reaction akin to that found for **1** is always operative in the Fe(II)-containing system. This reaction leads to the formation of two equivalents of benzoic acid and carbon monoxide. When water is added, a new reaction pathway is

enabled wherein one equivalent each of benzoic acid and benzoylformic acid are generated. Because complex **1** exhibits only the first type of reactivity, comparative studies of the reactivity of **1** and **3-X** enable us to probe for the chemical factors that enable α -keto acid formation. From these studies we find that regardless of metal ion or water content of the system, the initial step is the two-electron oxidation of the acireductone by dioxygen to form a triketone and the hydroperoxide anion as intermediates. This proposal is supported by our previous mechanistic studies of the O_2 reaction of **1**, as well as kinetic studies that show a similar rate-determining step for the oxidation of **1** and **3-X** in the presence or absence of water. The involvement of triketone and hydroperoxide intermediates is also supported by studies involving authentic triketone and hydrogen peroxide in the presence of the corresponding [(6- Ph_2TPA) $M(CH_3CN)_x$] $^{2+}$ ($M = Ni$ ($x = 2$) or Fe ($x = 1$)) complex. In these reactions we observed similar regioselectivity, as in the reaction of **1** or **3-X**, indicating that it is at the triketone level that a differentiation in the chemistry occurs.

In the absence of water, the triketone intermediate formed in the O_2 reactions of **1** and **3-X** will undergo reaction with the hydroperoxide anion to selectively cleave the C(1)-C(2) and C(2)-C(3) bonds and release CO. This chemistry is consistent with that previously reported by Pochapsky wherein 2,3,4-pentanetrione was shown to undergo reaction with H_2O_2 to give two equivalents of acetic acid and carbon monoxide.³⁶ For **3-X** in the presence of water, we propose that an additional reaction pathway is operative due to hydration of the triketone intermediate. Triketone hydration is a well-known process, and the central carbonyl of diphenyltriketone is the most electrophilic and therefore will be the site of initial hydration.³⁷ Once formed, we propose that the hydrated

triketone may interact with the iron center to form a five-membered chelate ring (Scheme 2-11), which becomes susceptible to attack by hydroperoxide at an activated terminal carbonyl moiety. Formation of a four-membered dioxetane ring via loss of water would generate the species from which C(1)-C(2) bond cleavage and α -ketoacid formation could occur.



Scheme 2-11. Proposed reaction pathway involving triketone hydration as a means to generate Fe-ARD'-type products containing oxygen atoms derived from both O₂ and H₂O.

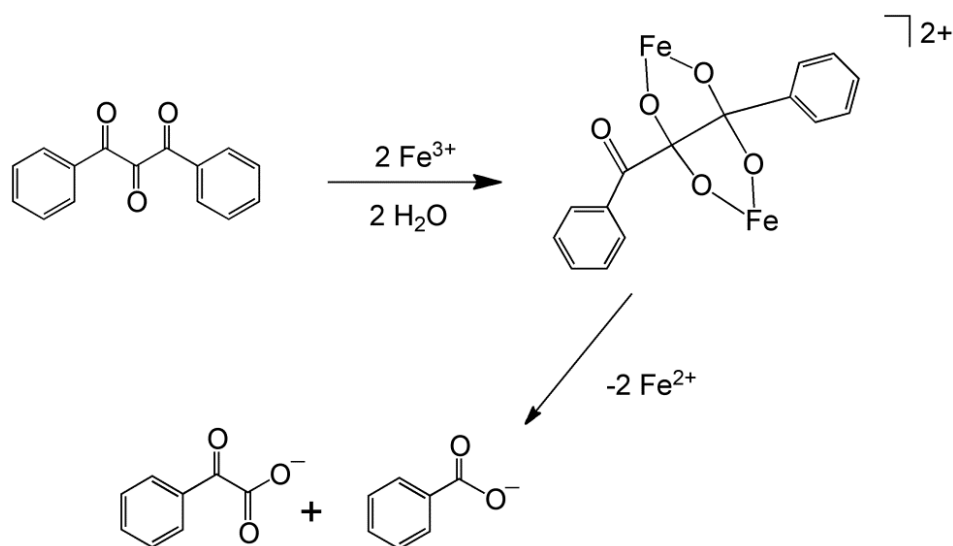
The reaction pathway outlined in Scheme 2-11 shows that it is the hydration and subsequent coordination of an intermediate, not differences in chelation involving the acireductone substrate itself (chelate hypothesis), that determine the regioselectivity of the reaction. This is in contrast to the reaction pathways of other metal-containing dioxygenases and their model systems wherein changes in the primary and/or secondary environment of the metal center determine the regioselectivity of carbon-carbon bond cleavage.³⁸ In terms of ARD enzymes, it is important to note that the active site in Fe-ARD' is much more open, and thus solvent-exposed, when compared to the Ni-ARD

active site wherein a tryptophan loop maintains a hydrophobic microenvironment.³⁰ The reaction pathway shown in Scheme 2-11 provides a means for ¹⁸O incorporation from ¹⁸O₂ in the α-ketoacid product. The substoichiometric ¹⁸O incorporation that is found in the α-keto acid generated in the O₂ reaction of **3-X** (~50%), and in the dioxygenase reactivity of Fe-ARD' (~78%),³⁹ suggests that water exchange may be important for both the model system and the enzyme. The involvement of a triketone-type intermediate in the enzymatic system cannot currently be ruled out on the basis of either experimental or computational studies. Therefore, our future work will involve approaches toward examining the feasibility of a triketone-type pathway in reactions involving C(1)-H-containing ARD substrates. We note that recent advances in the synthesis of C(1)-H triketones will be instrumental in carrying out this work.⁴⁰

Of course the question then arises as to why the C(1)-C(2) cleavage pathway leading to α-keto acid formation is not operative for the nickel-containing complex **1**. Our working hypothesis is that the Ni(II) center does not effectively mediate the hydration of the triketone intermediate, preventing this species from forming in significant amounts during the reaction progression. This hypothesis is supported by the differing anaerobic, water-dependent bulky acireductone isomerization chemistry of the nickel and iron complexes **1** and **3-X**. While **1** does not undergo isomerization of the acireductone, **3-X** undergoes rapid isomerization in the presence of water (Scheme 2-4). Similar water-dependent isomerization of the acireductone to the ester, as well as subsequent hydrolysis, was also observed in solutions containing the cobalt complex **5**. Interestingly, the solid state structures of the solvate complexes [(6-Ph₂TPA)M(CH₃CN)_x]²⁺ are pentacoordinate, with a single solvent molecule when M =

Fe or Co, but hexacoordinate with two solvent molecules when $M = \text{Ni}$.¹⁹ The differing coordination preferences for the metal ions in these systems may be responsible for the differences in Lewis acid activation for the triketone and/or water that would influence the formation of hydrated triketone and acireductone isomerization.

We note that an alternative route for α -keto acid formation could involve the direct oxidation a hydrated triketone by ferric ions generated in solution (Scheme 2-12). In this regard, it would be expected that ferric ions could rapidly promote hydration of the triketone, and previous studies have demonstrated ferric-mediated oxidative cleavage of vicinal triketones in aqueous solutions to give α -keto acid and carboxylic acid products.³² While this type of reactivity is certainly viable in our systems, it would not explain the observed isotope incorporation data, wherein ^{18}O from $^{18}\text{O}_2$ is incorporated into the α -keto acid product.⁴¹ In this regard, our studies do not exclude a pathway wherein the HO_2^-



Scheme 2-12. Proposed sequence for hydrated triketone aliphatic carbon-carbon bond cleavage promoted by ferric iron species.

produced in the reaction of **3-X** with O₂ first oxidizes Fe(II) to Fe(III), which then acts as Lewis acid to mediate triketone hydration. The hydrated triketone could then react with an additional equivalent of HO₂⁻ to give Fe-ARD' type products wherein the ¹⁸O label from ¹⁸O₂ would be incorporated.

Conclusion

The chelate hypothesis had remained unchallenged in the literature to date as an explanation for the differing regiospecificity of Ni-ARD and Fe-ARD' without the need to invoke metal-centered redox chemistry, which has not been observed in the native enzymes. In this first study of an iron-containing model system, designed to directly probe this hypothesis, we have found that the chelate hypothesis is not necessary to explain the differentiation in reactivity. Rather, in our model system, a difference between nickel and iron in the hydration of a triketone intermediate allows a change in regioselectivity of the reaction. This is an alternative proposition for the Fe-ARD' reaction, as it would be accounted for by the differences in solvent accessibility in the active sites of Ni-ARD and Fe-ARD' without a need to dismiss the similarity in absorption spectra for the enzyme-substrate adducts. The notion of hydration of an intermediate as the key factor differentiating regioselectivity also provides a potential framework for understanding how oxidation of an acireductone may occur in anaerobic systems using oxidants other than dioxygen.

References

- [1] Lange, S. J.; Que, L. Jr. *Curr. Opin. Chem. Biol.* **1998**, *2*, 159-172.
- [2] Bugg, T. D. H.; Ramaswamy, S. *Curr. Opin. Chem. Biol.* **2008**, *12*, 134-140.
- [3] Broderick, J. B. *Essays Biochem.* **1999**, *34*, 173-189.
- [4] Straganz, G. D.; Glieder, A.; Brecker, L.; Ribbons, D. W.; Steiner, W. *Biochem. J.* **2003**, *369*, 573-581.
- [5] Hopper, D. J.; Kaderbhai, M. A. *Biochem. J.* **1999**, *344*, 397-402.
- [6] Cicchillo, R. M.; Zhang, H.; Blodgett, J. A.; Whitteck, J. T.; Li, G.; Nair, S. K.; van der Donk, W. A.; Metcalf, W. W. *Nature* **2009**, *459*, 871-874.
- [7] Wray, J. W.; Abeles, R. H. *J. Biol. Chem.* **1993**, *268*, 21466-21469.
- [8] Albers, E. *IUBMB Life* **2009**, *61*, 1132-1142
- [9] Pochapsky, T. C.; Ju, T.; Dang, M.; Beaulieu, R.; Pagani, G. M.; OuYang, B. In *Metal Ions in Life Sciences*; Sigel, A., Sigel, H., Sigel, R. K. O., Eds.; Wiley-VCH: Weinheim, Germany, 2007; Vol. 2, pp 473-500.
- [10] Dai, Y.; Wensink, P. C.; Abeles, R. H. *J. Biol. Chem.* **1999**, *274*, 1193-1195.
- [11] Motterlini, R.; Otterbein, L. E. *Nat. Rev. Drug Discov.* **2010**, *9*, 728-743.
- [12] Szajna, E.; Arif, A. M.; Berreau, L. M. *J. Am. Chem. Soc.* **2005**, *127*, 17186-17187.
- [13] Berreau, L. M.; Borowski, T.; Grubel, K.; Allpress, C. J.; Wikstrom, J. P.; Germain, M. E.; Rybak-Akimova, E. L.; Tierney, D. L. *Inorg. Chem.* **2011**, *50*, 1047-1057.
- [14] Roberts, J. D.; Smith, D. R.; Lee, C. C. *J. Am. Chem. Soc.* **1951**, *73*, 618-625.

- [15] Armarego, W. L. F.; Perrin, D. D. *Purification of Laboratory Chemicals*, 4th ed., Butterworth–Heinemann, Boston, MA, 1996.
- [16] Hagen, K.S. *Inorg. Chem.* **2000**, *39*, 5867-5869.
- [17] So, J.-H.; Boudjouk, P. *Inorg. Chem.* **1990**, *29*, 1592-1593.
- [18] Plietker, B. *J. Org. Chem.* **2003**, *68*, 7123-7125.
- [19] Makowska-Grzyska, M. M.; Szajna, E.; Shipley, C.; Arif, A. M.; Mitchell, M. H.; Halfen, J. A.; Berreau, L. M. *Inorg. Chem.* **2003**, *43*, 7472-7488.
- [20] Szajna-Fuller, E.; Rudzka, K.; Arif, A. M.; Berreau, L. M. *Inorg. Chem.* **2007**, *46*, 5499–5507.
- [21] Grubel, K.; Ingle, G. K.; Fuller, A. L.; Arif, A. M.; Berreau, L. M. *Dalton Trans.* **2011**, *40*, 10609-10620.
- [22] Szajna, E.; Dobrowolski, P.; Fuller, A. L.; Arif, A. M.; Berreau, L. M. *Inorg. Chem.* **2004**, *43*, 3988–3997.
- [23] Evans, D. F. J. *Chem. Soc.* **1959**, 2003-2005.
- [24] Achord, J. M.; Hussey, C. L. *Anal. Chem.* **1980**, *52*, 601-602.
- [25] Wolsey, W. C. *J. Chem. Educ.* **1973**, *50*, A335-A337.
- [26] Addison, A. W.; Rao, T. N.; Reedijk, J.; van Rijn, J.; Vershcoor, G. C. *J. Chem. Soc., Dalton Trans.* **1984**, 2177-2184.
- [27] The X-ray crystallographically-characterized Ni(II) bulky acireductone complex **1** and its dibenzoylmethane analog, [(6-Ph₂TPA)Ni(PhC(O)CHC(O)Ph)]ClO₄, exhibited a similar ¹H NMR spectral congruence. Szajna-Fuller, E.; Rudzka, K.; Arif, A. M.; Berreau, L. M. *Inorg. Chem.* **2007**, *46*, 5499-5507.

- [28] (a) Park, H.; Baus, J. S.; Lindeman, S. V.; Fiedler, A. T. *Inorg. Chem.* **2011**, *50*, 11978-11989. (b) Park, H.; Bittner, M. M.; Baus, J. S.; Lindeman, S. V.; Fiedler, A. J. *Inorg. Chem.* **2012**, *51*, 10279-10289.
- [29] Diebold, A. R.; Neidig, M. L.; Moran, G. R.; Straganz, G. D.; Solomon, E. I. *Biochemistry* **2010**, *49*, 6945-6952.
- [30] Ju, T.; Goldsmith, R. B.; Chai, S. C.; Maroney, M. J.; Pochapsky, S. S.; Pochapsky, T. C. *J. Mol. Biol.* **2006**, *363*, 823-834.
- [31] Mukherjee, A.; Cranswick, M. A.; Chakrabarti, M.; Paine, T. K.; Fujisawa, K.; Münck, E.; Que, L., Jr. *Inorg. Chem.* **2010**, *49*, 3618-3628.
- [32] Mecinović, J.; Hamed, R. B.; Schofield, C. J. *Angew. Chem., Int. Ed. Engl.* **2009**, *48*, 2796-2800.
- [33] Taqui Khan, M. M.; Martell, A. E. *J. Am. Chem. Soc.* **1967**, *89*, 4176-4185.
- [34] Kim, Y. J.; Feng, X.; Lippard, S. J. *Inorg. Chem.* **2007**, *46*, 6099-6107.
- [35] (a) Singh, J.; Tabita, F. R. *J. Bacteriology* **2010**, *192*, 1324-1331. (b) Sekowska, A.; Déneraud, V.; Ashida, H.; Michoud, K.; Haas, D.; Yokota, A.; Danchin, A. *BMC Microbiology*, **2004**, *4*:9. (c) Imker, H. J.; Fedorov, A. A.; Fedorov, E. V.; Almo, S. C.; Gerlt, J. A. *Biochemistry*, **2007**, *46*, 4077-4089.
- [36] Dai, Y.; Pochapsky, T. C.; Abeles, R. H. *Biochemistry* **2001**, *40*, 6379-6387.
- [37] Rubin, M.B.; Gleiter, R. *Chem. Rev.* **2000**, *100*, 1121-1164.
- [38] Costas, M.; Mehn, M. P.; Jensen, M. P.; Que, L., Jr. *Chem. Rev.* **2004**, *104*, 939-986.
- [39] Wray, J. W.; Abeles, R. H. *J. Biol. Chem.* **1995**, *270*, 3147-3153.

- [40] Goswami, S.; Maity, A. C.; Fun, H.-K.; Chantrapromma, S. *Eur. J. Org. Chem.* **2009**, 1417-1426.
- [41] No isotope incorporation from dioxygen into the ferric-oxidized products was observed in the previous study.³²
- [42] Strukul, G. *Angew. Chem. Int. Ed. Engl.* **1998**, 37, 1198-1209.

CHAPTER 3

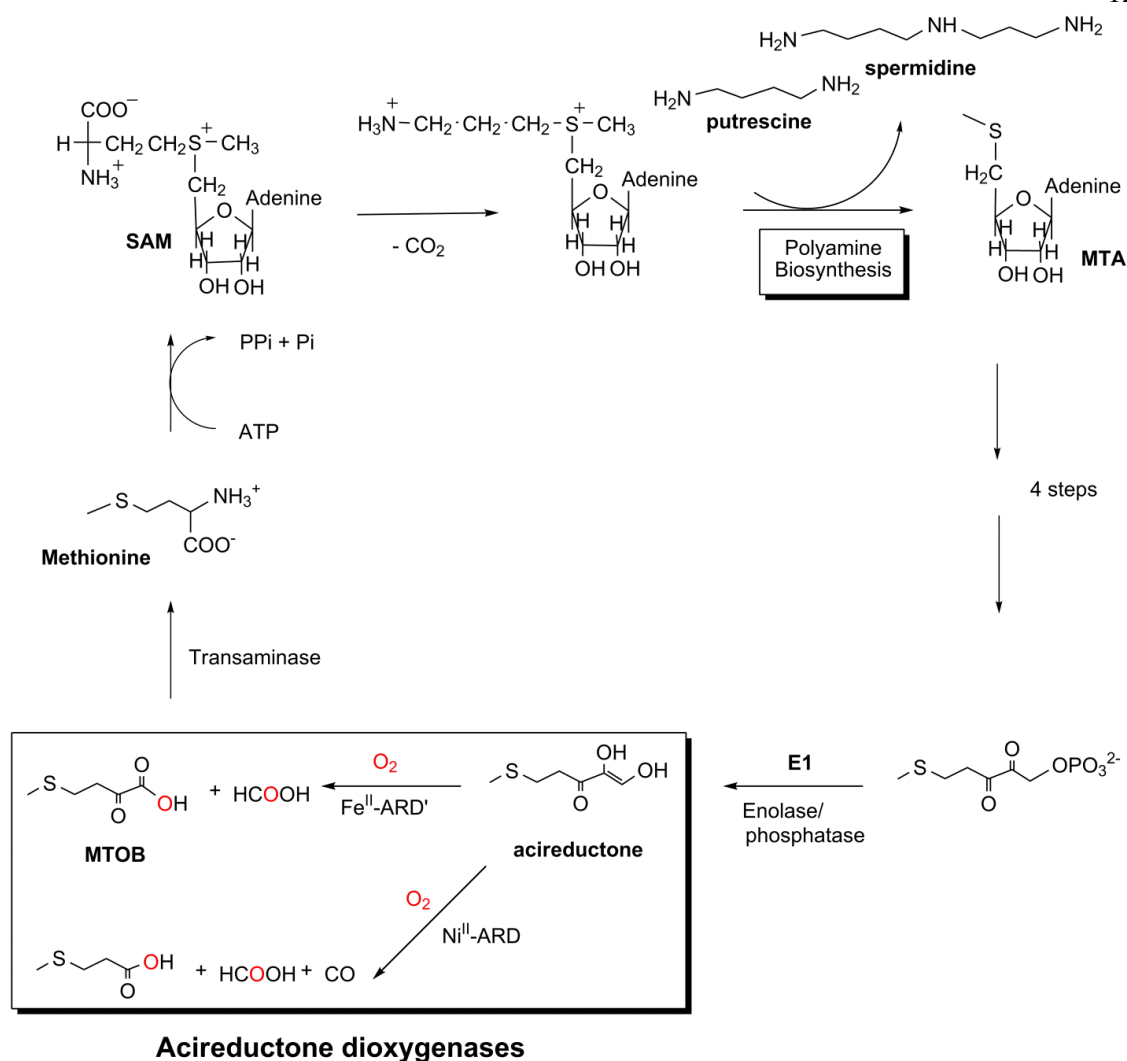
IRON- AND NICKEL-CONTAINING MODEL SYSTEMS OF
ACIREDUCTONE DIOXYGENASE THAT UTILIZE A C(1)H ACIREDUCTONE
SUBSTRATE**Abstract**

An acetylated tautomer of phenyl reductone, 1-Acetoxy-3-phenylpropan-2,3-dione (**5**), has been synthesized by a non-enzymatic route from commercially available precursors. Mononuclear complexes ($[(6\text{-Ph}_2\text{TPA})\text{M}(\text{PhC}(\text{O})\text{C}(\text{O})\text{CHOC}(\text{O})\text{CH}_3)]\text{ClO}_4$ (**7**: M = Ni; **8**: M = Fe) containing the mono-anion of **5** bound to a divalent metal center supported by the 6-Ph₂TPA chelate ligand (6-Ph₂TPA = *N,N*-bis((6-phenyl-2-pyridyl)methyl)-*N*-(2-pyridylmethyl)amine) have been synthesized. Complexes **7** and **8** have been characterized by ¹H NMR, UV-vis, infrared spectroscopy, mass spectrometry and elemental analysis. Exposure of solutions of **7** or **8** to O₂ does not lead to their decay over the course of several hours. Complexes **7** and **8** may be deprotected by the addition of excess nucleophilic base to generate a mononuclear species with a dianionic acireductone bound (**I**); this species subsequently anaerobically decays with loss of the 6-Ph₂TPA ancillary ligand. Exposure of the *in situ* generated mononuclear dianionic acireductone complex **I** to O₂ leads to oxidative cleavage of the diketonate. This is the first example of a strategy that allows examination of the oxidative reactivity of a mononuclear dianionic acireductone complex of relevance to the acireductone dioxygenase enzymes.

Introduction

Methionine is an essential amino acid that plays an important role in protein structure, biosynthetic pathways and is the start codon for translation in eukaryotic cells.¹ Its function in biosynthetic pathways is dominated by its enzymatic derivatization by adenosine triphosphate (ATP) to form S-adenosylmethionine (SAM).^{2, 3} SAM has numerous important biological functions due in part to its sulfonium cation with three S-C bonds.^{3, 4} These functions include: as a co-substrate for methyltransferases, which leads to the loss of the methyl group and formation of S-adenosylhomomethionine;⁵ as a co-factor in radical SAM enzymes;⁶ and as a source of n-propylamine during polyamine biosynthesis, leading to the formation of methylthioadenosine (MTA)⁷. Polyamines such as spermine and spermidine are associated with cell growth, and defects in polyamine biosynthesis regulation are associated with oncogenesis.⁸ Therefore, metabolic pathways that regulate polyamine synthesis are a potentially therapeutically important area of study. One such pathway is the methionine salvage pathway (MSP), a ubiquitous enzymatic pathway in eukaryotic organisms that functions to recycle the methylthio unit into methionine after SAM has been converted to MTA during polyamine biosynthesis.^{7, 9}

A pair of enzymes known as the acireductone dioxygenases catalyze the dioxygenolytic cleavage of an acireductone intermediate within the MSP.¹⁰ These enzymes represent the only known branch-point within this pathway, and thus are of current interest. In *Klebsiella pneumonia* the on-pathway reaction is catalyzed by an iron-containing enzyme (Fe-ARD'), while the off-pathway reaction is catalyzed by a nickel-containing enzyme (Ni-ARD).¹¹⁻¹³ These enzymes cleave the carbon-carbon bond(s) of



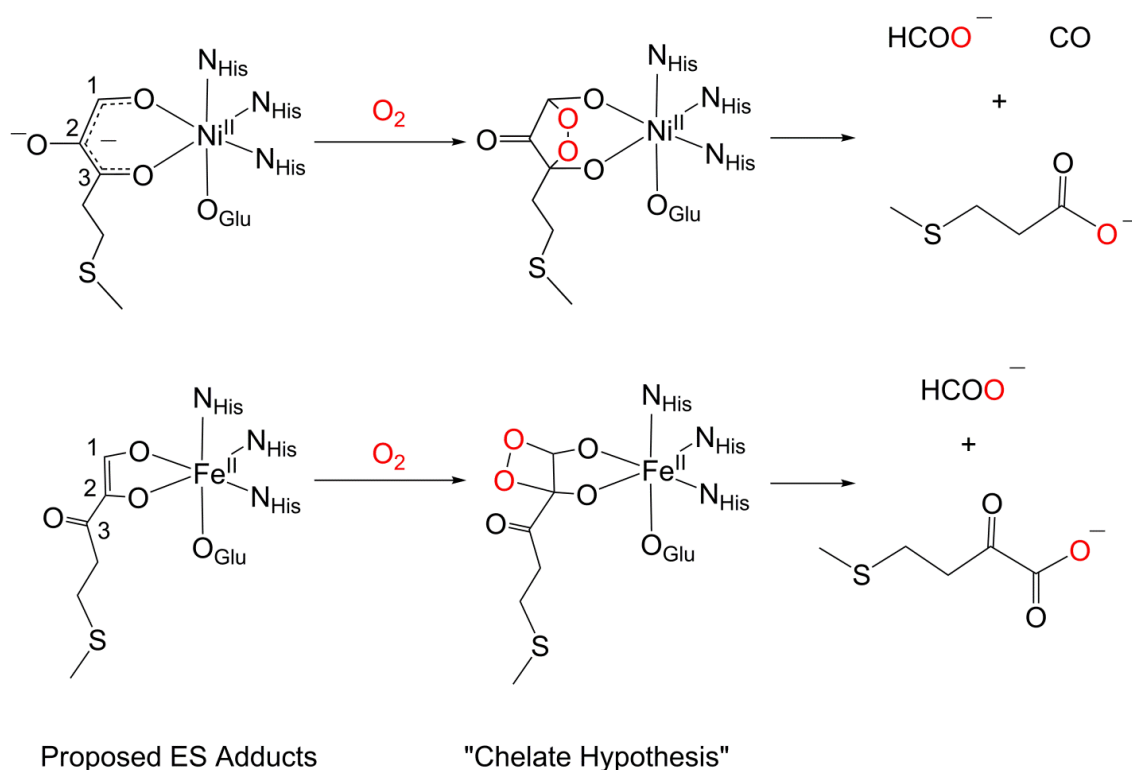
Scheme 3-1. An overview of the methionine salvage pathway in *K. pneumoniae*.

their substrate with differing regiospecificity (Scheme 3-1), and are particularly interesting from a chemical standpoint as the only constitutive difference between the enzymes is the identity of the metal ion at the active site (Fe^{II} or Ni^{II}).¹³ The reaction catalyzed by Ni-ARD also produces CO, a well-known cellular signaling molecule with therapeutic potential,¹⁴ thereby combining a regulatory junction with the production of a cellular signal. Efforts to gain an understanding of the chemical factors that control the

regiospecificity of the acireductone dioxygenase cleavage reactions are therefore warranted.

The original proposal for the changes in regiospecificity inferred changes in the binding mode of the acireductone to the metal center, from a five-membered chelate ring in Fe-ARD' to a six-membered chelate ring in Ni-ARD, would respectively activate the C(1) and C(2) or C(1) and C(3) carbons towards attack by dioxygen (Scheme 3-2).¹⁵

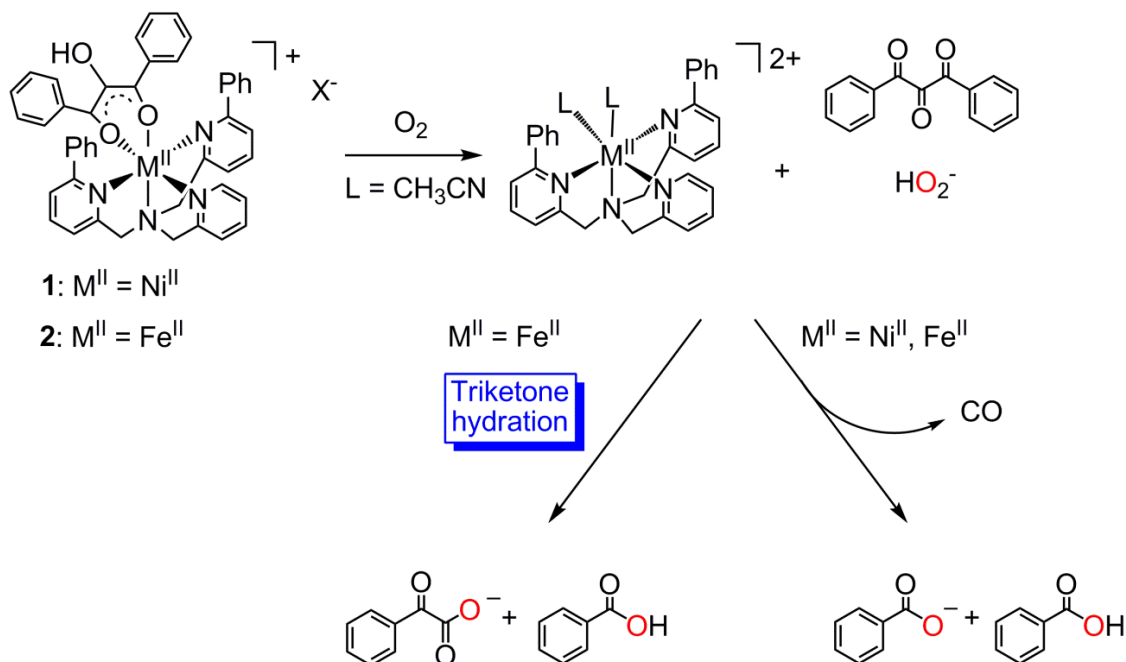
Subsequent collapse of the resulting dioxetane rings would lead to the observed



Scheme 3-2. The proposed reaction pathways for Ni-ARD (top) and Fe-ARD' (bottom), wherein a change in the binding mode of the acireductone activates different carbon atoms to attack by dioxygen.

regiospecificity of products. This “chelate hypothesis” was borne out by NMR studies of the tertiary structure of the enzymes, wherein it was found that the position of a tryptophan arm in the Ni-ARD active site could favor the six-membered chelate binding mode of the substrate.¹⁶ However, direct spectral probes of the enzyme-substrate adducts, including UV-vis spectroscopy and XAS, did not give conclusive evidence of a change in binding mode between Fe-ARD' and Ni-ARD.^{17, 18}

As an alternative to enzymatic studies as a method for investigating the mechanistic details of the acireductone dioxygenases, we have previously synthesized functional small molecular models of Ni-ARD and Fe-ARD'.^{19, 20} To model the 3-His, 1-Glu binding motif and hydrophobic pocket at the active site we utilized the ligand *N,N*-bis((6-phenyl-2-pyridyl)methyl)-*N*-(2-pyridylmethyl)amine (6-Ph₂TPA) and as a model substrate we synthesized the bulky acireductone 2-hydroxy-1,3-diphenylpropan-1,3-dione, which is not known to be a substrate for the native enzymes. The models of the enzyme-substrate adducts, [(6-Ph₂TPA)Ni(PhC(O)C(OH)C(O)Ph)]ClO₄ (**1**) and [(6-Ph₂TPA)Fe(PhC(O)C(OH)C(O)Ph)]ClO₄ (**2**), undergo a dioxygenolytic reaction via the formation of an intermediate triketone/hydroperoxide pair (Scheme 3-3).^{20, 21} The triketone intermediate was initially identified by the detection of benzil, the product of a Lewis acid-mediated decarbonylation of 1,3-diphenylpropantrione.²² Due to the identical binding mode of the model acireductone substrate in these complexes, they were an ideal test-case for the chelate hypothesis. It was found that the regioselectivity of the reaction of **1** and **2** with O₂ was identical in dry solvent, consistent with the chelate hypothesis. However, in the presence of H₂O a change in regioselectivity was observed in the reaction of **2**, but not for **1**, suggesting that the chelate hypothesis was not sufficient to



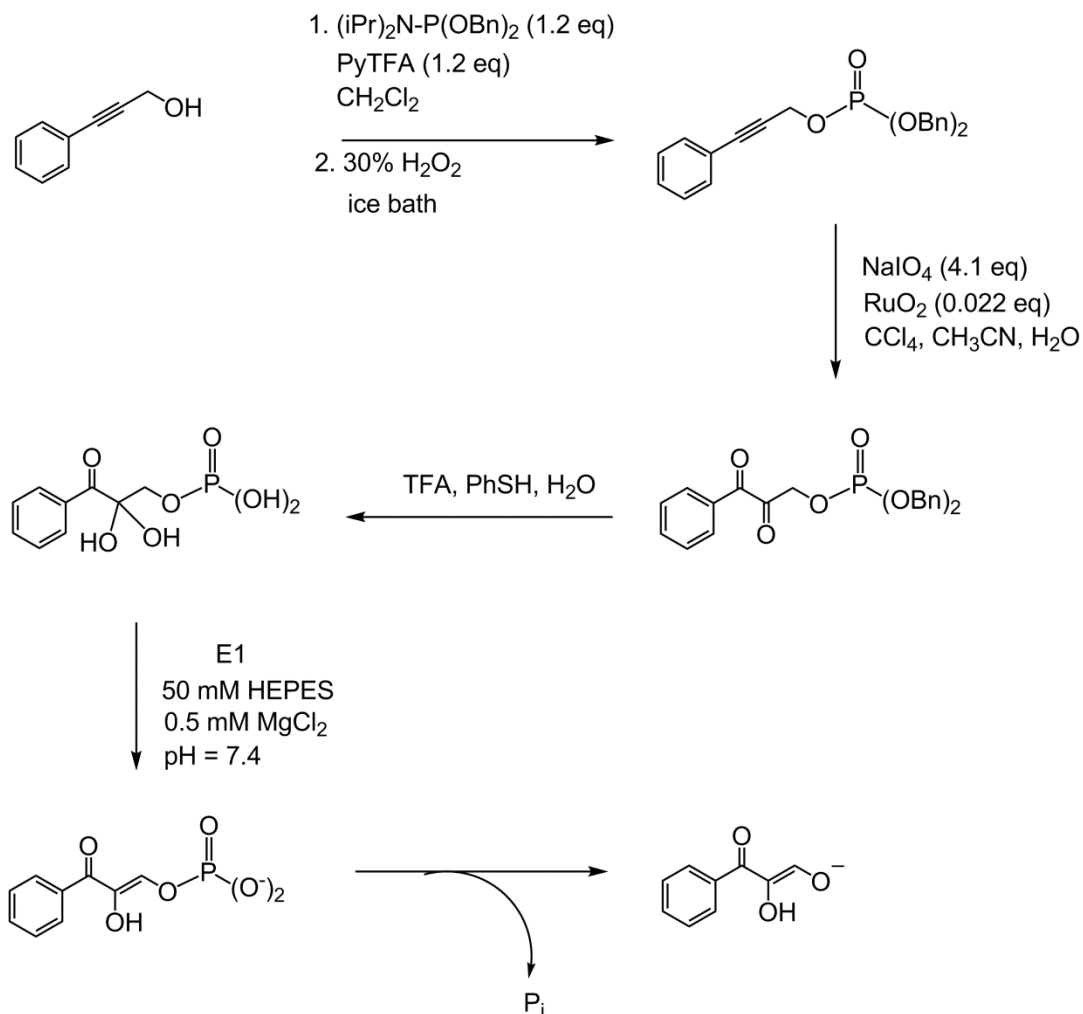
Scheme 3-3. Reaction pathways of **1** and **2** with O_2 via the formation of 1,3-diphenylpropantrione as an intermediate. Both complexes may react via a Ni-ARD pathway in which both the C(1)-C(2) and C(2)-C(3) bonds within the propyl chain are cleaved, releasing CO. When water is added to the reaction, a new reaction pathway becomes accessible only for **2**, in which only the C(1)-C(2) bond is cleaved.

explain the chemistry in these model systems.²¹ We thereby proposed a new reaction pathway for **2** wherein the ferrous center promoted hydration of a triketone intermediate, facilitating the change in regioselectivity (Scheme 3-3). Unfortunately, this model system is not truly biomimetic since it reacts at a mono-anion protonation level (whereas the enzyme is proposed to react at a di-anionic protonation level) and utilizes an acireductone that is likely too bulky to fit into the active site of the acireductone dioxygenases.¹⁰ Computational studies have additionally suggested significant differences in the electronic structure and thus reactivity between acireductones that have a phenyl group or a hydrogen atom at the C(1) position.^{21, 23} In order to provide better insight into the

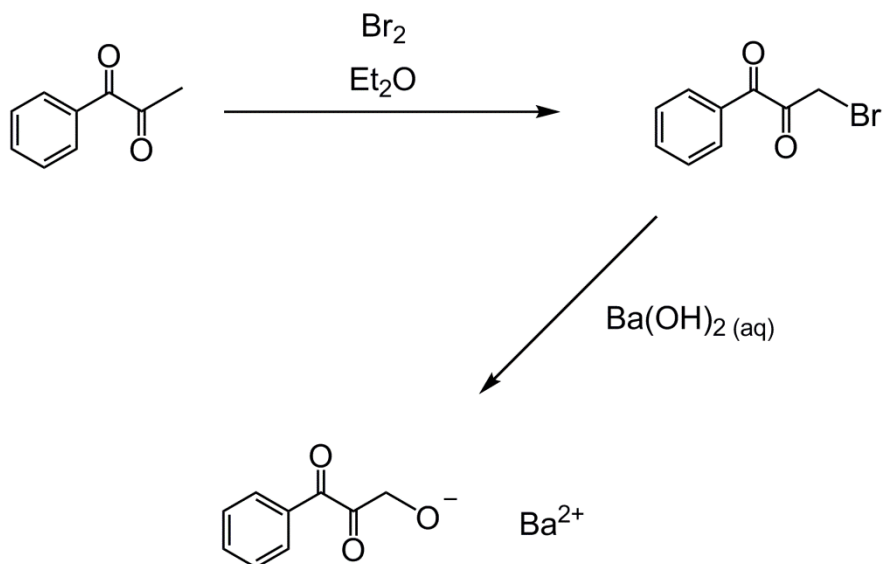
acireductone dioxygenase reaction pathways, we have therefore endeavoured to utilize a C(1)H acireductone that is a substrate for the native enzyme. As a target we have chosen 3-oxo-3-phenylpropen-1,2-diol (phenyl reductone), which has been reported as a substrate for the enzyme, due to its amenable UV-vis features ($\lambda_{\text{max}} = 320 \text{ nm}$ as a mono-anion).¹⁷

There are no reported chemical syntheses of the native substrate of the acireductone dioxygenases (1,2-dihydroxy-3-oxo-*S*-methylthiopentene), presumably due to the presence of the methylthio unit.²⁴ Synthetic routes to desthio analogues, such as phenyl reductone, have focused on generating a phosphorylated precursor to an acireductone, and subsequently using the E1 enolase/phosphatase enzyme from the MSP to dephosphorylate the precursor (Scheme 3-4).²⁵ The resulting acireductone mono-anion is normally utilized *in situ*, although it has been isolated as a sodium salt with purity of up to ~90 %, as evaluated by ¹H NMR.²⁶ An attempted alternative, entirely chemical synthetic route to phenyl reductone has generated a barium salt of the mono-anion, but the purity of this salt was not reported (Scheme 3-5).²⁷ The difficulty in isolating the acireductone is due to its propensity to oxidize under alkaline conditions utilized in its synthesis, and also due to a facile isomerization reaction that breaks a C-C bond to form an ester.^{27, 28}

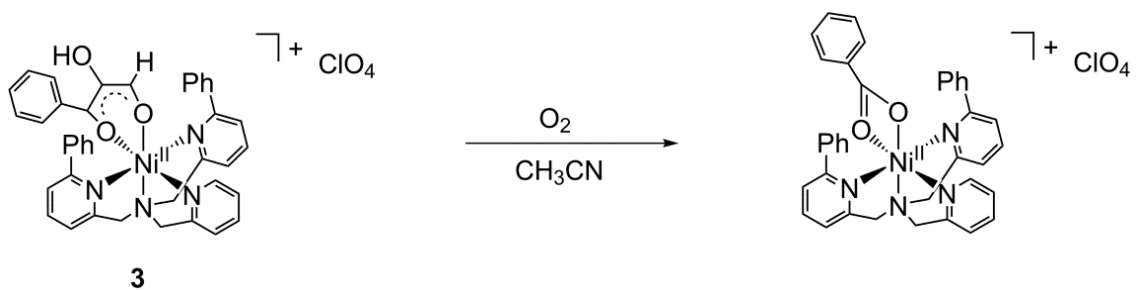
We have previously generated a small molecular model of the enzyme-substrate adduct of Ni-ARD *in situ*, by utilizing the sodium salt of phenyl reductone (Scheme 3-6). Based on its ¹H NMR and UV-vis features ($\lambda_{\text{max}} = 378 \text{ nm}$), the complex is formulated as [(6-Ph₂TPA)Ni(PhC(O)COHC(O)H)]ClO₄ (**3**).²⁶ Exposure of a solution of this complex to O₂ results in the slow decay of the 378 nm absorption feature. Analysis of the product



Scheme 3-4. A combined chemical-enzymatic route for the synthesis of a C(1)H acireductone mono-anion that utilizes the E1 enolase/phosphatase enzyme from the methionine salvage pathway to generate a mono-anion *in situ*, with ~90% purity. All reactions were performed under a nitrogen atmosphere.



Scheme 3-5. A solely chemical synthetic route for the synthesis of a C(1)H acireductone has been used to generate the Ba^{2+} salt of the mono-anion. All reactions were performed under a nitrogen atmosphere.



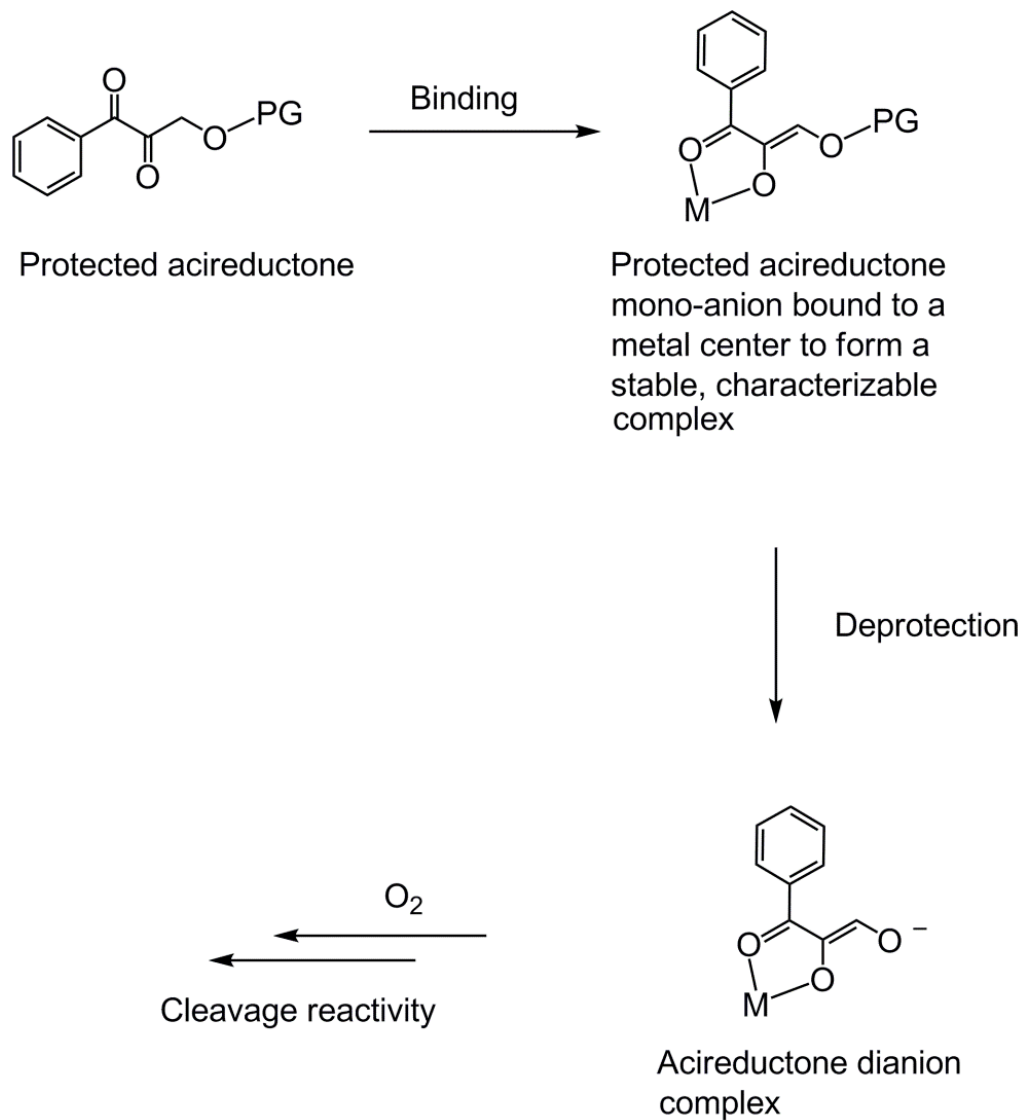
Scheme 3-6. A possible structure of an *in situ* generated phenyl reductone complex (**3**), and the product of its reaction with O_2 in CH_3CN .

mixture by ^1H NMR and HRMS allowed the identification of $[(6\text{-Ph}_2\text{TPA})\text{Ni}(\text{PhC}(\text{O})\text{O})]^+$ as a product. No other products have yet been identified. No mixture by ^1H NMR and HRMS allowed the identification of $[(6\text{-Ph}_2\text{TPA})\text{Ni}(\text{PhC}(\text{O})\text{O})]^+$ as a product. No other products have yet been identified. No analogous complex containing a ferrous center has yet been synthesized, and the reactivity of the complex in the presence of exogenous base (to generate the di-anion) has not been investigated.

In order to generate model systems of direct relevance to the acireductone dioxygenases, our current goal is to generate nickel and iron complexes with a di-anionic phenyl reductone moiety bound. Our strategy is outlined in Scheme 3-7 and involves the generation of a protected acireductone. Binding of this protected acireductone to a metal center will allow us to generate a well-defined, analytically pure complex by eliminating the acireductone isomerization reaction. Subsequent deprotection and exposure to O_2 will allow us to investigate the role that iron and nickel play in directing the regioselectivity of acireductone cleavage.

Experimental

General Methods. All reagents were obtained from commercial sources and were used without additional purification unless otherwise noted. Solvents were dried according to published procedures and were purified by distillation under N_2 prior to use.²⁹ Air-sensitive reactions were performed in an MBraun Unilab glovebox under a N_2 atmosphere or by using standard Schlenk techniques. The 6- Ph_2TPA (*N,N*-bis((6-phenyl-2-pyridyl)methyl)-*N*-(2-pyridylmethyl)amine) ligand, $[(6\text{-$



Scheme 3-7. Strategy for generating a well-defined C(1)H acireductone complex and subsequently deprotecting it to investigate the reactivity of a dianionic acireductone with O₂.

$\text{Ph}_2\text{TPA}]\text{Ni}(\text{CH}_3\text{CN})(\text{H}_2\text{O})](\text{ClO}_4)_2$, and $[(6\text{-Ph}_2\text{TPA})\text{Fe}(\text{CH}_3\text{CN})](\text{ClO}_4)$ were synthesized by following previously published procedures.^{30, 31, 20}

Physical Methods. ^1H NMR spectra of organic compounds were obtained using a JEOL ECX-300 spectrometer; chemical shifts were referenced to the residual solvent peak in CD_2HCN (1.94 ppm, quintet). ^{13}C NMR spectra of organic compounds were obtained using a Bruker ARX-400 spectrometer. ^1H NMR spectra of paramagnetic complexes were obtained using a Bruker ARX-400 spectrometer and parameters as previously described.³² UV-vis data was collected on an HP8453A spectrometer at ambient temperature. IR spectra were recorded on a Shimadzu FTIR-8400 spectrometer as KBr pellets. GC-MS data was obtained on a Shimadzu GCMS-QP5000 gas chromatograph/mass spectrometer with a GC-17A gas chromatograph, using an Alltech EC5 30 m \times 25 mm \times 25 μm thin film capillary column and temperature program: T_{initial} : 70 $^\circ\text{C}$ (5 min); temperature gradient: 23 $^\circ\text{C min}^{-1}$; T_{Final} : 250 $^\circ\text{C}$ (10 min). GC-TCD data for analysis of reaction headspace gas was collected using an Agilent 3000A Micro gas chromatograph. Mass spectral data for metal complexes was collected by the Mass Spectrometry Facility, University of California, Riverside. Elemental analyses were performed by Atlantic Microlabs Inc., Norcross, GA.

3-Phenyl-2-propynylacetate (4). 3-phenyl-2-propyn-1-ol (1.00 g, 7.57 mmol) and NEt_3 (1 mL) were dissolved in Ac_2O (5 mL) and stirred together for 16 hours under a N_2 atmosphere. The resulting orange solution was diluted with 150 mL EtOAc and washed repeatedly with 100 mL portions of H_2O . The organic layer was passed through an activated charcoal filter and dried over anhydrous Na_2SO_4 . The solvent was then removed under reduced pressure to yield a yellow oil (1.10 g, 83%). ^1H NMR (300 MHz,

CD₃CN): δ = 7.46-7.35 (5H, m), 4.87 (2H, s), 2.07 (3H, s); ¹³C NMR (100 MHz, CD₃CN): δ = 171.01, 132.54, 129.94, 129.58, 122.90, 86.47, 84.54, 53.23, 20.88.

1-Acetoxy-3-phenylpropan-2,3-dione (5). NaIO₄ (1.07 g, 5.00mmol) was dissolved in 15 mL H₂O and combined with RuCl₃ (0.037 mmol) to form a yellow solution. 3-Phenyl-2-propynylacetate (0.215 g, 1.23 mmol), dissolved in a mixture of 10 mL CCl₄ and 10 mL CH₃CN was added to the aqueous solution, and the resulting slurry stirred for 15 minutes, monitoring carefully by TLC. The slurry was then diluted with 150 mL CH₂Cl₂ and filtered. The filtrate was cooled in an ice bath and then carefully mixed with 100 mL Na₂SO₃ (1.0 M). The resulting suspension was placed in a separatory funnel, and the aqueous layer extracted with 3 × 100 mL CH₂Cl₂. The organic layers were combined, dried over anhydrous Na₂SO₄, and the solvent removed under reduced pressure. The crude yellow product mixture was purified by column chromatography using a silica gel solid phase and eluting with 4:1 hexanes:EtOAc (180 mg, 71%). ¹H NMR (300 MHz, CD₃CN): δ = 8.01 (2H, d, ³J(H,H) = 8.2 Hz), 7.73 (1H, t, ³J(H,H) = 7.2 Hz), 7.57 (2H, t, ³J(H,H) = 7.9 Hz), 5.21 (2H, s), 2.13 (3H, s); ¹³C NMR (100 MHz, CD₃CN) : δ = 196.23, 191.26, 171.24, 135.95, 132.94, 131.07, 129.92, 67.19, 20.49. UV-vis (Et₂O) λ_{\max} , nm (ϵ , M⁻¹cm⁻¹): 255 (12000).

Caution! *Perchlorate salts of metal complexes with organic ligands are potentially very explosive. Only small amounts of material should be prepared, and these should be handled with extreme caution.*³³

In situ generation of [(6-Ph₂TPA)Ni(PhC(O)COHC(O)H)]ClO₄ (3). Under a N₂ atmosphere, 1-acetoxy-3-phenylpropan-2,3-dione (5) (19 mg, 0.091 mmol) was dissolved in a mixture of 100 mL MeOH and 5 mL H₂O. 20 drops concentrated HCl_(aq)

was added and the solution stirred for 12 hours. The solvent was then removed under reduced pressure to yield a yellow solid. The solid was washed with H₂O and redissolved in 0.7 mL CD₃CN. By integration of the aromatic region in the ¹H NMR, the sample consisted of ~50% 2,3-dioxo-3-phenylpropanol (**6**). ¹H NMR (300 MHz, CD₃CN): δ = 7.99 (2H, d, ³J(H,H) = 8.6 Hz), 7.62 (1H, t, ³J(H,H) = 7.2 Hz), 7.49 (2H, t, ³J(H,H) = 7.9 Hz), 4.70 (2H, d, ³J(H,H) = 4.5 Hz; CH₂), 3.37 (1H, t, ³J(H,H) = 5.4 Hz; OH). A 0.7 mL CD₃CN solution of Ni(ClO₄)₂•6H₂O (19 mg, 0.051 mmol) was stirred with 6-Ph₂TPA (22 mg, 0.051 mmol) for 15 minutes to form a pale purple solution. This solution was combined with the solution of **6**. Me₄NOH•5H₂O (9 mg, 0.05 mmol) was then added and the resulting slurry stirred for 1 hour, during which time the color became yellow.

[(6-Ph₂TPA)Ni(PhC(O)C(O)CHOC(O)CH₃)]ClO₄ (7**).** Under a N₂ atmosphere, a CH₃CN (5 mL) solution of [(6-Ph₂TPA)Ni(CH₃CN)(H₂O)](ClO₄)₂ (0.078 mmol) was stirred with 1-acetoxy-3-phenylpropan-2,3-dione (16 mg, 0.078 mmol) until it was completely dissolved. This solution was then added to LiHMDS (14 mg, 0.082 mmol) in Et₂O (1 mL) and stirred overnight. The solvent was removed under reduced pressure, and the solid redissolved in CH₂Cl₂ then filtered through a glass wool/Celite plug to remove the insoluble LiClO₄. The CH₂Cl₂ solution was concentrated under reduced pressure, and then layered with hexanes to yield a pale yellow precipitate. The precipitate was collected, triturated with Et₂O and then dried under vacuum for 48 hours (36 mg, 54%). HRMS (ESI): *m/z* calculated for [C₄₁H₃₅N₄NiO₄]⁺: 705.2012 ([M-ClO₄]⁺); found: 705.2010. FTIR (KBr, cm⁻¹): 1749 (ν_{CO}), 1609 (ν_{CO}), 1451, 1355, 1094 (ν_{ClO₄}), 765, 623 (ν_{ClO₄}). UV-vis (MeOH) λ_{max}, nm (ε, M⁻¹cm⁻¹): 350 (6100). Analysis calculated for

$C_{41}H_{35}ClN_4NiO_8 \cdot 0.5CH_2Cl_2$: C, 58.74; H, 4.28; N, 6.61. Found: C, 59.17; H, 4.67; N, 7.09.

[(6-Ph₂TPA)Fe(PhC(O)C(O)CHOC(O)CH₃)]ClO₄ (8). Under a N₂ atmosphere, 1-acetoxy-3-phenylpropan-2,3-dione (14 mg, 0.068 mmol) was dissolved in Et₂O (2 mL) was added to LiHMDS (12 mg, 0.071 mmol) in Et₂O (1 mL) and stirred for 15 minutes to form a slurry. The solvent was then removed under reduced pressure. This solid was then combined with a CH₃CN (5 mL) solution of [(6-Ph₂TPA)Fe(CH₃CN)](ClO₄)₂ (0.068 mmol) and allowed to stir overnight. The solvent was removed under reduced pressure, and the solid redissolved in CH₂Cl₂ then filtered through a glass wool/Celite plug to remove the insoluble LiClO₄. The CH₂Cl₂ solution was concentrated under reduced pressure, and then layered with hexanes to yield a brown precipitate. The precipitate was collected, triturated with Et₂O and then dried under vacuum for 48 hours (28 mg, 49%). FTIR (KBr, cm⁻¹): 1750 (ν_{CO}), 1595 (ν_{CO}), 1451, 1094 (ν_{ClO4}), 765, 698, 623 (ν_{ClO4}). UV-vis (CH₃CN) λ_{max}, nm (ε, M⁻¹cm⁻¹): 339 (8400), 518 (1100). HRMS (ESI): *m/z* calculated for [C₄₁H₃₅N₄FeO₄]⁺: 703.2008 ([M-ClO₄]⁺); found: 703.2013. Analysis calculated for C₄₁H₃₅ClN₄FeO₈·0.5CH₂Cl₂: C, 58.93; H, 4.29; N, 6.63. Found: C, 58.71; H, 4.40; N, 6.22.

Treatment of 7 and 8 with NaOMe. For UV-vis experiments, a ~0.2 mM MeOH stock solution of 7 or 8 was prepared. A 2.4 mL aliquot of this solution (~0.48 μmol) was placed in a quartz UV-vis cell. This solution was then combined with a 200 μL aliquot of a 12 mM solution of NaOMe (2.4 μmol). For NMR experiments, ~2.5 mg complex (3 μmol) was dissolved in 0.75 mL CD₃OD. Then, 15 μmol NaOMe was also dissolved in 0.25 mL CD₃OD and the solutions combined.

Treatment of 7 with LiHMDS. A ~0.2 mM CH₃CN stock solution of **7** was prepared. A 2.4 mL aliquot of this solution (~0.48 μmol) was placed in a quartz UV-vis cell. This solution was then combined with a 200 μL aliquot of a 12 mM Et₂O solution of LiHMDS (2.4 μmol).

O₂ Reactivity. Solutions for monitoring by UV-vis or ¹H NMR were prepared as described above. The solutions monitored included: a solution of **7**; a solution of **8**; a solution of **7** that had been treated with NaOMe; and a solution of **8** that had been treated with NaOMe. Oxygen was introduced by purging the solutions with dry O₂ gas for 30 seconds, and then the reaction vessels were sealed. In an alternative set of experiments, solutions of **7** and **8** were purged with O₂ and then subsequently treated with 5 equivalents of NaOMe.

To analyze the products of reactions, MeOH solutions containing 2 mg/mL (~2.5 mM) of **7** and **8** were prepared. The solutions were then purged with O₂ for 30 seconds. The aerated solutions were then combined with 0.6 mg solid NaOMe per mL of solution, giving a NaOMe concentration of ~12.5 mM (5 eq). The solutions were then repurged with O₂ for 30 seconds, sealed with a rubber septum and stirred for 12 hours. The solvent was then removed under reduced pressure and the products analyzed as described below.

Detection of Formate. To detect the presence of formate, we derivatized it using 4-phenylphenacylbromide to generate 4-phenylphenacylformate. If formate had been present in the crude reaction mixture, a M⁺ ion with m/z = 240 would be present, corresponding to 4-phenylphenacylformate, and with a retention time matching that of an authentic sample of 4-phenylphenacylformate. The crude solid reaction mixture was dissolved in 10 mL CH₃CN and 10 mL benzene. To this reaction mixture was added 10

equivalents of 4-phenylphenacylbromide and 5 equivalents of 18-crown-6. The resulting slurry was refluxed under nitrogen for 18 hours. The solvent was removed under reduced pressure and the solid extracted with CH_2Cl_2 . The CH_2Cl_2 solution was then passed through a short silica plug and analyzed by GCMS. 4-phenylphenacylformate was detected in the analysis of the products of the reactions of both **7** and **8**.

Analysis of Phenyl-Containing Products. The crude reaction mixture was redissolved in a small amount of CH_3CN and passed through a short silica column, eluting with ethyl acetate. The organic products were then analyzed by GC-MS and identified by comparison to molecular ions, fragmentation patterns and retention times of authentic samples.

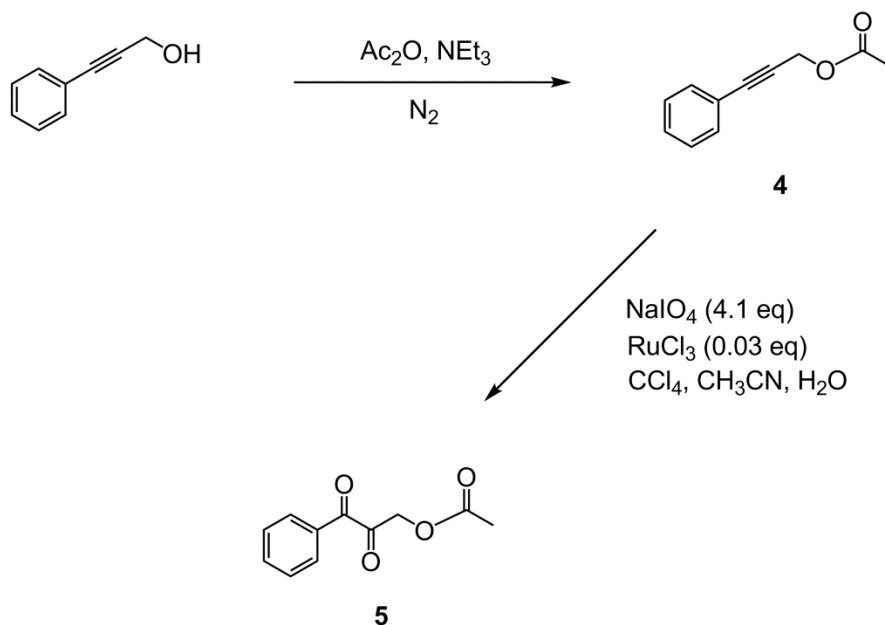
Analysis of Gaseous Products. Complex **7** or **8** (0.01 mmol), dissolved in 1.0 mL MeOH, was placed in a 50 mL round-bottomed flask equipped with a stir bar. The flask was filled with O_2 gas at atmospheric pressure and sealed with a rubber septum. A solution of NaOMe (0.05 mmol) in 1.0 mL MeOH was injected into the round-bottomed flask using a gas-tight syringe. The resulting solution was stirred for 12 hours. 10 mL of the headspace gas was removed by gas-tight syringe and analyzed by GC-TCD. The yield of CO generated in the reactions were determined using calibration curves generated using gas mixtures of O_2 and CO.

Results and Discussion

Synthesis of Protected Phenyl Reductone. 3-phenyl-2-propyn-1-ol was acylated using acetic anhydride to generate 3-phenyl-2-propynylacetate (**4**) (Scheme 3-8).

Oxidation of the alkyne with NaIO_4 and a RuCl_3 catalyst generated the diketone (**5**).

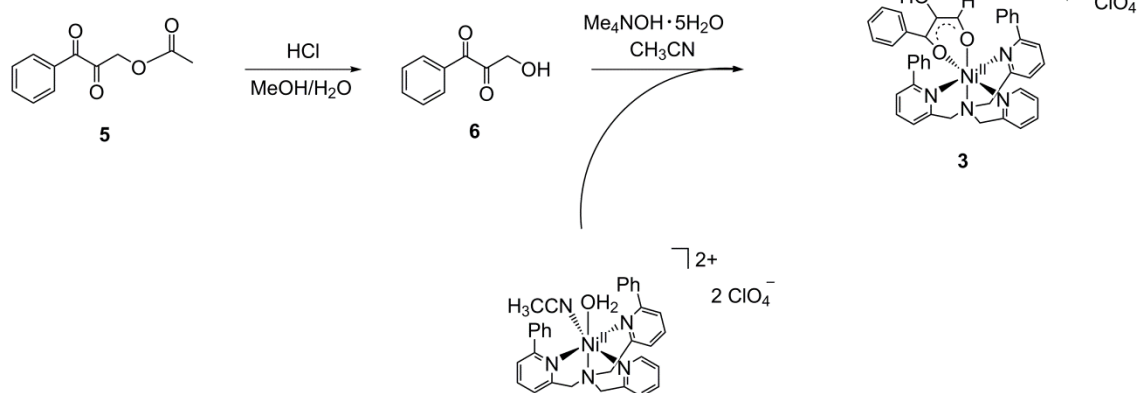
Careful monitoring of this reaction by TLC was necessary due to the propensity of **5** to



Scheme 3-8. Synthesis of 1-Acetoxy-3-phenylpropan-2,3-dione (**5**), a protected acireductone, from 3-phenyl-2-propyn-1-ol.

over-oxidize to give carboxylic acids, presumably via an initial hydrolytic cleavage of the acetyl protecting group. Due to the formation of byproducts, purification by column chromatography was necessary. The diketone tautomeric form of **5** was confirmed by the presence of two ketone ¹³C signals (196.23, 191.26 ppm), an integral of two protons for the methylene group by ¹H NMR, and by a UV absorption band at 255 nm.

Synthesis and Characterization of Metal Complexes. While our goal was to generate metal complexes containing a protected acireductone, we also determined whether our protected acireductone (**5**) could be used to generate a mono-anionic complex such as **3**. Hydrolysis of **5** under acidic conditions led to the generation of a new species **6** that has not yet been purified and isolated (Scheme 3-9). The ¹H NMR signals of **6** are consistent with the formulation 2,3-dioxo-3-phenylpropanol, as evidenced by the coupling between a doublet methylene signal at 4.70 ppm and a triplet proton at 3.37



Scheme 3-9. Route to the *in situ* synthesis of **3** from **5** via the formation of a phenyl reductone tautomer (**6**).

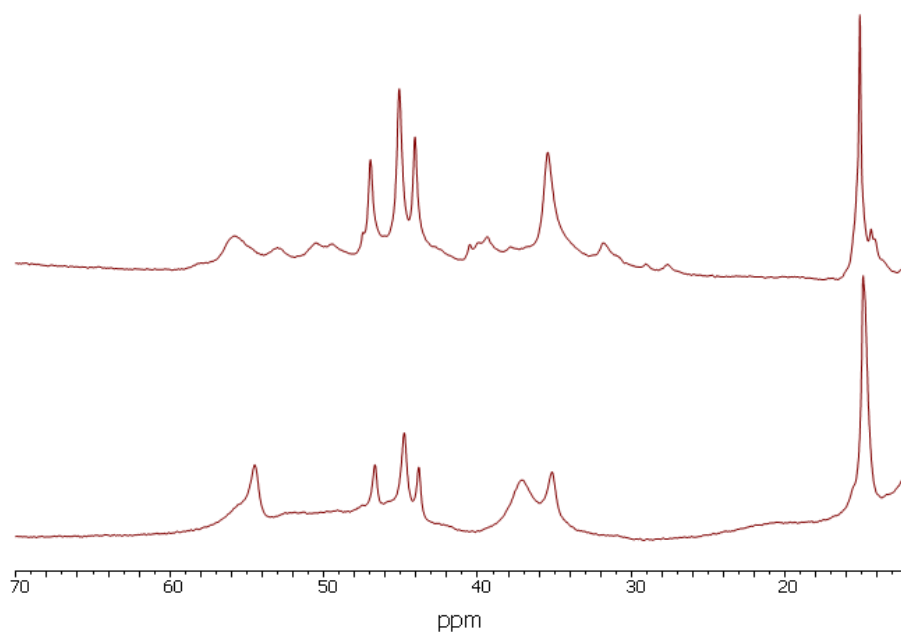
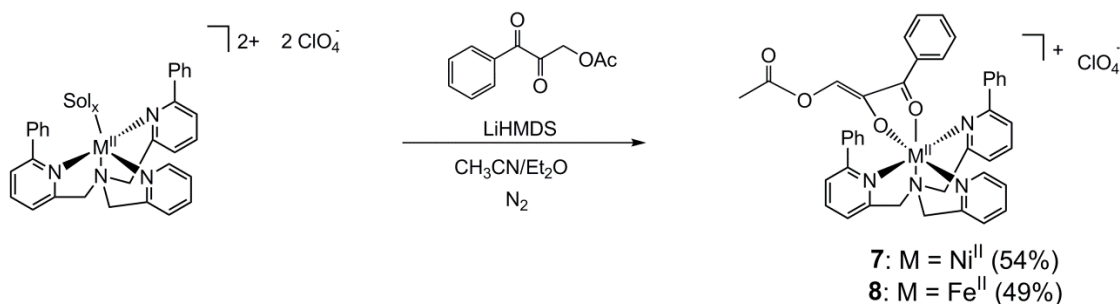


Figure 3-1. Selected portion of the paramagnetically-shifted ^1H NMR spectrum of the previously reported compound **3** (top), and our *in situ* generated compound, assigned as **3** (bottom). The peaks at 55 and 37 ppm in the bottom spectrum are likely impurities. Both spectra were recorded using a 400 MHz spectrometer in CD_3CN at 25°C .

ppm. Notably, the proton peak at 3.37 ppm disappears upon the addition of a drop of D₂O to the NMR tube, consistent with its assignment as an exchangeable hydroxyl proton.

Combination of **6** with [(6-Ph₂TPA)Ni(CH₃CN)(H₂O)](ClO₄)₂ in the presence of base led to the formation of a species that has ¹H NMR signals consistent with those previously reported for **3**, albeit with additional signals due to impurities (Figure 3-1).²⁶ Thus, our entirely chemically-generated, protected C(1)H acireductone provides a relatively high yielding route to generate precursors that can be converted to complexes of relevance to acireductone dioxygenases. This general method should be applicable to the synthesis of a broad array of C(1)H acireductones in which the phenyl-group is replaced with other aromatic or aliphatic groups.

Deprotonation of **5** by LiHMDS, a non-nucleophilic base, in Et₂O led to the formation of a pale yellow slurry. Combination of this with [(6-Ph₂TPA)M(sol)_x](ClO₄)₂ (M = Ni, Fe) led to the formation of the complexes [(6-Ph₂TPA)Ni(PhC(O)C(O)CHOC(O)CH₃)]ClO₄ (**7**) and [(6-Ph₂TPA)Fe(PhC(O)C(O)CHOC(O)CH₃)]ClO₄ (**8**) in moderate yields (Scheme 3-10). Single crystals of **8** were grown by slow diffusion of hexanes into a concentrated CH₂Cl₂ solution. The brown needle-like crystals produced a diffraction pattern, but were too



Scheme 3-10. Synthesis of complexes **7** and **8**.

small to generate a complete electron density map. Elemental analysis to determine the bulk purity of **7** and **8** was fit with 0.5 equivalents of CH_2Cl_2 , which was visible by ^1H NMR in each case, despite trituration and extensive drying. We note that other transition metal complexes with the same aryl-appended tris(pyridylmethyl)amine ligand have also exhibited a strong affinity for CH_2Cl_2 .^{34, 35}

Complexes **7** and **8** have been evaluated by HRMS, and each exhibit a $[\text{M-ClO}_4]^+$ molecular ion with excellent agreement to calculated exact masses and isotopic distributions. UV-vis spectroscopy of **7** and **8** show that each contain an absorption feature due to the coordinated enolate, at 350 and 339 nm, respectively. Consistent with

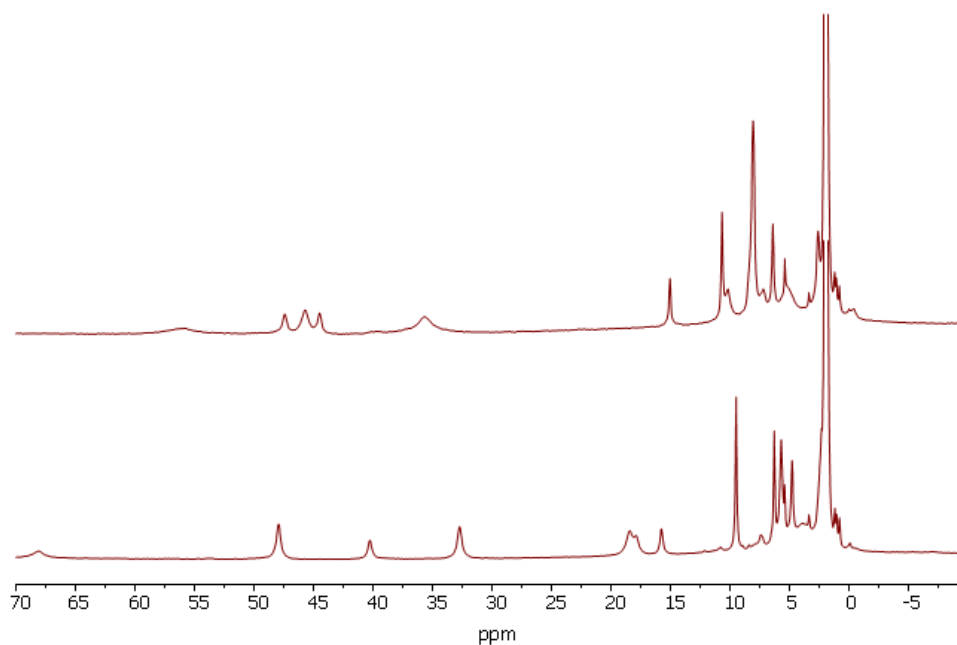


Figure 3-2. Selected portion of the paramagnetically-shifted ^1H NMR spectra of **7** (top) and **8** (bottom). Both spectra were collected using a 400 MHz spectrometer using CD_3CN as a solvent at 25 °C.

our proposed coordination motif, the FTIR spectrum of each complex has bands at ~ 1750 cm^{-1} , attributable to the acetyl ester group, and at ~ 1600 cm^{-1} , due to the non-enolized ketone carbonyl group vicinal to the phenyl ring. ^1H NMR of **7** and **8** (Figure 3-2), collected using paramagnetic parameters, show features consistent with those exhibited by other enolate complexes with the same 6- Ph_2TPA ancillary ligand.^{19, 20, 35}

Anaerobic Reactivity. Addition of 5 equivalents of NaOMe to a MeOH solution of **7** leads to decay of the 350 nm absorption feature with concomitant growth of a new feature centered at 390 nm (Figure 3-3 (left)), consistent with nucleophilic substitution at the acetyl group, to generate methyl acetate and a complex with a bound dianionic acireductone. By contrast, addition of a strong, non-nucleophilic base, such as LiHMDS in CH_3CN , does not lead to any change in the position of the 350 nm absorption maximum in the UV-vis spectrum. Removal of solvent from the reaction of **7** with NaOMe under reduced pressure and subsequent analysis of the product by FTIR, as KBr

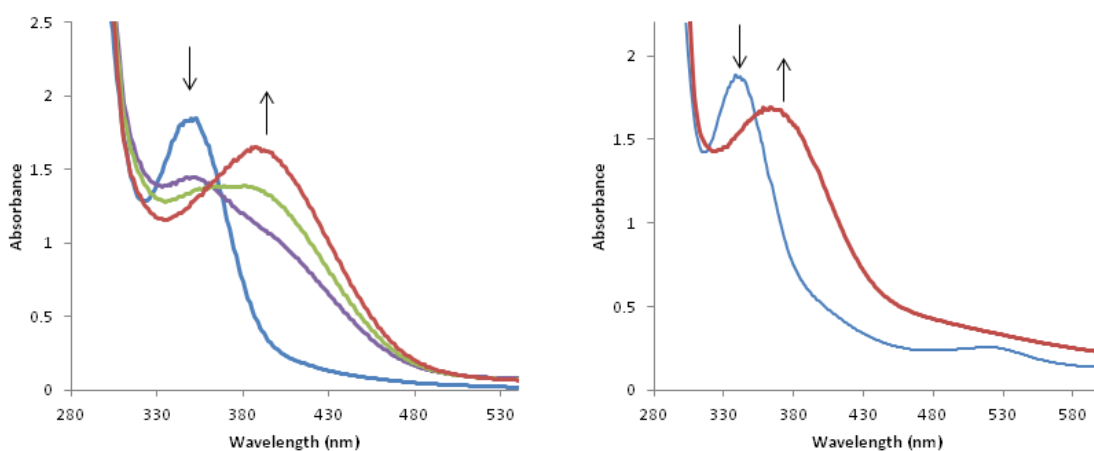


Figure 3-3. UV-vis spectra showing the effects of adding excess NaOMe to MeOH solutions of **7** (left) and **8** (right).

pellets, shows the disappearance of the 1749 cm^{-1} band, consistent with removal of the acetyl group and its subsequent volatilization as methyl acetate. When the reaction is carried out at higher concentrations, a white precipitate of NaClO_4 is also formed as the reaction proceeds. Similarly to **7**, the reaction of **8** with 5 equivalents of NaOMe leads to a shift of the 339 nm absorption feature in the UV-vis spectrum to 365 nm (Figure 3-3 (right)), and loss of the 1750 cm^{-1} band in the infrared spectrum.

Aerobic Reactivity. Exposure of CH_3CN or MeOH solutions of **7** or **8** to O_2 does not lead to decomposition over the course of 24 hours, as monitored by ^1H NMR and UV-vis. This is an expected result as, due to the acetate protecting group on the bound acireductone, the acireductone should not be reactive with O_2 . However, once deprotected these complexes should react rapidly with O_2 . Methanolic solutions of **7** and **8** were first deprotected by the addition of 5 equivalents of NaOMe. Once the deprotection was complete, as monitored by UV-vis spectroscopy, the resulting solutions were purged with O_2 . This led to rapid decay of the absorption features at 390 nm and 365 nm for the solutions generated from **7** and **8** respectively (Figure 3-4 (top)), consistent with oxidative cleavage of the acireductone enolate.

As an alternative route to induce O_2 reactivity, methanolic solutions of **7** and **8** were prepared and purged with O_2 . These O_2 solutions were then mixed with 5 equivalents of NaOMe, and the subsequent decay monitored by UV-vis (Figure 3-4 (bottom)), leading to the decay of the 350 nm absorption feature for complex **7** and the 339 nm absorption feature for complex **8**, without any observation of growth of the peak at 390 or 365 nm for **7** and **8** respectively. This is consistent with rapid oxidative cleavage of the acireductone enolate (Scheme 3-11).

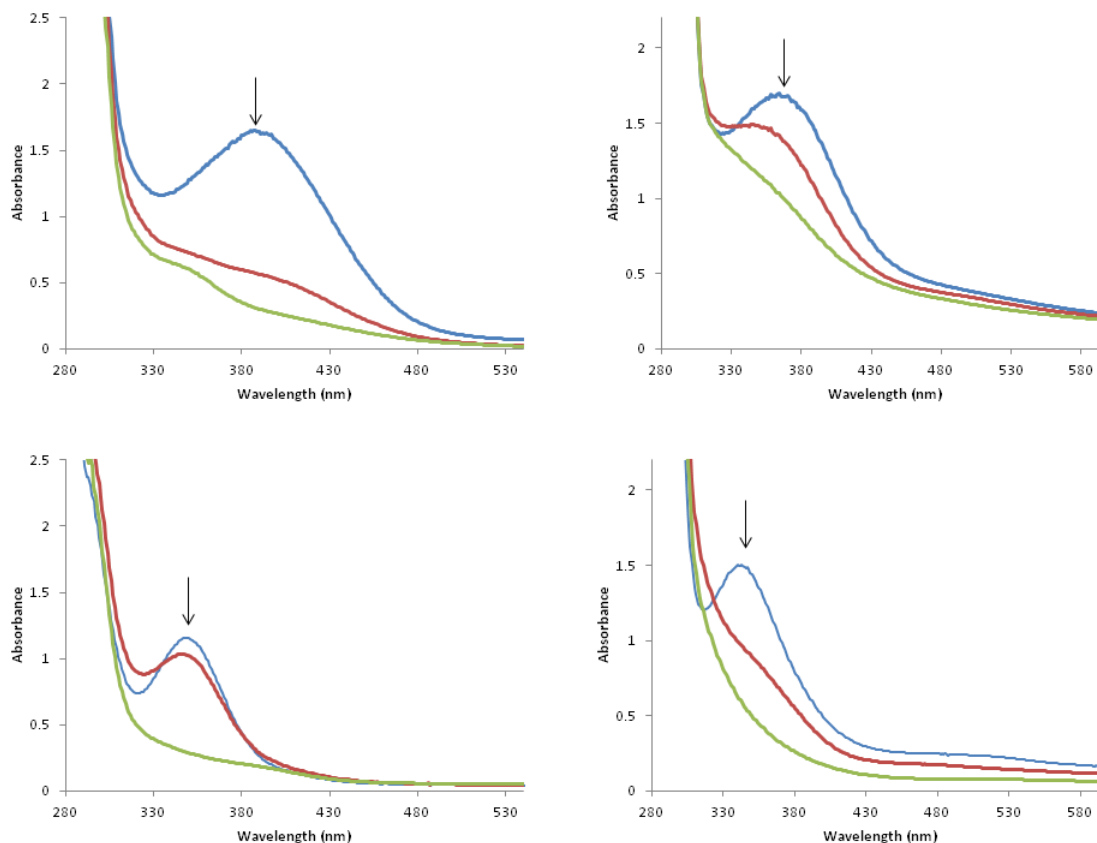
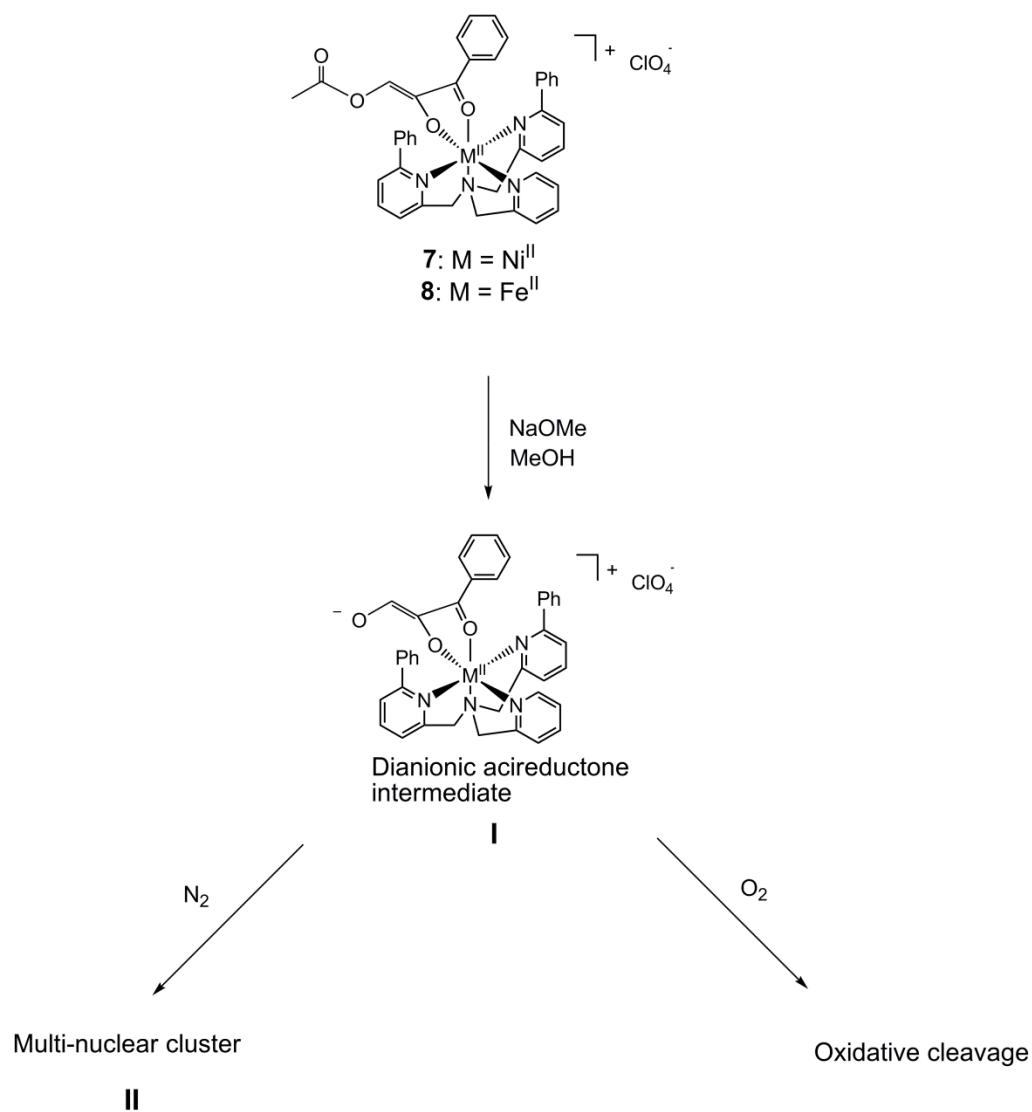


Figure 3-4. UV-vis spectra during the reactions of various species with O₂ in MeOH. Top left: the reaction with O₂ of a solution of **7** that had already been treated with 5 equivalents of NaOMe; a decrease in the 390 nm band was observed. Top right: the reaction with O₂ of a solution of **8** that had already been treated with 5 equivalents of NaOMe; a decrease in the 365 nm band was observed. Bottom left: the reaction when an O₂ purged solution of **7** was treated with 5 equivalents of NaOMe; a decrease in the 350 nm band was observed. Bottom right: the reaction when an O₂ purged solution of **8** was treated with 5 equivalents of NaOMe; a decrease in the 339 nm band was observed.



Scheme 3-11. Proposed reaction pathways for the reactions of **7** and **8** with a nucleophilic base (NaOMe) in the presence and absence of O_2 .

¹H NMR Studies. In addition to monitoring the reaction in real-time by UV-vis, we have also utilized ¹H NMR to follow the progression of the reaction. Analysis of the reaction of **7** with 5 equivalents of NaOMe under anaerobic conditions by ¹H NMR, in CD₃OD as a solvent, shows the initial growth of a new species, followed by the gradual disappearance of the paramagnetically-shifted peaks associated with the methylene and pyridyl ring protons on the 6-Ph₂TPA ligand (Figures 3-5 and 3-6 (top)). Analysis of the diamagnetic region at the end of the reaction shows the presence of peaks consistent with the presence of free 6-Ph₂TPA ligand, albeit broadened due to the presence of paramagnetic species in the solution (Figure 3-7). These results are consistent with the formation of an intermediate in which the 6-Ph₂TPA ligand remains coordinated to the metal center, followed by its subsequent demetallation (Scheme 3-11). We speculate that the intermediate is likely to be the neutral mononuclear complex [(6-Ph₂TPA)M(PhC(O)COCHO)] (**I**), in which the acetyl protecting group has been cleaved to generate an acireductone that has a dianionic protonation level.

In previous attempts to isolate a dianionic acireductone nickel complex, with an alternative acireductone substrate, various degrees of ancillary ligand displacement to form hexa-nickel or tri-nickel species were observed (Scheme 3-12).³⁶ In these complexes, the metal centers are bridged by the alkoxide groups of the dianionic acireductone. The displacement of the ancillary ligand is assumed to be due to the poor affinity of the phenyl pyridyl groups for Ni(II) relative to the affinity of the enolate moieties of the acireductone. It seems likely, therefore, that the displacement of 6-Ph₂TPA in the reaction of **7** and **8** with excess NaOMe is due to the formation of multi-nuclear clusters (**II**), likely bridged by the alkoxide groups of the dianionic acireductone.

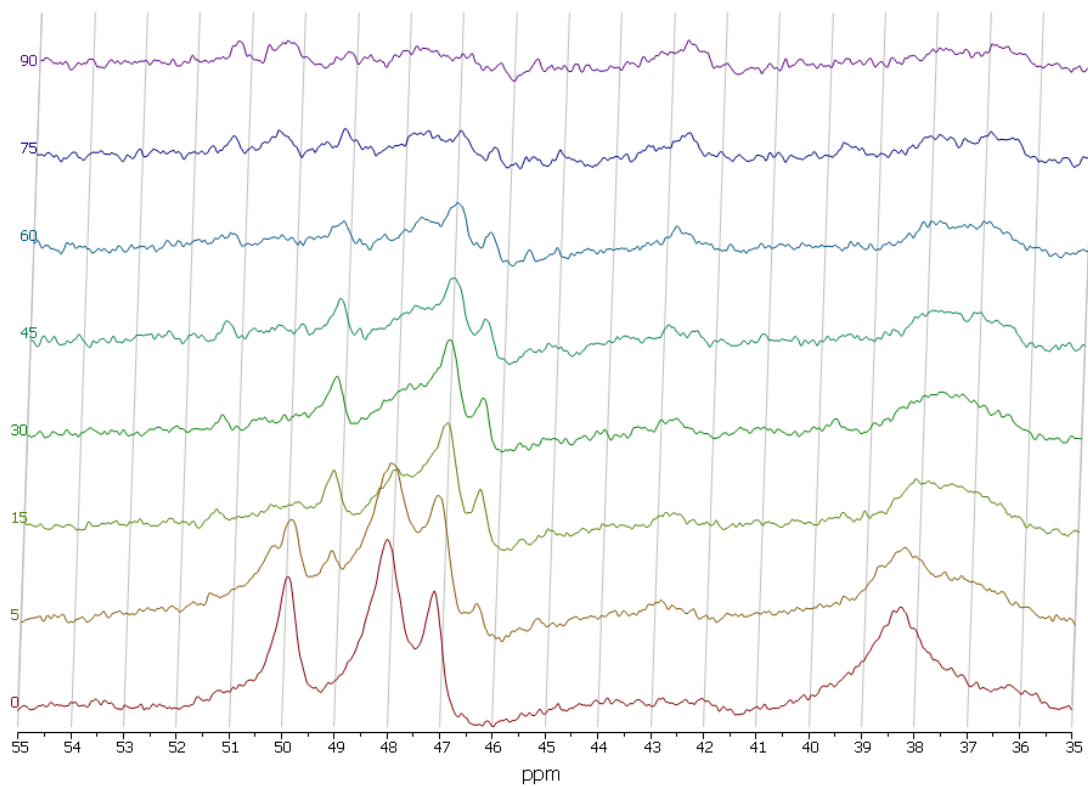


Figure 3-5. Selected regions of the ^1H NMR spectra collected during the reaction of **7** with 5 equivalents of NaOMe in CD_3OD under a nitrogen atmosphere. The spectra were recorded at varying time intervals, as shown in minutes. All spectra were collected using a 400 MHz spectrometer in CD_3OD at 25 $^\circ\text{C}$.

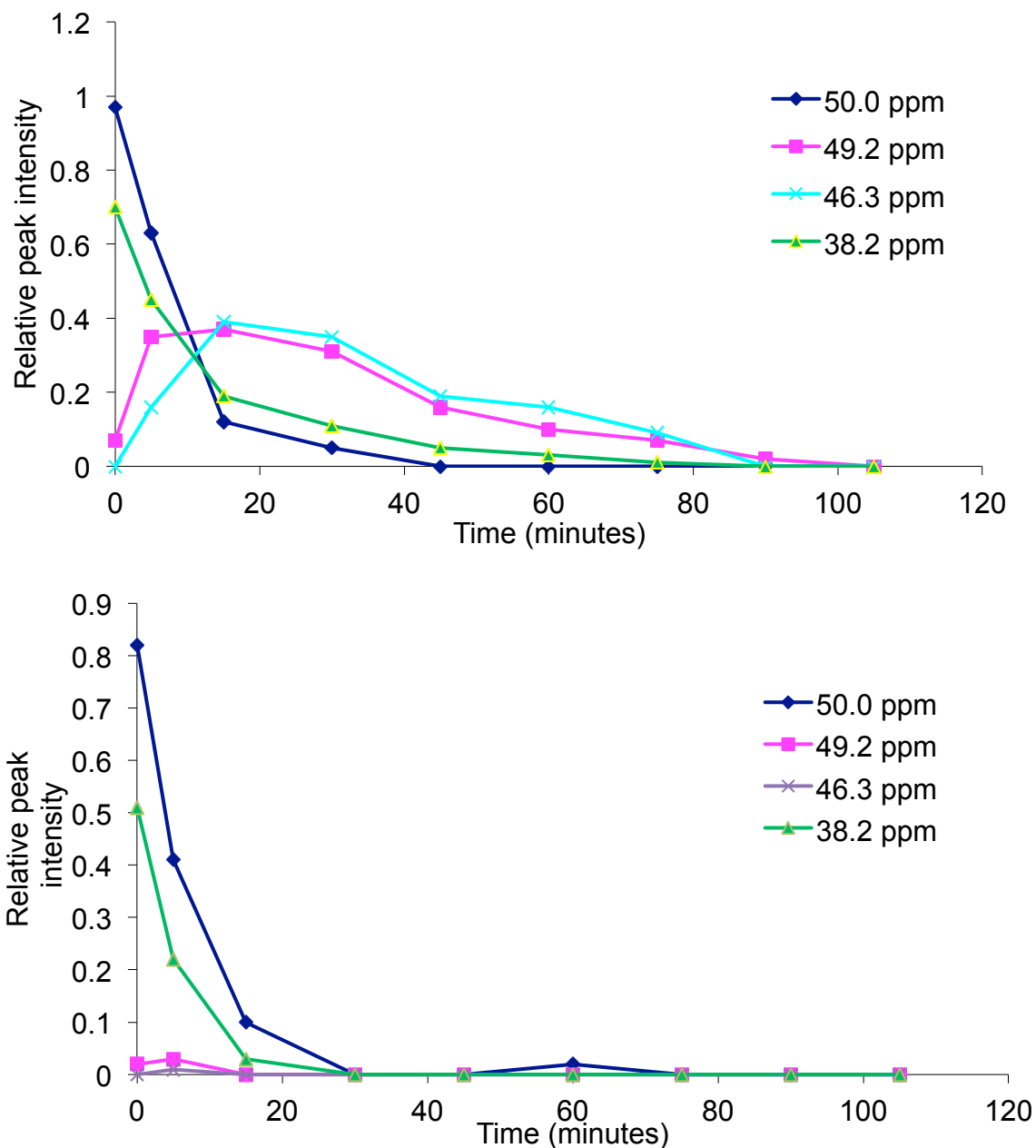


Figure 3-6. Plot of the relative intensities of selected features in the ^1H NMR during the reaction of **7** with 5 equivalents of NaOMe in CD_3OD under a nitrogen atmosphere (top) and under an oxygen atmosphere (bottom). The features at 50.0 and 38.2 ppm correspond to the starting material, while the features at 49.2 and 46.3 ppm correspond to an intermediate in the reaction. Notably, in the presence of oxygen the intermediate is no longer observed.

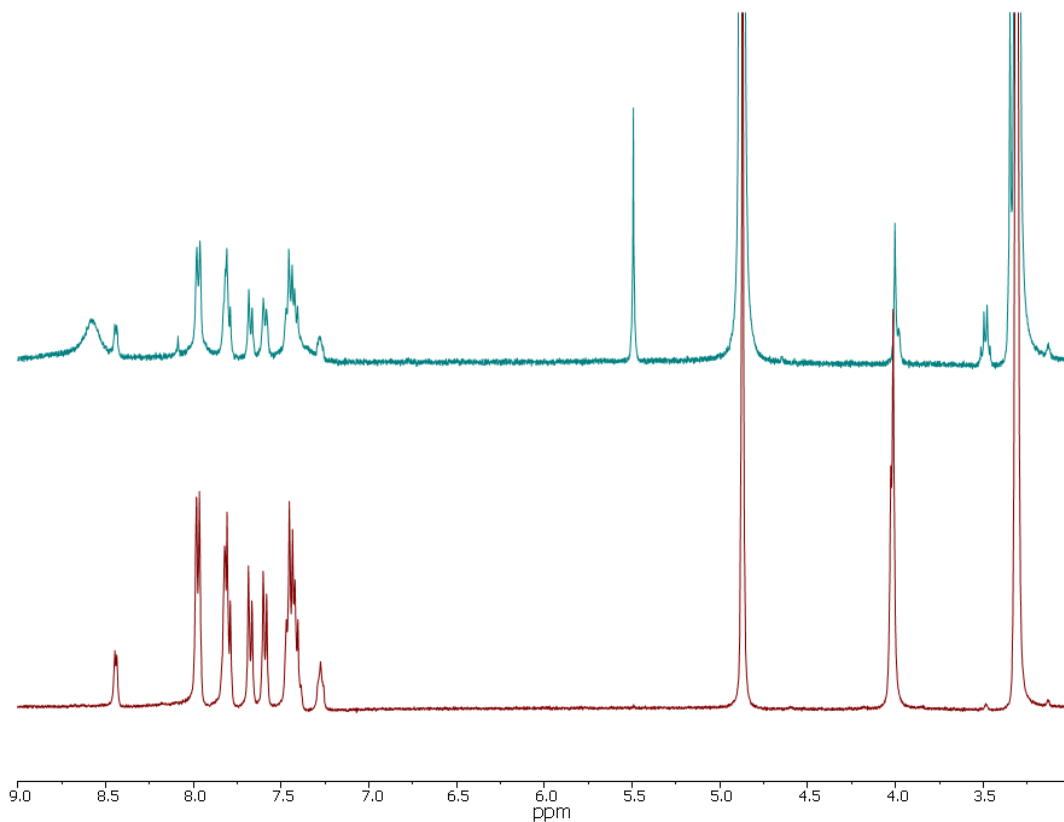
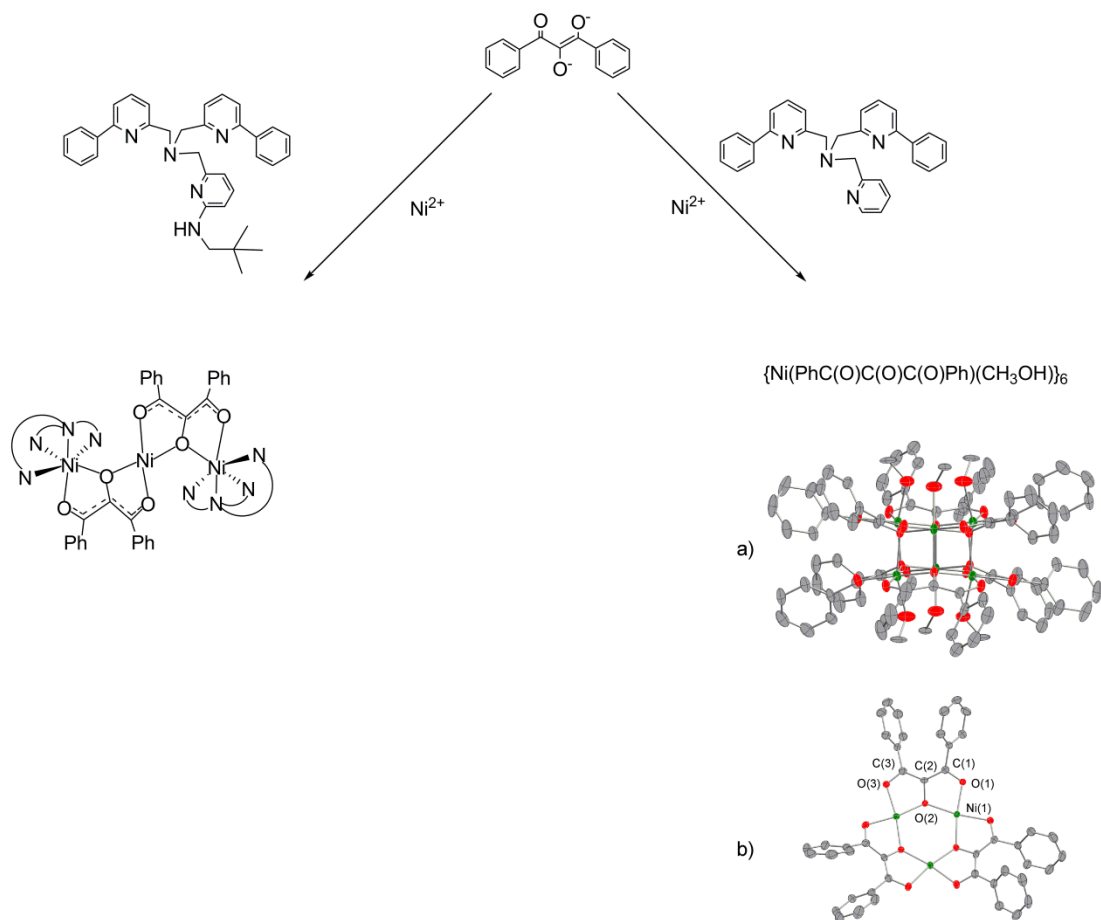


Figure 3-7. ¹H NMR spectra of the 6-Ph₂TPA ligand (bottom) and the product mixture of the reaction of **7** with 5 equivalents of NaOMe under a nitrogen atmosphere (top). Both spectra were recorded using a 400 MHz spectrometer using CD₃OD as a solvent and at 25 °C.



Scheme 3-12. Previous attempts to generate a mononuclear nickel acireductone dianionic complex have resulted in displacement of the ancillary chelate ligand. Treatment of a bulky acireductone dianion with one equivalent of Ni^{2+} and one equivalent of *N,N*-bis((6-phenyl-2-pyridyl)methyl)-*N*-(6-neopenylamino-2-pyridylmethyl)amine led to the formation of a trinuclear nickel complex with displacement of one equivalent of ancillary ligand (left). Treatment of a bulky acireductone anion with one equivalent of Ni^{2+} and one equivalent of 6- Ph_2TPA led to the formation of a hexanuclear nickel complex with displacement of six equivalents of ancillary ligand (right).

We note that an enolate absorption feature is still present in the UV-vis spectrum at this point in the reaction. It is only after addition of O₂ that the enolate is cleaved, which suggests that the cluster species is oxidatively sensitive. This is consistent with the previously reported reactivity of other nickel acireductone di-anion clusters, which in the presence of O₂ will cleave to form carboxylate products.³⁶

We also monitored the addition of NaOMe to an oxygenated solution of **7** by ¹H NMR (Figure 3-8). As we had seen in the reaction of **7** with NaOMe under anaerobic conditions, the peaks corresponding to **7** disappeared (Figure 3-6 (top)). Interestingly, the peaks that had previously been seen corresponding to the intermediate **I** were not observed in this aerobic reaction. In both cases, peaks associated with free 6-Ph₂TPA were present in the diamagnetic region at the end of the reaction. This strongly suggests that O₂ is in fact reacting directly with intermediate **I**, which appears to correspond to a mononuclear dianionic acireductone complex, in a very fast reaction. Thus, the intermediate is never observed spectroscopically as it is rapidly intercepted by the addition of O₂.

The goal of this work is to understand the reactivity of small molecular enolate complexes of structural relevance to the active sites of the acireductone dioxygenase enzyme substrate adducts. With this goal in mind, we have utilized the 6-Ph₂TPA ligand to mimic the 3-His, 1-Glu primary coordination sphere of these enzymes and attempted to generate a dianionic substrate bound to the metal center. The formation of a multi-nuclear cluster species (**II**) is detrimental to this goal despite its O₂ reactivity, as the resulting species has no structural relevance to the enzyme-substrate adduct. In order to investigate

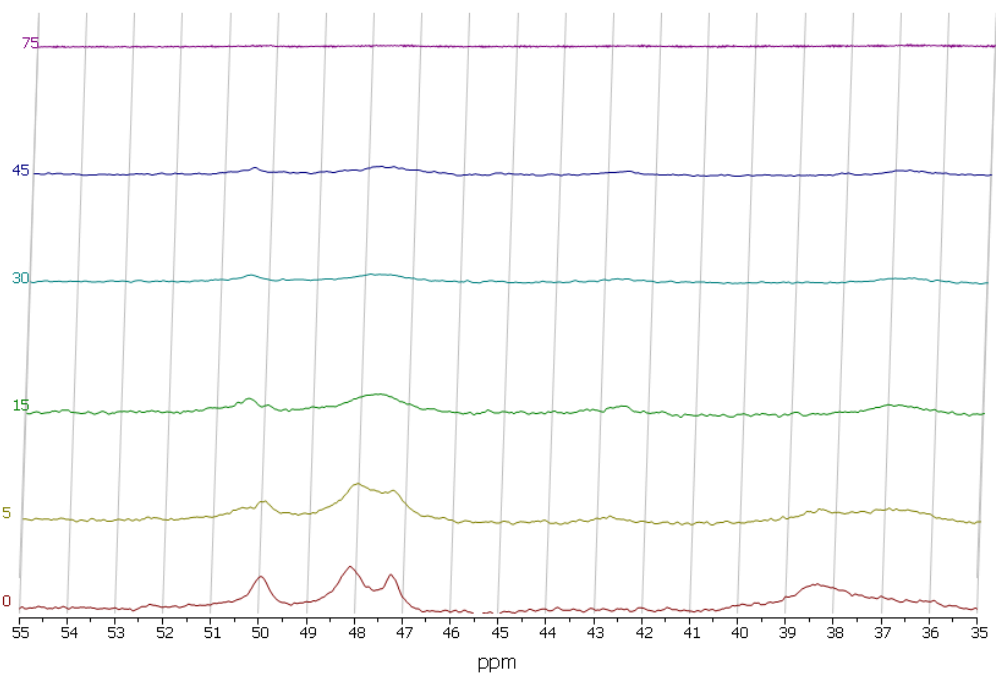
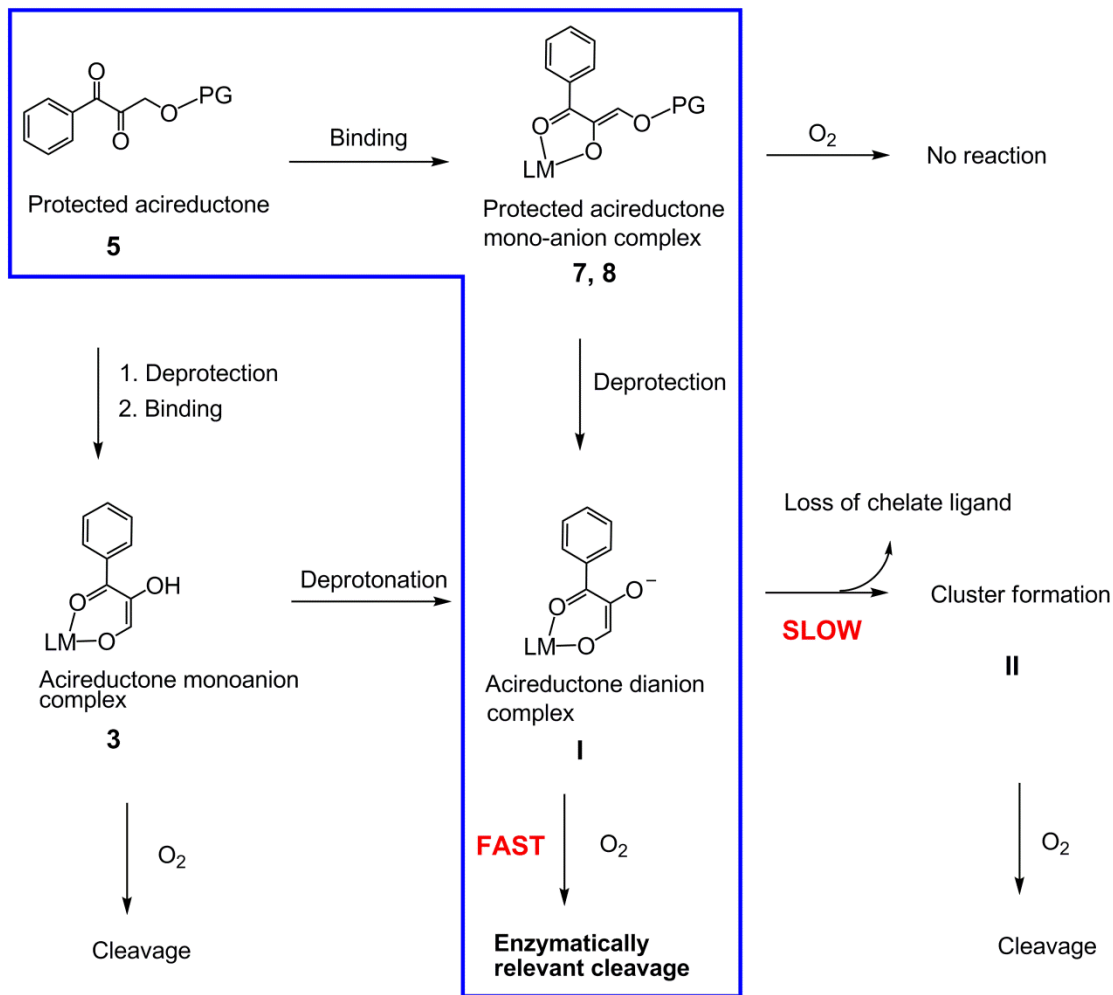


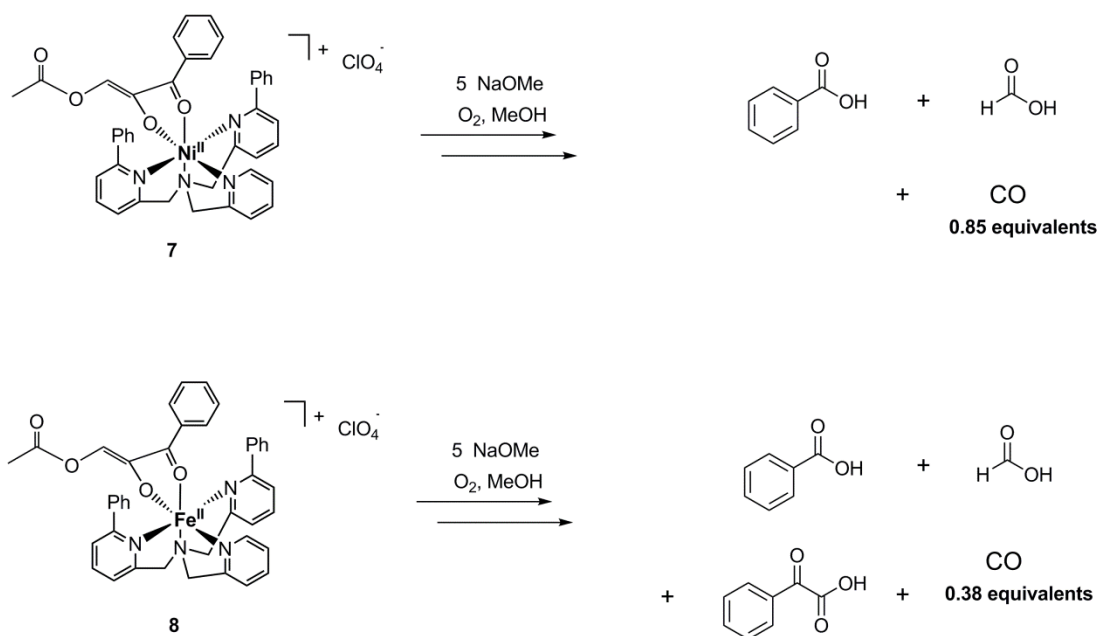
Figure 3-8. Selected regions of the ^1H NMR spectra collected during the reaction of **7** with 5 equivalents of NaOMe in CD_3OD under an oxygen atmosphere. The spectra were recorded at varying time intervals, as shown in minutes. All spectra were collected using a 400 MHz spectrometer in CD_3OD at 25 $^\circ\text{C}$.



Scheme 3-13. A summary of the various routes to oxidation of the C(1)H acireductone-derived species presented in this work. The use of complexes **7** and **8** as precursors for investigating the O₂ reaction of the enzymatically-relevant dianionic acireductone species **I** is advantageous as it avoids the inherent reactivity of **3**. Additionally, the observed fast reaction rate of **I** with O₂ allows the avoidance of oxidative chemistry associated with cluster species (**II**), which form at a much slower rate.

the O₂ reactivity of an enzymatically relevant species, we would need to work in a regime in which the O₂ reactivity of both the mono-anionic acireductone precursor, and the cluster, which is the thermodynamic product anaerobically, are excluded (Scheme 3-13). Our use of protected C(1)H acireductone complexes (**7** and **8**) is fortuitous as they do not react directly with O₂, in contrast to **3** which proves to be unsuitable for these investigations due to its inherent oxygenase reactivity. The observation by NMR that the mononuclear intermediate species **I** can be rapidly intercepted by the addition of O₂, on a time scale much faster than its subsequent decay to form a cluster, shows that these complexes can also exclude cluster-based oxygenation chemistry. Thus, we have discovered a method for generating an enzymatically relevant mononuclear dianionic complex *in situ* and monitoring its reactivity with oxygen (Scheme 3-13).

Product Analysis. Analysis of the headspace gas once the reaction of **7** with 5 equivalents of NaOMe in the presence of O₂ had proceeded to completion showed that 0.85 ± 0.01 equivalents CO had been produced in the reaction (Scheme 3-14). CO is an expected product if both the C(1)-C(2) and C(2)-C(3) bonds of the phenyl reductone substrate were to be cleaved. The yield of CO gas suggests that this cleavage reactivity is a major reaction pathway for **7**. However, the substoichiometric yield implies that there may be additional reaction pathways available to **7** that do not lead to the production of CO gas. In contrast to **7**, the reaction of **8** with 5 equivalents NaOMe in the presence of O₂ produced only 0.38 ± 0.10 equivalents of CO. As for **7**, the less-than-quantitative yield of CO suggests additional reaction pathways other than the oxidative cleavage of the C(1)-C(2) and C(2)-C(3) bonds. However, in the case of **8** these other reaction pathways appear to be responsible for a much more significant portion of the reaction products.



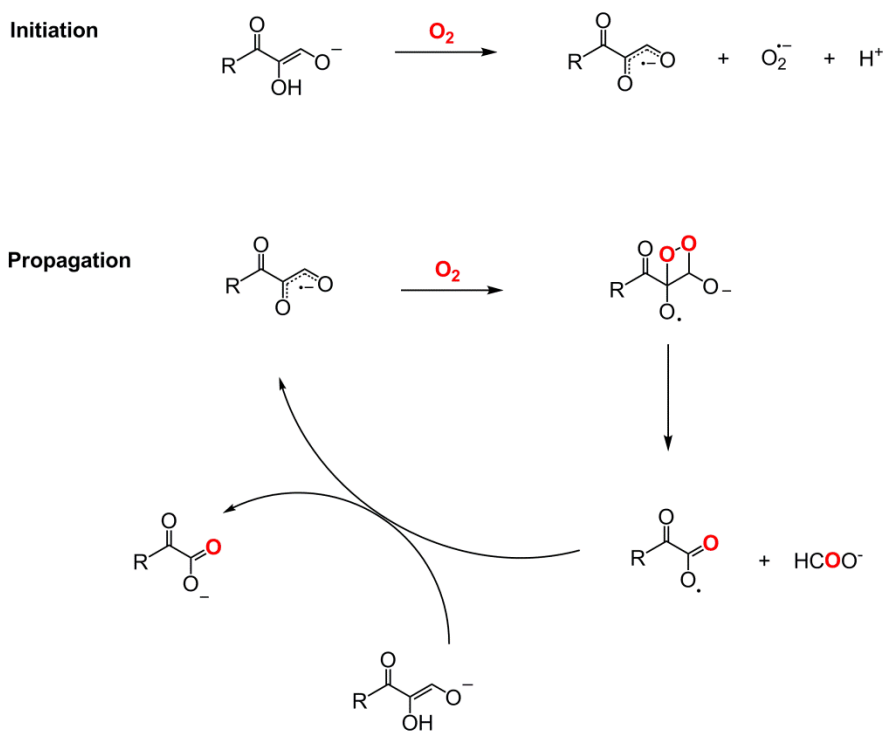
Scheme 3-14. Metal-dependent products of the oxidative enolate cleavage reactivity in the reactions of **7** and **8** with NaOMe in the presence of O_2 .

If the C(1)-C(2) and C(2)-C(3) bonds are being oxidatively cleaved then, in addition to CO, benzoate and formate are the expected products. The detection of formate in the presence of a paramagnetic metal center proves to be difficult, and thus we have utilized a previously reported method for the analysis of low molecular weight carboxylates and derivatized the crude reaction mixture using 4'-phenylphenacylbromide.¹¹ Subsequent analysis by GC-MS shows the production of 4'-phenylphenacylformate from the reaction mixtures of both **7** and **8**, consistent with the generation of formate in these reactions. In addition to formate, we have also detected the presence of benzoic acid in the reactions of both **7** and **8** (Scheme 3-14). Interestingly in the reaction mixture of **8** we have also detected benzoylformic acid which, along with formate, would be the expected product of oxidative cleavage of only the C(1)-C(2) bond of phenylreductone.

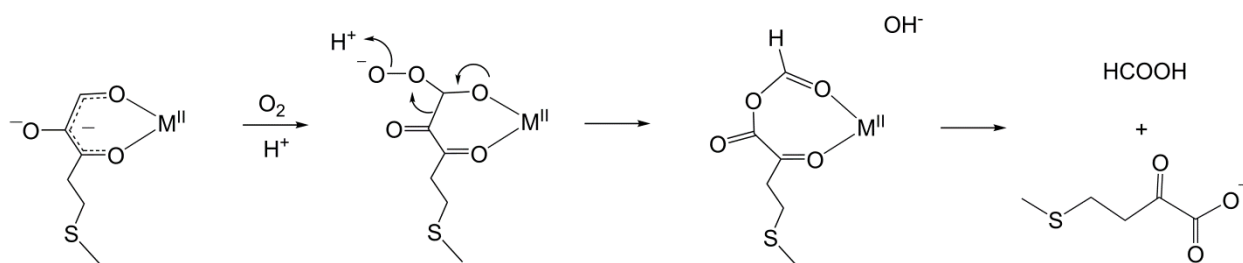
Mechanistic Implications. The reactions of **7** and **8** with excess NaOMe in the presence of O₂ show differences in the regioselectivity of their oxidative carbon-carbon bond cleavage reactions. Complex **7** predominantly reacts to cleave both the C(1)-C(2) and C(2)-C(3) bonds of its substrate, resulting in high yields of CO, while for complex **8** the yield of CO is significantly lower and an alternative pathway that cleaves only the C(1)-C(2) bond to generate benzoylformic acid accounts for a larger portion of the products. This difference in regioselectivity of reaction is somewhat unexpected based on our prior work investigating the metal-dependence of oxidative cleavage of a bulky acireductone substrate.

In the prior work, differences in regioselectivity were observed between the nickel-containing system (**1**) and the iron-containing system (**2**) only when water was present.²⁰ This led us to propose a mechanistic pathway in which the ferrous center had a much greater ability than nickel to promote hydration of a vicinal triketone intermediate, leading to a differentiation in the regioselectivity (Scheme 3-3). In the present work, a differentiation in regioselectivity as a function of metal ion is observed in the absence of water, suggesting that hydration chemistry is not relevant to the cleavage of this dianionic C(1)H acireductone. Thus, we have discovered that differences between a bulky acireductone substrate and a C(1)H acireductone substrate are significant enough to induce changes in reaction pathway.

This is not the first proposal for a change in the regioselectivity of the acireductone dioxygenases without invoking a water-dependent mechanism. A computational study has shown the lowest energy pathway for the reaction of a C(1)H acireductone mono-anion with oxygen in the absence of a metal center is via a radical



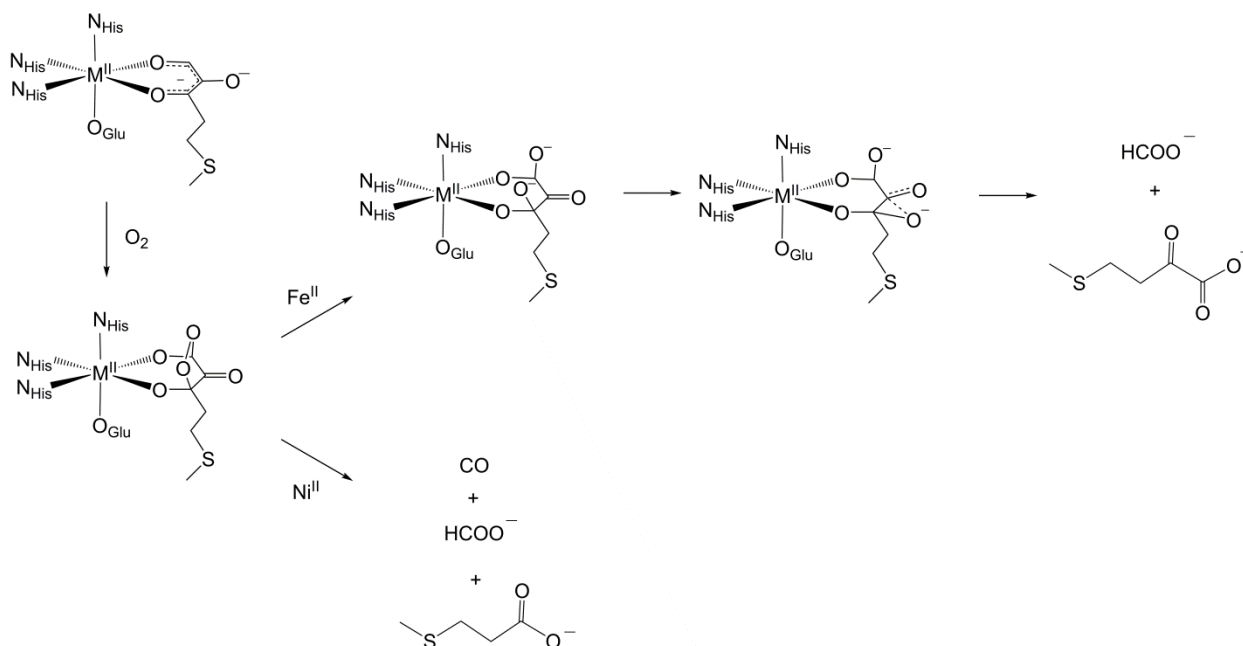
Scheme 3-15. A proposed radical propagation pathway to give Fe-ARD²-type products. This pathway was proposed based on a computational study.



Scheme 3-16. A proposed Baeyer-Villiger reaction to give Fe-ARD²-type products. This has been investigated computationally for a C(1)H acireductone monoanion in the absence of a metal center.

propagation pathway (Scheme 3-15).²³ This computed pathway correctly predicts the cleavage products of C(1)H acireductones in the absence of a metal center (an alpha-keto carboxylate and formate – the same as for Fe-ARD'), but the relevance of a radical propagation pathway to the enzymatic system is unclear.

A Baeyer-Villiger reaction pathway to form Fe-ARD'-type products has also been proposed (Scheme 3-16). In computational studies of the cleavage of the mono-anion of the bulky acireductone 2-hydroxy-1,3-diphenylpropan-1,3-dione, it was found that the Baeyer-Villiger reaction to form Fe-ARD' products was only 3.5 kcal/mol higher in energy than the observed reaction to form Ni-ARD products, suggesting that the Baeyer-Villiger reaction is a viable reaction pathway with appropriate tuning of the electronic structure.²¹ A recent mixed QM/DMD study on Ni-ARD and Fe-ARD' has also showed



Scheme 3-17. Pathways proposed by QM/DMD simulations for the reactions catalyzed by the acireductone dioxygenases.

that there does not appear to be a difference in binding mode between the two enzymes.³⁷ Rather, the lower occupation of the Fe^{II} d-orbitals (by two electrons compared to Ni^{II}), and greater redox flexibility, facilitated a key O-O bond cleavage step that was not accessible in Ni-ARD (Scheme 3-17). This reaction pathway is qualitatively quite similar to the Baeyer-Villager reaction pathway, albeit invoking direct metal-mediated electron transfer during the reaction progression. And, this general Baeyer-Villager type reaction pathway in which electronic differences between Ni^{II} and Fe^{II} provide for changes in regioselectivity is our current favoured explanation for the differences in reactivity observed for complexes **7** and **8**.

Conclusions

A high-yielding, relatively simple synthetic route to C(1)H acireductone precursors has been developed. This route can be utilized to generate tautomers of C(1)H acireductones, and has also allowed the synthesis of nickel and iron complexes with a protected C(1)H acireductone bound. This methodology will be expandable to the synthesis of a variety of C(1)H acireductones. Additionally, this work provides the first viable route to investigate the oxidative reactivity of mononuclear complexes with a coordinated acireductone dianion. Differences in regioselectivity are observed as a function of metal ion, suggesting that differences in the redox flexibility of Fe(II) and Ni(II) may be responsible for the reactivity differences.

References

- [1] a) Finkelstein, J. D. *J. Nutr. Biochem.* **1990**, *1*, 228-237. b) Valley, C. C.; Cembran, A.; Perlmutter, J. D.; Lewis, A. K.; Labello, N. P.; Gao, J.; Sachs, J. N. *J. Biol. Chem.* **2012**, *287*, 34979-34991. c) Cavuoto, P.; Fenech, M. F. *Cancer Treat. Rev.* **2012**, *38*, 726-736. d) Nakamoto, T. *Gene* **2009**, *432*, 1-6.
- [2] Pajares, M. A.; Markham, G. D. In *Advances in Enzymology and Related Areas of Molecular Biology*; Toone, E. J., Ed.; John Wiley & Sons, Inc.: Hoboken, New Jersey, 2011; Vol. 78, pp 449-521.
- [3] Stipanuk, M. H. *Ann. Rev. Nutr.* **1986**, *6*, 179-209.
- [4] Loenen, W. A. M. *Biochem. Soc. Trans.* **2006**, *34*, 330-333.
- [5] a) Schubert, H. L.; Blumenthal, R. M.; Cheng, X. *Trends Biochem. Sci.* **2003**, *28*, 329-335. b) Struck, A. -W.; Thompson, M. L.; Wong, L. S.; Micklefield, J. *Chem. Bio. Chem.* **2012**, *13*, 2642-2655.
- [6] a) Frey, P. A.; Hegeman, A. D.; Ruzicka, F. J. *Crit. Rev. Biochem. Mol. Biol.* **2008**, *43*, 63-88. b) Shisler, K. A.; Broderick, J. B. *Curr. Opin. Struct. Biol.* **2012**, *22*, 701-710.
- [7] Sauter, M.; Moffatt, B.; Saechao, M. C.; Hell, R.; Wirtz, M. *Biochem. J.* **2013**, *451*, 145-154.
- [8] a) Martinez, M. E.; O'Brien, T. G.; Fultz, K. E.; Babbar, N.; Yerushalmi, H.; Qu, N.; Guo, Y. J.; Boorman, D.; Einspahr, J.; Alberts, D. S.; Gerner, E. W. *Proc. Natl. Acad. Sci.* **2004**, *100*, 7859-7864. b) Pascale, R. M.; Simile, M. M.; Di Miglio, M. R.; Feo, F. *Alcohol* **2002**, *27*, 193-198.

- [9] a) Albers, E. *IUBMB Life* **2009**, *61*, 1132-1142. b) Sekowska, A.; Dénervaud, C.; Ashida, H.; Michoud, K.; Haas, D.; Yokota, A.; Danchin, A. *BMC Microbiol.* **2004**, *4*, 9. c) Avila, M. A.; García-Trevijano, E. R.; Lu, S. C.; Corrales, F. J.; Mato, J. M. *Int. J. Biochem. Cell Biol.* **2004**, *36*, 2125-2130.
- [10] Pochapsky, T. C.; Ju, T.; Dang, M.; Beaulieu, R.; Pagani, G. M.; OuYang, B. In *Metal Ions in Life Sciences*; Sigel, A., Sigel, H., Sigel, R. K. O., Eds.; Wiley-VCH: Weinheim, Germany, 2007; Vol. 2, pp 473-500.
- [11] Wray, J. W.; Abeles, R. H. *J. Biol. Chem.* **1995**, *270*, 3147-3153.
- [12] Wray, J. W.; Abeles, R. H. *J. Biol. Chem.* **1993**, *268*, 21466-21469.
- [13] Day, Y.; Wensink, P.C.; Abeles, R. H. *J. Biol. Chem.* **1999**, *274*, 1193-1195.
- [14] Motterlini, R.; Otterbein, L. E. *Nat. Rev. Drug Discov.* **2010**, *9*, 728-743.
- [15] Pochapsky, T. C.; Pochapsky, S. S.; Ju, T.; Mo, H.; Al-Mjeni, F.; Maroney, M. J. *Nat. Struct. Biol.* **2002**, *9*, 966-972.
- [16] (a) Ju, T.; Goldsmith, R. B.; Chai, S. C.; Maroney, M. J.; Pochapsky, S. S.; Pochapsky, T. C. *J. Mol. Biol.* **2006**, *393*, 823-834. (b) Pochapsky, T. C.; Pochapsky, S. S.; Ju, T.; Hoefler, C.; Liang, J. *J. Biomol. NMR.* **2005**, *34*, 117-127. (c) Pochapsky, S. S.; Sunshine, J. C.; Pochapsky, T. C. *J. Am. Chem. Soc.* **2008**, *130*, 2156-2157.
- [17] Dai, Y.; Pochapsky, T. C.; Abeles, R. H. *Biochemistry*, **2001**, *40*, 6379-6387.
- [18] Chai, S. C.; Ju, T.; Dang, M.; Goldsmith, R. B.; Maroney, M. J.; Pochapsky, T. C. *Biochemistry* **2008**, *47*, 2428-2438.
- [19] Szajna, E.; Arif, A. M.; Berreau, L. M. *J. Am. Chem. Soc.* **2005**, *127*, 17186-17187.

- [20] Allpress, C. J.; Grubel, K.; Szajna-Fuller, E.; Arif, A. M.; Berreau, L. M. *J. Am. Chem. Soc.* **2013**, *135*, 659-668.
- [21] Berreau, L. M.; Borowski, T.; Grubel, K.; Allpress, C. J.; Wikstrom, J. P.; Germain, M. E.; Rybak-Akimova, E. L.; Tierney, D. L. *Inorg. Chem.* **2011**, *50*, 1047-1057.
- [22] Roberts, J. D.; Smith, D. R.; Lee, C. C. *J. Am. Chem. Soc.* **1951**, *73*, 618-625.
- [23] T. Borowski, *J. Mol. Structure: Theochem*, **2006**, *772*, 89-92.
- [24] Myers, R.W.; Wray, J. W.; Fish, S.; Abeles, R. H. *J. Biol. Chem.* **1993**, *268*, 24785-24791.
- [25] Zhang, Y.; Heinsen, M. H.; Kostic, M.; Pagani, G. M.; Riera, T. V.; Perovic, I.; Hedstrom, L.; Snider, B. B.; Pochapsky, T. C. *Bioorg. Med. Chem.* **2004**, *12*, 3847-3855.
- [26] Rudzka, K., Ph.D. Dissertation, Department of Chemistry and Biochemistry, Utah State University, 2008.
- [27] Cocker, W.; Jenkinson, D. S.; Schwarz, P. *J. Chem. Soc.* **1953**, 1631-1634.
- [28] Grubel, K.; Ingle, G. K.; Fuller, A. L.; Arif, A. M.; Berreau, L. M. *Dalton Trans.* **2011**, *40*, 10609-10620.
- [29] Armarego, W. L. F.; Perrin, D. D. *Purification of Laboratory Chemicals*, 4th ed., Butterworth-Heinemann, Boston, MA, 1996.
- [30] Makowska-Grzyska, M. M.; Szajna, E.; Shipley, C.; Arif, A. M.; Mitchell, M. H.; Halfen, J. A.; Berreau, L. M. *Inorg. Chem.* **2003**, *43*, 7472-7488.
- [31] Szajna-Fuller, E.; Rudzka, K.; Arif, A. M.; Berreau, L. M. *Inorg. Chem.* **2007**, *46*, 5499-5507.
- [32] Szajna, E.; Dobrowolski, P.; Fuller, A. L.; Arif, A. M.; Berreau, L. M. *Inorg. Chem.* **2004**, *43*, 3988-3997.

- [33] Wolsey, W. C. *J. Chem. Educ.* **1973**, *50*, A335-A337.
- [34] (a) Allpress, C. J.; Arif, A. M.; Houghton, D. T.; Berreau, L. M. *Chem. Eur. J.* **2011**, *17*, 14962-14973. (b) Grubel, K.; Rudzka, K.; Arif, A. M.; Klotz, K. L.; Halfen, J. A.; Berreau, L. M. *Inorg. Chem.* **2010**, *49*, 82-96.
- [35] Szajna-Fuller, E.; Rudzka, K.; Arif, A. M.; Berreau, L. M. *Inorg. Chem.* **2007**, *46*, 5499-5507.
- [36] a) Rudzka, K.; Arif, A. M.; Berreau, L. M. *Inorg. Chem.* **2008**, *47*, 10832-10840.
b) Rudzka, K.; Grubel, K.; Arif, A. M.; Berreau, L. M. *Inorg. Chem.* **2010**, *49*, 7623-7625.
- [37] Sparta, M.; Valdez, C. E.; Alexandrova, A. N. *J. Mol. Biol.* **2013**, *425*, 3007-3018.

CHAPTER 4

PHOTOCHEMICALLY-INITIATED OXIDATIVE CARBON-CARBON BOND
CLEAVAGE REACTIVITY IN CHLORODIKETONATE DIVALENT NICKEL
COMPLEXES[†]**Abstract**

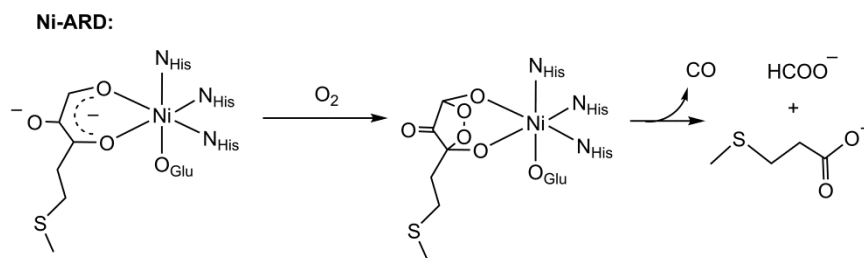
Three mononuclear Ni^{II} complexes having a 2-chloro-1,3-diketonate ligand and supported by the 6-Ph₂TPA chelate (**4-6**), as well as analogs that lack the 2-chloro substituent on the β-diketonate ligand (**7-9**), have been prepared and characterized. Upon irradiation at 350 nm under aerobic conditions, complexes **4-6** undergo reaction to generate products resulting from oxidative cleavage, α-cleavage, and radical-derived reactions involving the 2-chloro-1,3-diketonate ligand. Mechanistic studies suggest that the oxidative cleavage reactivity, which leads to the production of carboxylic acids, is a result of the formation of superoxide, which occurs via reaction of reduced nickel complexes with O₂. The presence of the 2-chloro substituent was found to be a prerequisite for oxidative carbon-carbon bond cleavage reactivity, as **7-9** did not undergo reaction following prolonged irradiation. The novel approach toward investigating oxidative reactivity of metal β-diketonate species outlined herein has yielded results of relevance to the proposed mechanistic pathways of metalloenzyme-catalyzed β-diketonate oxidative cleavage reactions.

[†] Coauthored by Caleb J. Allpress, Atta M. Arif, Dylan T. Houghton and Lisa M. Berreau. Reproduced in a modified format with permission from *Chem. Eur. J.* **2011**, *17*, 14962-14973.

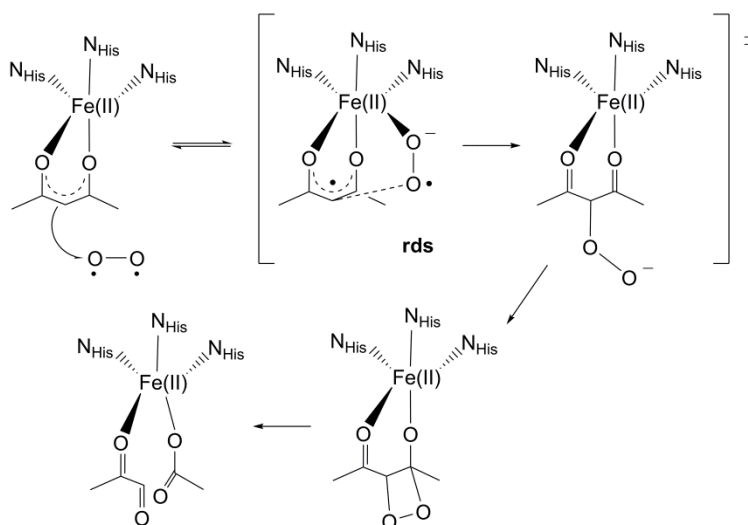
Introduction

Reaction pathways leading to the oxidative cleavage of the aliphatic carbon-carbon bonds of β -diketonate type molecules are of current interest due to the identification of enzymes that catalyze the cleavage of these strong bonds.¹ Of primary interest toward broadly understanding the chemistry of such systems is the elucidation of how changes in the nature of the metal center, or the structural and/or electronic features of the β -diketonate, influence the reaction mechanism. One potential role of the metal center is to act as a Lewis acid to stabilize a particular protonation level of a substrate. An example of a metalloenzyme of this class is acireductone dioxygenase (ARD), which uses a mononuclear Ni^{II} center as a Lewis acid to stabilize a dianionic form of the acireductone substrate in a β -diketonate type coordination motif (Scheme 4-1 (top)).² The acireductone dianion acts as a reductant toward O₂. Transfer of two electrons from the enediolate to O₂ is proposed to occur via an initial single electron transfer to form superoxide and an organic radical, followed by collapse of the radical pair by attack of superoxide at the terminal carbon to yield an organoperoxo species. Attack of the terminal oxygen of the peroxy moiety at the other carbonyl produces a five-membered dioxetane ring from which aliphatic oxidative carbon-carbon bond cleavage and CO release is proposed to occur.

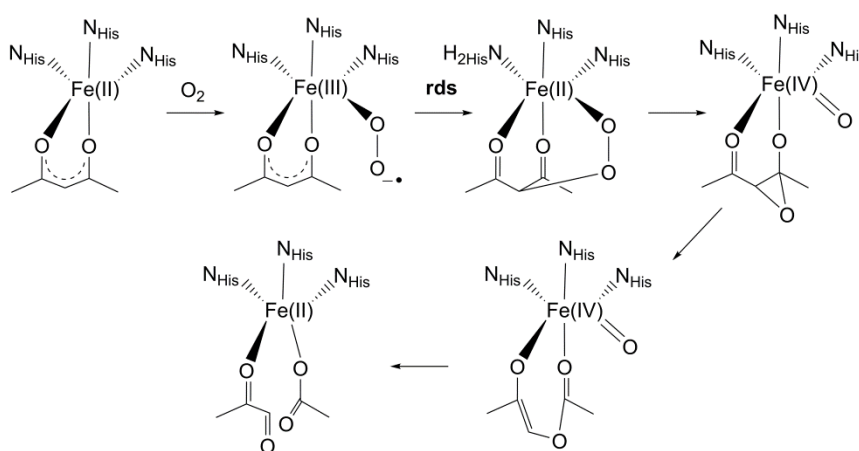
Alternative roles for the metal center can include orbital mixing to help overcome the spin forbidden reaction between ground state (triplet) dioxygen and the singlet ground state β -diketonate, or the reductive activation of dioxygen to form a superoxide species. Both of these roles for a metal center have been proposed as potential roles for the Fe^{II} center in the reaction pathway of acetylacetone dioxygenase (Dke1), which catalyzes the



Dke1: Reaction of coordinated enolate with O₂:



Dke1: Metal-centered activation of O₂:



Scheme 4-1. Proposed reaction pathways for the aliphatic carbon-carbon bond cleavage reactions catalyzed by Ni-ARD (top) and Dke1. For Dke1, both a direct reaction of O₂ with the diketonate substrate (middle) and a metal-centered reductive activation of O₂ (bottom) have been proposed.

oxidative decomposition of acetylacetonate to acetate and methyl glyoxal.^{3,4} Kinetic studies on the enzyme suggest that the role of the Fe^{II} center is to help overcome the spin forbidden nature of the reaction between triplet dioxygen with the singlet substrate by delocalization of electron density via orbital mixing of the HOMOs of the β -diketonate and Fe^{II} center (Scheme 4-1 (middle)). Electron transfer from the coordinated β -diketonate is suggested to occur in a concerted fashion with C-O bond formation at C(2) to give a peroxide species from which carbon-carbon bond cleavage occurs.^{4a} An alternative reaction pathway has been suggested by computational studies and involves the initial formation of Fe^{III}-O₂⁻ species which proceeds to C-C cleavage via an Fe^{IV}=O intermediate (Scheme 4-1 (bottom)).^{4b} It should be noted that substitution of the Fe^{II} in Dke1 by other divalent metal ions, including Ni^{II}, results in a loss of catalytic activity.^{4a}

A useful technique that provides insight into the reaction pathway of complicated enzymatic systems is the use of small molecular model systems that can be definitively characterized. In model studies of relevance to Dke1, Limberg et al. have shown that while [Tp*Fe(acac)] (Tp* = hydridotris(3,5-dimethylpyrazol-1-yl)borato) does not undergo reaction with O₂ to give products of acetylacetonate oxidative cleavage, a structurally similar complex of the more electron rich diethylphenylmalonate β -diketonate, [Tp*Fe(Phmal)], catalyzes O₂-dependent carbon-carbon bond cleavage reactivity to give Dke1-type products (ethyl benzoylformate, ethoxide and CO₂ via decomposition of EtOCO₂⁻).⁵ Control studies indicate that the formation of a Fe(III) superoxide species is necessary in this model system for the observed reactivity. In a very recent study of relevance to Dke1, Nunes et al. have reported the formation of [Ni(en)₂(CH₃CO₂)]PF₆ via treatment of [Ni(acac)₂(H₂O)₂] with ethylenediamine in

aerobic, aqueous solution. The oxidative cleavage of acac^- to give acetate is suggested to involve superoxide generated in the reaction mixture, however no further details were provided.⁶

As can be seen in the chemistry of Ni^{II} -ARD and Dke1, and related model systems, specific combinations of β -diketonate ligand and metal ion impart oxidative carbon-carbon bond cleavage reactivity. In Ni^{II} -ARD, a typically redox-inactive metal center stabilizes the dianionic form of a β -diketonate type substrate having inherent reductive reactivity toward O_2 . In Dke1, a potentially redox active Fe^{II} center is partnered with the O_2 -stable acetylacetone substrate. In this latter case the metal center is important for either substrate activation or stabilization, or for redox reactivity with O_2 , to initiate the oxidative cleavage process.

We have previously shown that the β -diketonate complex [(6- Ph_2TPA) $\text{Ni}(\text{PhC}(\text{O})\text{C}(\text{OH})\text{C}(\text{O})\text{Ph})$] ClO_4 (**1**, Figure 4-1) reacts with O_2 to give products (carboxylates and CO) akin to those generated in the Ni^{II} -ARD catalyzed reaction.⁷ The mechanism by which this occurs involves two electron oxidation of the enediolate moiety to give an intermediate triketone species which subsequently undergoes reaction with HOO^- generated in the reaction mixture to give aliphatic carbon-carbon bond cleavage products.⁸ While this mechanism differs from that proposed for the enzyme¹, this system does mimic Ni^{II} -ARD in terms of incorporating the combination of an inherently O_2 -reactive β -diketonate ligand with a redox-inactive Ni^{II} center.

Complexes that are structurally similar to **1** but instead have an unsubstituted β -diketonate ligand, such as [(6- Ph_2TPA) $\text{Ni}(\text{PhC}(\text{O})\text{CHC}(\text{O})\text{Ph})$] ClO_4 (**9**), are stable with respect to O_2 under ambient conditions.⁷ As described herein, Ni^{II} complexes having a

mildly electron withdrawing chloride at the C(2) position, e.g. [(6-Ph₂TPA)Ni(PhC(O)C(Cl)C(O)Ph)]ClO₄ (**6**), are also stable with respect to O₂ under ambient conditions. The lack of dioxygen reactivity for **6** and **9** is not unexpected, as the reduced electron density within the π system of the β-diketonate moiety makes these anions poorer reducing agents than the α-hydroxy-containing analog.

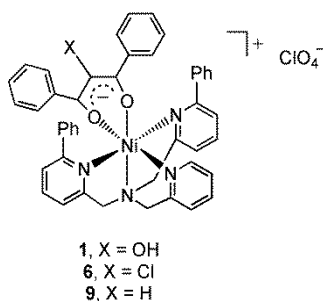
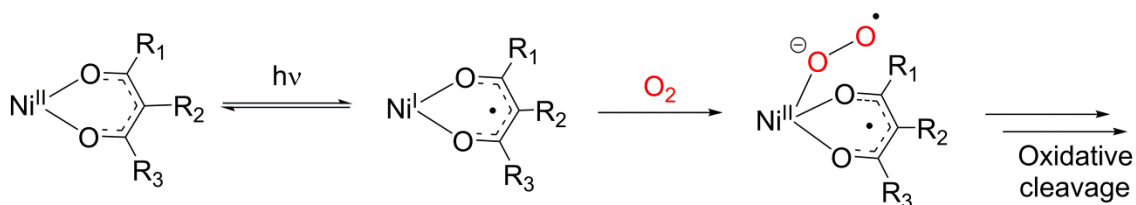


Figure 4-1. Structures of a synthetic complex studied as a model system for Ni^{II}-containing acireductone dioxygenase **1** and analogues **6** and **9** that are O₂-stable under ambient conditions.

Prior studies of Ni^{II} β-diketonate species have shown that it is possible to photochemically induce redox activity at the nickel center. It is known, for example, that Ni(acac)₂ undergoes photoreduction to produce transient Ni^I complexes in the presence of stabilizing ligands.⁹ This led us to consider how this approach might be used to induce redox activity at the nickel center of **6** and **9** as a means toward promoting oxidative carbon-carbon bond cleavage reactivity. Based on this literature precedent, if Ni^I β-diketonate species can be photochemically generated starting from complexes such as **6** and **9**, this offers the possibility of producing a combination of a Ni^I center and a β-diketonate radical. The Ni^I could then activate O₂ to generate Ni^{II} and O₂⁻ from which subsequent oxidative chemistry may occur (Scheme 4-2).¹⁰ This net transfer of one

electron from the β -diketonate to O_2 would be similar to the mechanism proposed for the Dke1 enzyme wherein the ligand is also oxidized by one electron to form superoxide (Scheme 4-1 (middle)), albeit in the nickel case this would involve direct electron transfer rather than orbital mixing.



Scheme 4-2. Proposed mechanism by which a Ni^{II}- β -diketonate unit may be photochemically activated to generate a superoxo-diketonyl radical pair.

We outline herein the results of studies of the photochemical reactivity of **6** and **9** and para-substituted analogs. The results show that oxidative cleavage products are generated for systems containing a 2-chloro substituent on the coordinated enolate.

Experimental

General Methods. All reagents and solvents were obtained from commercial sources, and were used without further purification unless noted. The 6-Ph₂TPA ligand *N,N*-bis-((6-phenyl-2-pyridyl)methyl)-*N*-((2-pyridyl)methyl)amine, 1,3-di-(4-tolyl)-propane-1,3-dione (**2b**), [(6-Ph₂TPA)Ni(PhC(O)CHC(O)Ph]ClO₄ (**9**), [(6-Ph₂TPA)NiCl(CH₃CN)]ClO₄ (**10**), [(6-Ph₂TPA)Ni(CH₃CN)₂](ClO₄)₂ (**13**) were synthesized according to literature procedures.^{7, 11-13} 1,3-di-(4-methoxyphenyl)-propane-1,3-dione and 1,3-di-phenyl-propane-1,3-dione were purchased from TCI and ACROS, respectively, and were used as received. Dry acetonitrile was prepared according to a literature procedure¹⁴ and was used in the metal complex syntheses.

Physical Methods. ^1H NMR spectra of organic compounds were obtained using a JEOL ECX-300 or Bruker ARX-400 NMR spectrometer. Chemical shifts were referenced to the residual solvent peak in CD_2HCN (1.94 ppm, quintet). ^1H NMR spectra of paramagnetic Ni^{II} complexes were obtained using a Bruker ARX-400 spectrometer and parameters as previously described.¹¹ FT-IR data collected on a Shimadzu FTIR-8400 spectrometer as KBr pellets. UV-vis data was collected on a HP8453A spectrometer at ambient temperature. Photoreactions were carried out in a Srinivasan-Griffin Rayonet photochemical reactor equipped with 8 RPR-3500 lamps, having $\lambda_{\text{max}} = 350$ nm. GC-MS data was obtained with a Shimadzu GCMS-QP5000 gas chromatograph/mass spectrometer with a GC-17A gas chromatograph, using an Alltech EC-5 $30 \text{ m} \times 0.25 \text{ mm} \times 0.25 \text{ }\mu\text{m}$ thin film capillary column and temperature program: $T_{\text{Initial}} 30^\circ\text{C}$ (3 min); temperature gradient $23^\circ\text{C}/\text{min}$; $T_{\text{Final}} 250^\circ\text{C}$ (10 min). Quantum yields were determined by ferrioxalate actinometry, using an integrative analysis method.¹⁵ Anaerobic electrochemical measurements were carried out in a drybox under N_2 in CH_3CN with 0.1 M $[\text{Bu}_4\text{N}][\text{ClO}_4]$ as the supporting electrolyte using a model ED401 computer controlled potentiostat (eDAQ). A three-electrode configuration with a glassy carbon working electrode, a Ag wire quasi-reference electrode with a Fc/Fc^+ internal reference, and a platinum wire auxiliary electrode was used. Aerobic electrochemical studies were performed after purging the cell with O_2 . The potential values were referenced to an internal ferrocenium/ferrocene couple, which is reported to be $+0.38 \text{ V}$ vs. SCE in CH_3CN using $[\text{NBu}_4][\text{ClO}_4]$ as a supporting electrolyte.¹⁶

Preparation of 2-chloro-1,3-di(4-methoxyphenyl)-propane-1,3-dione (3a). A solution comprised of acetonitrile (20 mL), aqueous NH_4Cl (1.0 M, 20 mL) and aqueous

RuCl₃ (0.10 M, 250 μL) was cooled in an ice-bath. Oxone (4.08 g, 6.64 mmol) was added to this solution, which resulted in the formation of a yellow suspension. The mixture was then warmed to room temperature. Dropwise addition of a solution of 1,3-di-(4-methoxyphenyl)-propane-1,3-dione (0.382 g, 1.34 mmol) in ethyl acetate (10 mL) resulted in darkening to a purplish color. After stirring overnight at ambient temperature, the solution was again a yellow color. The suspension was then diluted with water (100 mL) and the mixture was extracted with ethyl acetate (3 × 100 mL). The combined organic fractions were dried over anhydrous Na₂SO₄, filtered, and the filtrate was brought to dryness under reduced pressure. The pale yellow solid was recrystallized from hot ethanol to give pale yellow crystals (338 mg, 79%), m.p. 94-96 °C; ¹H NMR (300 MHz, CD₃CN, 25°C): δ = 7.96 (d, ³J(H,H) = 8.9 Hz, 4H; Ar-H), 7.03 (d, ³J(H,H) = 8.9 Hz, 4H; Ar-H), 6.83 (s, 1H; CH), 3.87 ppm (s, 6H; CH₃); ¹³C{¹H} NMR (100 MHz, CD₃CN, 25°C): δ = 189.8 (C=O), 166.0 (C_q^{Ar}), 132.8 (CH^{Ar}), 128.1 (C_q^{Ar}), 115.7 (CH^{Ar}), 62.8 (CHCl), 56.9 ppm (CH₃); IR (KBr): ν = 1687 (C=O), 1659, 1601, 1572 cm⁻¹; GC-MS: *m/z* = 320 (38%), 318 (18%).

Preparation of 2-chloro-1,3-bis(4-methylphenyl)-propane-1,3-dione (3b) and 2-chloro-1,3-bis-phenyl-propane-1,3-dione (3c). These compounds were prepared in a similar manner to **3a**. **3b** (32%): m.p. 140-141°C; ¹H NMR (300 MHz, CD₃CN, 25°C): δ = 7.87 (d, ³J(H,H) = 8.5 Hz, 4H; Ar-H), 7.35 (d, ³J(H,H) = 8.5 Hz, 4H; Ar-H), 6.89 (s, 1H; CH), 2.45 ppm (s, 6H; CH₃); ¹³C{¹H} NMR (100 MHz, CD₃CN, 25°C): δ = 191.0 (C=O), 147.3 (C_q^{Ar}), 132.8 (C_q^{Ar}), 131.1 (CH^{Ar}), 130.4 (CH^{Ar}), 62.7 (CHCl), 22.1 ppm (CH₃); IR (KBr): ν=1695 (C=O), 1674, 1604 cm⁻¹; GC-MS: *m/z* (%) = 286 (1.1), 288 (0.4); elemental analysis calcd (%) for C₁₇H₁₅ClO₂·0.2H₂O: C 70.31, H 5.35; found: C

70.50, H 5.31. **3c** (83%): m.p. 71-72 °C; $^1\text{H NMR}$ (300 MHz, CD_3CN , 25°C): $\delta = 7.98$ (d, $^3J(\text{H,H}) = 7.2$ Hz, 4H; Ar-H), 7.69 (t, $^3J(\text{H,H}) = 8.4$ Hz, 2H; Ar-H), 7.55 (t, $^3J(\text{H,H}) = 6.7$ Hz, 4H; Ar-H), 6.97 ppm (s, 1H; CH); IR (KBr): $\nu = 1699$ (C=O), 1680, 1595, 1580 cm^{-1} ; GC-MS: m/z (%) = 258 (1.5), 260 (0.5).

Caution! *Perchlorate salts of metal complexes with organic ligands are potentially explosive. Only small amounts of material should be prepared, and these should be handled with great care.*¹⁷

Preparation of [(6-Ph₂TPA)Ni((4-OCH₃Ph)C(O)C(Cl)C(O)(4-OCH₃Ph))]ClO₄ (4**).** Ni(ClO₄)₂•6H₂O (29 mg, 79 μmol) was dissolved in dry acetonitrile, (2 mL) and this solution was added to solid 6-Ph₂TPA (35 mg, 79 μmol) and the resulting solution was stirred for 15 minutes during which time it became a pale purple. This solution was added to solid 2-chloro-1,3-di(4-methoxyphenyl)-propane-1,3-dione (25 mg, 79 μmol) and the resulting mixture was stirred until completely dissolved. The pale purple solution was then added to solid Me₄NOH•5H₂O (13 mg, 79 μmol) and the mixture was stirred overnight at ambient temperature during which time it became yellow. The solvent was removed from the reaction mixture under vacuum and the remaining solid was redissolved in CH₂Cl₂, and the solution was filtered through a glass wool/Celite plug. Concentration of the filtrate under vacuum, followed by the addition of excess hexanes, resulted in the deposition of a yellow solid (50 mg, 70%) that was dried under vacuum. IR (KBr): $\nu = 1603, 1346, 1094$ (ClO₄), 623 cm^{-1} (ClO₄); HRMS (ESI): m/z calcd for C₄₇H₄₀N₄ClO₄Ni⁺: 817.209 [M-ClO₄]⁺; found: 817.209; elemental analysis calcd (%) for C₄₇H₄₀N₄Cl₂O₈Ni: C 61.45, H 4.39, N 6.10; Found: C 61.48, H 4.90, N 5.99.

Preparation of [(6-Ph₂TPA)Ni((4-CH₃Ph)C(O)C(Cl)C(O)(4-CH₃Ph))]ClO₄ (5), [(6-Ph₂TPA)Ni(PhC(O)C(Cl)C(O)Ph)]ClO₄ (6), [(6-Ph₂TPA)Ni((4-OCH₃Ph)C(O)CHC(O)(4-OCH₃Ph))]ClO₄ (7) and [(6-Ph₂TPA)Ni((4-CH₃Ph)C(O)CHC(O)(4-CH₃Ph))]ClO₄ (8). Compounds **5-8** were prepared and crystallized in a manner similar to that described for **4** using appropriate starting materials. **5** (62%): IR (KBr): $\nu=1346, 1094$ (ClO₄), 623 cm^{-1} (ClO₄); HRMS (ESI) m/z calcd for C₄₇H₄₀N₄ClO₂Ni⁺: 785.219 ([M-ClO₄]⁺); found: 784.219; elemental analysis calcd (%) for C₄₇H₄₀N₄Cl₂O₆Ni·1.5CH₂Cl₂: C 57.46, H 4.27, N 5.53; found: C 57.19, H 4.26, N 5.50. **6** (83%): IR (KBr): $\nu = 1352, 1096$ (ClO₄), 623 cm^{-1} (ClO₄); HRMS (ESI) m/z calcd for C₄₅H₃₆N₄ClO₂Ni⁺: 757.188 ([M-ClO₄]⁺); found: 757.189; elemental analysis calcd (%) for C₄₅H₃₆N₄Cl₂O₆Ni: C 62.95, H 4.23, N 6.53; found: C 63.22, H 4.18, N 6.65. **7** (80%): IR (KBr): $\nu = 1094$ (ClO₄), 623 cm^{-1} (ClO₄); elemental analysis calcd (%) for C₄₇H₄₁N₄ClO₈Ni·0.2(CH₂Cl₂): C 62.90, H 4.63, N 6.22; found: C 62.84, H 4.65, N 6.18. **8** (80%): IR (KBr): $\nu = 1094$ (ClO₄), 623 cm^{-1} (ClO₄); elemental analysis calcd (%) for C₄₇H₄₁N₄ClO₆Ni: C 66.67, H 5.14, N 6.42; found: C 66.80, H 5.50, N 6.48.

Preparation of [(6-Ph₂TPA)Ni(O₂C(4-OCH₃Ph))]ClO₄ (11). Solid Ni(ClO₄)₂·6H₂O (22 mg, 61 μ mol) was dissolved in acetonitrile, and this solution was added to 6-Ph₂TPA (27 mg, 61 μ mol) and the resulting mixture was stirred for one hour to form a purple homogeneous solution. Anisic acid (9.3 mg, 61 μ mol) was dissolved in methanol (1 mL) and this solution was added to the Ni^{II} complex solution. The resulting mixture was stirred 15 minutes and was then added to solid Me₄NOH·5H₂O (11 mg, 61 μ mol) and the mixture was stirred overnight during which time a blue/green solution formed. The solvent was removed under reduced pressure, and the residue was dissolved

in CH₂Cl₂. This solution was passed through a glass wool/Celite plug twice and then the filtrate was reduced in volume under reduced pressure. The final product was precipitated by the addition of excess hexanes and was dried under vacuum (26 mg, 47%). IR (KBr): $\nu = 1607, 1096$ (ClO₄), 623 cm^{-1} (ClO₄); HRMS (ESI): m/z calcd for C₃₈H₃₃ClN₄NiO₇⁺: 651.1906 ([M-ClO₄]⁺); found: 651.1913; elemental analysis calcd (%) for C₃₈H₃₃ClN₄NiO₇·0.2C₆H₁₄: C 61.83, H 4.76, N 7.25; found: C 61.73, H 4.62, N 7.66.

Preparation of [(6-Ph₂TPA)Ni(O₂C(4-OCH₃Ph))₂] (12). Solid Ni(ClO₄)₂·6H₂O (30 mg, 81 μ mol) dissolved in acetonitrile (1 mL) was added to 6-Ph₂TPA (40 mg, 80 μ mol) and the resulting solution was stirred for one hour during which time it became pale purple. Anisic acid (25 mg, 162 μ mol) was dissolved in acetonitrile (1 mL) and this solution was added to solid Me₄NOH·5H₂O (29 mg, 162 μ mol) and the resulting mixture was stirred for 1 h during which time the solution became yellow. The Ni^{II}-containing solution was combined with the anisic acid/ Me₄NOH·5H₂O solution and the mixture was stirred overnight, forming a blue/green homogeneous solution. The solvent was then removed under reduced pressure and the remaining solid was dissolved in CH₂Cl₂ and filtered through a glass wool/Celite plug. The filtrate was brought to ~1 mL in volume under reduced pressure and the final product was precipitated by the addition of hexanes (41 mg, 63%). IR (KBr): $\nu = 1605\text{ cm}^{-1}$; HRMS (ESI): m/z calcd for C₃₈H₃₃ClN₄NiO₇⁺: 651.1906 ([M-(CH₃OC₆H₄CO₂)⁺]; found: 651.1918; elemental analysis calcd (%) for C₄₆H₄₀N₄O₆Ni·1.5H₂O: C 66.51, H 5.22, N 6.75; found: C 66.72, H 5.18, N 6.81.

Product recovery for photochemical reactions. To identify products of the photo-reactions, acetonitrile solutions (5.0 mL, 2.0 mM) of complexes **4-6** were irradiated for 20 hours. The solvent was then removed under reduced pressure and the

crude reaction mixtures were analyzed by ^1H NMR using paramagnetic parameters. To extract the organic component, each crude reaction mixture was passed through a short silica column, eluting with ethyl acetate and yield was greater than 80% (~2.5 mg) of the expected mass of the β -diketonate in the starting compound. The inorganic fraction was also recovered by eluting with acetonitrile, followed by methanol. The organic fraction was then analyzed by ^1H NMR and GC-MS and the inorganic fraction by ^1H NMR using paramagnetic parameters. As a control reaction, 0.01 mmol of complex **4** was passed through a short silica column using the same solvents, and dissociation of the complex to form the 2-chloro-1,3-dione (**3a**, 85% recovery) and $[(6\text{-Ph}_2\text{TPA})\text{Ni}(\text{CH}_3\text{CN})_2](\text{ClO}_4)_2$ (**13s**) was observed.

Reactivity studies. For UV-vis experiments, solutions of the complexes **4-6** in acetonitrile (0.04 mM) were prepared. These solutions were found to be stable in the absence of light under aerobic or anaerobic conditions. Aliquots of these solutions (3.0 mL) were placed in a UV-vis cell. The cell was then irradiated at 350 nm, monitoring the reaction by UV-vis spectroscopy. For anaerobic reactions, the solutions were prepared in a Vacuum Atmosphere glovebox under an atmosphere of N_2 , and the UV-vis cell was sealed with a Teflon stopcock. For reactions that included dihydroanthracene, solutions were prepared as above with the addition of dihydroanthracene (2.0 mM).

Reactivity of 4-6 with KO_2 . Acetonitrile solutions (4.0 mL, 2.0 mM) of **4-6** were treated with KO_2 (1.0 mg, 0.014 mmol) in the presence of 18-crown-6 (3.7 mg, 0.014 mmol) and stirred for 15 minutes. The color of the solution rapidly faded from yellow to colorless. The solvent was then removed under reduced pressure, and the organic components of the reactions separated by silica column and analyzed by GC-MS, similar

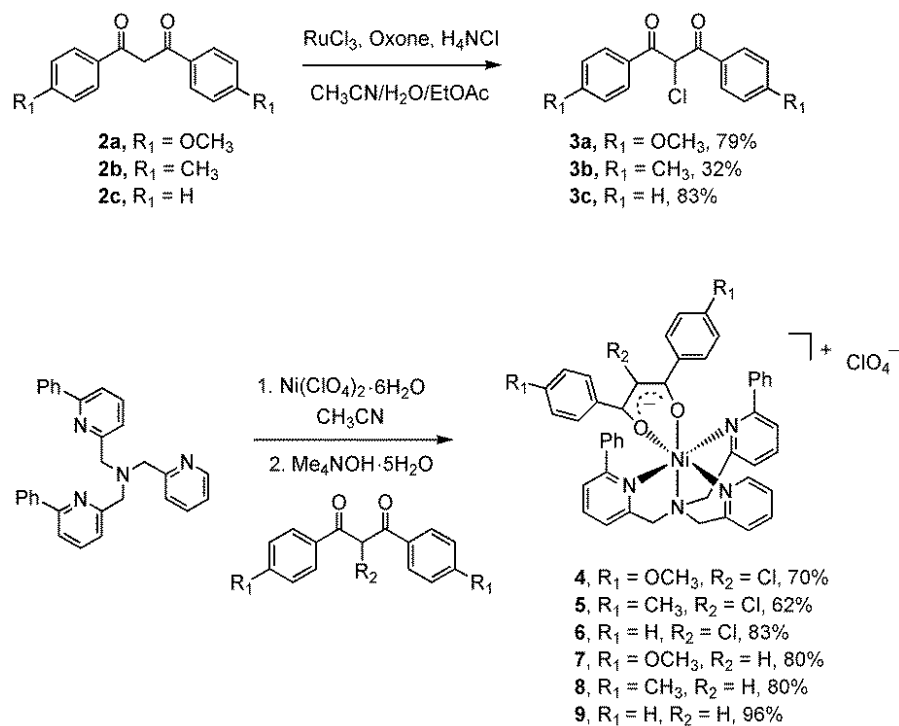
to the photochemical reactions. In all cases, the major organic product, as determined by GC-MS, was the corresponding benzoic acid derivative **I**.

X-ray Crystallography. Single crystal samples of **5**, **6**, and **8** were mounted on a glass fiber using a viscous oil and then transferred to a Nonius KappaCCD diffractometer (Mo K α , $\lambda = 0.71073 \text{ \AA}$) for data collection at 150(1) K. Methods for determination of cell constants and unit cell refinement have been previously reported.¹⁸ Each structure was solved using a combination of direct methods and heavy atom using SIR97. All non-hydrogen atoms were refined with anisotropic displacement coefficients.

Complexes **5**, **6** and **8** crystallize in the triclinic crystal system in the space group *P*-1. All hydrogen atoms in these complexes were assigned isotropic displacement coefficients $U(\text{H}) = 1.2 U(\text{C})$ or $1.5 U(\text{C}_{\text{methyl}})$ and their coordinates were allowed to ride on their respective carbon using SHELXL97. For **5** and **6**, $Z = 2$, whereas for **8**, $Z = 4$ and two independent molecules are present in the asymmetric unit. For **5**, three atoms of the perchlorate anion were found to be disordered over two positions (0.68:0.32). One disordered molecule of Et₂O is present per formula unit in the structure of **5**. In the structure of **6**, two oxygen atoms of the perchlorate anion are disordered over two positions (0.86:0.14). For **8**, there are two molecules of CH₂Cl₂ per formula unit.

Results and Discussion

Preparation of 2-chloro-1,3-diones. β -diketones can be chlorinated at the α position using various reagents.¹⁹ Recent studies in this area have focused on the use of hypervalent iodine reagents²⁰ and reactions performed using *N*-chlorosuccinimide in an ionic liquid²¹ or CCl₄.²² In a new synthetic route (Scheme 4-3 (top)), we have found that treatment of the appropriate β -diketone **2a-2c** with RuCl₃/Oxone/NH₄Cl in



Scheme 4-3. Synthesis of 2-chloro-1,3-diones (top) and Ni^{II} 2-chloro-1,3-diketonate complexes supported by the 6-Ph₂TPA ligand (bottom).

CH₃CN/H₂O/EtOAc gives the 2-chloro compounds (**3a-3c**) as crystalline solids in high purity following recrystallization(s).

Complex synthesis and characterization: A series of mononuclear Ni^{II} 2-chloro-1,3-diketonate complexes (**4-6**) supported by the 6-Ph₂TPA ligand was prepared as outlined in the bottom equation in Scheme 4-3. Crystalline solids were isolated in yields greater than 70%. For reactivity comparison, structurally similar β-diketonate complexes lacking the 2-chloro substituent (**7-9**) were generated. We note that complex **9** has been previously reported.⁷ Each new complex was characterized by elemental analysis, IR, ¹H NMR, UV-vis, and in some cases, mass spectrometry and/or X-ray crystallography.

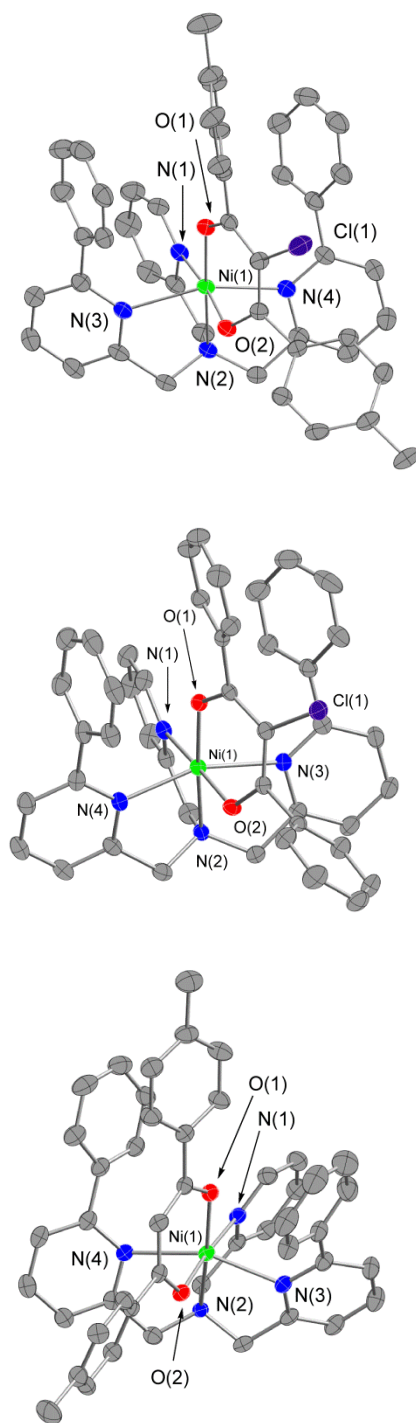


Figure 4-2. Thermal ellipsoid representations of the cationic portions of **5** (top), **6** (middle) and **8** (bottom). Ellipsoids are drawn at the 50% probability level. Hydrogen atoms have been omitted for clarity.

Table 4-1. Crystallographic data for **5**, **6**, and **8**.

	5 ·C ₄ H ₁₀ O	6	8 ·2CH ₂ Cl ₂
formula	C ₄₇ H ₄₀ Cl ₂ N ₄ NiO ₆ ·C ₄ H ₁₀ O	C ₄₅ H ₃₆ Cl ₂ N ₄ NiO ₆	C ₄₉ H ₄₁ ClN ₄ NiO ₆ ·2CH ₂ Cl ₂
<i>M_r</i>	960.56	858.39	1021.85
T [K]	150(1)	150(1)	150(1)
crystal size [mm]	0.30x0.28x0.20	0.38x0.15x0.13	0.30x0.22x0.12
crystal system	triclinic	triclinic	triclinic
space group	<i>P</i>$\bar{1}$	<i>P</i>$\bar{1}$	<i>P</i>$\bar{1}$
<i>a</i> [Å]	11.96810(10)	9.7136(1)	13.5383(2)
<i>b</i> [Å]	13.6006(2)	13.2959(2)	17.0153(2)
<i>c</i> [Å]	16.1278(3)	16.7754(3)	23.0279(3)
α [°]	108.5037(6)	77.5113(7)	97.2779(7)
β [°]	104.6479(9)	76.7675(10)	92.9850(7)
γ [°]	102.9892(9)	68.7334(9)	112.8856(7)
<i>V</i> [Å ³]	2271.55(6)	1944.11(5)	4817.82(11)
<i>Z</i>	2	2	4
ρ_{calcd} [gcm ⁻³]	1.404	1.466	1.409
μ [mm ⁻¹]	0.603	0.693	0.733
F(000)	1004	888	2112
Θ range [°]	1.91–27.48	2.34–27.49	1.71–27.44
Index ranges	-14 ≤ <i>h</i> ≤ 15 -17 ≤ <i>k</i> ≤ 17 -20 ≤ <i>l</i> ≤ 20	-12 ≤ <i>h</i> ≤ 12 -17 ≤ <i>k</i> ≤ 17, -21 ≤ <i>l</i> ≤ 21	-16 ≤ <i>h</i> ≤ 17 -22 ≤ <i>k</i> ≤ 21 -29 ≤ <i>l</i> ≤ 29
reflns collected	19512	16726	40512
unique reflns	10319 [<i>R</i> (int) = 0.0235]	8901 [<i>R</i> (int) = 0.0237]	21813 [<i>R</i> (int) = 0.0420]
<i>R</i> _{int}	0.0235	0.0237	0.0420
data/restr./param	10319/24/632	8901/0/533	21813/12/1184
GoF (<i>F</i> ²)	1.024	1.027	1.026
<i>R</i> ₁ , w <i>R</i> ₂ [<i>I</i> > 2σ(<i>I</i>)]	0.0427, 0.1055	0.0364, 0.0816	0.0497, 0.1106
<i>R</i> ₁ , w <i>R</i> ₂ (all data)	0.0617, 0.1163	0.0553, 0.0889	0.0944, 0.1293
Max. and min. transmission	0.8889 and 0.8398	0.9153 and 0.7786	0.9172 and 0.8101
$\Delta\rho_{(\text{max/min})}$ [eÅ ⁻³]	0.441/-0.664	0.333/-0.510	0.0820/-0.862

Table 4-2. Selected bond lengths (Å) and angles (°).

	5·C ₄ H ₁₀ O	6	8·2CH ₂ Cl ₂
Ni(1)-N(1)	2.0569(18)	2.0404(15)	2.068(2)
Ni(1)-N(2)	2.0635(17)	2.0882(15)	2.085(2)
Ni(1)-N(3)	2.3041(17)	2.3174(15)	2.283(2)
Ni(1)-N(4)	2.2261(18)	2.1890(15)	2.238(2)
Ni(1)-O(1)	1.9709(14)	1.9748(12)	1.9796(16)
Ni(1)-O(2)	1.9968(14)	1.9883(13)	1.9885(17)
C(37)-C(38)	1.418(3)	1.422(3)	1.401(3)
C(38)-C(39)	1.411(3)	1.397(3)	1.405(3)
C(38)-Cl(1)	1.760(2)	1.7571(18)	-
O(1)-Ni(1)-O(2)	88.78(6)	89.13(5)	91.57(7)
O(1)-Ni(1)-N(1)	97.65(6)	94.17(6)	90.92(8)
O(2)-Ni(1)-N(1)	172.50(6)	176.66(6)	175.39(8)
O(1)-Ni(1)-N(2)	178.06(6)	174.91(5)	171.45(8)
O(2)-Ni(1)-N(2)	89.74(6)	93.15(6)	95.57(7)
N(1)-Ni(1)-N(2)	83.91(7)	83.51(6)	82.29(8)
O(1)-Ni(1)-N(4)	100.33(6)	102.77(5)	103.07(8)
O(2)-Ni(1)-N(4)	85.78(6)	92.08(5)	93.47(7)
N(1)-Ni(1)-N(4)	96.80(7)	87.69(6)	82.18(8)
N(2)-Ni(1)-N(4)	78.31(7)	81.71(6)	81.23(8)
O(1)-Ni(1)-N(3)	101.07(6)	98.63(5)	100.47(7)
O(2)-Ni(1)-N(3)	94.50(6)	84.69(5)	82.25(7)
N(1)-Ni(1)-N(3)	80.52(7)	94.29(6)	101.11(8)
N(2)-Ni(1)-N(3)	80.30(7)	77.08(6)	75.92(8)
N(4)-Ni(1)-N(3)	158.60(7)	158.31(6)	156.18(7)
O(1)-Ni(1)-O(2)	88.78(6)	89.13(5)	91.57(7)
O(1)-Ni(1)-N(1)	97.65(6)	94.17(6)	90.92(8)
O(2)-Ni(1)-N(1)	172.50(6)	176.66(6)	175.39(8)
O(1)-Ni(1)-N(2)	178.06(6)	174.91(5)	171.45(8)
O(2)-Ni(1)-N(2)	89.74(6)	93.15(6)	95.57(7)
N(1)-Ni(1)-N(2)	83.91(7)	83.51(6)	82.29(8)
O(1)-Ni(1)-N(4)	100.33(6)	102.77(5)	103.07(8)
O(2)-Ni(1)-N(4)	85.78(6)	92.08(5)	93.47(7)
N(1)-Ni(1)-N(4)	96.80(7)	87.69(6)	82.18(8)

Single crystal X-ray structures were obtained for **5**, **6**, and **8**. Details of the data collection and refinement are given in Table 4-1. Selected bond distances and angles are given in Table 4-2. These complexes all contain a pseudo-octahedral Ni^{II} cation with bidentate coordination of the corresponding β -diketonate (Figure 4-2). Bond lengths within the six-membered nickel- β -diketonate chelate ring in each complex are typical for nickel β -diketonates.⁷ The C-Cl bond lengths in **5** and **6** are within the range previously reported for metal-bound 2-chloro-1,3-diketonates (1.68-1.81 Å), being particular close to that reported for Cu^{II} complexes (1.739(3) and 1.755(3) Å).²³ As can be seen in Table 4-2, there are only subtle changes in the Ni-N/O bond lengths as the nature of the substituents on the β -diketonate is changed. Comparison of the structural features of **6** to those of [(6-Ph₂TPA)Ni(PhC(O)C(OH)C(O)Ph)]ClO₄ (**1**, Figure 4-1) revealed that the Ni-N_{PhPy} bonds are slightly elongated in the 2-hydroxy-1,3-diketonate complex relative those found in the 2-chloro analog **6** (Ni-N_{PhPy}, **1**: av 2.30 Å; **6**: av. 2.25Å).

Selected spectroscopic data for **4-9** is given in Table 4-3. Each β -diketonate complex has an absorption feature at ~370 nm which may be assigned as a $\pi \rightarrow \pi^*$

Table 4-3. Selected spectroscopic features for **4-9**.

	4	5	6	7	8	9
λ_{\max} (nm) ^a	378	374	372	374	370	368
ϵ (10 ⁴ M ⁻¹ cm ⁻¹)	1.03	1.16	0.80	2.38	2.16	1.30
β -py ^b	48.4 42.8	48.1 43.5	48.4 43.5	46.0 44.1	47.0 44.4	46.6 44.1
β' -py	46.0 34.8	46.0 34.6	46.4 34.7	44.1 33.8	44.1 33.9	44.9 34.3
γ -py	15.4	15.5	15.5	14.9	15.0	15.1
α -CH	-	-	-	-14.1	-13.9	-13.6

^a UV-vis spectra obtained in CH₃CN. ^b ¹H NMR spectra obtained in CD₃CN at ambient temperature at 400 MHz. Chemical shifts are reported in ppm.

involving the β -diketonate ligand. Comparison of the 2-chloro-1,3-diketonate complexes (**4-6**) with their unsubstituted analogs (**7-9**) revealed a red shift of 4 nm for the former.

The ^1H NMR features of **1** and **9** have been previously reported.^{7, 24} Resonances in selected regions of the ^1H NMR spectra of **4-6**, **7** and **8** can be assigned on the basis of chemical shift, integrated intensity, and comparison to previously studied complexes.^{7, 11, 24} All of the complexes (**4-9**) exhibit C_s symmetry in CD_3CN on the NMR time scale, as evidenced by the presence of only two resonances for the β' pyridyl protons (Figure 4-3), indicating that the phenyl-appended pyridyl rings are equivalent. Diagnostic resonances for the pyridyl ring β -H's and phenyl-appended pyridyl ring β' -H's (Figure 4-3) are found in the region of 44-48 ppm (Table 4-3). The effect of changing the para-substituent on the aryl groups of the β -diketonate ligand can be seen in the shift of the pyridyl γ -H's in the series **4-6** and **7-9**, and in a shift of the β -diketonate methyne proton in **7-9**. In the latter set of complexes, the pyridyl β , β' , and γ proton resonances are shifted upfield by 1-2 ppm relative to the 2-chloro analogues.

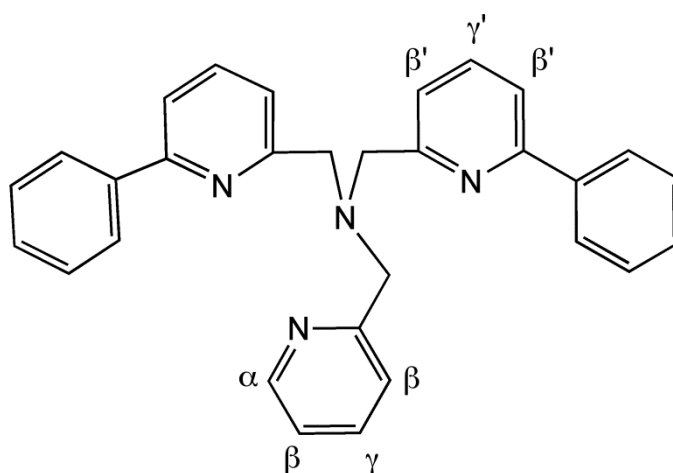


Figure 4-3. Labeling scheme for the 6-Ph₂TPA ligand.

Reactivity studies: It was found that the yellow color of acetonitrile solutions of the 2-chloro-1,3-diketonate complexes **4-6** faded upon exposure to UV light ($\lambda_{\text{irr}} = 350$ nm) over the course of several hours under aerobic conditions. As shown in Figure 4-4 for the methoxy-substituted **4**, this corresponds to loss of the $\pi \rightarrow \pi^*$ absorption band of the β -diketonate at 378 nm. An isosbestic point for the reaction was identified at 269 nm.

The products of each aerobic photochemical reaction were determined after irradiating a 0.002 M acetonitrile solution of each complex (**4-6**) at 350 nm for 20 h under an aerobic atmosphere. The Ni^{II} -containing products were determined using ^1H

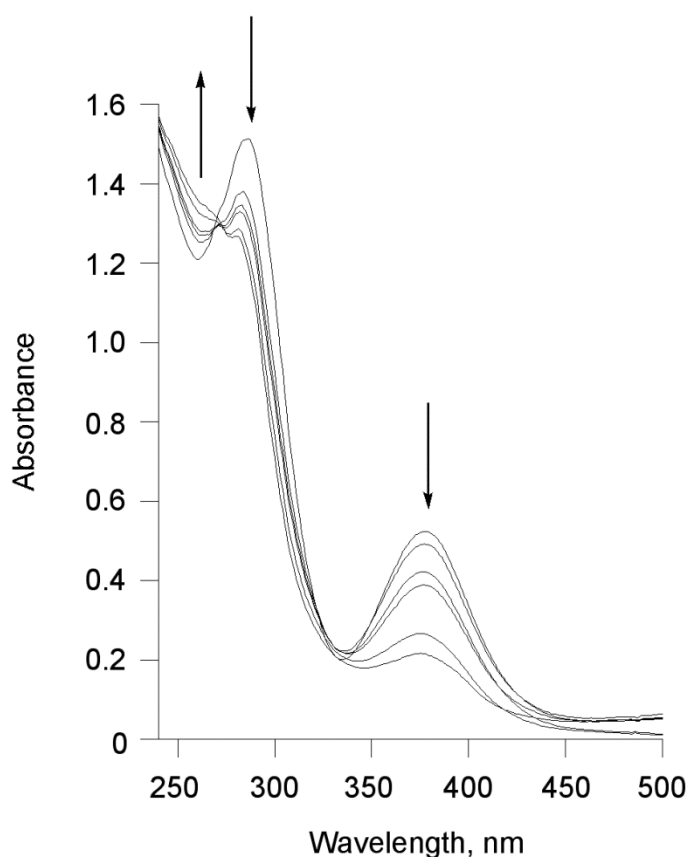


Figure 4-4. Absorption changes over time observed for the aerobic photochemical reaction of **4**.

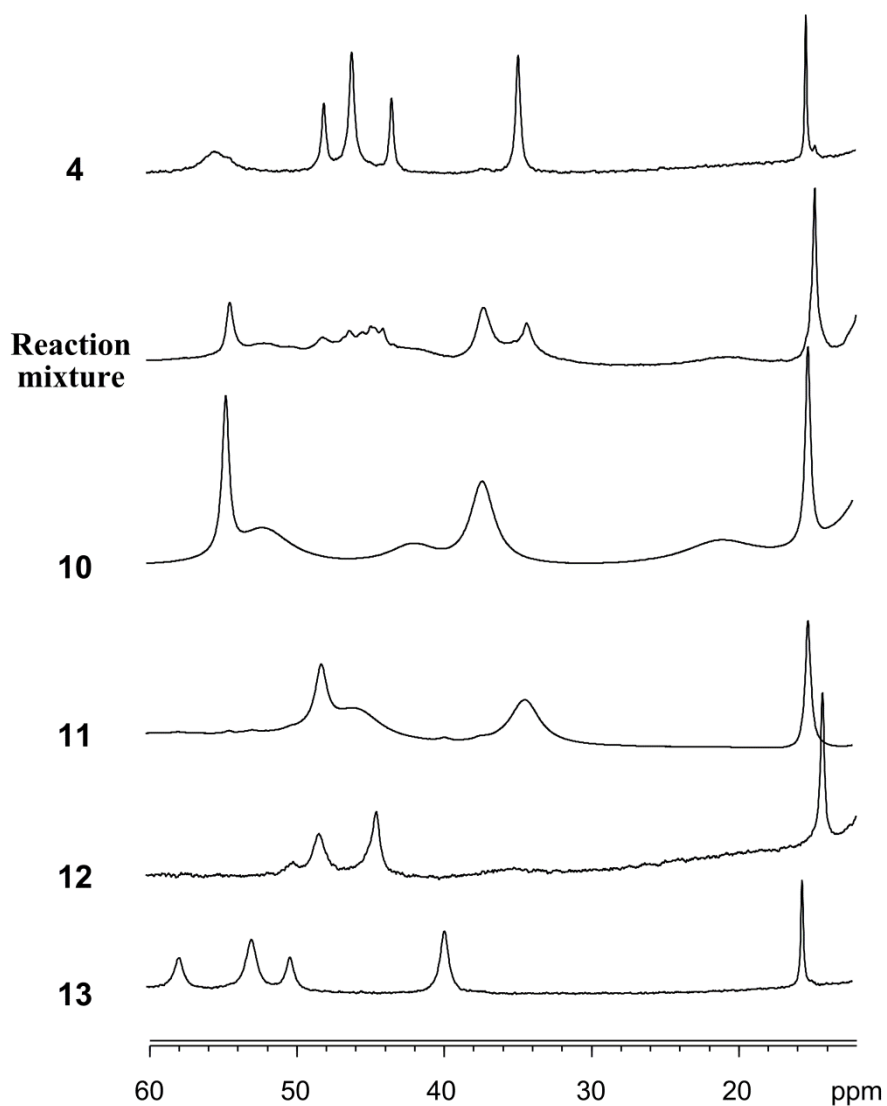
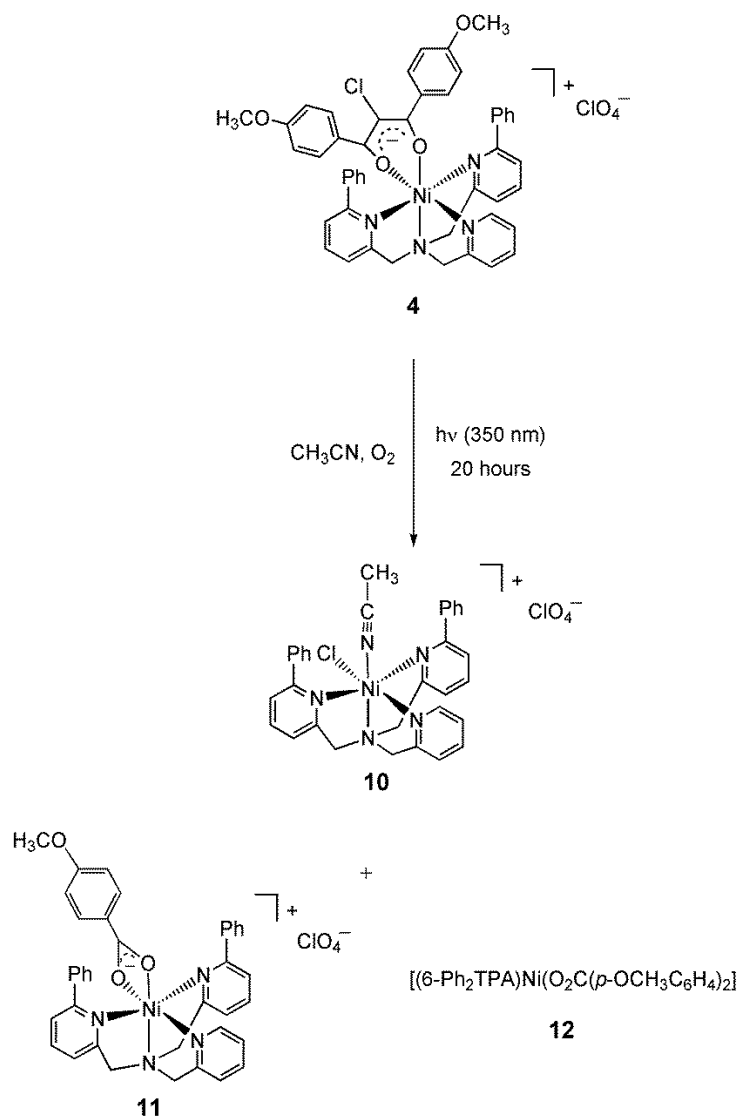


Figure 4-5. Selected features of the paramagnetic region of the ¹H NMR spectra of analytically pure **4** and **10-13** and the reaction mixture produced upon irradiation of **4** under aerobic conditions at 350 nm for 20 hours in CH₃CN. All spectra were obtained using a 400 MHz spectrometer at 298 K in CD₃CN.



Scheme 4-4. Ni^{II} complexes generated upon irradiation of **4** at 350 nm for 20 hours in an aerobic solution of CH_3CN .

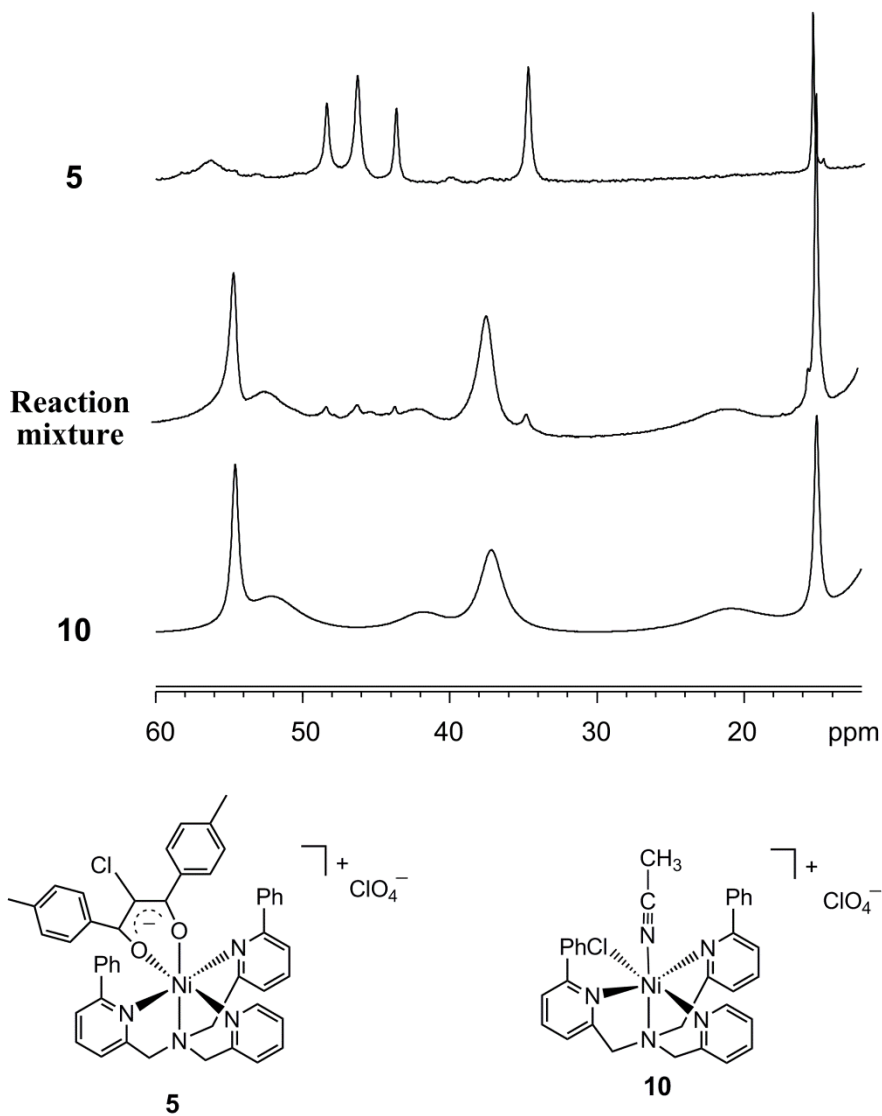


Figure 4-6. Selected features of the paramagnetic region of the ^1H NMR spectra of analytically pure **5** and **10** and the reaction mixture produced upon irradiation of **5** under aerobic conditions at 350 nm for 20 hours in CH_3CN . All spectra were obtained using a 400 MHz spectrometer at 298 K in CD_3CN .

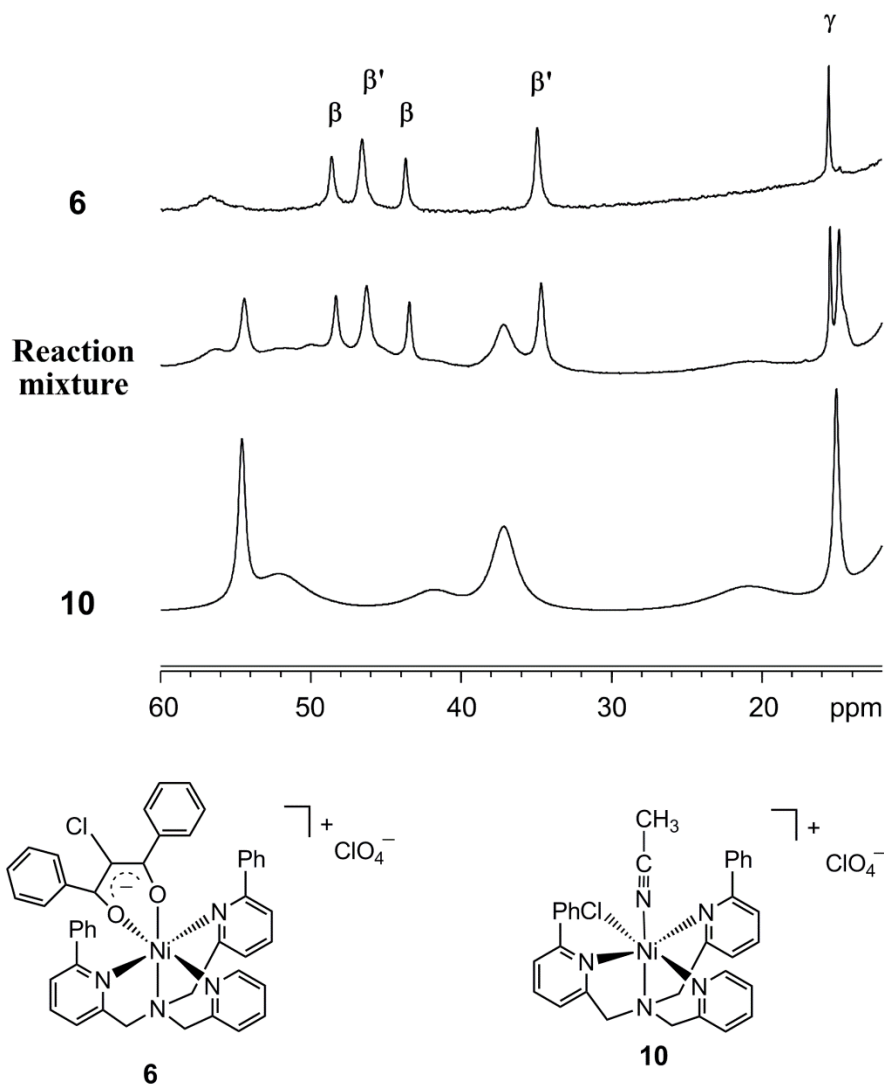


Figure 4-7. Selected features of the paramagnetic region of the ¹H NMR spectra of analytically pure **6** and **10** and the reaction mixture produced upon irradiation of **6** under aerobic conditions at 350 nm for 20 hours in CH₃CN. All spectra were obtained using a 400 MHz spectrometer at 298 K in CD₃CN.

NMR (Figures 4-5, 4-6 and 4-7) and ESI-MS. The most reactive compound was found to be the methoxy derivative **4** (Figure 4-5). A major Ni^{II} product in this reaction is the chloride complex [(6-Ph₂TPA)NiCl(CH₃CN)]ClO₄ (**10**)¹¹, as evidenced by the presence of resonances at 54 and 37 ppm, respectively. Also present are resonances associated with a monoanisate complex [(6-Ph₂TPA)Ni(O₂C(*p*-OCH₃C₆H₄))]ClO₄ (**11**) and the dianisate complex [(6-Ph₂TPA)Ni(O₂C(*p*-OCH₃C₆H₄))₂] (**12**). Complexes **11** and **12** were independently synthesized and characterized to confirm the assignment. The formation of **10-12** in the photochemical reaction of **4** is supported by ESI-MS investigations which confirmed the presence of the corresponding [M-ClO₄]⁺ and [M-C₈H₇O₃]⁺ ions. From comparison of ¹H NMR spectra, it is evident that the aerobic photochemical reaction of **4** goes to completion in the 20 h irradiation period, as no signals for the starting compound could be identified. A summary of the reaction of the methoxy-substituted **4** is presented in Scheme 4-4.

The reaction of the methyl-substituted **5** under aerobic conditions (Figure 4-6) also leads primarily to the formation of the chloro complex [(6-Ph₂TPA)NiCl(CH₃CN)]ClO₄ (**10**), although minor peaks that appear to correspond to the starting complex are also visible.¹¹ The reaction of **6** (Figure 4-7) differs from that of **4** and **5** in that ¹H NMR resonances from the starting complex are clearly evident in ¹H NMR and ESI-MS spectra after 20 h of irradiation, indicating that **6** reacts significantly slower than the other complexes. Note that as a control reaction, 0.002 M solutions of **4-6** in CD₃CN were stored in the dark under aerobic conditions at ambient temperature and pressure for several days and produced no decomposition products, as determined by ¹H NMR.

For each reaction described above, the organic products could not be analyzed in the presence of the Ni^{II} complex(es). Therefore these products were separated via filtration of each reaction mixture through a short silica plug, using ethyl acetate as the eluent. Each sample was analyzed by ¹H NMR and GC-MS. The amount of organic material isolated from each reaction mixture corresponds to >80% by mass of that expected from the respective starting 2-chloro-1,3-diketonate ligand. Control reactions indicate that the coordinated 1,3-diketonate ligand in **4-6**, and the anisate ligands in **11** and **12**, are released upon passage of the complexes through the silica plug. Thus the presence of 2-chloro-1,3-dione in the organic products is further evidence for incomplete reaction. The inorganic residue on the silica is eluted by washing with acetonitrile, followed by methanol. ¹H NMR analysis of the inorganic fractions showed the presence of [(6-Ph₂TPA)Ni(CH₃CN)₂](ClO₄)₂ (**13**, Figure 4-5), which was not present in the reaction mixtures prior to work-up.

Upon irradiation of **4** for 20 h under aerobic conditions, the primary organic product generated is *p*-anisic acid (**I**), along with lesser amounts of *p*-anisil methyl ketone (**II**), anisaldehyde, deoxyanisoin (**III**), and halogenated species (e.g. 2-chloro, 1-4-

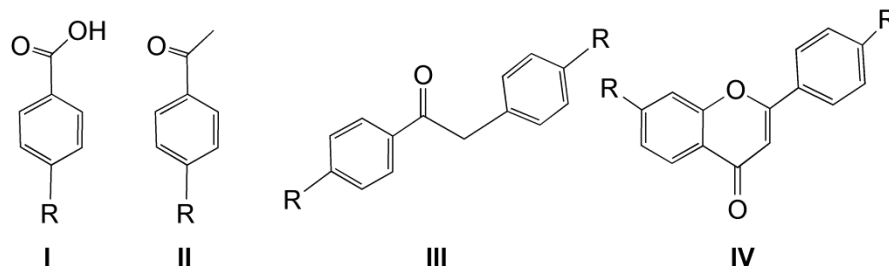


Figure 4-8. Structures of the organic products generated in photochemical reactions of **4-6** under aerobic or anaerobic conditions with irradiation at 350nm for 20 hours in CH₃CN.

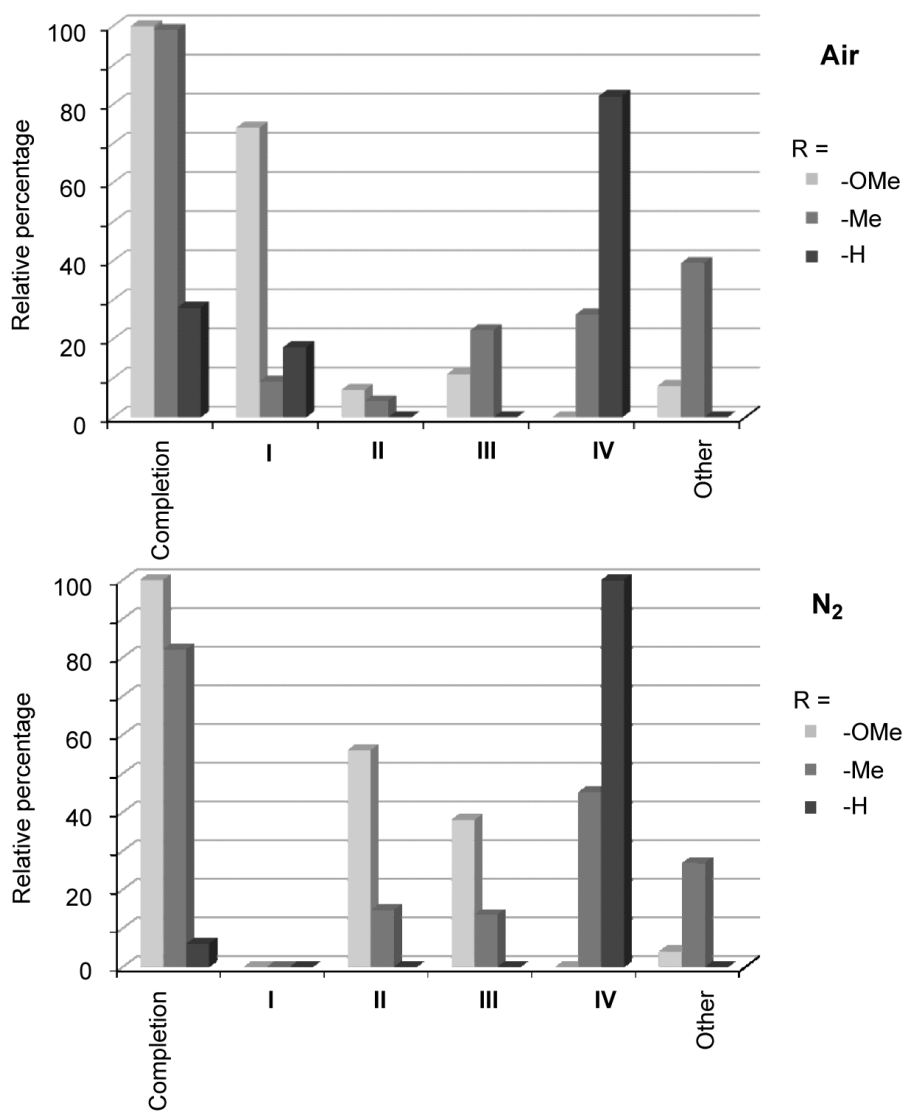
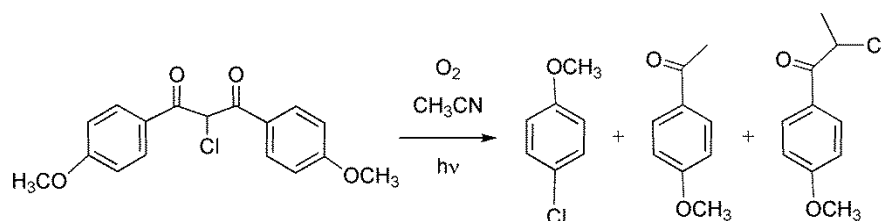


Figure 4-9. Relative amounts of the organic products generated during the 350 nm irradiation of **4-6** in CH₃CN for 20 hours under aerobic (top) and anaerobic conditions (bottom). In each graph the column labeled completion corresponds to the relative percentage of reaction completion observed after 20 hours. The relative percentages of **I-IV** refer to the amount of product generated as a percentage of the overall amount of 2-chloro-1,3-diketonate that underwent reaction under the prescribed conditions. Other refers to species such as *para*-R-arylaldehyde, chloro-containing compounds and unidentified compounds.

methoxyphenylpropan-1-one) (Figure 4-8 and Figure 4-9 (top)). Notably, performing the same reaction with **4** under N₂ results in the formation of only α -cleavage products (e.g. **II** and **III**, Figure 4-9 (bottom)). Thus, oxygen is required for the generation of the carboxylic acid product. The photoreactivity of the methoxy-substituted 2-chloro-1,3-dione **3a** has previously been evaluated by Kosmrlj et al.²⁵ After irradiation of a 0.002 M solutions of the diketone at 350 nm for 2 h under aerobic conditions they noted the formation of only α -cleavage products (Scheme 4-5). Thus, the presence of nickel is required for oxidative cleavage reactivity involving the 2-chloro-1,3-dione.



Scheme 4-5. α -Cleavage products formed from the photoirradiation of **3a** at 352 nm in aerobic CH₃CN for 2 hours.

The aerobic photochemical reaction involving the methyl-containing Ni^{II} 2-chloro-1,3-diketonate complex **5** results in the formation of multiple products (Figure 4-9) including flavone and deoxytoluoin, with lesser amounts of *p*-toluic acid, *p*-tolualdehyde and methyl-*p*-tolyl ketone. Under a N₂ atmosphere, the reaction involving **5** reached only ~80% completion. The organic products were a similar mixture to that found under aerobic conditions, except *p*-toluic acid is not generated. As the photoreactivity of the methyl-substituted **3b** had not been previously reported, we performed this reaction under the conditions previously employed for **3a** and **3c** (0.002 M in CH₃CN under aerobic conditions with irradiation at 350 nm for 2 h).²⁵ The primary

reaction products generated were the α -cleavage products methyl-*p*-tolyl ketone and *p*-tolualdehyde, with no *p*-toluic acid.

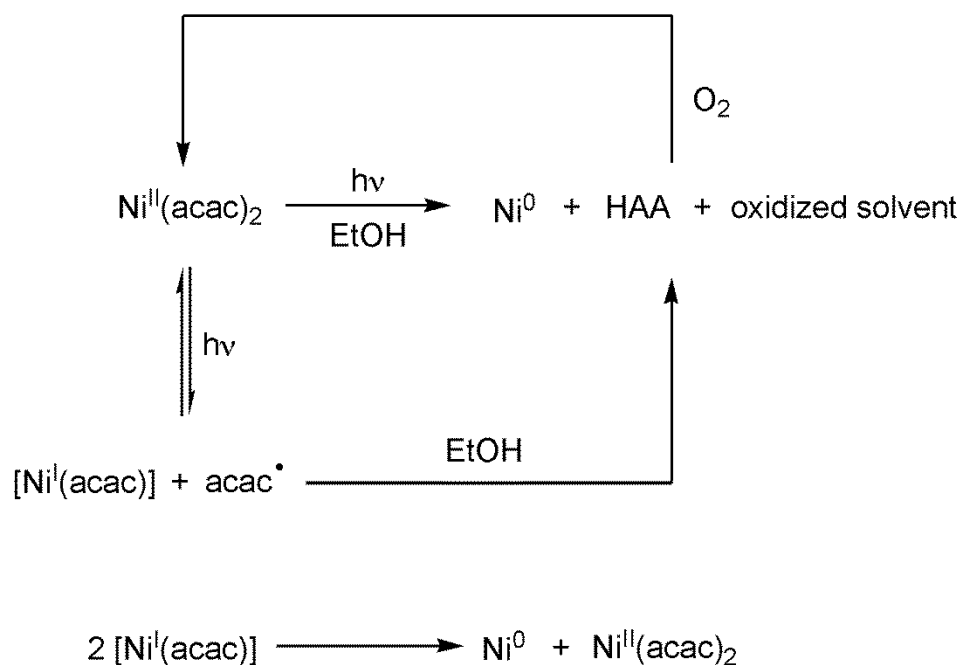
As noted above, the photochemical reaction of **6** under aerobic conditions does not go to completion after 20 h of irradiation at 350 nm. Hence the primary organic product isolated from the reaction mixture is the unreacted 2-chloro-1,3-dione **3c**. However, of the remaining organic compounds generated, flavone is the primary product (Figure 4-9) along with a small amount of benzoic acid. Performing the irradiation of **6** under a N₂ atmosphere resulted in less than 10% of the starting complex undergoing reaction, with only trace amounts of flavone generated. Kosmrlj et al., previously reported that irradiation of unsubstituted 2-chloro-1,3-dione **3c** yielded the photocyclization flavone product **IV** as the sole product in ~50% yield regardless of conditions (air, argon or oxygen atmosphere).²⁵

Complexes **7-9** were tested for photoreactivity under both aerobic and anaerobic conditions identical to those used for the 2-chloro-1,3-diketonate complexes **4-6**. Analysis of the product mixtures by ¹H NMR using paramagnetic parameters showed no change from the starting material.

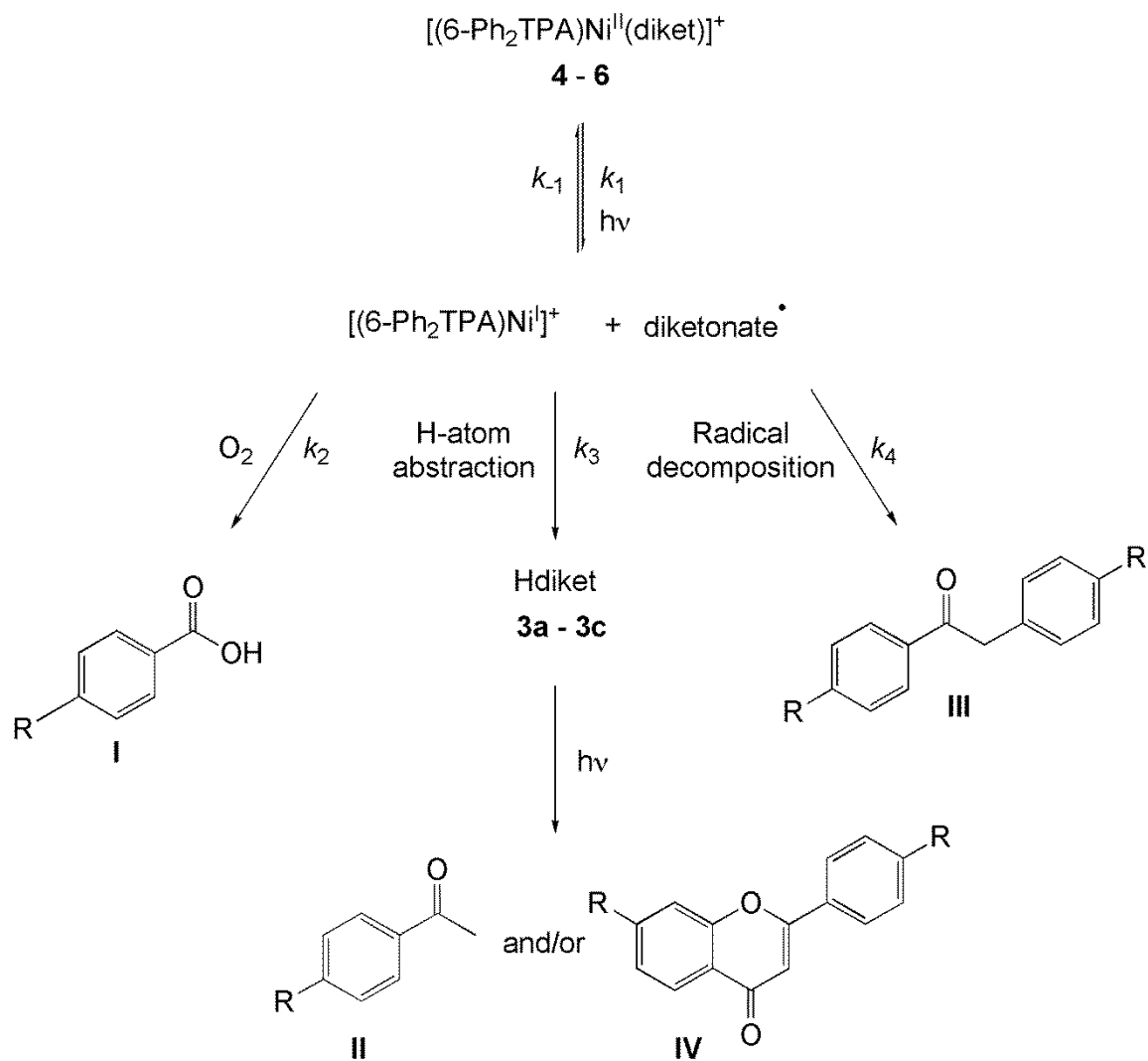
Mechanistic Experiments. The differing product distributions found for the reactions of **4-6**, and the overall lack of reactivity found for **7-9** was evaluated through consideration of literature precedent and the results of additional mechanistic experiments. In pioneering work by Lintvedt et al., it was found that when Ni(acac)₂ is irradiated at 252 nm in ethanol in the absence of O₂, free Hacac is produced along with a colloidal suspension of Ni⁰ or a Ni⁰ film (Scheme 4-6).^{26, 27} The mechanism for reduction of the Ni^{II} center in Ni(acac)₂ is thought to involve a π - π^* transition to a vibrationally-

excited π^* state from which the reduction can take place. However the involvement of ligand-to-metal charge transfer has also been proposed. In either scenario, an initial single-electron reduction of Ni^{II} to Ni^{I} can occur (Scheme 4-6).⁹ The Ni^{I} formed could then react with a second Ni^{I} species in solution to disproportionate to form Ni^{II} and Ni^0 . Interestingly, photochemical reduction of $\text{Ni}(\text{acac})_2$ is not observed to occur in the presence of O_2 .²⁶ However, this observed overall lack of reactivity may represent the sum of a photochemical reduction followed by rapid reoxidation of the reduced nickel and complexation to give $\text{Ni}(\text{acac})_2$ (Scheme 4-6). This is consistent with the fact that the anaerobically generated photoreduction products of $\text{Ni}(\text{acac})_2$ readily oxidize in O_2 to regenerate the starting material.²⁷

Given the literature precedent described above, we hypothesize that low-valent nickel complexes, likely Ni^{I} , are generated upon photoirradiation of the 6- Ph_2TPA -ligated



Scheme 4-6. Proposed reaction sequence for photoreduction of $\text{Ni}(\text{acac})_2$.



Scheme 4-7. Proposed photochemical reaction pathways for **4-6** leading to the formation of **I-IV** (diket = diketonate).

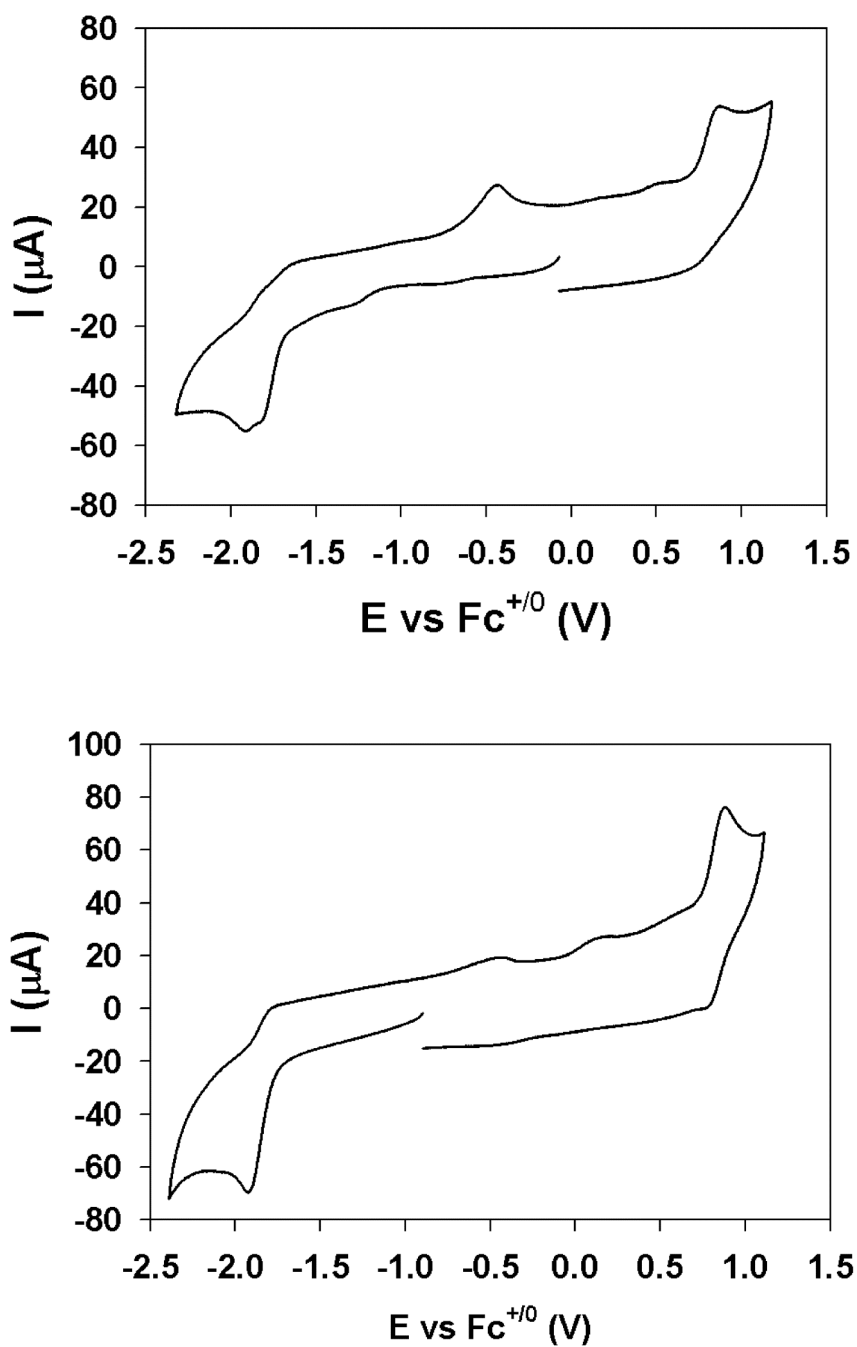
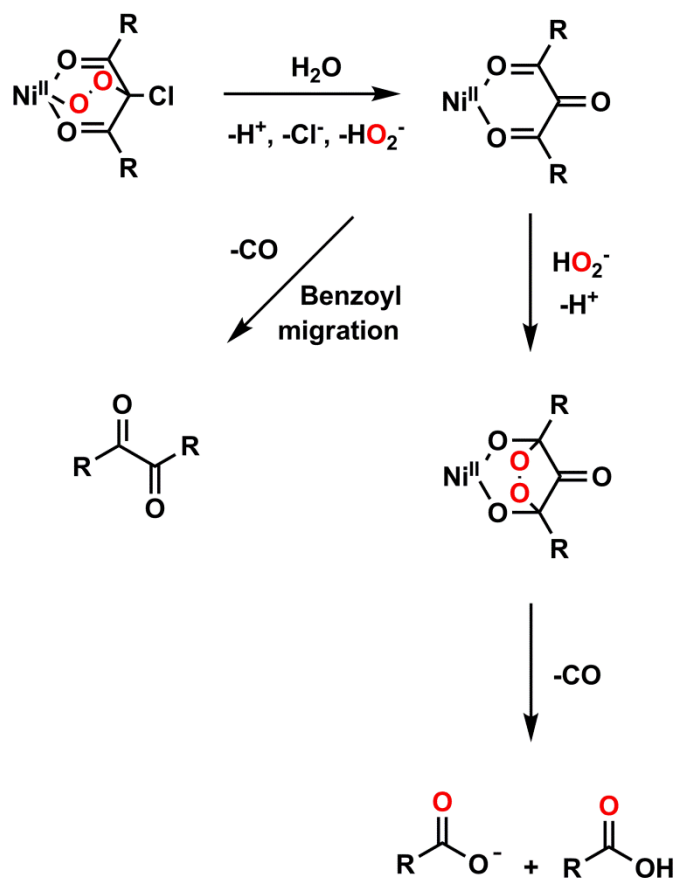


Figure 4-10. Cyclic voltammograms of **4** (top) and **7** (bottom) obtained in freshly distilled CH₃CN (0.1 M [Me₄N][ClO₄]) with an analyte concentration of 1.0 mM (**4**; 1.3 mM for **7**) under an atmosphere of N₂. Scan rate: 200 mV/s. Temperature: 298 K.

Ni^{II} β -diketonate complexes. Irradiation on the high-energy shoulder of the π - π^* transition that is present at 368-380 nm could produce a high energy electronic state on the β -diketonate with reducing character, leading to one-electron reduction of Ni^{II} to Ni^I and the formation of a β -diketonate radical (Scheme 4-7). While we cannot directly probe the Ni^I/ β -diketonate radical species, to provide insight into the redox properties of the Ni^{II} 2-chloro-1,3-diketonate complex **4**, as well as an unsubstituted analog **7**, cyclic voltammetry studies were performed. Complex **4** exhibits two poorly reversible cathodic features at approximately -1.82 and -1.91 V vs. Fc/Fc⁺ (Figure 4-10 (top)), respectively, suggesting that an initially formed Ni^I β -diketonate anion species is susceptible to further reduction and/or a chemical reactivity that limits reversibility. A new oxidative wave at -0.44 mV generated after the cathodic scan indicates the formation of a possibly electrode deposited nickel species. Complex **7** exhibits a quasireversible cathodic wave at approximately -1.93 V (Figure 4-10 (bottom)), indicating that the stability of the Ni^I β -diketonate anion species is influenced by the nature of the enolate ligand. In the presence of O₂, solutions of **4** and **7** exhibit only a quasireversible cathodic wave consistent with the reduction of O₂ to O₂⁻.²⁸ The reversibility of this feature improves in the absence of complex, indicating that the electrochemically generated superoxide is reacting with the complex (either **4** or **7**). Notably, we have found that the Ni^{II} β -diketonate complexes **4** and **7** are reactive with potassium superoxide (solubilized by 18-crown-6) in acetonitrile. In the reaction of **4** with KO₂, the carboxylic acid product **I** was detected as the major β -diketonate-derived product. In sum, these observations suggest that a nickel-superoxo species forms, and this species is capable of oxidatively cleaving the diketonyl unit, as had been suggested in Scheme 4-2.

Literature precedent, as well as experimental evidence, suggests that the oxidative reactivity leading to carboxylic acid formation in the photoreactions of **4-6** likely involves the formation of a trione intermediate. Tada et al. have proposed that in situ generated α -I- β -diketones undergo reaction with O_2 upon irradiation with fluorescent light to produce 1,3-diphenylpropanetrione, $PhC(O)C(O)C(O)Ph$.²⁹ We have shown that the same trione is generated as a reactive intermediate upon reaction of **1** with O_2 .⁸ The trione is a transient intermediate that may then react with in situ generated peroxide to form the observed carboxylate cleavage products. Alternatively, triones with aryl groups



Scheme 4-8. Possible triketone formation and subsequent degradation pathways to form either diketone or carboxylate products.

in the C(1) and C(3) positions may undergo a Lewis acid-promoted benzoyl migration and subsequent decarbonylation to form benzil (PhC(O)C(O)Ph), making the detection of benzil a potential probe for the detection of triketone intermediates.³⁰ Careful examination of the products generated in the photoreaction of **6** (labeled as "other" in Figure 4-8) shows the presence of a small amount of benzil, strongly suggesting the formation of the triketone intermediate.³¹ A possible route leading to the formation of a triketone intermediate, starting from a nickel diketone peroxo species (formed by the combination of the proposed diketonyl and superoxo radicals from Scheme 4-2), and its subsequent cleavage is outlined in Scheme 4-8.

To probe the formation of a trione intermediate, ¹⁸O labeling studies were undertaken and the results obtained for the aerobic photoreaction of **6** are consistent with previous reports. Specifically, the amount of benzoic acid containing one ¹⁸O label (36%) is generally similar to that found for the reaction of **1** (~50%).⁸ Labeling studies were also undertaken to further explore the photoinduced oxidative cleavage reactivity of **4** under aerobic conditions. Irradiation of **4** in the presence of ¹⁸O₂ (99%) resulted in the isolation of a sample of *p*-anisic acid that is ~31% unlabeled, ~46% containing one ¹⁸O, and ~23% containing two ¹⁸O atoms (Figure 4-11). We are cautious to avoid overinterpreting this labelling data in the absence of a more thorough kinetic analysis of the reactions. However, we tentatively propose that the observed formation of double-labeled anisic acid in the reaction of **4** could be a result of previously-reported scrambling reactions in the presence of the electron-donating methoxy substituent.³²

To gain additional insight into the effect of the *p*-substituent on the reactivity of the 2-chloro-1,3-diketonate ligands in **4-6**, the rates of the aerobic photoreactions were

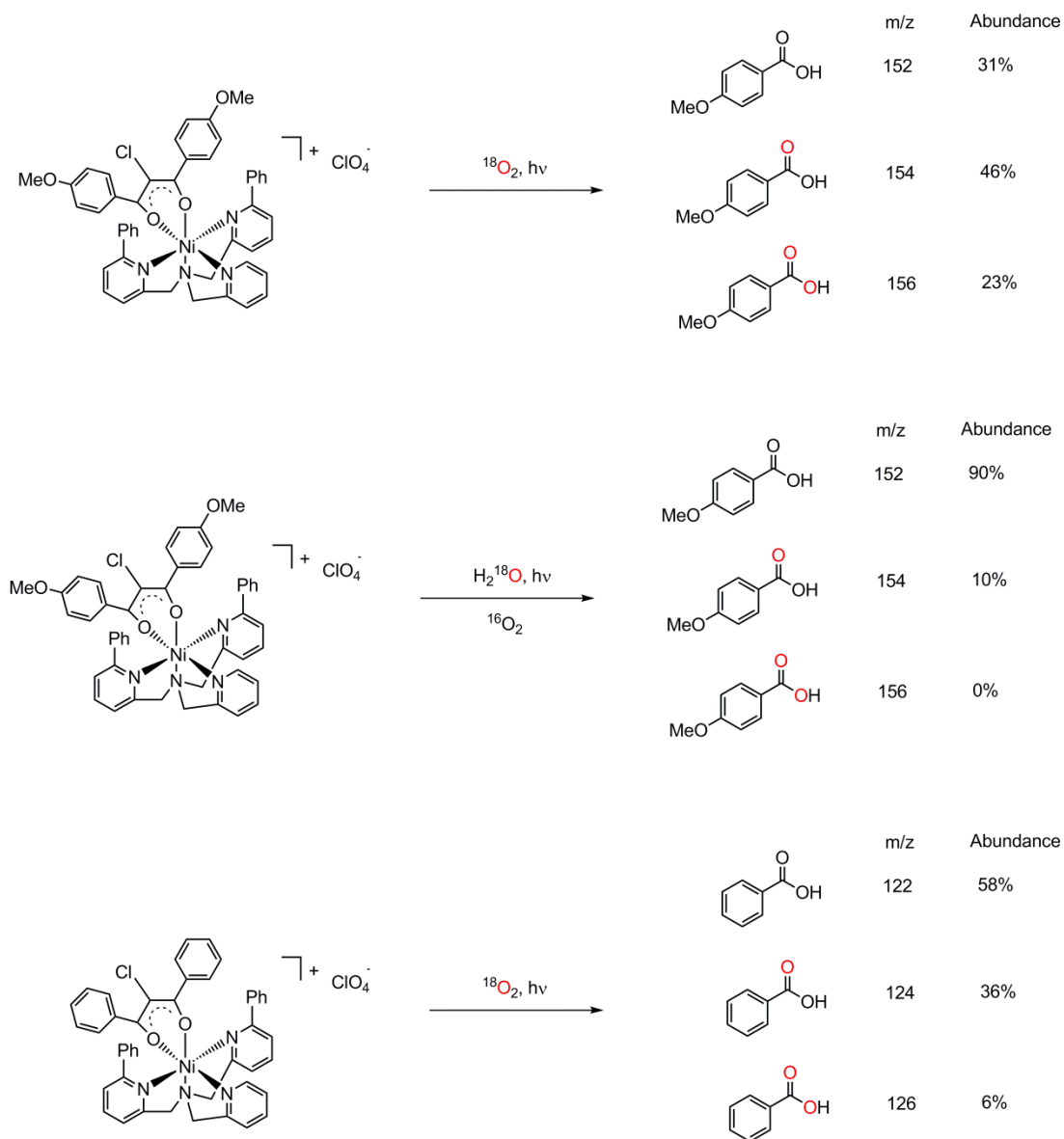


Figure 4-11. ^{18}O labelling studies for the photochemical reactions of **4** and **6**.

Incorporation of isotope into the carboxylate products was determined by the relative abundance of the $[\text{M}]^+$, $[\text{M}+2]^+$ and $[\text{M}+4]^+$ ions by GCMS.

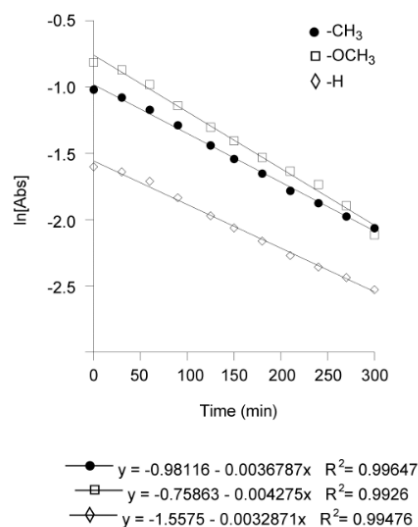


Figure 4-12. First-order plot for the photoreaction of **4-6** in aerobic CH₃CN at 29(1)^oC, irradiating at 350 nm. Reactions were monitored at 378, 374 and 372 nm for **4-6** respectively.

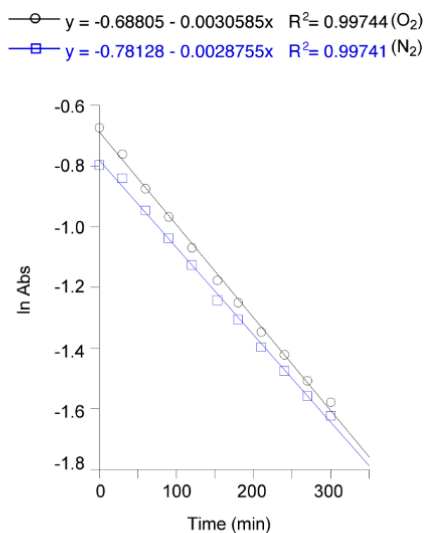


Figure 4-13. Representative first order plots of side-by-side studies of the photochemical reaction of **4** under O₂ and N₂ at ~29^oC. Several repeat runs produced similar results wherein the reaction performed under oxygen was slightly faster. The data shown here were obtained monitoring at 378nm.

comparatively investigated. Monitoring the change in absorbance at 378 nm (Figure 4-4) as a function of time for the photochemical reaction of **4** under aerobic conditions indicated a first-order process (Figure 4-12). Similar experiments performed using **5** and **6** demonstrated that the reaction slows in the order $4 > 5 > 6$. This is consistent with quantum yields measured for the reactions wherein **4** (0.00038 ± 0.00002) $>$ **5** (0.00032 ± 0.00003) $>$ **6** (0.00020 ± 0.00007). Thus, enhanced electron density within the 2-chloro-1,3-diketonate ligand increases the quantum yield and the rate of the reaction. As shown in Scheme 4-7, the overall low quantum yield of these reactions may be attributed to recombination of the Ni^{I} species with the β -diketonate radical.

The formation of the other organic products (**II-IV**) in the photoreactions of **4-6** can be rationalized on the basis of the chemistry of the β -diketonate radical. The production of **II** and **IV** suggests that free neutral 2-chloro-1,3-dione is generated in the reaction mixture and subsequently undergoes the photochemical reactions previously reported by Kosmrlj et al.²⁵ The formation of free neutral **3a-3c** most likely occurs via hydrogen atom abstraction reactivity involving the β -diketonate radical. Although we have not definitively identified the H-atom donor in the system, we have found that an aerobic photochemical experiment involving **4** in the presence of the H-atom donor 9,10-dihydroanthracene does significantly increase the rate of disappearance of the 2-chloro-1,3-diketonate complex.

The formation of **III** has not been reported in the photochemical reactions of **3a** and **3c**,²⁵ although it has been detected as a product in the photochemical reactions of dibenzoyldiazomethane, suggesting decomposition involving the β -diketonyl radical.³³

As depicted in Scheme 4-7, we propose that the observed rate of reaction for **4-6** will be influenced by the magnitude of the pseudo first order rate constants k_2 , k_3 and k_4 as compared to k_{-1} . For example, the rate should increase in the presence of O_2 as the pathway represented by k_2 becomes operative. Addition of an H-atom donor compound, such as 9,10-dihydroanthracene, would also be expected to increase the rate, as the magnitude for k_4 would increase and k_2 may also increase due to the ability of a hydrogen atom donor to trap a nascent superoxide radical. The relative rates of reaction for **4** under an aerobic or nitrogen atmosphere (Figure 4-13), and in an aerobic mixture containing 9,10-dihydroanthracene, were determined and qualitatively support the proposed reaction scheme. The reactivity trend **4** > **5** > **6** described earlier can be explained either in terms of the increased electron richness decreasing the magnitude of k_{-1} or increasing the magnitude of at least one of k_2 - k_4 . In fact, the two effects may be viewed as synergistic. Specifically, the electron-donating methoxy groups will stabilize the one-electron oxidized form of the β -diketonate with respect to reduction, decreasing k_{-1} , and the increased electron density should facilitate oxidation, thereby increasing k_2 .

The observed lack of reactivity for the unsubstituted Ni^{II} β -diketonate complexes **7-9** was investigated using a crossover type experiment. Specifically, an acetonitrile solution containing equimolar amounts of the methoxy-substituted **7** with the sodium salt of dibenzoylmethane was irradiated for 20 h after which time the reaction was evaluated using 1H NMR under paramagnetic conditions. At this point a mixture of **7** and **9** was present. In the absence of irradiation, formation of a similar mixture took >7 days to form. These combined results indicate that similar to **4-6**, the unsubstituted complexes **7-9** undergo a photochemical reaction that labilizes the β -diketonate ligand. The lack of

formation of oxidation, α -cleavage, or flavone products in these systems appears to be due to the lack of the reactive 2-chloro moiety in that labilized β -diketonate radical species. The chloro substituent may be necessary as a leaving group³⁴ to enable formation of a vicinal triketone, or to enhance the electrophilic character of the α -carbon center.

Conclusion

Oxidative carbon-carbon bond cleavage reactions of relevance to biological processes are of current interest, including those involving aliphatic carbon-carbon bond cleavage in β -diketone substrates. Herein we demonstrate that this type of oxidative chemistry can be achieved via photochemical reduction of Ni^{II} 2-chloro-1,3-diketonate complexes under aerobic conditions. We propose that the reduced nickel center generated in these reactions activates dioxygen to form superoxide and initiate a reaction sequence that ultimately results in the formation of carboxylic acid products. This novel reactivity has relevance to that proposed for the iron-containing Dke1 enzyme wherein the metal center mediates electron transfer from the β -diketonate ligand to O₂ leading to the formation of superoxide. Overall, this work outlines a new approach toward examining chemistry of relevance to metal-containing dioxygenase enzymes that cleave a β -diketone ligand.

References

- [1] G. Grogan, *Biochem. J.* **2005**, *388*, 721-730.
- [2] T. Pochapsky in *Metal Ions in Life Sciences, Vol. 2, Nickel and Its Surprising Impact in Nature* (Eds: A. Sigel, H. Sigel, R. K. O. Sigel), Wiley, Chichester, West Sussex, England, **2007**, pp. 473-500.

- [3] G. D. Straganz, B. Nidetzky, *J. Am. Chem. Soc.* **2005**, *127*, 12306-12314.
- [4] a) S. Leitgeb, G. D. Straganz, B. Nidetzky, *Biochem. J.* **2009**, *418*, 403-411. b) A. R. Diebold, G. D. Straganz, E. I. Solomon, *J. Am. Chem. Soc.* **2011**, *133*, 15979-15991.
- [5] I. Siewert, C. Limberg, *Angew. Chem., Int. Ed.* **2008**, *47*, 7953-7956.
- [6] M. G. M. B. Martin, M. Hörner, M. B. Behm, F. S. Nunes, *Z. Anorg. Allg. Chem.* **2011**, *637*, 1229-1233.
- [7] E. Szajna-Fuller, K. Rudzka, A. M. Arif, L. M. Berreau, *Inorg. Chem.* **2007**, *46*, 5499-5507.
- [8] L. M. Berreau, T. Borowski, K. Grubel, C. J. Allpress, J. P. Wickstrom, M. E. Germain, E. V. Rybak-Akimova, D. L. Tierney, *Inorg. Chem.* **2011**, *50*, 1047-1057.
- [9] a) Y. L. Chow, H. Li, M. S. Yang, *J. Chem. Soc., Perkin Trans. 2* **1990**, 17-24. b) Y. L. Chow, H. Li, *Can. J. Chem.* **1986**, *64*, 2229-2231. c) Y. L. Chow, G. E. Buono-Core *J. Chem. Soc., Chem. Commun.* **1985**, 592-594.
- [10] a) M. T. Kieber-Emmons, C. G. Riordan *Acc. Chem. Res.* **2007**, *40*, 618-625. b) A. Company, S. Yao, K. Ray, M. Driess, *Chem. Eur. J.* **2010**, *16*, 9669-9675.
- [11] E. Szajna, P. Dobrowolski, A. L. Fuller, A. M. Arif, L. M. Berreau, *Inorg. Chem.* **2004**, *43*, 3988-3997.
- [12] T. Choshi, S. Horimoto, C. Y. Wang, H. Nagase, M. Ichikawa, E. Sugino, S. Hibino, *Chem. Pharm. Bull.* **1992**, *40*, 1047-1049.
- [13] P. K. Dhondi, P. Carberry, J. D. Chisholm, *Tetrahedron Lett.* **2007**, *48*, 8743-8746.
- [14] W. L. F. Armarego, D. D. Perrin, *Purification of Laboratory Chemicals*, 4th ed., Butterworth-Heinemann, Boston, MA, 1996.

- [15] a) H. J. Kuhn, S. E. Braslavsky, R. Schmidt, *Pure Appl. Chem.* **2004**, *76*, 2105-2146. b) C. G. Hatchard, C. A. Parker, *Proc. R. Soc. London* **1956**, *A235*, 518-536.
- [16] W. Connelly and W. Geiger, *Chem. Rev.* 1996, *96*, 877-910.
- [17] W. C. Wolsey, *J. Chem. Educ.* **1973**, *50*, A335.
- [18] E. Szajna, M. M. Makowska-Grzyska, C. C. Wasden, A. M. Arif, and L. M. Berreau, *Inorg. Chem.* **2005**, *44*, 7595-7605. Crystallographic files in CIF format for compounds **5**•C₄H₁₀O (CCDC-827741), **6** (CCDC-827742) and **8**•2CH₂Cl₂ (CCDC-827743) have been deposited in The Cambridge Crystallographic Data Center. This data can be obtained free of charge on the internet via www.ccdc.cam.ac.uk/data_request/cif.
- [19] R. C. Larock, *Comprehensive Organic Transformations*, 2nd ed., Wiley-VCH, New York, 1999, p. 715.
- [20] A. Podgorsek, M. Jurisch, S. Stavber, M. Zupan, J. Iskra, J. A. Gladysz, *J. Org. Chem.* **2009**, *74*, 3133-3140.
- [21] H. M. Meshram, P. N. Reddy, P. Vishnu, K. Sadashiv, J. S. Yadav, *Tetrahedron Lett.* **2006**, *47*, 991-995.
- [22] G. I. Roshchupkina, Y. V. Gatilov, T. V. Rybalova, V. A. Reznikov, *Eur. J. Org. Chem.* **2004**, 1765-1773.
- [23] (a) J. C. Taylor, A. B. McLaren, *J. Chem. Soc.* **1979**, *3*, 460-464. b) V. G. Isakova, I. A. Baidina, N. B. Morozova, I. K. Igumenov, *Polyhedron*, **2000**, *19*, 1097-1103. c) D. C. Ware, W. R. Wilson, W. A. Denny, C. E. F. Rickard, *Chem. Comm.* **1991**, *17*, 1171-1173. d) C. A. Vock, A. K. Renfrew, R. Scopelliti, L. Juillerat-Jeanneret, P. J. Dyson, *Eur. J. Inorg. Chem.* **2008**, *10*, 1661-1671. e) E. D. Estes, R. P. Scaringe, W. E.

Hatfield, D. J. Hodgson, *Inorg. Chem.* **1976**, *15*, 1179-1182. f) C. A. Kavounis, L. C. Tzavellas, C. J. Cardin, Y. Zubavichus, *Struct. Chem.* **1999**, *10*, 411. g) S. Sans-Lenain, A. Gleizes, *Inorg. Chim. Acta.* **1993**, *211*, 67-75. h) V. V. Sharutin, O. K. Sharutina, O. P. Zadachina, A. N. Zakharova, V. A. Reutov, N. P. Shapkin, V. K. Belsky, *Russ. J. Gen. Chem.* **2000**, *70*, 1672.

[24] E. Szajna, A. M. Arif, L. M. Berreau, *J. Am. Chem. Soc.* **2005**, *127*, 17186-17187.

[25] B. Kosmrlj, B. Sket, *Org. Lett.* **2007**, *9*, 3993-3996.

[26] R. L. Lintvedt, H. D. Gafney, *J. Am. Chem. Soc.* **1970**, *92*, 6996-6997.

[27] F. D. Lewis, A. M. Miller, G. D. Salvi, *Inorg. Chem.* **1995**, *34*, 3173-3181.

[28] P. S. Singh, D. H. Evans, *J. Phys. Chem. B.* **2006**, *110*, 637-644.

[29] N. Tada, M. Shomura, H. Nakayama, T. Miura, A. Itoh, *Synlett* **2010**, 1979-1983.

[30] J. D. Roberts, D. R. Smith, C. C. Lee, *J. Am. Chem. Soc.* **1951**, *73*, 618-625.

[31] We could not conclusively identify the formation of the benzil analog 4,4'-dimethoxybenzil in the product mixture generated from the reactions of **4**. This may be influenced by the presence of the methoxy substituent, as the propensity of the triketone to undergo migration reactivity leading to benzil formation will be influenced by the relative electrophilicity of carbonyl centers. V. H. Le Dao, F. Dayer, L. Duc, H. Rode-Gowal, H. Dahn, *Helv. Chim. Acta* **1974**, *47*, 2215-2223.

[32] a) L. Shu, Y. Shi, *Tetrahedron* **2001**, *57*, 5213-5218. b) N. A. Porter, H. Yin, D. A. Pratt, *J. Am. Chem. Soc.* **2000**, *122*, 11272-11273.

[33] K. Nakatani, J. Shirai, R. Tamaki, I. Saito, *Tetrahedron Lett.* **1995**, *36*, 5363-5366.

- [34] S. J. Coats, H. H. Wasserman, *Tetrahedron Lett.* **1995**, 36, 7735-7738.

CHAPTER 5

DIOXYGENASE-TYPE CARBON-CARBON BOND CLEAVAGE IN A
MONONUCLEAR COPPER(II) CHLORO-DIKETONATE COMPLEX**Abstract**

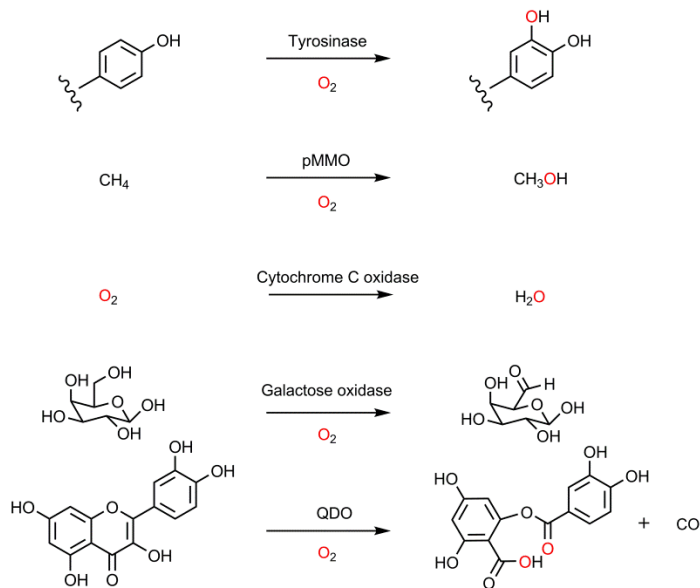
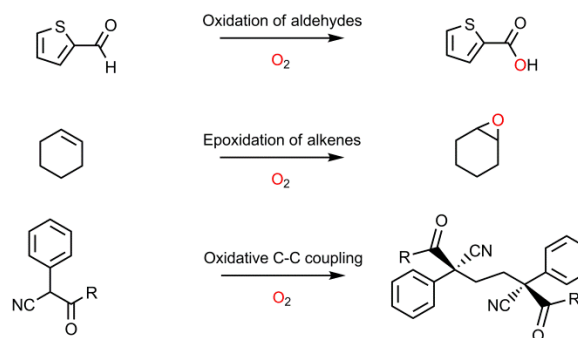
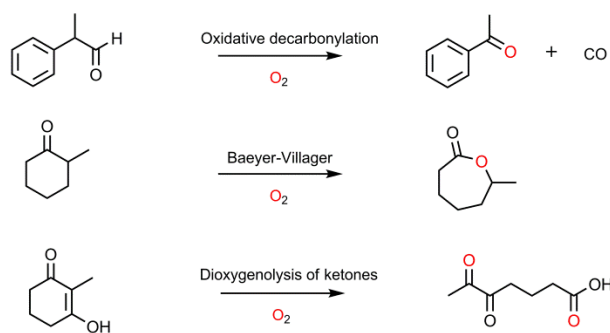
The scope of copper dioxygenase chemistry in well-defined synthetic systems has not been widely investigated, excepting the oxidative cleavage of flavonols by model systems of relevance to quercetin dioxygenase. In this article we report the synthesis and characterization of a mononuclear copper chloro-diketonate complex, [(6-Ph₂TPA)Cu(PhC(O)CClC(O)Ph)](ClO₄) (**1**). Complex **1** is a five-coordinate complex with a bidentate coordination mode of the diketonate and has been characterized by UV-vis, FTIR, EPR, magnetic susceptibility, elemental analysis, HRMS, and X-ray crystallography. Exposure of **1** to dioxygen in CH₃CN leads to cleavage of the diketonate carbon-carbon bonds at ambient temperature and pressure to generate carboxylate products and [(6-Ph₂TPA)CuCl]ClO₄ (**2**). Mechanistic and computational studies show an important role for *in situ* generated chloride ions in promoting this oxidative cleavage reaction.

Introduction

One of the most important challenges for chemists in the 21st century is to develop new ways for converting chemical feedstocks (including biomass) into useful products, including pharmaceuticals, polymers, and fuels, in an environmentally benign and cost-efficient manner.¹ One area of chemistry that is still underdeveloped in this regard is the development of methods for the selective oxidative activation of carbon-carbon bonds.²

The principles of Green Chemistry provide a guiding framework for accomplishing such oxidations, including advocacy of the use of low-cost, non-toxic catalysts, renewable feedstocks, and low temperature and pressure conditions.³ Ideally, oxidations could be achieved using the abundant gas dioxygen as a terminal oxidant, cheap and relatively non-toxic first-row transition metals as catalysts, and at ambient temperature and pressure.⁴ With this in mind, copper is a late first-row transition metal that appears ideally suited as a catalyst for selective carbon-carbon bond activations due to the rich redox chemistry available to it. This is due to its ability to access Cu(0), Cu(I), Cu(II) and Cu(III) oxidation states through appropriate tuning of its ligand environment.⁵

The chemistry of copper and dioxygen is rich and varied.⁶ Nature employs copper centers to facilitate numerous oxygen-involving reactions in enzymatic systems, including tyrosinase, particulate methane monooxygenase (pMMO), cytochrome C oxidase and galactose oxidase (Scheme 5-1 (top)).⁷⁻¹⁰ These reactions have been studied extensively both by direct investigation of the enzymatic systems and by the synthesis of well-defined copper coordination compounds that can act as model systems of the more complex enzyme active sites.⁶⁻¹¹ A large focus within the synthetic inorganic community has been on understanding the spectroscopy and reactivity of Cu-O₂ adducts, both to better understand enzymatic systems and to investigate their ability to oxidatively activate bonds for applications in energy-related applications, such as the oxidation of methane to methanol.¹¹⁻¹³ Thus, there have been a wide variety of synthetic copper-containing systems identified that are capable of selectively activating X-H (X = C, N, O) bonds, often via the initial synthesis of a Cu(I) center, or a dicopper core (Figure 5-1).¹¹ While the activation of X-H bonds has been extensively studied, the activation of C-C

Cu-containing enzymes:**Cu-catalyzed reactions:****Cu-catalyzed C-C cleavage:**

Scheme 5-1. Selected examples of copper oxygen chemistry including examples from enzymatic systems (top), catalytic reactions for synthesis (middle), and reactions that lead to C-C bond cleavage (bottom). Many of these reactions also require a coreductant for the reaction to proceed.

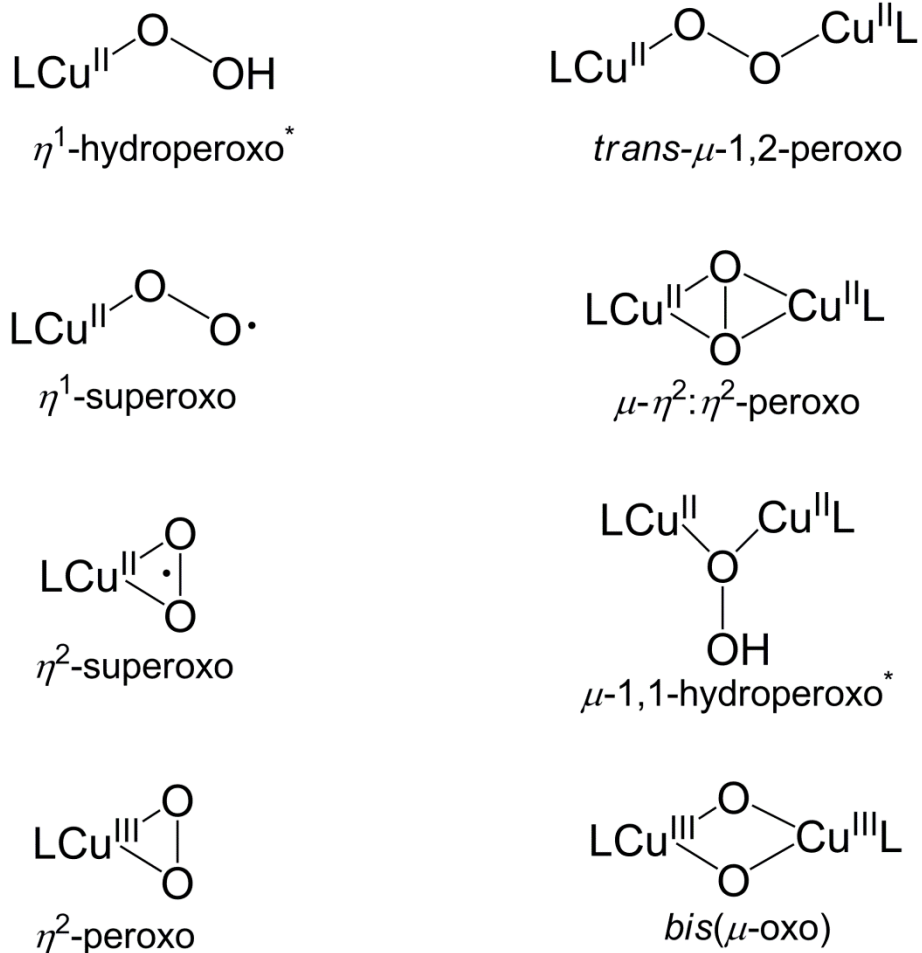
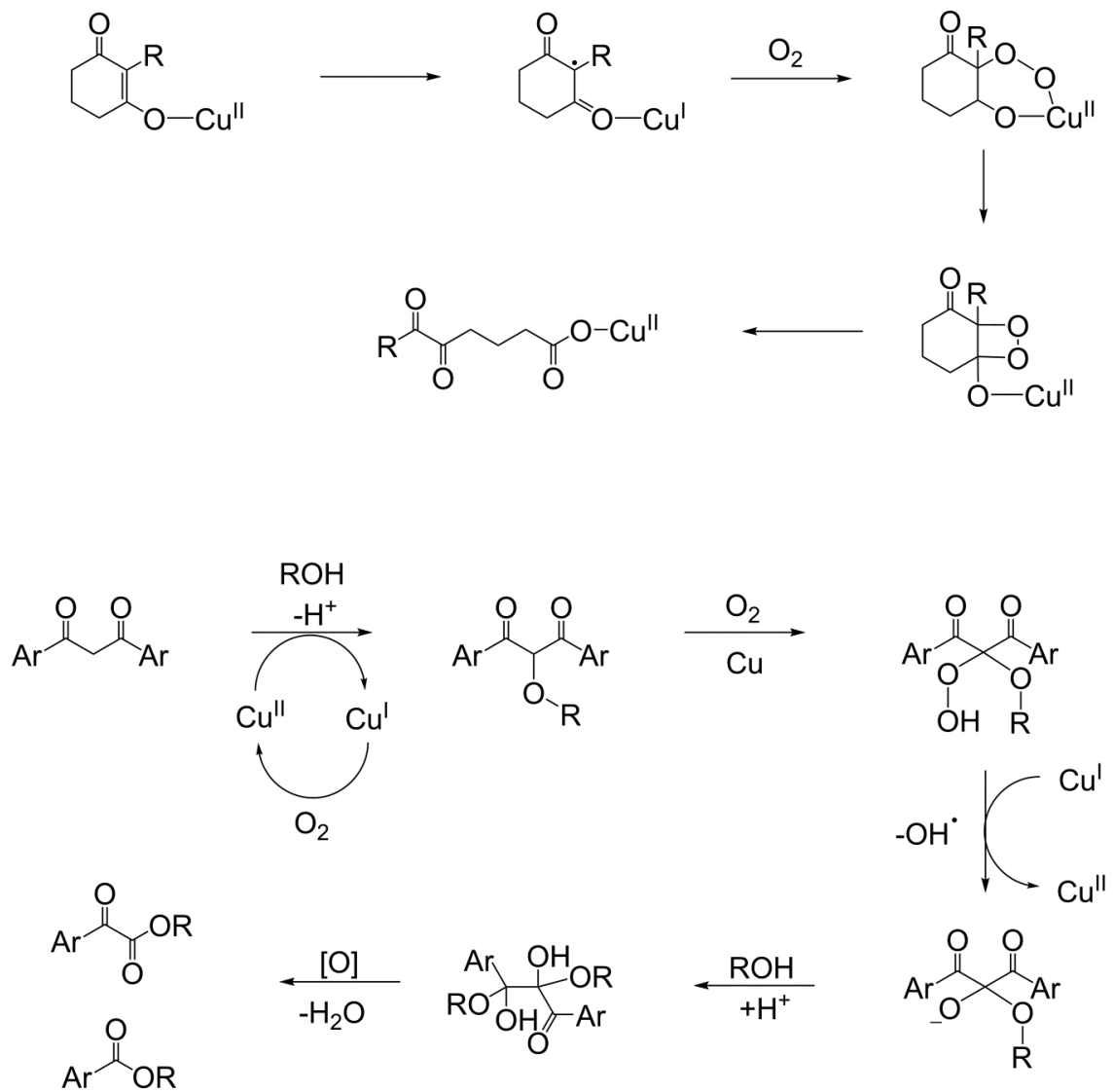


Figure 5-1. A subset of Cu/O₂ adducts that have been investigated for their spectroscopic features and reactivity to provide insight into a variety of copper-containing enzymatic systems. All of these Cu/O₂ adducts are formed by the reaction of O₂ with a Cu(I) center(s). * The formation of the η^1 -hydroperoxo and μ -1,1-hydroperoxo structures require the addition of a hydrogen atom and a proton, respectively.

bonds in well-defined copper complexes has only been extensively studied in model systems of a single family of enzymes – the quercetin dioxygenases.¹⁴

Synthetic organic chemists have also utilized the oxygen chemistry of copper for numerous organic transformations, many of these inspired by enzymatic systems.^{5, 15-23} These oxidations range from functional group interconversions, such as the oxidation of aldehydes to carboxylic acids, to monooxygenase reactions involving the insertion of oxygen into hydrocarbon C-H bonds or during the epoxidation of alkenes, to oxidase reactions such as coupling reactions generating C-C bonds (Scheme 5-1 (middle)).¹⁷⁻¹⁹ Within the scope of oxidative C-C bond cleavage, copper catalysts have often been used in decarbonylation reactions of aldehydes, aldehyde-mediated Baeyer-Villiger-type monooxygenase cleavage reactions of ketones to form esters, and in the cleavage of cyclic ketones via a dioxygenase-type pathway (Scheme 5-1 (bottom)).²⁰⁻²²

The oxidative cleavage of cyclic ketones is very interesting as it does not require the presence of a co-reductant (Scheme 5-2 (top)), which is a major draw-back in the copper-catalysed Baeyer-Villiger reactions. The reaction is reported to be catalyzed by simple Cu(II) salts at room temperature in CH₃CN, and uses O₂ as the terminal oxidant.²² By analogy with the copper-catalyzed, aldehyde-mediated Baeyer Villager reaction, a reaction pathway has been proposed that involves the generation of a Cu(I)-ketonyl radical pair which intercepts dioxygen (Scheme 5-2 (top)). This proposal is very similar to that proposed for the reaction of quercetin dioxygenase (QDO, *vide infra*).¹⁴ No mechanistic studies have been reported, which might have provided insight into the appropriateness of the proposed mechanism. It is worth noting that the cleavage of acyclic ketones was not reported, suggesting that alleviation of ring strain may be



Scheme 5-2. Proposed reaction mechanisms for the copper-catalyzed oxidative cleavage of cyclic ketones (top) and of acyclic β -diketones (bottom).

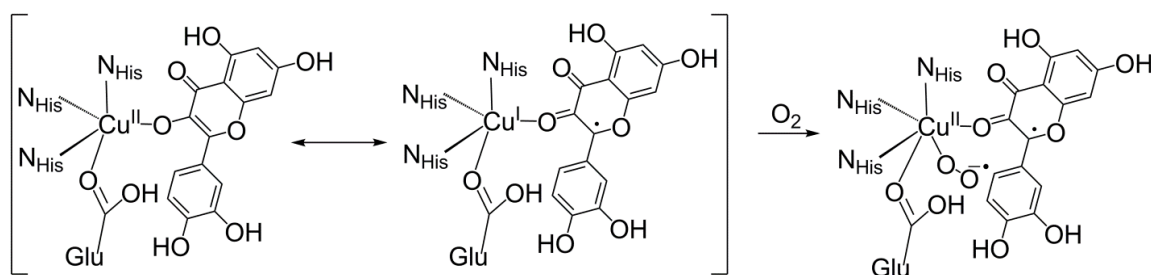
involved in facilitating the reaction.

Recently, the copper-catalyzed oxidative cleavage of an acyclic β -diketonate substrate has also been reported (Scheme 5-2 (bottom)).²³ The reaction proceeds by combining a CuBr or CuBr₂ salt, pyridine, the diketone substrate and oxygen in toluene at 90°C. While some mechanistic experiments were undertaken, suggesting that the reaction may proceed via generating a superoxide intermediate, the poorly defined catalytic complex precluded any useful conclusions being drawn about the reaction pathway. For example, while pyridine was found to be necessary for the reaction to proceed, its exact role is unknown. Varying the concentration of pyridine from 2 to 20 equivalents per copper had only minor effects on the reaction progression. EPR experiments appeared to show that the presence of pyridine was required to oxidize CuBr using O₂ to generate superoxide, although the importance of this is unclear as the reaction still proceeds in similar yields and product distributions when only CuBr₂ is present as a copper source.

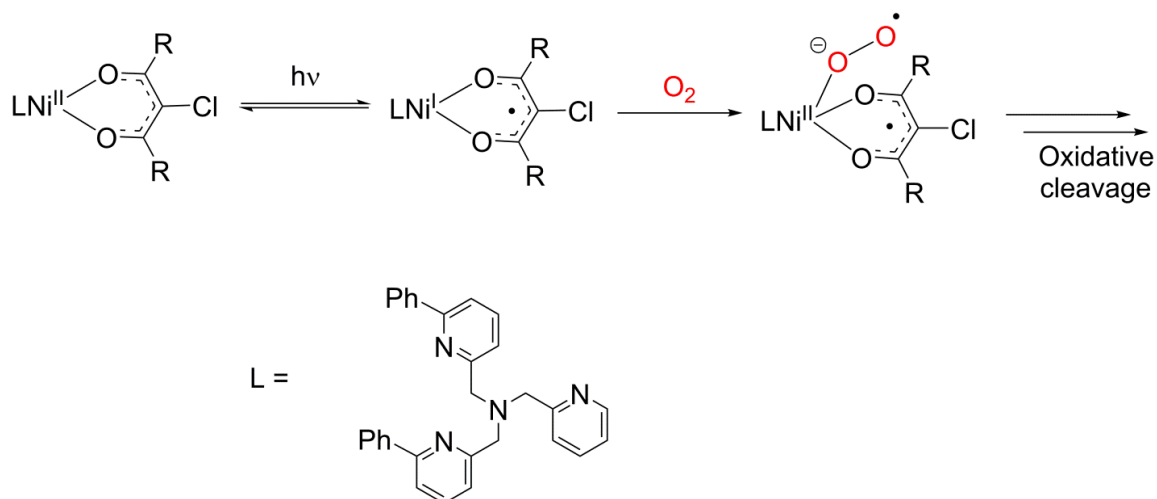
We are interested in utilizing well-defined copper coordination complexes to understand the chemical factors that influence the reactivity, and selectivity thereof, of copper-containing systems that oxidatively cleave C-C bonds using oxygen as the terminal oxidant and that proceed via a dioxygenase-type pathway. We are especially interested in these dioxygenase-type pathways as they do not require external co-reductants, like some oxidase or monooxygenase reactions, and also due to their relevance in understanding the role of the metal center in biologically important dioxygenase reactions.^{2a} Despite the prevalence of well-defined copper-containing systems for X-H bond activation, and the numerous copper-containing catalytic systems that can oxidatively cleave C-C bonds, there are very few well-defined copper-containing

systems that can cleave C-C bonds by a dioxygenase-type pathway.^{14b, 15b} We hope that such studies would inform design of future catalytic systems for organic synthesis. The only well-defined system to date that has allowed extensive mechanistic investigations of the role of the copper center in O₂ activation is quercetin dioxygenase (QDO).¹⁴

QDO is the only dioxygenase unambiguously known to contain copper.^{14b} It is also one of the few dioxygenase enzymes capable of cleaving aliphatic carbon-carbon bonds.^{2a} QDO contains a mononuclear Cu(II) center at the active site, ligated by three histidines, a water molecule and sometimes by a mobile carboxylate.²⁴ The enzyme-substrate adduct of QDO is proposed to react with dioxygen via the formation of a Cu(I)-substrate radical pair, facilitated by binding of the carboxylate residue that favours monodentate coordination of the flavonol substrate (Scheme 5-3).¹⁴ Functional model systems of QDO containing a copper ion have been able to replicate the dioxygenase reactivity of flavonol substrates and also exhibit rate enhancement in the presence of excess carboxylate.^{14c} These functional models only operate at elevated temperatures (>80°C), usually with DMF as a solvent. The wider scope of using a Cu(II)-substrate anion/Cu(I)-substrate radical equilibrium to dioxygenolytically cleave substrates has been rarely studied.²⁵ Our previous studies of the photo-induced dioxygenase-type reactivity of



Scheme 5-3. A proposed oxygen activation step in the dioxygenase reaction of quercetin dioxygenase.



Scheme 5-4. Photo-induced dioxygenase cleavage of a chloro-diketonate substrate utilizing a Ni(II) center. Since a Cu(I) center is more stable than Ni(I), it was proposed that it should allow facile oxidative cleavage of the diketonate substrate.

a nickel chloro-diketonate (Scheme 5-4) suggested that this substrate would be a candidate for this chemistry in a copper system.²⁶ Herein we report our discovery of dioxygenase-type aliphatic carbon-carbon bond cleavage in a copper chloro-diketonate system at ambient temperature. To our knowledge, this is the only example of facile Cu(II) dioxygenase chemistry in a well-defined synthetic system without elevated temperatures or photochemical activation.^{14b, 27}

Experimental

General methods: All reagents were obtained from commercial sources, and were used without further purification unless otherwise stated. Solvents were dried according to published procedures and purified by distillation under N₂ prior to use.²⁸ 6-Ph₂TPA (*N,N*-bis((6-phenyl-2-pyridyl)methyl)-*N*((2-pyridyl)methyl)amine) and 2-chloro-1,3-diphenylpropane-1,3-dione were prepared according to previously published

procedures.^{29, 30} All manipulations were carried out in an MBraun Unilab glovebox with a N₂ atmosphere, or using standard Schlenk techniques, unless otherwise noted.

Physical methods: ¹H NMR spectra were collected on a Bruker ARX-400 spectrometer at 25 °C; chemical shifts were referenced to the residual solvent peak in CD₂H₂CN (1.94 ppm, quintet). UV-vis data was collected on a HP8453A spectrometer at ambient temperature; kinetic measurements were performed at 21 °C in 1 mm pathlength quartz cells with Teflon stopcocks. FTIR spectra were collected on a Shimadzu FTIR-8400 as KBr pellets. Room temperature magnetic susceptibilities were determined by the Evans method, using a Bruker ARX-400 spectrometer.³¹ GC-MS data was collected on a Shimadzu GCMS-QP5000 GC-MS with a GC-17A gas chromatograph, using an Alltech EC5 30 m × 25 mm × 25 μm thin film capillary column. CO and CO₂ gases were detected on an Agilent 3000A Micro Gas Chromatograph, with molecular sieve and Plot U columns, and a thermal conductivity detector. Mass spectral data for the metal complexes were collected by the Mass Spectrometry Facility, University of California, Riverside. Elemental analyses were performed by Atlantic Microlabs Inc., Norcross, GA.

EPR: X-band EPR spectra were recorded with a Bruker EMX EPR spectrometer on degassed 50 μM 80/20 CH₂Cl₂/toluene solutions. Low temperature spectra were obtained using an Oxford ESR900 liquid helium cryostat. The spectra in Figure 5-3 represent the average of four scans each. Other conditions, unless otherwise noted: $\nu_{\text{MW}} = 9.385$ GHz (20 μW); 2 G field modulation (100 kHz); receiver gain = 50000; time constant/conversion time = 82 ms. Spectra were simulated using the program QPOW.³² The final simulations include weighted contributions from both ⁶³Cu and ⁶⁵Cu, and

uncorrelated m_I and frequency-dependent contributions to the observed line width,³³ totaling less than 20 % of the overall EPR line width.

Caution! *Perchlorates are potentially explosive, and should be handled with extreme care and in small quantities (<50 mg).*³⁴

Synthesis of [(6-Ph₂TPA)Cu(PhC(O)CClC(O)Ph)]ClO₄ (1) Cu(ClO₄)₂·6H₂O (18 mg, 0.047 mmol) was dissolved in CH₃CN (2 mL) and added to 6-Ph₂TPA (21 mg, 0.047 mmol). The resulting pale green solution was stirred together for 30 minutes until all solids had completely dissolved. 2-chloro-1,3-diphenylpropane-1,3-dione (12 mg, 0.047 mmol) was dissolved in Et₂O (1 mL), added to lithium bis(trimethylsilyl)amide (7.9 mg, 0.047 mmol) and the mixture was stirred for five minutes, resulting in a pale yellow suspension. The solutions were combined and stirred for 16 hours to produce a green solution. The solvent was removed under reduced pressure, and the crude material was dissolved in CH₂Cl₂ and filtered through a glass wool/Celite plug. The solution was then concentrated under reduced pressure, and the metal complex precipitated by addition of excess hexanes, yielding a green powder (36 mg, 88 % yield). Crystals suitable for x-ray diffraction were grown by vapour diffusion of Et₂O into a CH₂Cl₂ solution. Elemental analysis calculated (%) for C₄₅H₃₆Cl₂CuN₄O₆: C 62.59, H 4.21, N 6.49; found: C 62.79, H 4.47, N 6.49. HRMS: m/z calculated for C₄₅H₃₆ClCuN₄O₂: 762.1823 [M-ClO₄]⁺; found: 762.1806. UV-vis λ_{\max} , nm (ϵ , M⁻¹cm⁻¹): 253 (34000), 363 (10200). FTIR (KBr, cm⁻¹): 1541, 1339, 1105 (ν_{ClO_4}), 623 (ν_{ClO_4}). μ_{eff} 1.82 μ_{B} .

Synthesis of [(6-Ph₂TPA)CuCl]ClO₄ (2) Cu(ClO₄)₂·6H₂O (27 mg, 0.074 mmol) was dissolved in CH₃CN (3 mL) and added to 6-Ph₂TPA (33 mg, 0.074 mmol). The resulting pale green solution was stirred for half an hour until all solids had completely

dissolved. The solution was added to solid Me_4NCl (8.1 mg, 0.074 mmol) and stirred for four hours to produce a pale green solution. The solution was concentrated under reduced pressure, causing a precipitate to form. The precipitate was collected on a glass wool/Celite plug, washing with a small amount of CH_3CN . The precipitate was redissolved in CH_2Cl_2 , to generate a green solution. Addition of excess hexanes to this solution caused a precipitate to form. Decantation of the supernatant, followed by extensive drying *in vacuo* yielded a blue/green powder (43 mg, 90% yield). Elemental analysis calculated (%) for $\text{C}_{30}\text{H}_{26}\text{Cl}_2\text{CuN}_4\text{O}_4 \cdot 0.5\text{CH}_2\text{Cl}_2$: C 53.58, H 3.98, N 8.20; found: C 53.23, H 4.34, N 8.95. HRMS: m/z calculated for $\text{C}_{30}\text{H}_{26}\text{ClCuN}_4$: 540.1124 [$\text{M}-\text{ClO}_4$]⁺; found: 540.1143. FTIR (KBr, cm^{-1}): 1092 (ν_{ClO_4}), 624 (ν_{ClO_4}). μ_{eff} 1.83 μ_{B} .

Reaction of 1 with O₂. A CH_3CN solution of **1** (1.2 mM) was prepared under a N_2 atmosphere. Aliquots of this solution were purged for 30 seconds with O_2 . The reaction vessel was then sealed with a Teflon stopcock and stirred for 2 hours. The progression of the reactions was conveniently monitored by removing aliquots of solution and following the decay of the absorption feature at 363nm using a 1mm quartz UV-vis cell. In order to determine whether the reactions were photo initiated, as has been previously reported for some nickel-containing chloro-diketonate systems,²⁶ we performed the reactions in foil-wrapped glassware, and found that light was not required for the reaction to proceed. We also attempted irradiation of **1** at 350 nm in the presence of O_2 . By comparing the reaction progression of this irradiated sample with that of a sample kept in the dark, we found a slight increase in rate in the photo reaction. However, this photo reaction was very slow (quantum yield $\sim 10^{-4}$, as determined by ferrioxalate

actinometry),³⁵ and thus we focused our efforts on characterizing the more interesting thermal reaction.

The reactions were stopped by removing the solvent under reduced pressure. Analysis of the crude solid by HRMS showed a molecular ion at 540.1142 m/z consistent with a $[(6\text{-Ph}_2\text{TPA})\text{CuCl}]^+$ ion, and had a fragmentation pattern that matched that of an authentic sample of **2**. Vapor diffusion of Et_2O into a CH_2Cl_2 solution of the crude product mixture yielded green crystals of **2**. CH_2Cl_2 suitable for analysis by x-ray diffraction. The organic products of the reaction were analyzed as described below.

For consistency with the ^{18}O experiments, the reaction was also repeated with the addition of 10 μL H_2O to the reaction mixture per mL CH_3CN .

Analysis of Organic Products To separate the organic components of the product mixture from the metal-containing species, the crude product mixture was passed through a silica column, eluting with EtOAc . The total yield of these organic products was greater than 80%, determined as a percentage by mass of the diketonate in the starting material. The organic species were analyzed by GC-MS, and identified by comparing to retention times and fragmentation patterns of authentic samples. Four species were present, and were identified to be benzoic acid, benzil, benzoic anhydride and diphenylpropantrione. When the reactions were repeated with the addition of H_2O (see above), benzoic anhydride was no longer detected among the products.

Recovery of the Ligand 6-Ph₂TPA A CH_2Cl_2 solution of the crude product mixture was stirred vigorously with NH_3 (aq). The blue aqueous layer was removed by decantation, then the CH_2Cl_2 solution was dried over Na_2SO_4 and the solvent removed under reduced pressure. Yield by mass of chelate ligand was 85%. Analysis by ^1H NMR

showed peaks corresponding predominantly to the intact chelate ligand, in addition to a minor component of benzil.

¹⁸O Labeling Experiments To introduce ¹⁸O₂, a 1.2 mM CH₃CN solution of **1** was prepared under a N₂ atmosphere, and a 5 mL aliquot placed in a flask sealed with a stopcock. 50 μL H₂¹⁶O was introduced, and then the atmosphere removed from the flask by freeze-pump-thaw cycles. ¹⁸O₂ gas was then introduced to the frozen solution on a Schlenk line, the flask sealed, thawed, and allowed to stir for 12 hours.

To introduce H₂¹⁸O, 5 mL of a 1.2 mM CH₃CN solution of **1** was prepared under a N₂ atmosphere. 50 μL H₂¹⁸O was added and the solution purged with ¹⁶O₂ for 30 seconds. The reaction vessel was then sealed and allowed to stir for 12 hours.

In each case the organic products were isolated and analyzed as described above. Levels of ¹⁸O incorporation into benzoic acid were determined from the ratios of the [M]⁺, [M+2]⁺ and [M+4]⁺ ion intensities.

X-ray Crystallography: Single crystal samples of **1**, and the product of the O₂ reaction of **1**, which was determined to be the chloride complex [(6-Ph₂TPA)CuCl]ClO₄ (**2**), were mounted on a glass fiber using a viscous oil and then transferred to a Nonius KappaCCD diffractometer (Mo K_α, λ = 0.71073 Å) for data collection at 150(1) K. Methods for determination of cell constants and unit cell refinement have been previously reported.³⁶ Each structure was solved by a combination of direct methods and heavy atom using SIR97. All of the non-hydrogen atoms were refined with anisotropic displacement coefficients.

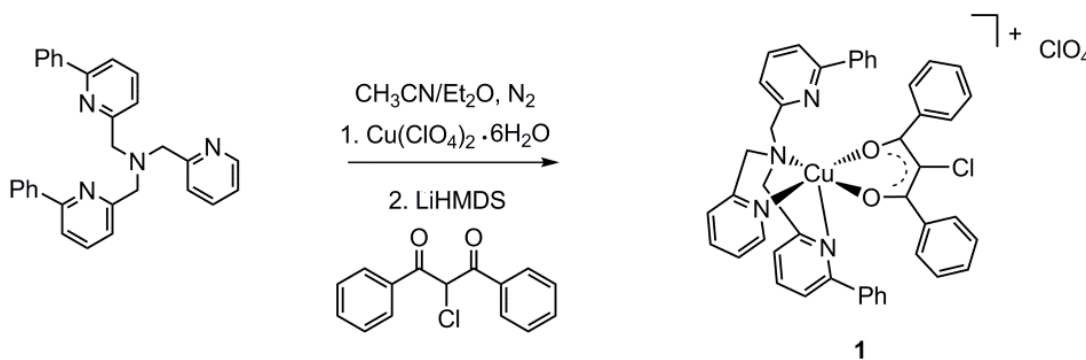
Complex **1** crystallizes in the orthorhombic space group *P bca* while complex **2** crystallizes in the monoclinic space group *P 2₁/a*. All hydrogen atoms were assigned

isotropic displacement coefficients $U(\text{H}) = 1.2(\text{C})$ or $1.5U(\text{C}_{\text{methyl}})$ and their coordinates allowed to ride on their respective carbons using SHELXL97. Complex **2** contains a single molecule of CH_2Cl_2 per formula unit.

Results and Discussion

Synthesis and Characterization: Admixture of a CH_3CN solution containing equimolar amounts of *N,N*-bis((6-phenyl-2-pyridyl)methyl)-*N*-((2-pyridyl)methyl)amine (6- Ph_2TPA) and $\text{Cu}(\text{ClO}_4)_2 \cdot 6\text{H}_2\text{O}$ in CH_3CN to a slurry of 2-chloro-1,3-diphenylpropan-1,3-dione and LiHMDS in Et_2O under a $\text{N}_2(\text{g})$ atmosphere generated a green solution (Scheme 5-5). Nucleophilic bases, such as hydroxides, were avoided in this step due to the potential for substitution at the C-Cl position. After removing the solvent under reduced pressure, the resulting green powder was redissolved in CH_2Cl_2 , filtered through a Celite/glass wool plug and precipitated with hexanes to generate analytically pure $[(6\text{-Ph}_2\text{TPA})\text{Cu}(\text{PhC}(\text{O})\text{CClC}(\text{O})\text{Ph})]\text{ClO}_4$ (**1**) in 88 % yield.

Crystals of **1** suitable for X-ray crystallography were grown by vapour diffusion of Et_2O into a CH_2Cl_2 solution (Tables 5-1 and 5-2). Crystallographic studies showed a five-coordinate copper center in which one of the phenylpyridyl arms of the 6- Ph_2TPA



Scheme 5-5. Synthesis of **1**.

Table 5-1. Summary of X-ray data collection and refinement.

	1	2 · CH₂Cl₂
Formula	C ₄₅ H ₃₆ Cl ₂ CuN ₄ O ₆	C ₃₁ H ₂₈ Cl ₄ CuN ₄ O ₄
M_r	863.22	725.91
Crystal system	Orthorhombic	Monoclinic
Space group	<i>Pbc</i> <i>a</i>	<i>P</i> $2_1/a$
$a/\text{Å}$	12.7335(2)	$a = 13.1354(2) \text{ Å}$
$b/\text{Å}$	19.3738(2)	$b = 15.4508(3) \text{ Å}$
$c/\text{Å}$	31.7858(4)	$c = 15.3363(3) \text{ Å}$
$\alpha/^\circ$	90	90
$\beta/^\circ$	90	90.3769(12)
$\gamma/^\circ$	90	90
$V/\text{Å}^3$	7841.44(18)	3112.47(10)
Z	8	4
$D_c/\text{Mg m}^{-3}$	1.462	1.549
T/K	150(1) K	150(1) K
Color	green	green
Crystal shape	Prism	needle
Crystal size/ mm	0.30 x 0.30 x 0.15	0.30 x 0.15 x 0.05
μ/mm^{-1}	0.750	1.089
$F(000)$	3560	1484
θ range/ $^\circ$	2.46-27.48	2.03-26.38
Completeness to $\theta/ \%$	27.48°/99.9 %	26.38°/99.9 %
Reflections collected	17118	12435
Independent reflections	8993	6371
R_{int}	0.0351	0.0237
Data/restraints/ parameters	8993 / 0 / 550	6371 / 12 / 434
GoF / F^2	1.011	1.017
$R_1, wR_2/ I > 2\sigma(I)$	0.0396, 0.0882	0.0394, 0.0970
$R_1, wR_2/ \text{all data}$	0.0729, 0.1008	0.0631, 0.1098
max./min. transmission	0.8958/0.8063	0.9476/0.7359
$\Delta\rho_{\text{max/min}}/ \text{eÅ}^{-3}$	0.348/-0.582	0.430/ -0.606 e.Å ⁻³
Radiation	Mo K α ($\lambda = 0.71073\text{Å}$)	Mo K α ($\lambda = 0.71073\text{Å}$)
Diffractometer	Nonius KappaCCD	Nonius KappaCCD

Table 5-2. Selected bond distances (Å) and angles (°) for **1** and **2·CH₂Cl₂**

1			
Cu(1)-O(1)	1.9199(14)	O(1)-Cu(1)-O(2)	91.01(6)
Cu(1)-O(2)	1.9245(15)	O(1)-Cu(1)-N(1)	95.46(7)
Cu(1)-N(1)	1.9992(18)	O(2)-Cu(1)-N(1)	155.95(7)
Cu(1)-N(2)	2.0333(17)	O(1)-Cu(1)-N(2)	179.79(7)
Cu(1)-N(3)	2.3394(18)	O(2)-Cu(1)-N(2)	89.07(7)
Cu(1)---N(4)	3.089(2)	N(1)-Cu(1)-N(2)	84.39(7)
Cl(1)-C(38)	1.747(2)	O(1)-Cu(1)-N(3)	102.74(6)
O(1)-C(37)	1.277(3)	O(2)-Cu(1)-N(3)	97.91(6)
O(2)-C(39)	1.277(3)	N(1)-Cu(1)-N(3)	103.17(7)
C(37)-C(38)	1.420(3)	N(2)-Cu(1)-N(3)	77.44(6)
C(38)-C(39)	1.402(3)		
2·CH₂Cl₂			
Cu(1)-N(2)	2.019(2)	N(2)-Cu(1)-N(1)	82.27(9)
Cu(1)-N(1)	2.033(2)	N(2)-Cu(1)-N(3)	78.67(9)
Cu(1)-N(3)	2.103(2)	N(1)-Cu(1)-N(3)	137.32(9)
Cu(1)-Cl(1)	2.1989(7)	N(2)-Cu(1)-Cl(1)	173.98(6)
Cu(1)-N(4)	2.247(2)	N(1)-Cu(1)-Cl(1)	97.71(7)
		N(3)-Cu(1)-Cl(1)	97.54(6)
		N(2)-Cu(1)-N(4)	76.79(8)
		N(1)-Cu(1)-N(4)	104.86(8)
		N(3)-Cu(1)-N(4)	107.35(8)
		Cl(1)-Cu(1)-N(4)	108.94(6)

chelate ligand has a distance of 3.089(2) Å between the nitrogen atom and the metal center (Figure 5-2). The second phenylpyridyl arm, which coordinates directly to the copper via its pyridyl nitrogen, is elongated by ~0.3 Å relative to the other nitrogen donors. Compared to the nickel-containing analogue [(6-Ph₂TPA)Ni(PhC(O)CClC(O)Ph)]ClO₄ (**3**), **1** has contracted M-O, M-N_{amine} and M-N_{Py} bond lengths by an average of 0.05 Å.²⁶ This is attributable to both the higher Lewis acidity of the Cu(II) center relative to Ni(II), as well as to the greater Jahn-Teller distortion of the Cu(II) center that led to dissociation of one of the N_{PhPy} arms. The geometry of the center is intermediate between square-based pyramidal and trigonal bipyramidal (τ value of 0.40).³⁷ Bond distances within the six-membered chelate ring formed by the diketonate binding to the metal center are consistent with a fully-delocalized diketonate (Table 5-2), and the C-Cl bond distance (1.747(2) Å) is in the

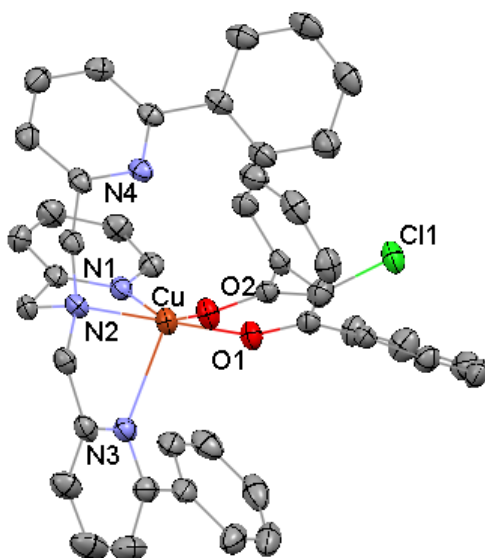


Figure 5-2. Thermal ellipsoid representation of the cationic portion of **1**. Ellipsoids are drawn at 50% probability and hydrogen atoms are omitted for clarity.

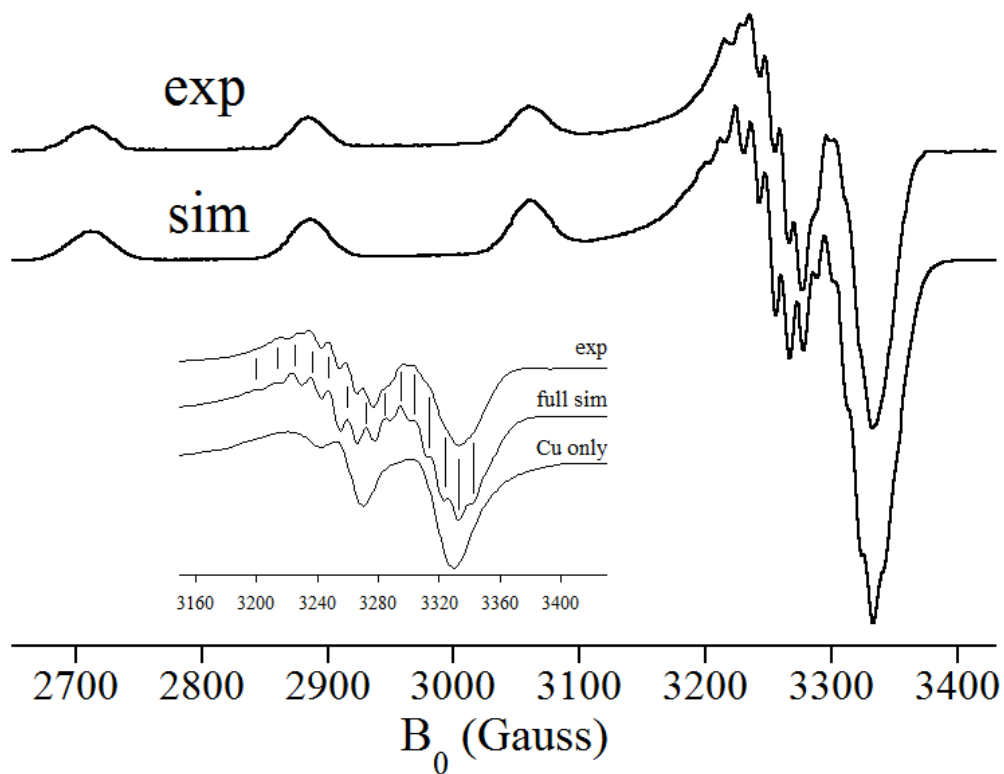


Figure 5-3. X-band EPR spectrum (top) and representative simulation (bottom) of **1** at 20 K. (Inset) Expanded view of the g_{\square} region. The vertical lines are added to facilitate comparison; the lower simulation represents the $^{63,65}\text{Cu}$ contribution to the line shape. For detailed simulation information, see Figure 5-4.

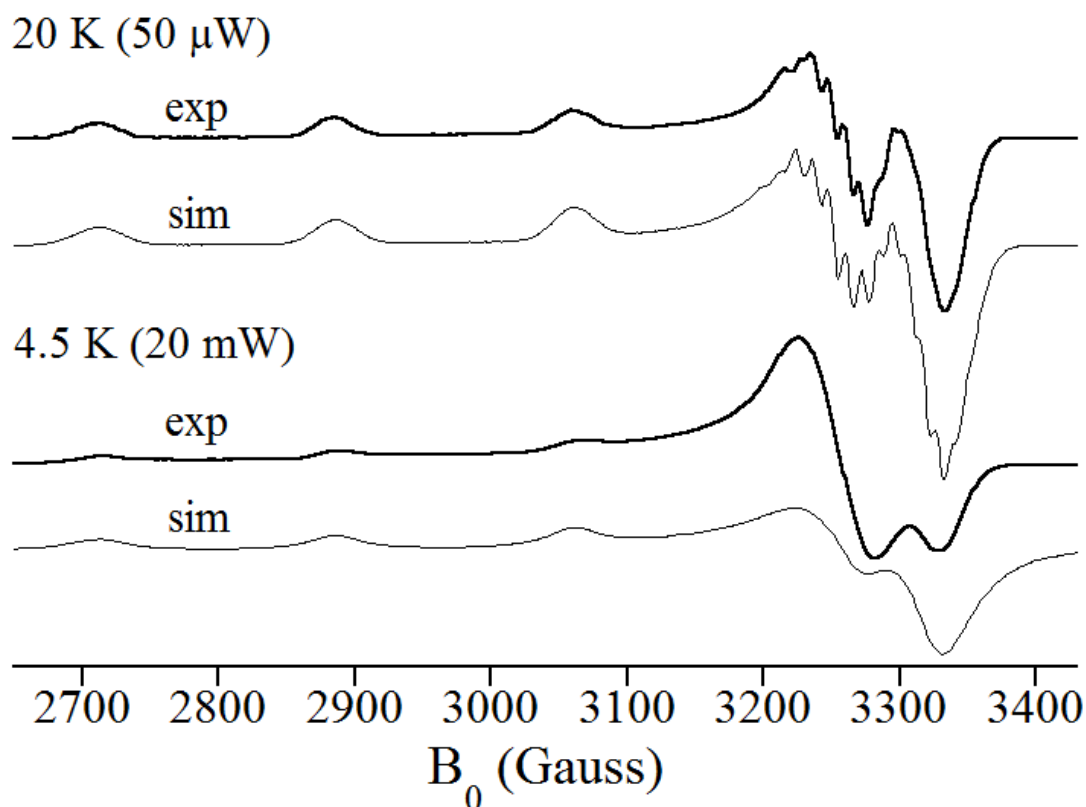


Figure 5-4. X-band EPR of **1** and representative simulations, (top) at elevated temperature and low power, and (bottom) at low temperature and high power. The simulations only differ in the presence (top) or absence (bottom) of three equivalent ^{14}N couplings, and in their line width parameters. In the 20 K simulation, an isotropic EPR line width of 10 MHz was used, with uncorrelated strains in both \mathbf{g} and \mathbf{A} of 2.5 MHz (25 %). In the 4.5 K simulation, the isotropic EPR line width was increased to 50 MHz, with the same uncorrelated strains in \mathbf{g} and \mathbf{A} (2.5 MHz, 5 %). Other parameters: (both) $\mathbf{g} = [2.058, 2.058, 2.260]$; $\mathbf{A}({}^{63,65}\text{Cu}) = [52, 52, 540]$ MHz; (top) $\mathbf{A}({}^{14}\text{N}) = [34, 34, 24]$ MHz. The value of $A_z({}^{14}\text{N})$ derives from poorly resolved hyperfine structure on the lowest field Cu hyperfine line in the 20 K spectrum.

range typically found for other chloro-diketonates (1.739-1.755 Å).³⁸

The low temperature EPR spectrum of **1** (Figure 5-3) is consistent with a five-coordinate Cu(II) ion in solution,³⁹ with axial **g** ($g_{\parallel, \square} = [2.058, 2.260]$) and **A** ($A_{\parallel, \square} = [52, 540]$ MHz). An adequate simulation could only be obtained by inclusion of three equivalent ¹⁴N atoms with largely isotropic hyperfine couplings, $A_{\parallel, \square}({}^{14}\text{N}) = [34, 23]$ MHz. Inclusion of two or four ¹⁴N did not reproduce all of the features near g_{\square} .

Aerobic reactivity: Complex **1** has a prominent absorption feature at 363 nm ($10200 \text{ M}^{-1}\text{cm}^{-1}$) (Figure 5-5). A similar feature was observed in the nickel-containing analogue of **1**, albeit red-shifted to 372 nm, and was assigned as a $\pi\text{-}\pi^*$ transition on the diketonate, with LMCT character on the high energy side of the band.²⁶ Exposure of

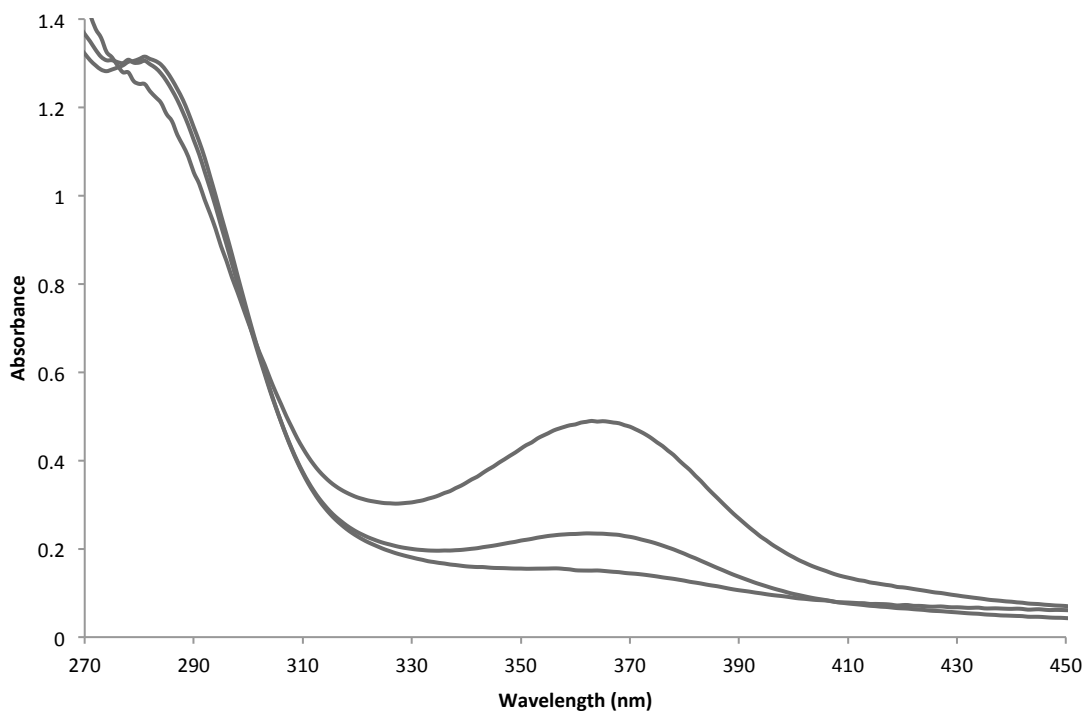


Figure 5-5. Selected UV-vis spectra during the decay of the 363 nm absorption feature of **1** upon exposure to O₂.

CH₃CN solutions of **1** to O₂ in CH₃CN at 25 °C in the absence of light leads to the decay of this feature within 1 hour, consistent with destruction of the diketonate unit. This was a very surprising observation as our previous studies on nickel-containing analogues of **1** required photo-activation for cleavage of the diketonate, while oxidative cleavage of enolates by copper-containing functional models of QDO typically require elevated temperatures (greater than 80 °C) to proceed.^{26, 14b}

Product Identification: Analysis of the crude reaction mixture by HRMS reveals an ion at $m/z = 540.1143$, with exact mass and isotope pattern consistent with the formulation [(6-Ph₂TPA)CuCl]ClO₄ (**2**); this formulation has been confirmed by comparison to the HRMS of an authentic sample of independently synthesized **2**. Removal of solvent followed by recrystallization of a CH₂Cl₂ solution of the product mixture by vapor diffusion of Et₂O yielded crystals suitable for X-ray crystallography (Tables 5-1 and 5-2). Crystallographic studies revealed a five-coordinate copper center (Figure 5-6) in a geometry intermediate between trigonal bipyramidal and square-based

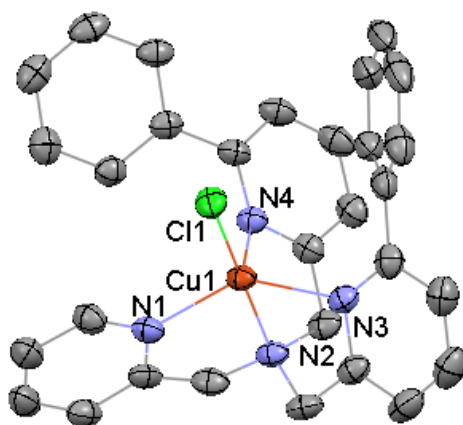


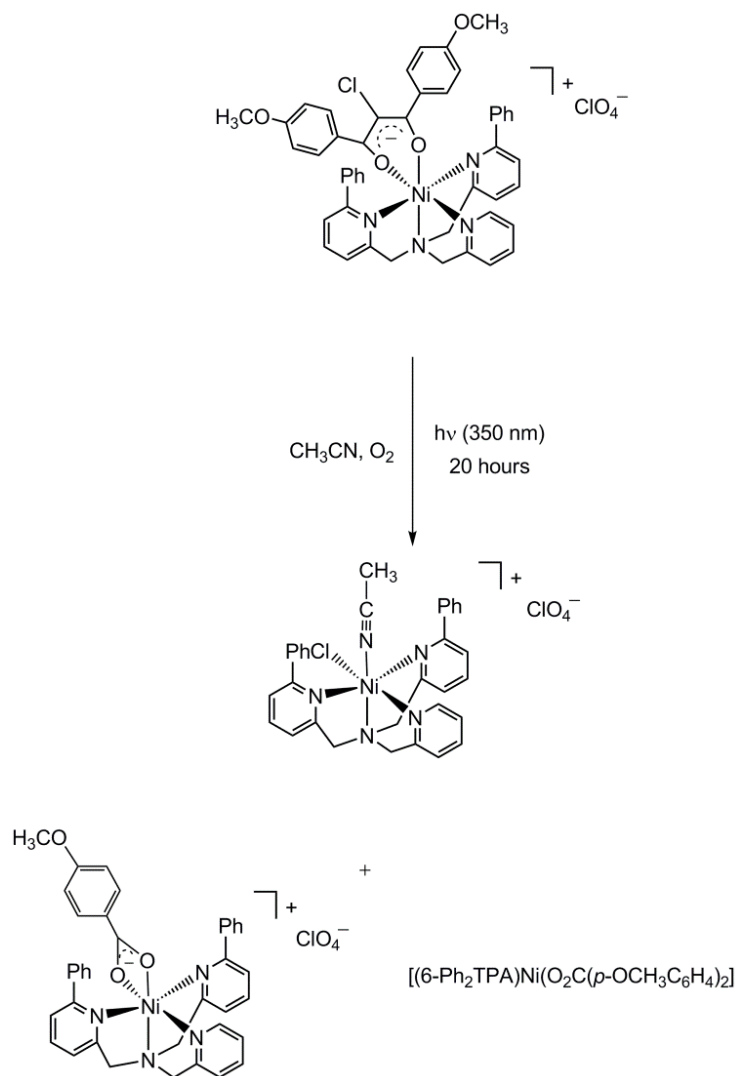
Figure 5-6. Thermal ellipsoid representation of the cationic portion of **2**. Ellipsoids are drawn at 50% probability and hydrogen atoms are omitted for clarity.

pyramidal ($\tau = 0.61$),³⁷ although with more trigonal bipyramidal character than **1**. In this structure, the Cu-N_{PhPy} bond lengths are roughly equivalent and only an average of ~0.2 Å longer than the other Cu-N bonds, in contrast to the structure of **1**. Notably, the Cu-Cl bond length in this structure (2.1989(7) Å) is, to our knowledge, the shortest reported Cu-Cl bond length in a mononuclear copper species with a tris(2-methylpyridyl)amine-based ligand, with the shortest other Cu-Cl bond lengths being 2.206(2) and 2.211(3) Å.⁴⁰

In reactions of chlorodiketonate Ni(II) complexes with O₂, products have included carboxylate species in addition to mono-chloride complexes (Scheme 5-6).²⁶

Carboxylates are the oxidative cleavage products of the diketonate substrate. To determine whether **2** was the sole Cu(II)-containing product, or if additional carboxylate species may be present, EPR was used to analyze the crude product mixture from the reaction of **1** with O₂. Upon exposure of **1** to O₂, there is a significant change in the EPR spectrum. While the Cu(II) ion g-tensor is largely unaffected, suggesting that it remains penta-coordinate, the ^{63,65}Cu hyperfine coupling becomes significantly more isotropic, $A(^{63,65}\text{Cu}) = [130, 375]$ MHz. Simulations showed the only way to reproduce the product complex spectrum is to include a second, strongly coupled $I = 3/2$ nucleus, consistent with formation of a chloride complex. This is demonstrated convincingly, on comparison of the product complex EPR spectrum to that of the synthetically prepared complex **2** (Figure 5-7). Thus, **2** is the only Cu(II)-containing species in the reaction of **1** (Scheme 5-7).

To determine the fate of the diketonate substrate, the product mixture was passed through a short silica column, eluting with ethyl acetate. The yield of the organics by this process was greater than 80%, and analysis by GCMS and ¹H NMR revealed the



Scheme 5-6. Products of the dioxygenolytic photoreactivity of a nickel chlorodiketonate include both chloride and carboxylate species.

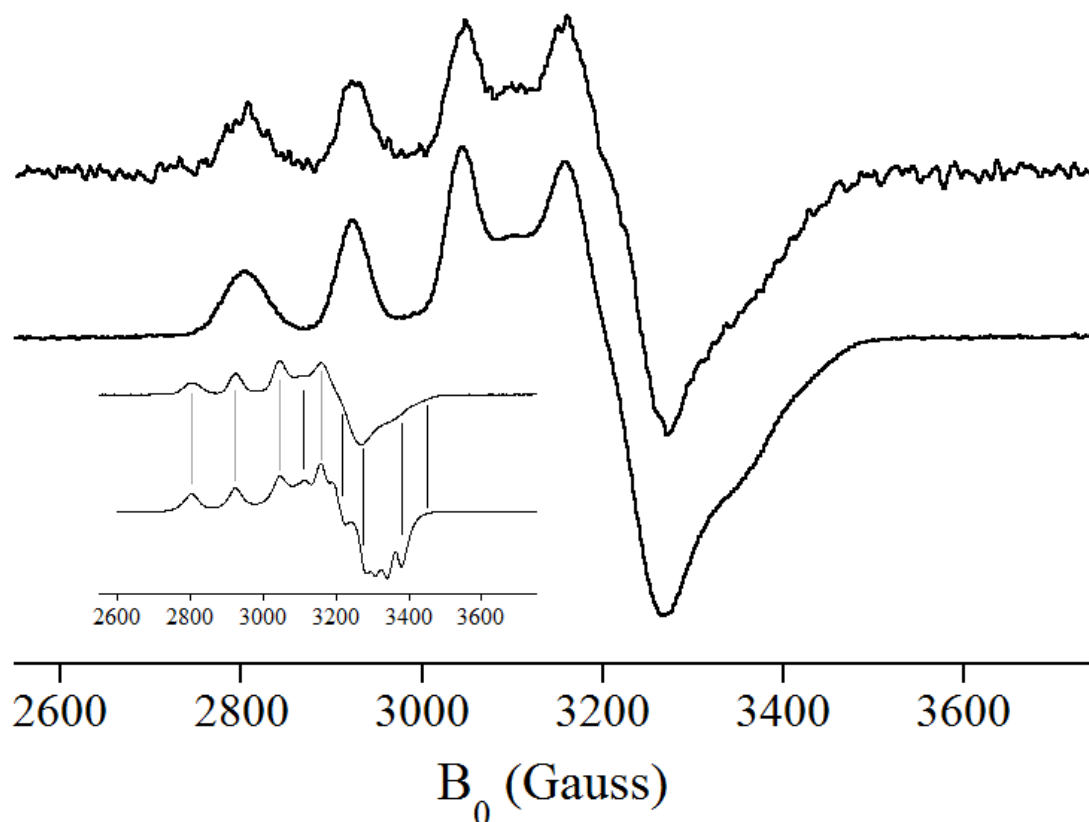


Figure 5-7. X-band EPR of **2** and the product mixture from the reaction of **1** with O₂. Top: **2** at 15 K (50 μW microwave power). Bottom: The product mixture from the reaction of **1** with O₂ at 10 K (200 μW). The patterns are adequately simulated (inset) with a pair of $I = 3/2$ nuclei (^{35,37}Cl and ^{63,65}Cu) that have similar A values at g_□, as expected in the Cl complex. Simulation parameters: $\mathbf{g} = [2.06, 2.06, 2.24]$; $\mathbf{A}({}^{63,65}\text{Cu}) = [130, 130, 375]$ MHz; $\mathbf{A}({}^{35,37}\text{Cl}) = [100, 100, 10]$ MHz; isotropic EPR line width of 50 MHz, uncorrelated strains in both \mathbf{g} and \mathbf{A} of 2.5 MHz (25 %). These parameters were adequate to match peak positions and the overall breadth of the pattern, but no combination of line shape parameters were found that would then match the final line shape.

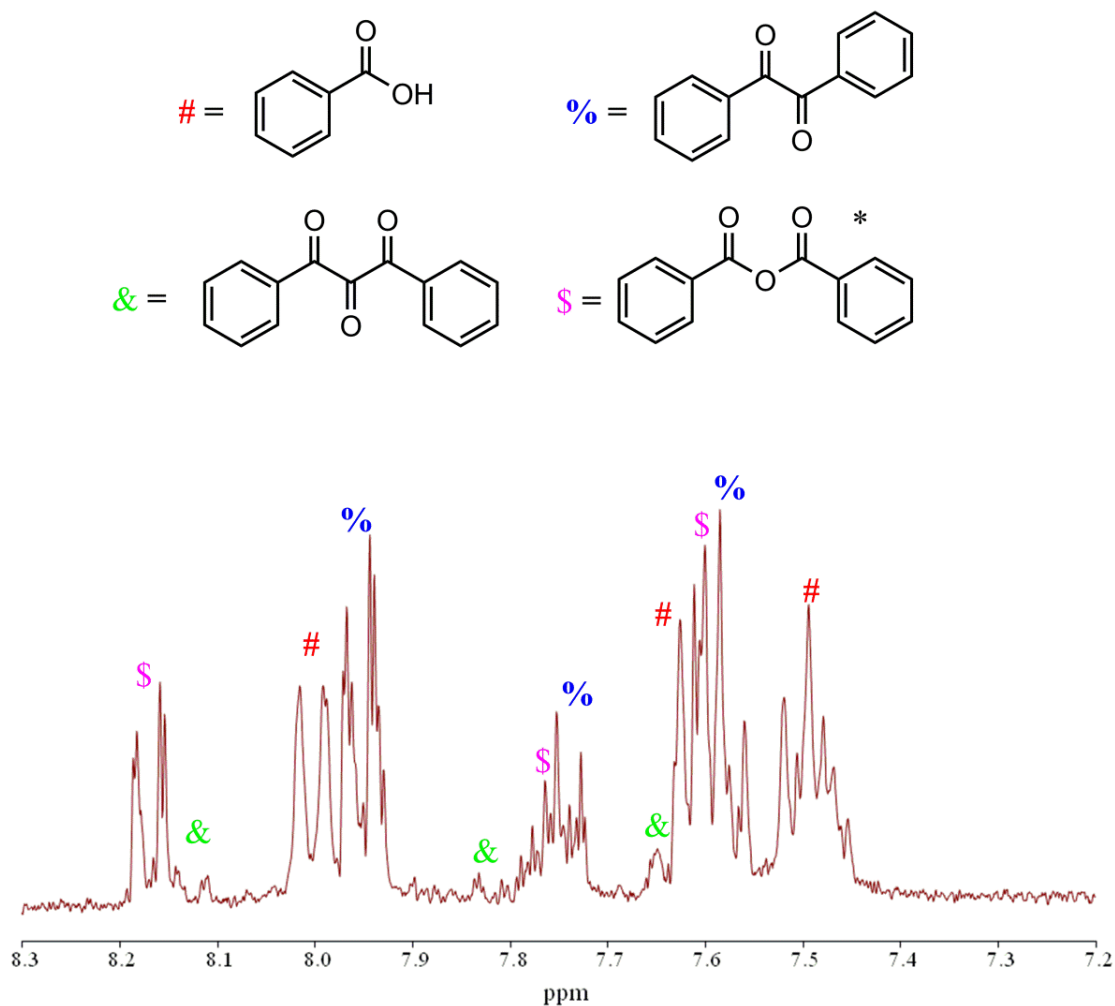
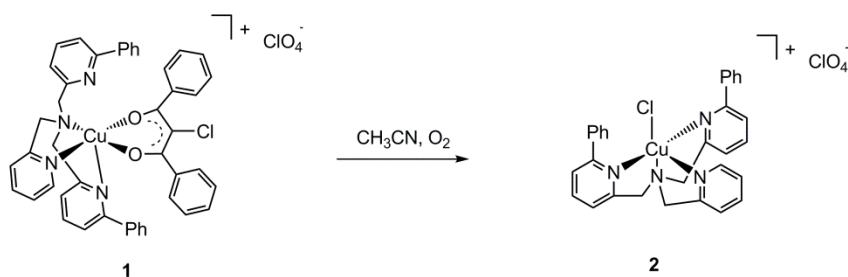


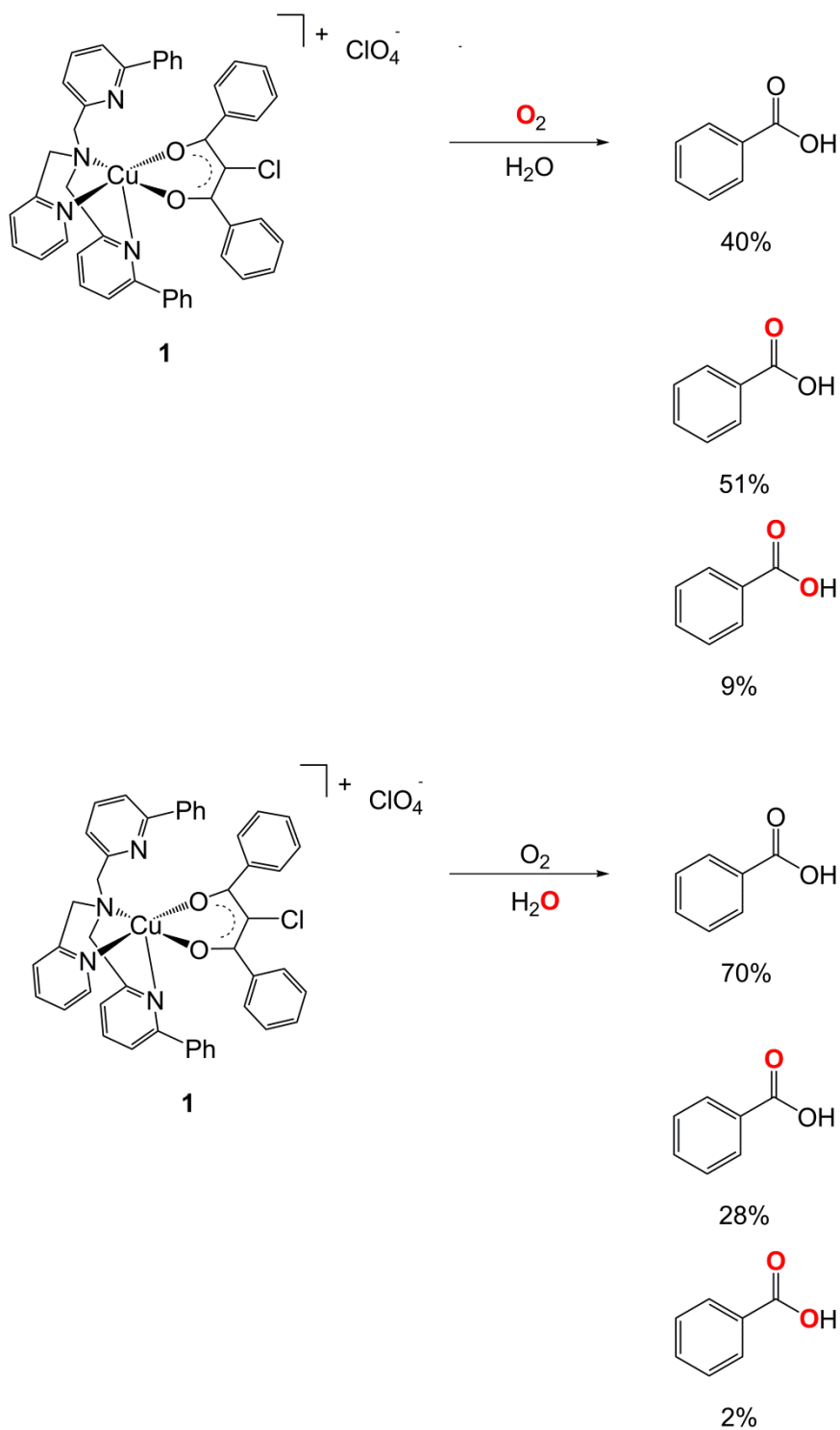
Figure 5-8. Organic species formed in the reaction of **1** with O_2 in CH_3CN (top) and identification of their corresponding aromatic signals in the ^1H NMR of the organic products (bottom). When the reaction is repeated in the presence of 1% H_2O , benzoic anhydride is no longer detected and a corresponding increase in the intensity of the benzoic acid peaks are observed.



Scheme 5-7. Reaction of **1** with O_2 in CH_3CN to form the chloride complex **2**.

presence of four species (Figure 5-8). The production of the carboxylate species benzoic acid and benzoic anhydride are indicative of oxidative cleavage of the diketonate unit in the reaction of **1** with O_2 . We note that benzoic anhydride is produced in a water-dependent manner, and may be completely removed from the product mixture by the addition of 1% water to the reaction. $^{18}O_2$ labelling studies in the presence of 1% $H_2^{16}O$ show incorporation of at least one oxygen atom into 60% of the benzoic acid. The corresponding $^{16}O_2/H_2^{18}O$ experiment shows incorporation into 30% of the benzoic acid (Scheme 5-8). The hydrolysis of benzoic anhydride presumably provides a route for incorporation of oxygen atoms from water. Using a separate extraction technique, adding $NH_{3(aq)}$ to the crude reaction products and extracting with CH_2Cl_2 , we have also determined that the supporting chelate ligand remains intact during the course of the reaction by 1H NMR (Figure 5-9).

Benzoic acid, benzil and diphenylpropantrione have previously been observed as products in model systems of nickel- and iron-containing acireductone dioxygenases, and were indicative of a reaction pathway in which an alpha-substituted diketonate reacts with dioxygen via a hydroperoxide-triketone intermediate (Scheme 5-9).^{41, 42} Two-electron oxidation of the α -chloro diketonate by dioxygen could lead to the formation of the intermediate **A** shown in Scheme 5-10. Subsequent hydrolysis of **A** would generate



Scheme 5-8. ^{18}O incorporation into benzoic acid during the reaction of **1** with O_2 in CH_3CN/H_2O . Isotope incorporation levels were determined from the relative intensities of the $[M]^+$, $[M+2]^+$ and $[M+4]^+$ ions in the GCMS spectrum.

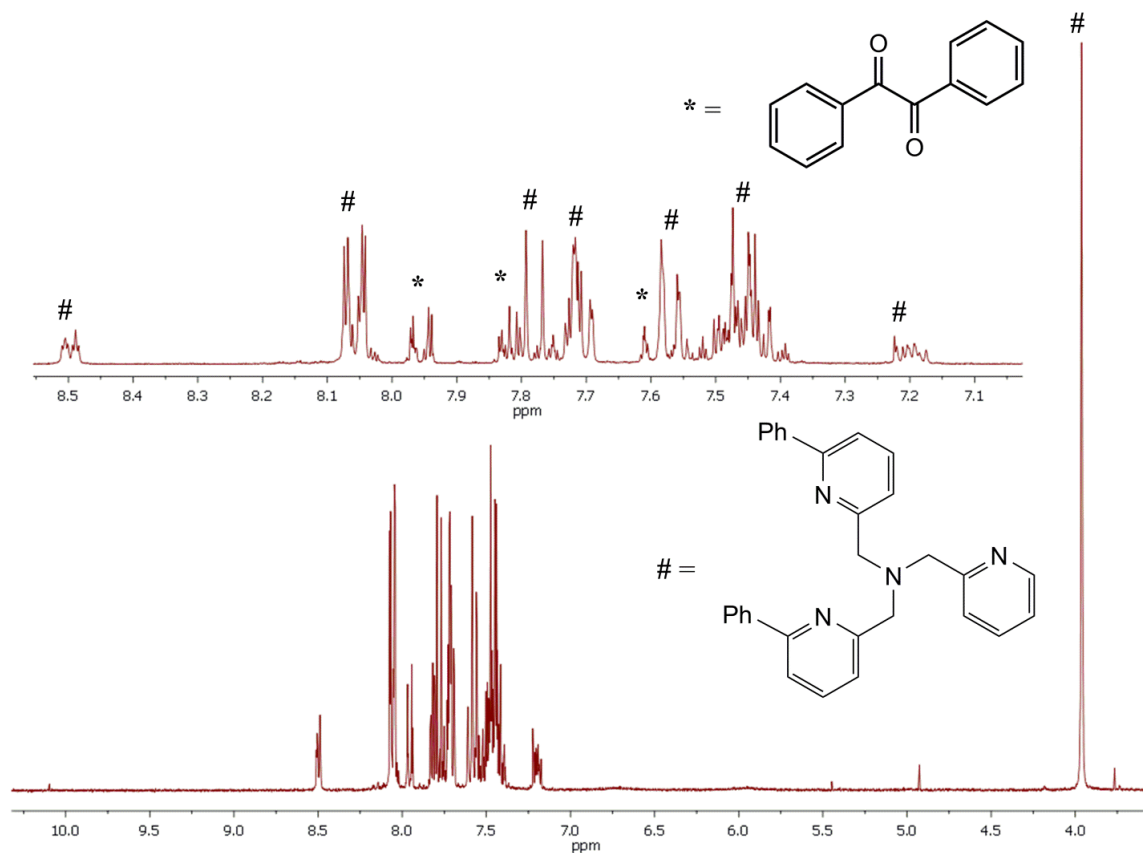
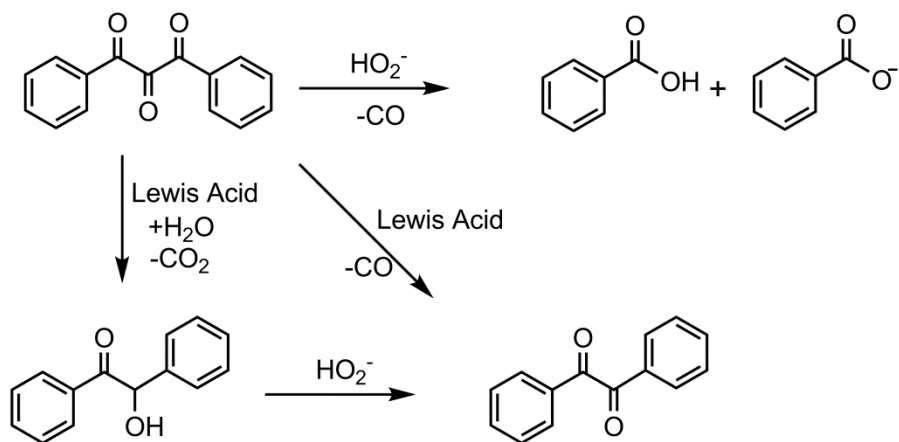
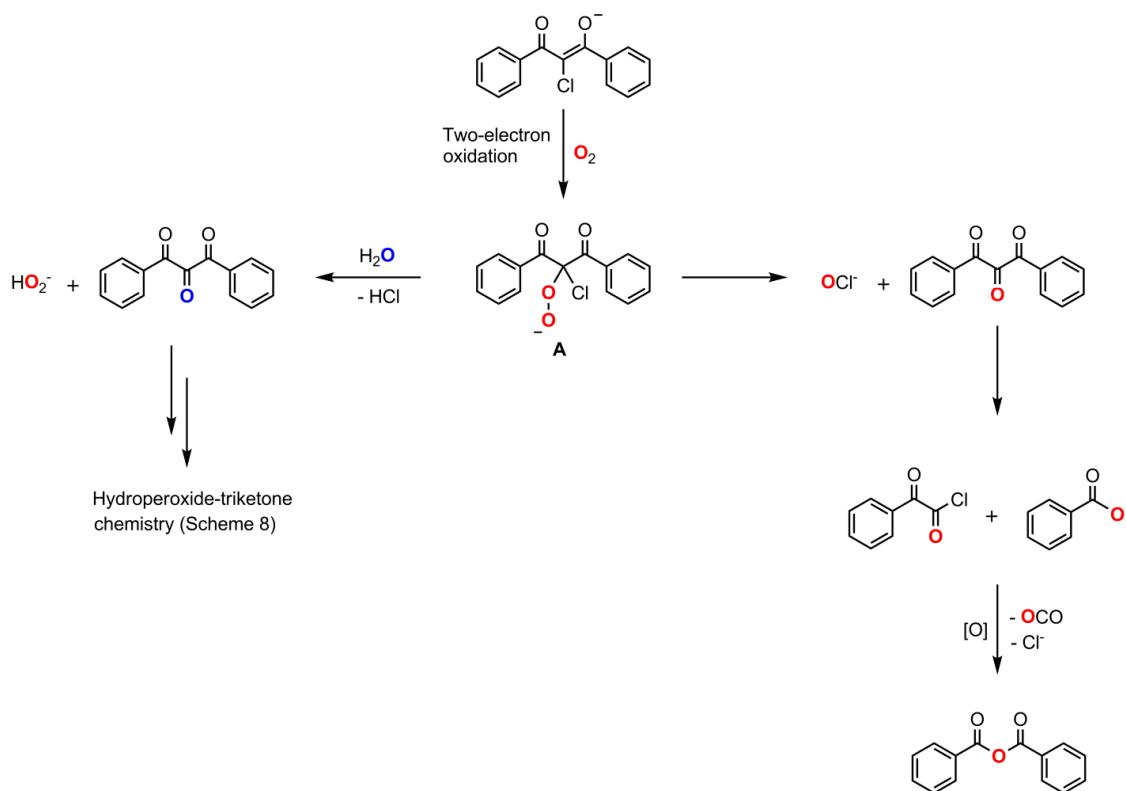


Figure 5-9. ^1H NMR spectrum (CD_3CN) of the recovered ligand.



Scheme 5-9. Reactions of diphenylpropantrione in the presence of hydroperoxide and a Lewis acid.



Scheme 5-10. Proposed reaction pathways for O_2 with the diketonate anion of α -chloro-1,3-diphenylpropan-1,3-dione.

the proposed hydroperoxide-triketone pair and a chloride ion. Analysis of the reaction headspace gas showed the production of both CO_2 and CO gases, however while 0.80 equivalents of CO_2 were produced, less than 0.05 equivalents of CO was detected. This suggests that a hydroperoxide-triketone pathway, which would produce predominantly CO_2 gas, is likely a minor pathway.^{41a}

Analysis of the products generated when **1** was allowed to react with $^{18}O_2$ in dry CH_3CN showed quantitative incorporation of one equivalent of ^{18}O into diphenylpropantrione. This suggested that rather than hydrolysis of intermediate **A** to form diphenylpropantrione and hydroperoxide, it instead extrudes hypochlorite (Scheme 5-10). To test the feasibility of this proposal, we reacted diphenylpropantrione with one

equivalent of NaOCl in the presence of one equivalent of $\text{Cu}(\text{ClO}_4)_2 \cdot 6\text{H}_2\text{O}$ and 6- Ph_2TPA in CH_3CN . Analysis of the organic products showed that the products were benzoic acid, benzoic anhydride, benzil and a minor amount of unreacted diphenylpropantrione. Additionally, analysis of the headspace gas showed the production of 0.79 equivalents of CO_2 and only a trace amount of CO . These are the same products as in the reaction of **1** with O_2 , validating the viability of this proposed hypochlorite pathway.

Kinetic Studies. In order to determine the role of the copper center in the oxidation reaction of **1**, we performed some kinetic studies. In the presence of excess O_2 , after a short induction period, this reaction proceeds with a first-order dependence on **1** (Figure 5-10). The first-order dependence on **1** suggests a mononuclear copper species is involved in the rate-determining step, precluding the involvement of a dinuclear copper species bridged by a reactive oxygen species (i.e. a structure similar to one of the dinuclear structures shown in Figure 5-1).

Mechanistic Studies. The induction period in the oxidation reaction is an interesting phenomenon, and implies the reaction proceeds via a slow initial step to generate some catalytic species, the presence of which greatly accelerates the rate of the reaction of **1** with O_2 . There are two related possibilities for the catalytic species. In the first possibility (termed the “pre-catalyst pathway”), the catalyst is a reaction intermediate that is originally generated by an initiation step, and then during the decay of this intermediate to products, it regenerates another equivalent of this catalyst via a propagation pathway. The second possibility for the identity of the catalyst (termed the “autocatalytic pathway”) would be that one of the reaction products may act as a catalyst for the oxidation reaction.⁴³

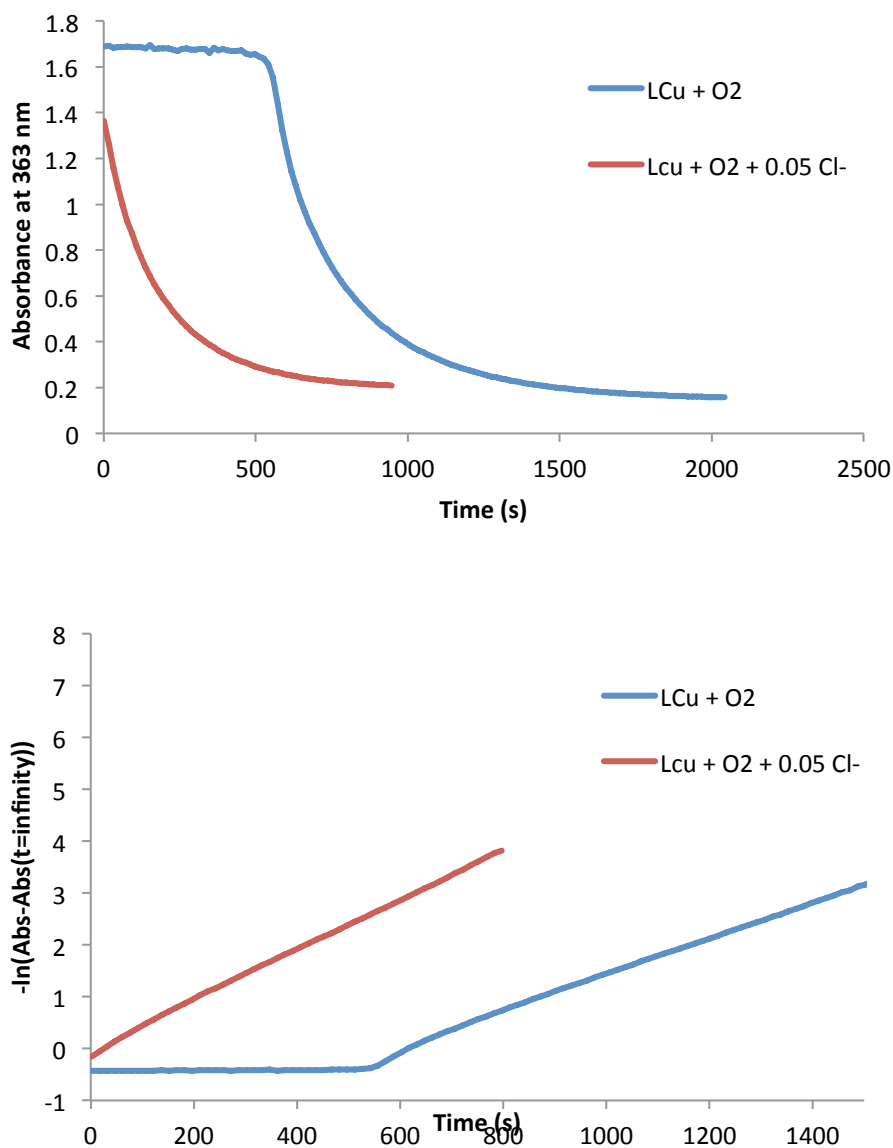
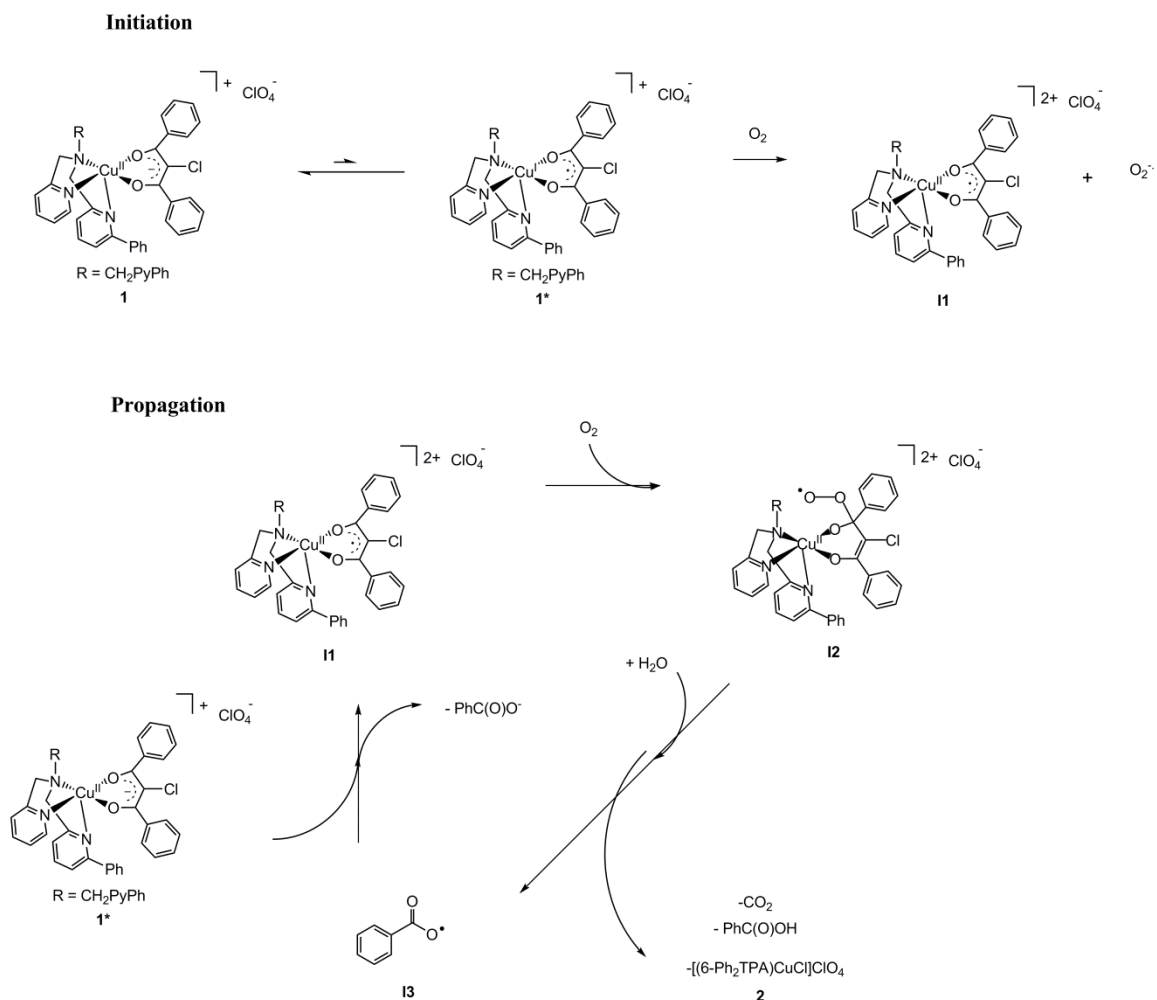


Figure 5-10. Time trace of the decay of **1** in the presence of O₂ (blue line), or in the presence of O₂ and Cl⁻ (red line) (top). A natural log plot shows that after the induction period, the reaction of **1** with O₂ is first order in **1** in either the presence of absence of Cl⁻ (bottom).



Scheme 5-11. A proposed radical propagation pathway for the reaction of **1** with O_2 .

One possibility for a pre-catalyst pathway that we have considered is a radical-initiated oxidative propagation pathway. We have outlined one possible reaction pathway in Scheme 5-11. In the first step of this pathway, we propose a very endergonic equilibrium between **1** and a Cu(I)-diketonyl radical pair. Addition of O_2 to this pair could oxidize the Cu(I) center to Cu(II), forming the intermediate **II** with concomitant loss of O_2^- . After this initiation step, **II** may react with a second equivalent of O_2 to form a diketonyl-superoxo species (**I2**). Decay of this species would lead to the formation of the observed copper-containing product (**2**), as well as an organic radical species. Decay

of the organic radical, coupled to oxidation of another molecule of **1**, leads to the production of observed carboxylate products. The oxidation of **1** to form **II** completes the propagation cycle. We note that a similar pathway has previously been computationally studied in the reactions of α -hydroxy diketonates with oxygen, albeit in the absence of a metal center.⁴⁴

To test the possibility of a radical-initiated propagation pathway, we attempted to use an exogenous radical initiator to generate radical species and eliminate the induction period. However, addition of AIBN to generate radicals by photolysis did not eliminate the induction period. We also attempted to trap radicals using 2,4-di-tertbutylphenol, however addition of this to the reaction greatly slowed the rate of reaction (less than 5% complete after 1 hour, as judged by UV-vis). We do not attribute the slowing of the reaction by 2,4-di-tertbutylphenol to its ability to act as a radical trap, as no coupling products were identified by ¹H NMR. In a separate experiment, we found that MeOH, which would not be expected to act as a radical trap, also slowed the rate of reaction, suggesting its coordinating or hydrogen-bonding properties were responsible for the slowing of reaction rate. Dihydroanthracene is an alternative radical trap due to its weak C-H bonds, which can be oxidized by radical species that abstract a hydrogen atom.²⁶ Addition of dihydroanthracene to the reaction did lead to its oxidation to produce anthracene (Figure 5-11), which suggests that a species capable of oxidizing weak C-H bonds, such as a putative O₂⁻ intermediate may be generated in the reaction.

We have also considered the feasibility of an auto-catalytic (product-catalyzed) reaction pathway. The crude product mixture from a reaction of **1** with O₂ that had reached completion was generated. A solution of **1** in MeOH was prepared at UV-vis

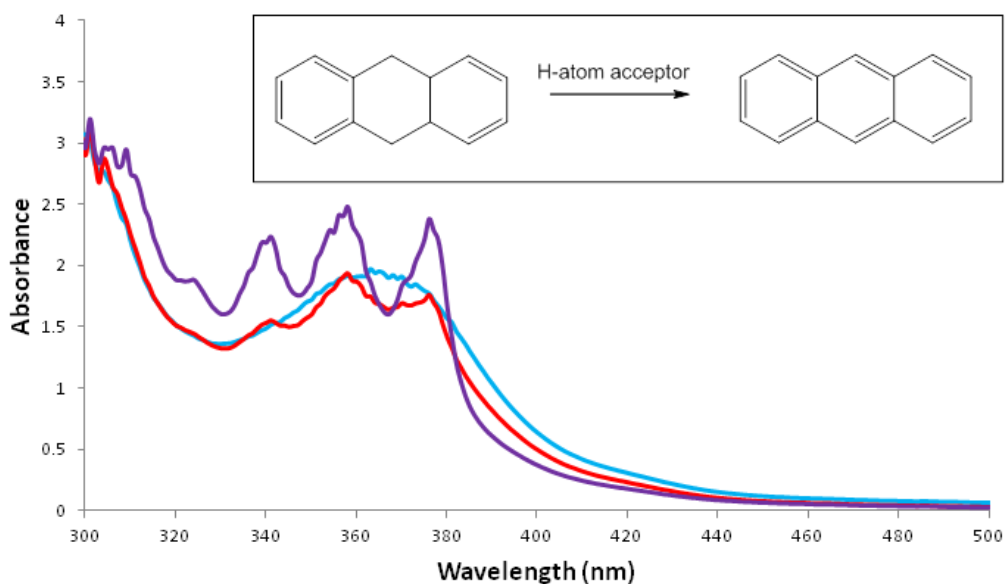
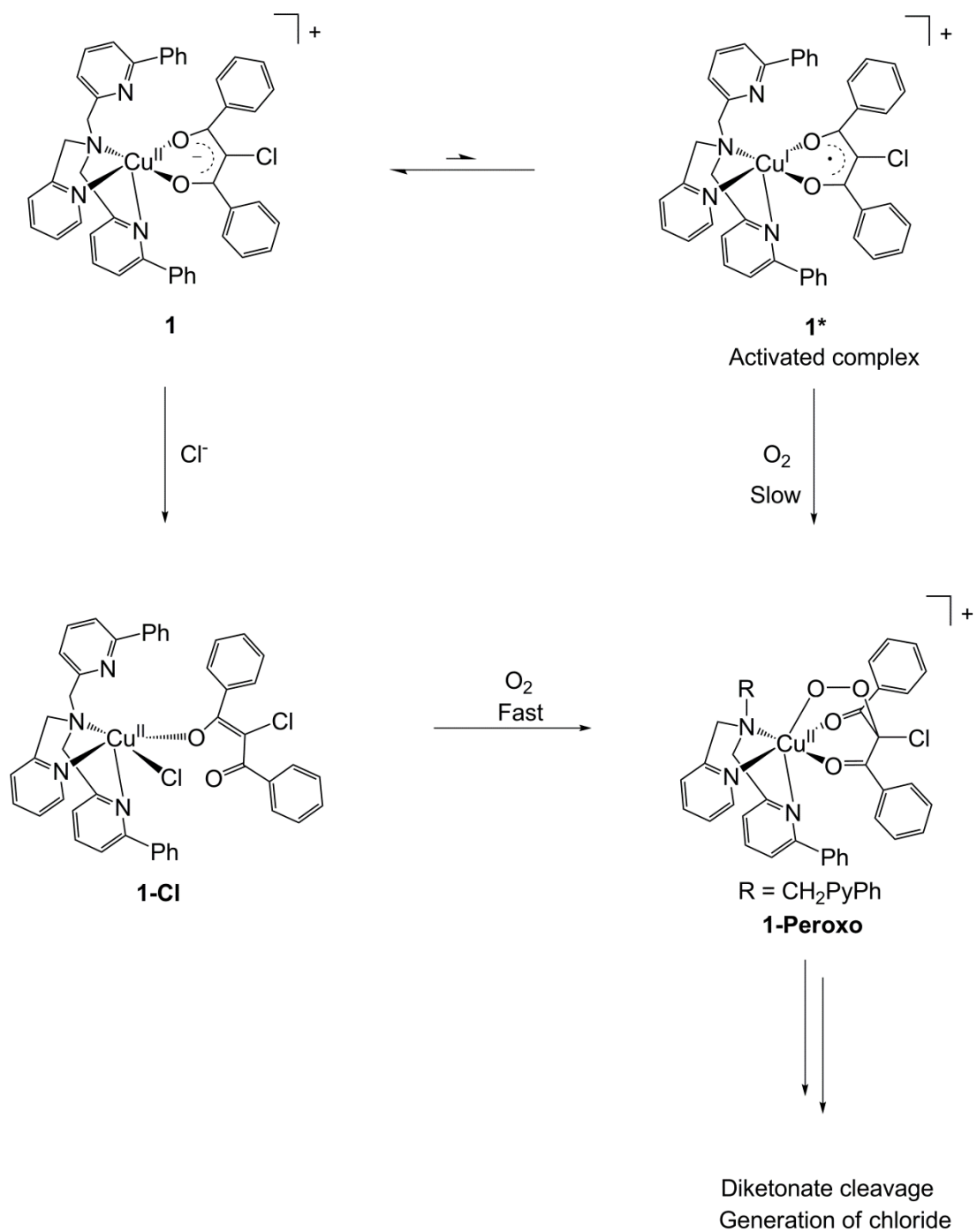


Figure 5-11. UV-vis spectra showing the appearance of characteristic peaks associated with anthracene during the loss of the 363 nm feature of **1** when a solution of **1** is exposed to O₂ in the presence of dihydroanthracene. Inset: the oxidation of dihydroanthracene in the presence of a H-atom acceptor to generate anthracene.

concentrations and combined with the crude product mixture. The decay of the diketone band of **1** upon addition of O₂ was then monitored by UV-vis spectroscopy, and no induction period was observed. This result strongly suggests that one of the products in the reaction has a catalytic role, and thus is responsible for the induction period. Addition of 0.05 equivalents tetramethylammonium chloride results in a total loss of the induction period (although a short induction period may have been present, albeit not observed, during the mixing time), and the reaction immediately exhibits a decay that is first-order in **1** (Figure 5-10). We therefore have assigned the induction period to the time required to build up a catalytic amount of chloride ion *in situ*. A possible reaction pathway is shown in Scheme 5-12, wherein an endergonic Cu(II)/Cu(I) equilibrium may be



Scheme 5-12. A possible reaction pathway for the auto-catalytic reaction of **1** with O_2 .

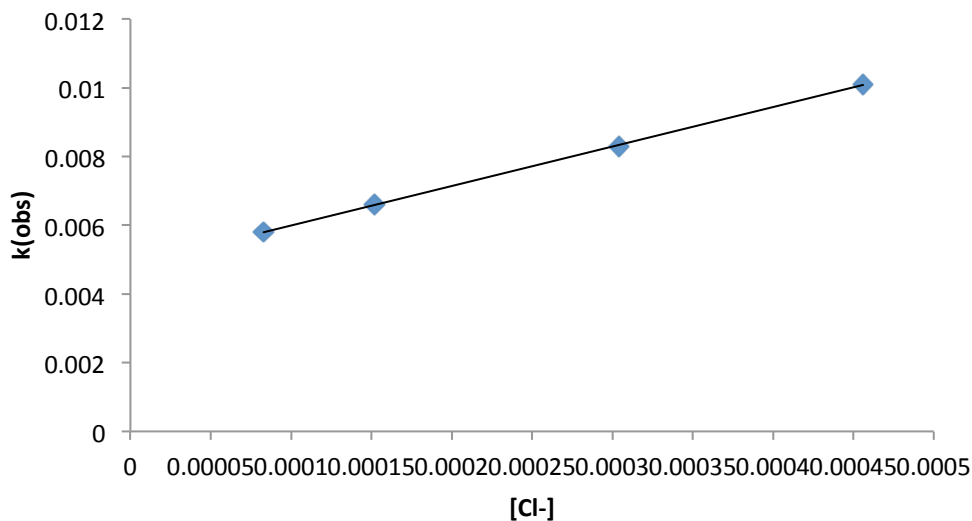
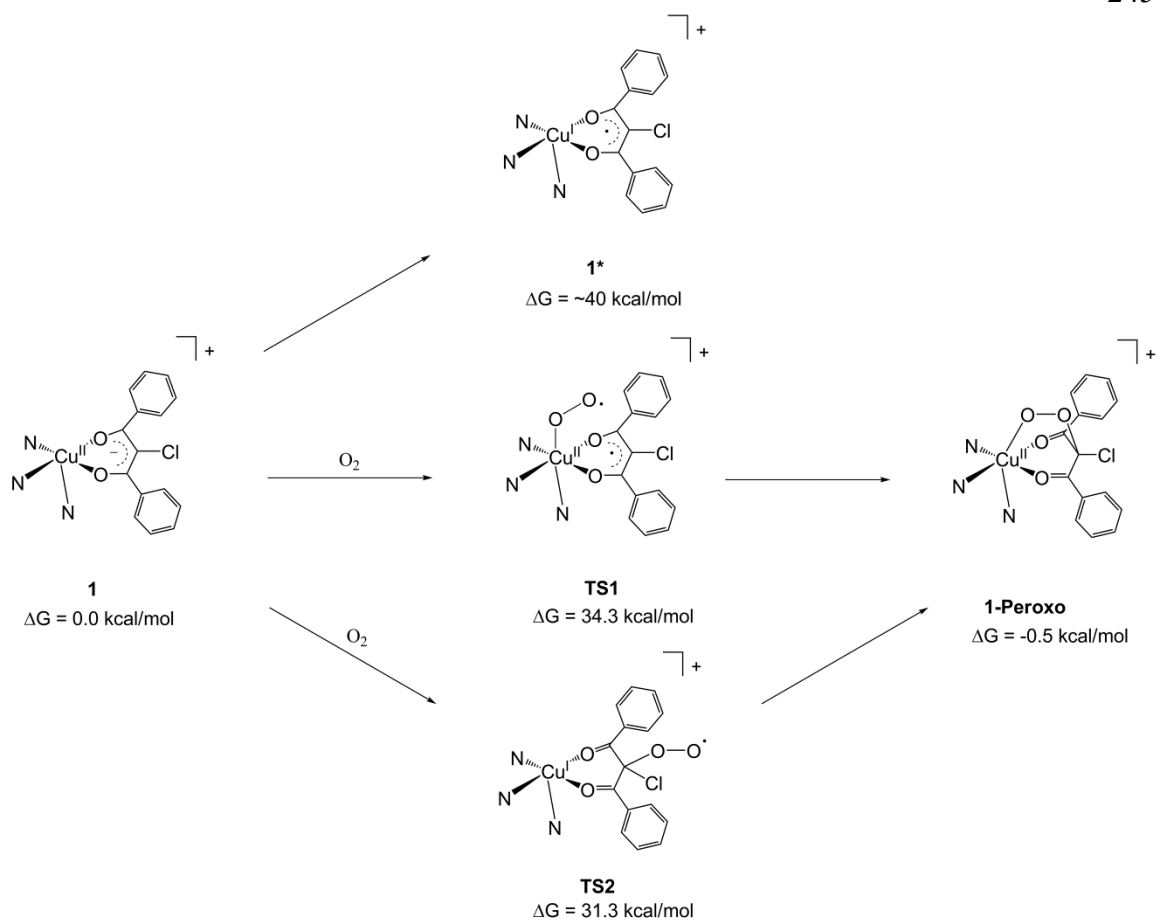


Figure 5-12. Linear dependence of k_{obs} on the concentration of added Cl^- salt.

intercepted with O_2 in a slow reaction to generate a catalytic amount of chloride. The catalytic amount of chloride could then generate an activated form of the complex, allowing the reaction to proceed rapidly. To test this, we have modified the concentration of chloride and found a linear dependence of the k_{obs} on $[\text{Cl}^-]$ (Figure 5-12).

Computational Studies. We have also undertaken computational studies of the reaction of **1** with O_2 (Scheme 5-13).⁴⁵ Consistent with the proposal outlined in Scheme 5-12, we have found that the reaction of **1** to form **1-Peroxo** is exergonic by -0.5 kcal/mol. Preliminary attempts to determine the role of copper show that the excitation of an electron from the Cu(II)-diketonate species (**1**) to form a Cu(I)-diketonyl species (**1***) is highly endergonic (by ~40 kcal/mol), suggesting that this species may not directly form. Rather, in attempts to locate transition states between **1** and **1-Peroxo**, we have found that one-electron oxidation of the diketonate by O_2 to form a Cu(II)-superoxo transition state (**TS1**), or two-electron oxidation of the diketonate by Cu(II) and O_2 to form **TS2**, provide reaction pathways with more reasonable free energies of 34.3 and 31.3



Scheme 5-13. Preliminary computational results for the reaction of **1** with O_2 to form **1-Peroxo**.

kcal/mol respectively. Thus the role of the Cu(II) effectively appears to be to act as a conduit for electrons from the diketonate to O₂ without ever forming a formally reduced state on the copper center. The role of the chloride ion in accelerating the rate is the subject of ongoing computational, as well as mechanistic, investigations.

Evaluation of Mechanistic Implications. The reaction of **1** with O₂ exhibits an induction period that implies that the reaction proceeds by a complicated mechanism. The induction period shows that the reaction proceeds by a slow initial step to generate a catalytic species that then enables the reaction to proceed much more rapidly. To explain this induction period, we have considered a radical-based pre-catalyst pathway (Scheme 5-11), which seems unlikely due to our inability to remove the induction period by the introduction of exogenous radical generators. We have also considered an auto-catalytic pathway, and found this pathway to be viable due to the ability of chloride ions to remove the induction period and accelerate the rate of reaction. A possible route for the auto-catalytic pathway is outlined in Scheme 5-12, and involves an initial simple Cu(II)-diketonate/Cu(I)-diketonyl radical equilibrium that may be intercepted by O₂ to form an organo-peroxo species (**1-Peroxo**) in a slow step, similar to QDO (Scheme 5-3).⁴⁶ However, whether a Cu(I) species ever actually forms in the reaction of **1** has been brought into doubt by our computational data. The diketonate-based fragment of **1-Peroxo** is similar to intermediate **A** in Scheme 5-10, so subsequent decay of this species would yield an equivalent of chloride. Additionally, formation of **1-Peroxo** has been found computationally to be viable (Scheme 5-13). Once a small amount of complex has reacted by this pathway, the chloride generated allows a new rapid reaction to proceed. This role of chloride was confirmed by observing a linear dependence of the rate on

chloride concentration. We note that the sigmoidal (albeit asymmetric) reaction profile is generally consistent with an auto-catalytic reaction pathway.⁴⁷

The exact role the chloride ion plays to accelerate the reaction rate so dramatically remains unclear. By analogy with the role of carboxylates in QDO, we have proposed the intermediate **1-Cl**, although it is by no means the only possible role of chloride. In **1-Cl** the chloride competes with the diketonate for access to the Cu center, favouring a monodentate coordination of the diketonate ligand. In computational studies of QDO enzyme-substrate adducts, it was found that bidentate binding of the substrate resulted in an equilibrium with the radical tautomer via the enolate π system, greatly stabilizing the bound flavonolate and preventing its reaction with O₂.⁴⁸ However, in the monodentate binding mode, the substrate exhibited no such stabilization, making it more reactive.

It is also worth noting that LCu(Fla)₂ complexes have been found to be more reactive with O₂ than the corresponding [LCu(Fla)]⁺ complexes, suggesting an alternative role for Cl⁻ may involve modulating the electron density on the Cu center itself.⁴⁹ A third possible role for Cl⁻ may be to aid in the generation of a Cu(I) center for reaction with O₂ via homolysis of the Cu-Cl bond.

Conclusions

We have synthesized and fully characterized the mononuclear α -chloro diketonate complex **1**, which has a five-coordinate geometry. Complex **1** was found to be inherently reactive with O₂ at room temperature in the absence of photoirradiation, a striking contrast to previous reported reactivity of nickel complexes of α -chloro diketonates. Analysis of the organic products confirmed that oxidative cleavage of the diketonate to form carboxylates had taken place. Typically, Cu(I) rather than Cu(II) is used to activate

O₂ to react with organic substrates, and so it was very surprising to find this facile thermal reactivity with a Cu(II) center. To our knowledge, this is the only example of room temperature and pressure dioxygenase-type thermal cleavage of aliphatic carbon-carbon bonds in a well-defined mononuclear Cu(II) complex. Other well-defined Cu(II) complexes that exhibit dioxygenase-type aliphatic carbon-carbon bond cleavage (most commonly functional model systems of QDO) require harsh reaction conditions (greater than 80 °C and often in DMF), or photochemical activation.^{14b, 27}

The potential of this Cu(II)-based activation of C-C bonds towards reaction with O₂ has not yet been extensively explored. We envision that this chemistry may well be expandable to other supporting ligand environments, as well as a potentially wide range of substrates. With this in mind, our well-defined coordination environment provides an excellent template for the continuation of these investigations. Further investigation of the role of the chloride ion, both by experimental and computational studies, will be of paramount importance in continuing this work.

References

- [1] (a) Gettys, N. S. *J. Chem. Ed.* **1998**, *75*, 665-668. (b) National Research Council (US) Chemical Sciences Roundtable. *Bioinspired Chemistry for Energy: A Workshop Summary to the Chemical Sciences Roundtable*. Washington (DC): National Academies Press (US); 2008. (c) National Research Council (US). *Health and Medicine: Challenges for the Chemical Sciences in the 21st Century*. Washington (DC): National Academies Press (US); 2004.

- [2] (a) Allpress, C. J.; Berreau, L. M. *Coord. Chem. Rev.* **2013**, *257*, 3005-3029. (b) Crabtree, R. H. *Nature*, **2000**, *408*, 415–416. (c) Jun, C.-H. *Chem. Soc. Rev.*, **2004**, *33*, 610–618.
- [3] Anastas, P. T.; Warner, J. C. *Green Chemistry: Theory and Practice*; Oxford University Press, Oxford, England, 1998.
- [4] Constable, D. J. C.; Dunn, P. J.; Hayler, J. D.; Humphrey, G. R.; Leazer, J. L., Jr.; Linderman, R. J.; Lorenz, K.; Manley, J.; Pearlman, B. A.; Wells, A.; Zaks, A.; Zhang, T. Y. *Green Chem.* **2007**, *9*, 411.
- [5] Allen, S. E.; Walvoord, R. R.; Padilla-Salinas, R.; Kozlowski, M. C. *Chem. Rev.* **2013**, *113*, 6234-6458.
- [6] Karlin, K.D.; Itoh, S. Eds. *Copper-Oxygen Chemistry*; John Wiley & Sons Inc., Hoboken, NJ, 2011.
- [7] Sánchez-Ferrer, A.; Rodríguez-López, J. N.; García-Cánovas, F.; García-Carmona, F. *Biochim. Biophys. Acta.* **1995**, *1247*, 1-11.
- [8] (a) Hakemian, A. S.; Rosenzweig, A. C. *Ann. Rev. Biochem.* **2007**, *76*, 223-241. (b) Balasubramanian, R.; Smith, S. M.; Rawat, S.; Yatsunyk, L. A.; Stemmler, T. L.; Rosenzweig, A. C. *Nature*, **2010**, *465*, 115-119.
- [9] Brzezinski, P.; Ojemyr, L. N.; Adelroth, P. *Biochim. Biophys. Acta.* **2013**, *1827*, 843-847.
- [10] Whittaker, J. W. *Adv. Protein Chem.* **2002**, *60*, 1-49.
- [11] (a) Lewis, E.A.; Tolman, W.B. *Chem. Rev.* **2004**, *104*, 1047-1076. (b) Mirica, L.M.; Ottenwaelder, X.; Stack, T.D.P. *Chem. Rev.* **2004**, *104*, 1013-1045.

- [12] Itoh, S. In *Copper-Oxygen Chemistry*; Karlin, K.D.; Itoh, S., Eds.; John Wiley & Sons Inc., Hoboken, NJ, 2011; pp 225-282.
- [13] (a) Chan, S. I.; Lu, Y. -J.; Nagababu, P.; Maji, S.; Hung, M. -C.; Lee, M. M.; Hsu, I. -J.; Minh, P. D.; Lai, J. C. -H.; Ng, K, Y.; Ramalingam, S.; Yu, S. S. -F.; Chan, M. K. *Angew. Chem. Int. Ed. Engl.* **2013**, *52*, 3731-3735. (b) Woertink, J. S.; Smeets, P. J.; Groothaert, M. H.; Vance, M. A.; Sels, B. F.; Schoonheydt, R. A.; Solomon, E. I. *Proc. Natl. Acad. Sci.*, **2009**, *106*, 18908-18913.
- [14] (a) Fetzner, S. *Appl. Environ. Microbiol.* **2012**, *78*, 2505-2514. (b) Kaizer, J.; Pap, J.S.; Speier, G. In *Copper-Oxygen Chemistry*; Karlin, K.D.; Itoh, S., Eds.; John Wiley & Sons Inc., Hoboken, NJ, 2011; pp 23-52. (c) Pap, J.S.; Kaizer, J.; Speier, G. *Coord. Chem. Rev.* **2010**, *254*, 781-793.
- [15] (a) Kozlowski, M.C. In *Copper-Oxygen Chemistry*; Karlin, K.D.; Itoh, S., Eds.; John Wiley & Sons Inc., Hoboken, NJ, 2011; pp 361-444. (b) Puniyamurthy, T.; Rout, L. *Coord. Chem. Rev.* **2008**, *252*, 134-154.
- [16] Some recent examples include: a) Zhang, C.; Zhang, L.; Jiao, N. *Adv. Synth. Catal.* **2012**, *354*, 1293-1300. b) Schröder, K.; Join, B.; Amali, A. J.; Junge, K.; Ribas, X.; Costas, M.; Beller, M. *Angew. Chem. Int. Ed.* **2011**, *50*, 1425-1429. c) Liu, Q.; Wu, P.; Yang, Y.; Zeng, Z.; Liu, J.; Yi, H.; Lei, A. *Angew. Chem. Int. Ed.* **2012**, *51*, 4666-4670. d) Wang, H.; Wang, Y.; Liang, D.; Liu, L.; Zhang, J.; Zhu, Q. *Angew. Chem. Int. Ed.* **2011**, *50*, 5678-5681. e) Xu, Z.; Zhang, C.; Jiao, N. *Angew. Chem. Int. Ed.* **2012**, *51*, 11367-11370. f) Du, F. -T.; Ji, J. -X. *Chem. Sci.* **2012**, *3*, 460-465. g) Li, X.; Huang, L.; Chen, H.; Wu, W.; Huang, H.; Jiang, H. *Chem. Sci.* **2012**, *3*, 3463-3467.
- [17] Tian, Q.; Shi, D.; Sha, Y. *Molecules* **2008**, *13*, 948.

- [18] Komiya, N.; Naota, T.; Oda, Y.; Murahashi, S.-I. *J. Mol. Catal. A: Chem.* **1997**, *117*, 21-37.
- [19] De Jongh, H. A. P.; De Jongh, C. R. H.; Mijs, W. J. *J. Org. Chem.* **1971**, *36*, 3160-3168.
- [20] van Rheenen, V. *Tetrahedron Lett.* **1969**, *10*, 985-988.
- [21] Bolm, C.; Schlingloff, G.; Weickhardt, K. *Tetrahedron Lett.* **1993**, *34*, 3405-3408.
- [22] (a) Atlamsani, A.; Brégeault, J. –M. *Synthesis*, **1993**, 79-81. (b) Cossy, J.; Belotti, D.; Brocca, B. D.; *Tet. Lett.* **1994**, *35*, 6089-6092. (c) Brégeault, J. –M.; Launay, F.; Atlamsani, A. *Surf. Chem. Cat.* **2001**, *4*, 11-26.
- [23] Zhang, C.; Feng, P.; Jiao, N. *J. Am. Chem. Soc.* **2013**, *135*, 15257-15262.
- [24] Steiner, R.A.; Kalk, K.H.; Dijkstra, B.W. *Proc. Natl. Acad. Sci.* **2002**, *99*, 16625-16630.
- [25] Kaizer, J.; Zsigmond, Z.; Ganzsky, I.; Speier, G.; Giorgi, M.; Réglie, M. *Inorg. Chem.* **2007**, *46*, 4660-4666.
- [26] Allpress, C.J.; Arif, A.M.; Houghton, D.T.; Berreau, L.M. *Chem. Eur. J.* **2011**, *17*, 14962-14973.
- [27] Grubel, K.; Marts, A.R.; Greer, S.M.; Tierney, D.L.; Allpress, C.J.; Anderson, S.N.; Laughlin, B.J.; Smith, R.C.; Arif, A.M.; Berreau, L.M. *Eur. J. Inorg. Chem.* **2012**, *29*, 4750-4757.
- [28] Armarego, W. L. F.; Perrin, D. D. *Purification of Laboratory Chemicals*, 4th ed., Butterworth-Heinemann, Boston, MA, 1996.
- [29] Szajna-Fuller, E.; Rudzka, K.; Arif, A. M.; Berreau, L. M. *Inorg. Chem.* **2007**, *46*, 5499-5507.

- [30] Allpress, C. J.; Arif, A. M.; Houghton, D. T.; Berreau, L. M. *Chem. Eur. J.* **2011**, *17*, 14962-14973.
- [31] Evans, D. F. *J. Chem. Soc.* **1959**, 2003-2005.
- [32] QPOW is available on request from Prof. Joshua Telser, Roosevelt University, Chicago, IL.
- [33] Froncisz, W.; Hyde, J. S., *J. Chem. Phys.*, **1980**, *73*, 3123-3131.
- [34] Wolsey, W. C. *J. Chem. Educ.* **1973**, *50*, A335.
- [35] Ferrioxalate actinometry was carried out as previously described.²⁶ A description of the actinometer may be found in: a) Kuhn, H. J.; Braslavsky, S. E.; Schmidt, R., *Pure Appl. Chem.* **2004**, *76*, 2105-2146. b) Hatchard, C. G.; Parker, C. A., *Proc. R. Soc. London* **1956**, *A235*, 518-536.
- [36] Szajna, E.; Makowska-Grzyska, M. M.; Wasden, C. C.; Arif, A. M.; Berreau, L. M., *Inorg. Chem.* **2005**, *44*, 7595-7605.
- [37] Addison, A.W.; Rao, T.N.; Reedijk, J.; van Rijn, J.; Vershcoor, G.C. *J. Chem. Soc., Dalton Trans.* **1984**, 2177-2184.
- [38] (a) J. C. Taylor, A. B. McLaren, *J. Chem. Soc.* **1979**, *3*, 460-464. (b) V. G. Isakova, I. A. Baidina, N. B. Morozova, I. K. Igumenov, *Polyhedron*, **2000**, *19*, 1097-1103. (c) D. C. Ware, W. R. Wilson, W. A. Denny, C. E. F. Rickard, *Chem. Comm.* **1991**, *17*, 1171-1173. (d) C. A. Vock, A. K. Renfrew, R. Scopelliti, L. Juillerat-Jeanneret, P. J. Dyson, *Eur. J. Inorg. Chem.* **2008**, *10*, 1661-1671. (e) E. D. Estes, R. P. Scaringe, W. E. Hatfield, D. J. Hodgson, *Inorg. Chem.* **1976**, *15*, 1179-1182. (f) C. A. Kavounis, L. C. Tzavellas, C. J. Cardin, Y. Zubavichus, *Struct. Chem.* **1999**, *10*, 411. (g) S. Sans-Lenain, A. Gleizes, *Inorg. Chim. Acta.* **1993**, *211*, 67-75. (h) V. V. Sharutin, O. K. Sharutina, O.

P. Zadachina, A. N. Zakharova, V. A. Reutov, N. P. Shapkin, V. K. Belsky, *Russ. J. Gen. Chem.* **2000**, *70*, 1672.

[39] (a) Peisach, J.; Blumberg, W. E. *Arch. Biochem. Biophys.*, **1974**, *165*, 691-708.

(b) Bubacco, L.; van Gastel, M.; Groenen, E. J. J.; Vijgenboom, E.; Canters, G. W. *J. Biol. Chem.*, **2003**, *278*, 7381-7389.

[40] (a) Harata, M.; Jitsukawa, K.; Masuda, H.; Einaga, H. *Chem. Lett.* **1995**, *24*, 61-

62. (b) Lucchese, B.; Humphreys, K. J.; Lee, D. -H.; Incarvito, C. D.; Sommer, R. D.; Rheingold, A. L.; Karlin, K. D. *Inorg. Chem.* **2004**, *43*, 5987-5998.

[41] (a) Berreau, L. M.; Borowski, T.; Grubel, K.; Allpress, C. J.; Wikstrom, J. P.;

Germain, M. E.; Rybak-Akimova, E. L.; Tierney, D. L. *Inorg. Chem.* **2011**, *50*, 1047-

1057. (b) Allpress, C. J.; Grubel, K.; Szajna-Fuller, E.; Arif, A. M.; Berreau, L. M. *J.*

Am. Chem. Soc. **2013**, *135*, 659-668.

[42] Benzil is formed by a Lewis acid-mediated benzoyl migration of diphenylpropantrione. Roberts, J. D.; Smith, D. R.; Lee, C. C. *J. Am. Chem. Soc.* **1951**, *73*, 618-625.

[43] Atkins, P. W. *Physical Chemistry*, 6th ed., Oxford University Press, Oxford, UK, 1998.

[44] Borowski, T., *J. Mol. Structure: Theochem*, **2006**, *772*, 89-92.

[45] Calculations performed by A. Miłaczewska and T. Borowski (Institute for Catalysis and Surface Chemistry, Polish Academy of Science).

[46] **1-Peroxo** likely forms by the initial generation of a superoxo species capable of abstracting a hydrogen atom from dihydroanthracene (Figure 5-11).

[47] Mata-Perez, F.; Perez-Benito, J. F. *J. Chem. Ed.* **1987**, *64*, 925-927.

- [48] Speier, G.; Tyeklar, Z.; Toth, P.; Speier, E.; Tisza, S.; Rockenbauer, A.; Whalen, A. M.; Alkire, N.; Pierpont, C. G. *Inorg. Chem.* **2001**, *40*, 5653–5659.
- [49] (a) Balogh-Hergovich, E.; Kaizer, J.; Speier, G.; Huttner, G.; Zsolnai, L. *Inorg. Chim. Acta.* **2000**, *304*, 72–77. (b) Balogh-Hergovich, E.; Kaizer, J.; Pap, J.; Speier, G.; Huttner, G.; Zsolnai, L. *Eur. J. Inorg. Chem.* **2002**, 2287–2295.

CHAPTER 6
CONCLUSIONS

Summary

The work that has been outlined in this dissertation has focused on generating complexes of relevance to dioxygenase enzymes that oxidatively cleave aliphatic carbon-carbon bonds (Figure 6-1), including nickel- and iron-containing acireductone dioxygenases (Ni-ARD and Fe-ARD'), acetylacetonate dioxygenase (Dke1) and quercetin

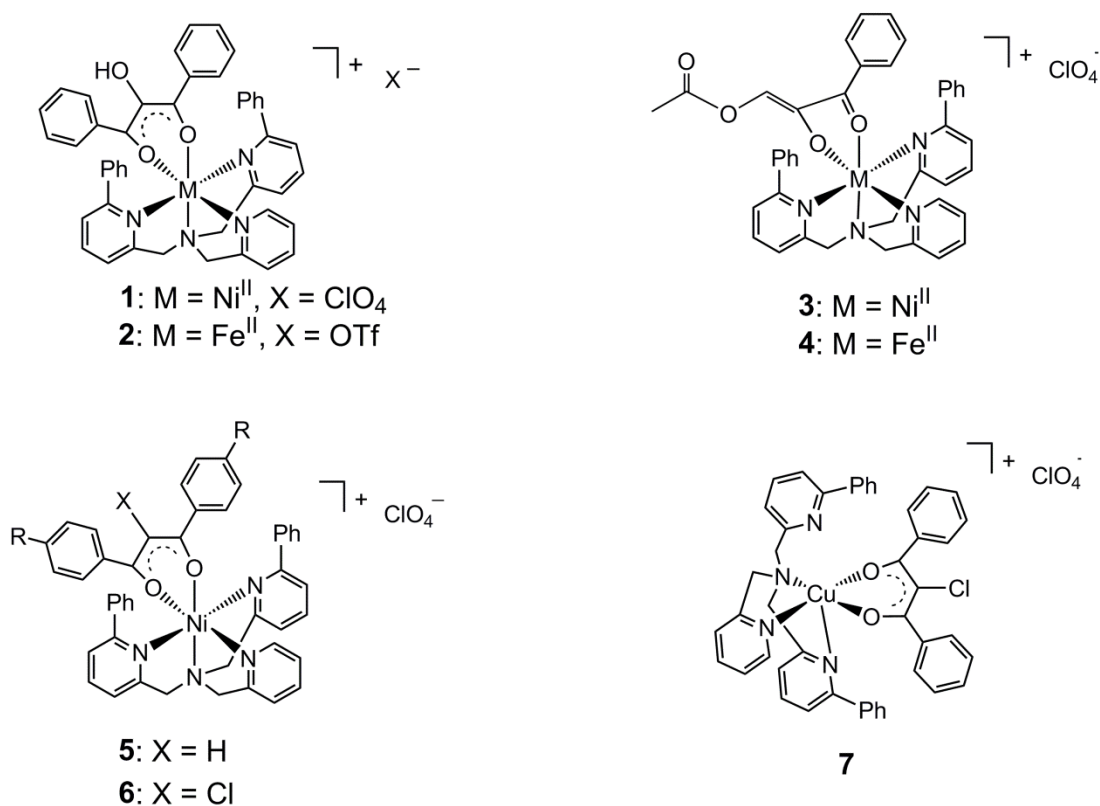
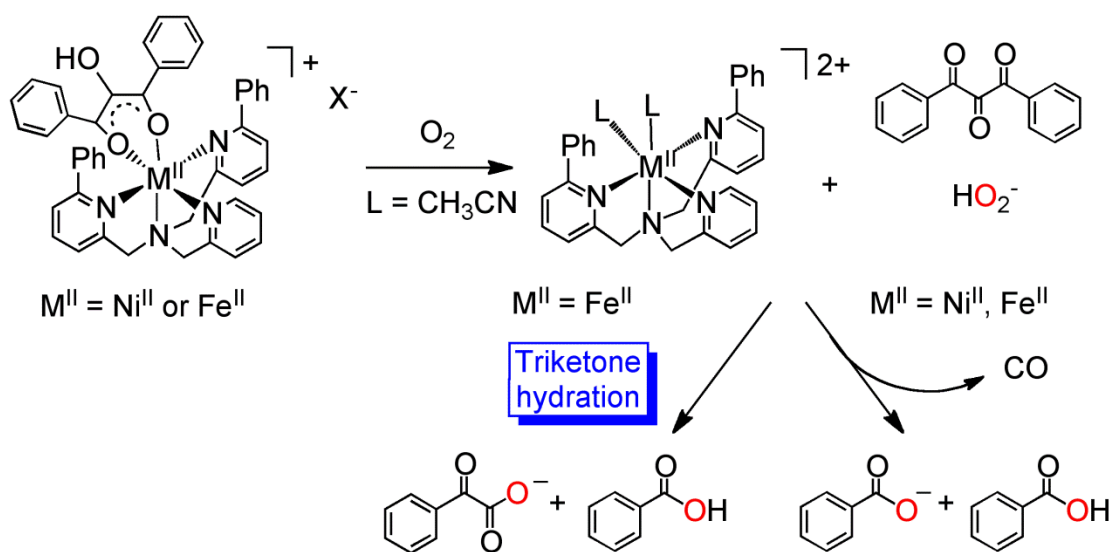


Figure 6-1. A selection of complexes investigated in this dissertation of relevance to C-C cleaving dioxygenases.

dioxygenase (QDO). The enzymes that carry out these reactions are diverse in terms of the identity of the metal co-factor at the active site, in terms of the amino acid residues that function as ligands at the active site, and in terms of the substrate that is cleaved.¹ We have utilized a variety of first-row transition metals supported by an aryl-appended tris(pyridylmethyl)amine ligand to investigate the reactivity of a number of enolizable substrates. The systems we have generated have focused on: understanding aspects of the regioselectivity of Ni-ARD and Fe-ARD'; probing mechanistic pathways that have relevance to Dke1; and studying unique ways to utilize late first-row transition metal divalent complexes for the activation of O₂.

Chapter 2. The acireductone dioxygenases are a unique pair of enzymes in biology in that, despite having identical peptide sequences, they catalyze the oxidative cleavage of their substrate with differing regiospecificity.² The only constitutive difference is the identity of the metal ion (either nickel or iron) at the active site.³ A generally-accepted reaction pathway was that changes in the tertiary structure of the enzymes favoured different binding modes of the acireductone substrate (either via a six- or five-membered chelate ring, for Ni-ARD and Fe-ARD' respectively).² This change in chelate ring size would activate different carbon atoms toward reaction with O₂, leading to a change in regiospecificity. Prior work on a nickel-containing model system, [(6-Ph₂TPA)Ni(PhC(O)COHC(O)Ph)]ClO₄ (**1**) in which the substrate bound via a six-membered chelate ring, led to Ni-ARD type products when the complex was exposed to O₂, consistent with the chelate hypothesis (Scheme 6-1).⁴ However, until the present work, no model systems investigating the role of the identity of the metal center on the reaction regioselectivity had been reported.

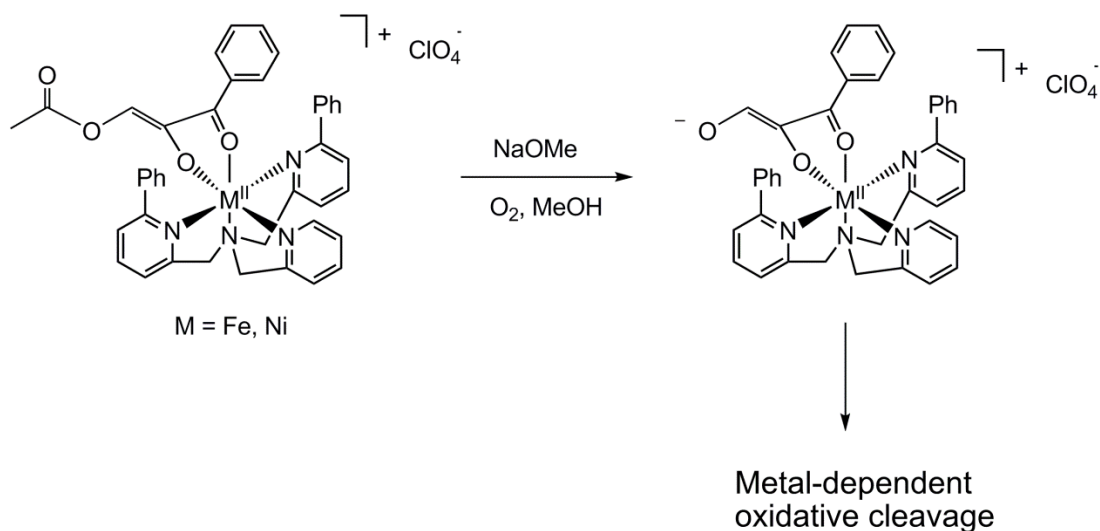
We have synthesized [(6-Ph₂TPA)Fe(PhC(O)COHC(O)Ph)]OTf (**2**), the first-ever model of the enzyme-substrate adduct of Fe-ARD'. The complex has been characterized by UV-vis, FTIR, ¹H NMR, magnetic susceptibility and elemental analysis. The characterization data is consistent with binding of the acireductone substrate via a six-membered chelate ring, as had previously been observed in the nickel analogue **1**.⁴ Thus, this complex was the ideal test-case for the chelate hypothesis. Reaction of **2** with O₂ was found to produce Ni-ARD like products under dry conditions, but in the presence of water produced Fe-ARD' like products (Scheme 6-1). This showed that the chelate hypothesis was not sufficient to explain the differences in reactivity between the nickel- and iron-containing systems, as water was not found to affect the binding mode of the substrate. Instead, we found that the iron-promoted hydration of an intermediate was likely the determining factor in the change in regioselectivity. This was



Scheme 6-1. O₂ reactivity of the acireductone dioxygenase model systems **1** and **2** in the presence and absence of water.

the first time such a notion had been proposed. We also found that *in situ* generated ferric species were capable of oxidatively cleaving the acireductone substrate.

Chapter 3. While our results highlighted that there could well be alternative explanations to a chelate-differentiated regioselectivity of C-C cleavage, our system was not truly biomimetic. Two issues that were not addressed in the prior work were: differences in electronic structure between our “bulky acireductone” substrate and native substrates for the enzyme, that all have a C(1)H functionality; and the protonation level of the substrate - mono-anionic in our model system, but believed to be di-anionic in the enzyme-substrate adduct.⁵ Prior methods for generating C(1)H acireductones have been low-yielding and involved multiple-step syntheses, often utilizing an enolase/phosphatase enzyme to generate an acireductone mono-anion *in situ*.⁶ We have developed a relatively simple, high-yielding, non-enzymatic synthetic route to an acetylated precursor of a C(1)H acireductone. This acetylated acireductone may either be bound to a metal center directly for subsequent deprotection, or deprotected to form a C(1)H acireductone tautomer and bound to a metal center. The former strategy was found to be advantageous, as it allowed us to investigate the O₂ reactivity of mononuclear di-anionic acireductone complexes that were generated *in situ* by deacetylation of the air-stable complexes [(6-Ph₂TPA)Ni(PhC(O)C(O)CHOC(O)CH₃)]ClO₄ (**3**) and [(6-Ph₂TPA)Fe(PhC(O)C(O)CHOC(O)CH₃)]ClO₄ (**4**) (Scheme 6-2). To date, all previous attempts at investigating the O₂ reactivity of mononuclear di-anionic acireductone complexes had failed due to the propensity for the ancillary ligand to be displaced to form multi-nuclear clusters, bridged by the acireductone, that were also O₂ reactive.⁷

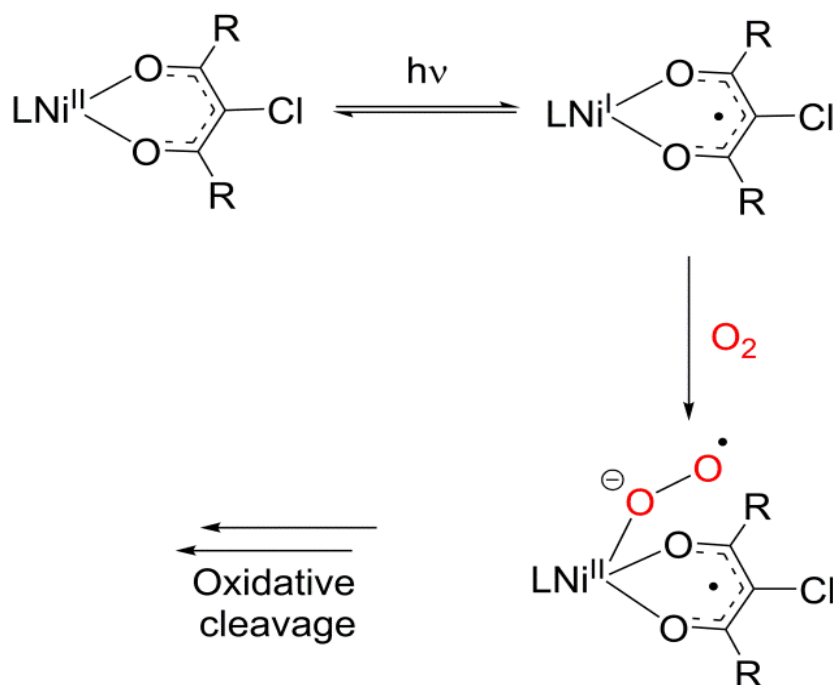


Scheme 6-2. *In situ* generation of mono-nuclear di-anionic C(1)H acireductone complexes from **3** and **4** allowed investigation of their O₂ cleavage reactivity.

Under anaerobic conditions **3** and **4** exhibit the same cluster formation. However, when the deprotection is carried out in the presence of O₂, a sufficiently long-lived mononuclear dianionic species is intercepted by O₂ allowing us to investigate the regioselectivity of cleavage of this species for the first time ever.

Chapter 4. One of the most important questions in studies of acetylacetonate dioxygenase (Dke1), is what the role of the metal center is in promoting the C-C cleavage reaction. Initial studies suggested that the role of the metal center was to act as an “electron conduit”, facilitating the spin-forbidden reaction between ³O₂ and the singlet substrate via a superoxo/substrate radical pair.⁸ More recent work in model systems suggested a redox-active role of the ferrous center to generate a ferric-superoxo adduct, while computational studies have postulated that a Fe(IV)O species may be involved.⁹ To test whether the “electron conduit” pathway would be viable, we have taken a unique approach to generating a superoxo/substrate radical pair and investigating its interaction with dioxygen.

We have synthesized a series of complexes with the formulation [(6-Ph₂TPA)Ni(ArC(O)CXC(O)Ar)]ClO₄ (**5**: X = H, **6**: X = Cl) and characterized them by UV-vis, FTIR, ¹H NMR, elemental analysis, HRMS and variably by x-ray crystallography. Photoirradiation in the presence of O₂ led to decay of the ~370 nm absorption feature associated with a combined enolate π-π* transition and a diketonate-based LMCT for the series of compounds **6** (Scheme 6-3), but for **5** no reactivity was observed. Analysis of the products in the reaction of **6** showed the production of carboxylic acids, and ¹⁸O labeling studies confirmed the cleavage proceeded by a dioxygenolytic mechanism. Mechanistic studies strongly supported the photogeneration of a Ni(I)-diketonyl radical species that could be intercepted by O₂ to form a Ni(II)-superoxo/diketonyl radical intermediate. Thus, we showed that reaction via a



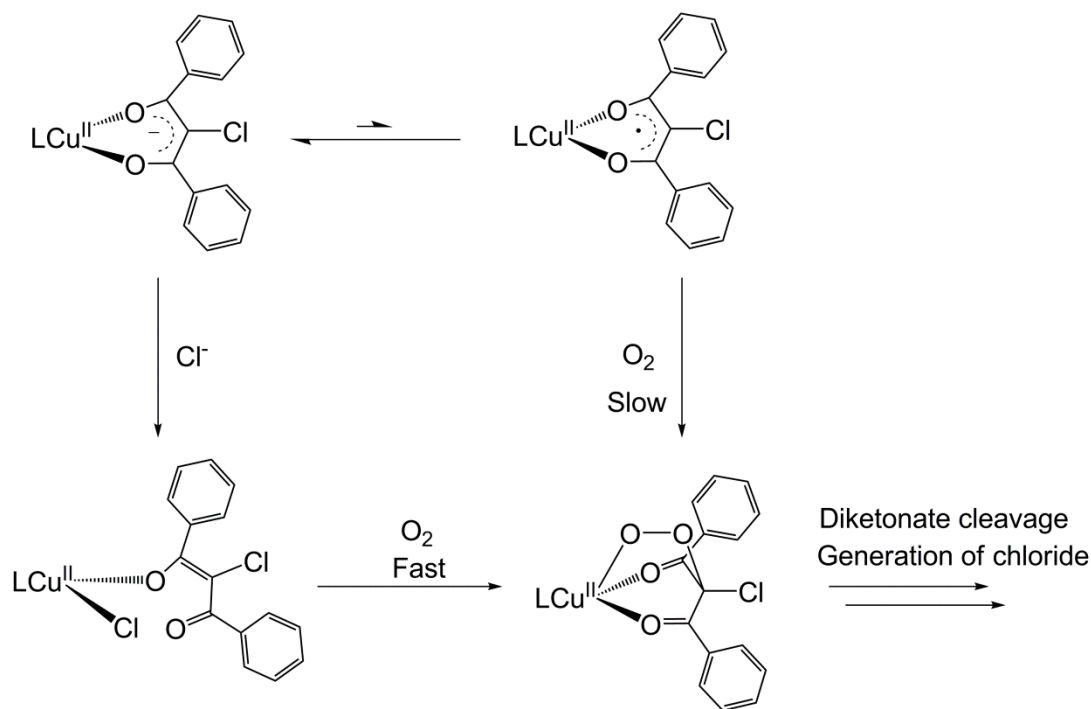
Scheme 6-3. Reaction pathway for the oxidative photo-cleavage of a Ni(II)-supported α-chloro diketonate.

superoxo/diketonyl radical pair was a viable route to C-C cleavage. However, the lack of reactivity of **5** showed the unexpected requirement of a chloride leaving group for this reaction to proceed.

Chapter 5. We attempted to expand the photo cleavage exhibited by **6** to a copper-containing system, expecting the potentially longer lifetime of the putative Cu(I)-diketonyl radical intermediate to result in higher reactivity. The complex [(6-Ph₂TPA)Cu(PhC(O)CClC(O)Ph)]ClO₄ (**7**) was synthesized and characterized by UV-vis, FTIR, magnetic susceptibility, EPR, elemental analysis, mass spectrometry and x-ray crystallography. It was found to undergo photoreaction similar to **6**, albeit with a disappointingly low quantum yield of $\sim 10^{-4}$. However, a facile thermal reaction was also discovered at room temperature in the presence of O₂ (Scheme 6-4). Interestingly, a short induction period was observed that could be removed by the addition of a catalytic amount of a soluble chloride salt. The exact role of the chloride ion in accelerating the rate of reaction has not yet been fully determined, and is the subject of ongoing computational investigations. Nonetheless, the discovery of thermal dioxygenolysis of C-C bonds at room temperature, mediated by a well-defined Cu(II) complex is very interesting and, to our knowledge, unique.

Significance

One of the most important challenges for chemists in the 21st century is the selective oxidative activation of carbon-carbon bonds.^{1, 10} Such reactions are of current interest due to their potential applications in the utilization of biomass for fuel production, applications in wastewater treatment and bioremediation, and in developing



Scheme 6-4. A proposed role of chloride in accelerating the thermal oxidative cleavage of an α -chloro diketonate by complex **7**.

new reactions for organic synthesis of fine chemicals including pharmaceuticals.¹¹ Ideally these reactions would be carried out with high atom economy at low temperatures and pressures, and using earth-abundant elements as reagents and catalysts.¹² With these points in mind, nature provides an ideal framework, carrying out its chemistry at ambient temperature and pressure. Enzymes that cleave C-C bonds by a dioxygenolytic pathway are particularly interesting as they utilize dioxygen as a terminal oxidant and also do not require any coreductants, maximizing atom economy. While dioxygenases that cleave aromatic C-C bonds have been extensively studied, those that cleave aliphatic C-C bonds have only recently become an area of extensive investigation.¹ We have focused on exploring the reaction pathways of several dioxygenase enzymes that cleave aliphatic C-C bonds, with the goal of understanding fundamental factors involved in the activation

and direction of cleavage of these bonds. These efforts have led to several important advances in understanding of the cleavage of C-C bonds.

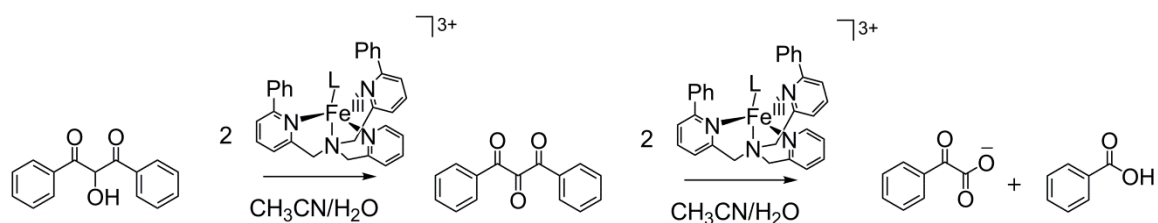
Chapters 2 and 3. Our work on model systems of the enzyme-substrate adducts of the acireductone dioxygenases allowed us to probe the reasons for the metal-dependent changes in regioselectivity of C-C cleavage of the substrate. In contrast to the widely-accepted chelate hypothesis,² we found in our model systems (complexes **1-4**) that the binding mode of the substrate was not sufficient to explain the observed changes in regioselectivity of C-C cleavage. Rather, the identity of the metal center (in conjunction with the presence of water in the case of **2**), either the redox inactive Ni(II) or the redox active Fe(II), was more important than substrate binding mode in determining the regioselectivity. This role of the redox activity of a metal center in determining regioselectivity may have some utility in organic syntheses, although the current lack of *a priori* predictive power of how redox activity may affect regioselectivity is a drawback. However, a more important aspect of this work is in highlighting the predictive power of small molecular model systems. A recent QM/DMD computational study has shown that, as we predicted, the binding mode of the substrate does not actually change between Ni-ARD and Fe-ARD'.¹³ It is, rather, differences in the electronic structure of the metal ion at the active site that alters the energy of an intermediate in the reaction pathway, leading to the observed changes in regioselectivity.

Our discovery that the reaction catalyzed by acireductone dioxygenases to cleave an acireductone substrate and form an α -keto acid (methylthiobutyrate (MTOB) in the enzymatic reaction) can be carried out under anaerobic conditions is also a very important discovery. The methionine salvage pathway, that regenerates methionine from

the toxic methylthioadenosine generated when S-adenosylmethionine is consumed during polyamine biosynthesis, is a ubiquitous pathway in eukaryotic organisms.¹⁴ However, despite the discovery of a methionine salvage pathway in anaerobic organisms, including a Rubisco-like protein that can carry out the same reactions as the enolase/phosphatase enzyme in the methionine salvage pathway of *Klebsiella oxytoca*, the route by which the resulting acireductone intermediate is converted to MTOB, and subsequently transaminated to form methionine, has remained unclear.¹⁵ It has been proposed that this reaction likely proceeds via a non-oxidative route. Our discovery, then, that ferric ions can both act as a terminal oxidant for the cleavage of an acireductone substrate, and do so in a regioselective manner (Scheme 6-5), suggests that an enzyme that carries out this reaction oxidatively under anaerobic conditions may yet be found.

Chapter 4. The utilization of complexes **5** and **6** to investigate the reactivity of a superoxo/diketonyl radical pair with O₂ provided some insight into the feasibility of this reaction pathway for the cleavage of acetylacetonone by Dke1. However, the real significance of this work is in the methodology of utilizing a Ni(II) center to activate O₂.

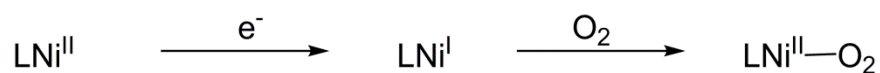
There is currently a strong interest in understanding how late first-row transition metals such as nickel and copper can be utilized to activate ³O₂ towards reactions with



Scheme 6-5. Oxidative cleavage of an acireductone by ferric species in a regioselective manner.

singlet ground state organic molecules.¹⁶ The typical current strategy involves the use of a ligand set that allows stabilization of a Ni(I) center as a precursor for the generation of a Ni(II)-superoxo species.¹⁷ This active oxidant is known to exhibit high reactivity, including via dioxygenase-type reaction pathways.¹⁸ However, the strategy of utilizing a Ni(I) center is not likely to be sustainable for catalysis, as it is generated by the use of a strong external reductant from a Ni(II) complex (Scheme 6-6).¹⁹ Our strategy of photoirradiation into a LMCT band of a Ni(II)-substrate complex to form a Ni(I)-substrate radical adduct (Scheme 6-3) provides an alternative pathway to activating O₂ at nickel as a superoxo. This strategy is likely to be expandable to the oxidative cleavage of other substrates using catalytic amounts of metal complex. However, a remaining challenge is increasing the quantum yields of these photoreactions, which will likely require the utilization of a ligand set that can better stabilize Ni(I), preventing recombination of the radical pair.

Chapter 5. Attempted expansion of the nickel photochemistry to a copper system did not improve the quantum yields of the photoreaction, but instead a much more interesting thermal oxidative cleavage of C-C bonds was discovered. The field of Cu-oxygen chemistry has been dominated by investigations of the reaction of Cu(I) species with O₂, or the reaction of Cu(II) species with peroxides.²⁰ This copper oxygen chemistry



Scheme 6-6. The most common current strategy for the activation of O₂ by a nickel system involves the initial reduction of a Ni(II) precursor by an external electron source to generate an O₂-reactive Ni(I) species.

has not been widely expanded to C-C cleavage reactivity. The only well-defined systems that have allowed investigations of the role of a Cu(II) ion in facilitating C-C cleavage by O₂ are models of the enzyme-substrate adducts of QDO, which react only under relatively harsh conditions with elevated temperatures, greater than 80 °C.²¹ The lack of well-defined systems that investigate how Cu(II) may be utilized is particularly surprising given reports of seemingly anomalous room temperature oxidative C-C cleavage of cyclic ketones catalyzed by simple Cu(II) salts.²² There is no experimental or theoretical framework currently in place to investigate the factors that lead to this facile reactivity.

The facile cleavage of a diketone substrate by our Cu(II) complex **7** is therefore particularly interesting. While experimental and computational studies are ongoing to fully understand the reasons this complex allows for facile room temperature C-C cleavage chemistry, the well-defined nature of the complex and the observation of a chloride-dependent induction period both provide an excellent starting point for elucidating important mechanistic details. We envision that this chemistry may well be expandable to other supporting ligand environments, as well as a potentially wide range of substrates. And, such chemistry will be of exceeding interest to both the organic synthetic community, which already uses some poorly defined copper catalysts for O₂ activation,^{20c} and the inorganic community. Therefore, although this chemistry is still at a very early stage, it may well be the most important area expounded upon in this dissertation with a view to moving forward.

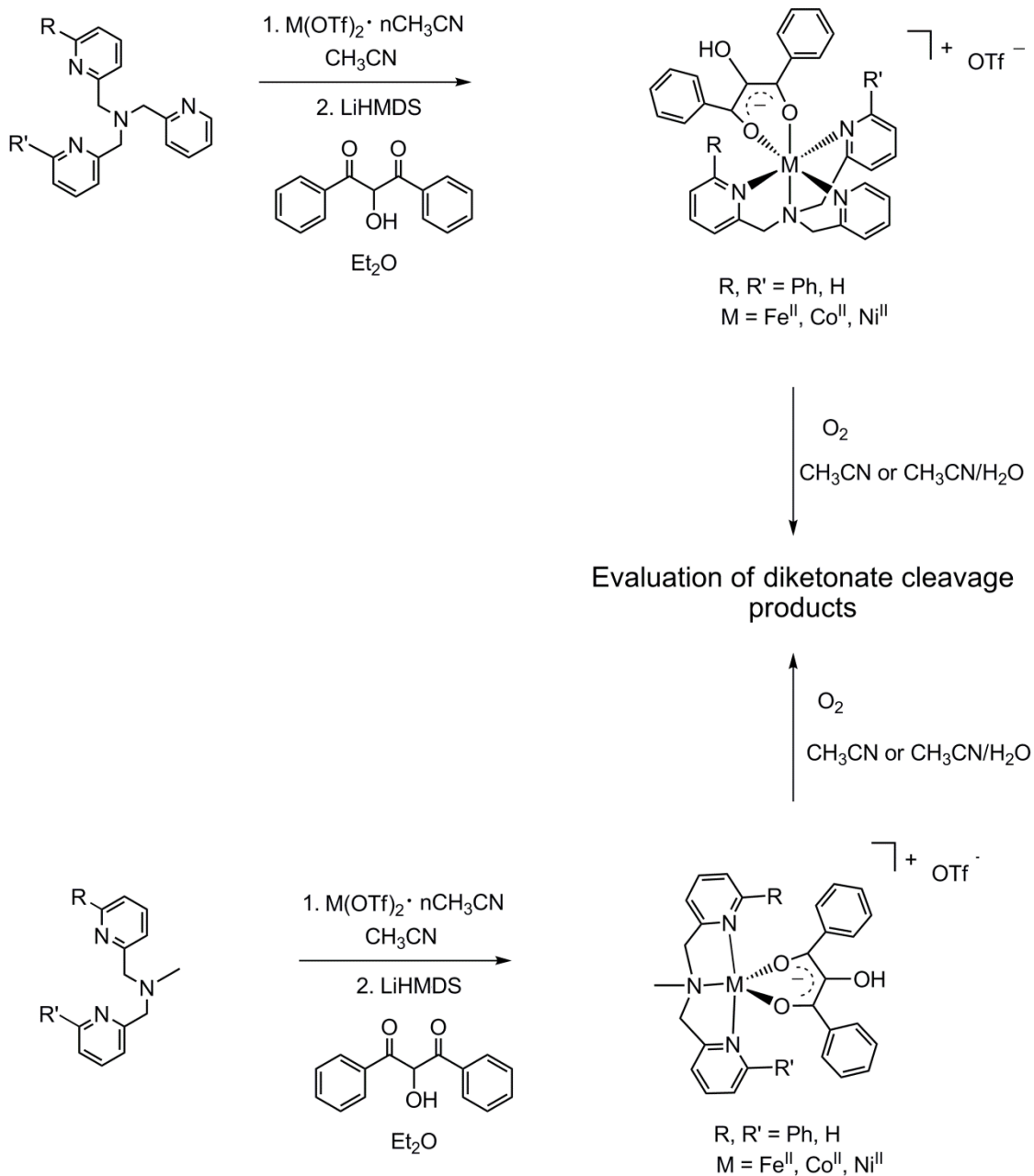
Future Directions

There are numerous potential avenues of research that build out of the work presented in this dissertation. Herein we discuss aspects of possibilities of future

directions in this work. While the directions presented here are by no means comprehensive, they highlight some areas that would provide much-desired mechanistic insight into aspects of C-C oxidative cleavage. Other avenues of investigation that would mark significant advances in the field but are not directly relevant to the mechanism of C-C cleavage are not actively discussed. These include, but are not limited to: extensions of LMCT-based photoreduction to induce O₂ reactivity in divalent complexes via ligand modification and introduction of antennae moieties; and extension of the chloride-mediated thermal cleavage of copper diketonates into catalytic systems.

Chapter 2. The differing reactivity of **1** and **2** in the presence of H₂O raises a number of interesting questions concerning the reasons why Fe(II) is able to promote the postulated hydration chemistry while Ni(II) is not, and what role (if any) the supporting 6-Ph₂TPA chelate ligand plays in directing the regioselectivity. While differences are observed in both coordination number preferences of the [(6-Ph₂TPA)M(sol)_x]²⁺ complex, and in its ability to facilitate a Lewis acid mediated side reaction, it is not clear that Ni(II) should be categorically unable to promote the same hydration chemistry. It is also unclear whether other metal centers, such as Co(II) can promote the reaction with any regioselectivity preferences (notably when the acireductone dioxygenase apo enzyme is reconstituted with Co(II), it exhibits Ni-ARD type reactivity). Another question that arises is whether the only role of H₂O is the hydration of the triketone intermediate, or if it also facilitates other processes such as acting as a hydrogen bond donor to promote dissociation of one of the phenylpyridyl arms of the tetradentate ligand.

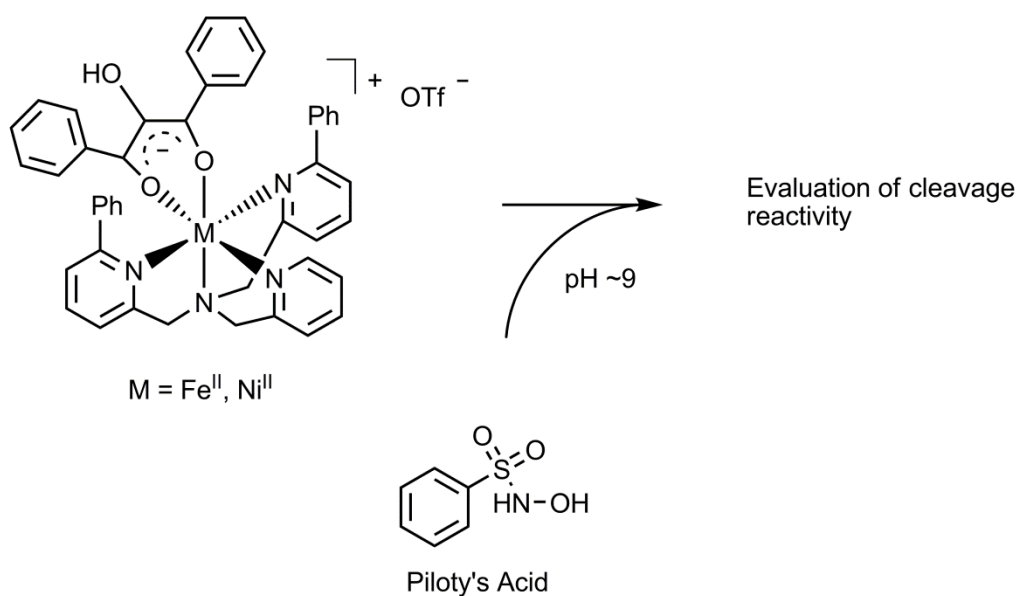
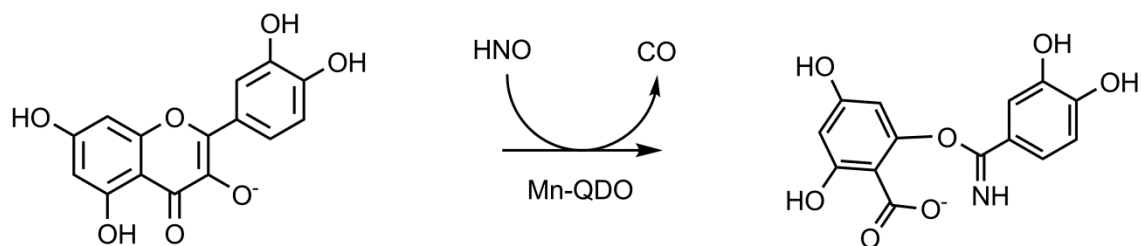
With these points in mind, an important advance in the modeling of acireductone dioxygenases would be the systematic construction of a series of divalent metal



Scheme 6-7. Proposed synthetic scheme for investigating the role of ligand bulkiness, coordination number and metal ion identity in determining the regioselectivity of the dioxygenolytic reaction of a bulky acireductone.

complexes with varying features on the supporting chelate ligand (Scheme 6-7). We do note that some attempts at this have been previously reported, that identified some metal- and ligand-dependent hydrolysis chemistry. However, the study was hindered by Lewis acid-promoted isomerization of the acireductone substrate to produce an ester in the presence of H₂O; this was minimized by some convoluted drying processes of the hydroxide base, but never fully eliminated to generate analytically pure material in all cases.²³ The exclusion of hydroxide bases to completely eliminate water from the reactions was not reported. However, our work utilizing anhydrous metal salts and lithium amide bases with the effect of the total exclusion of water provides a promising framework for advancing this chemistry. A series of potential synthetic targets is outlined in Scheme 6-7. We note that all proposed ligands are known compounds. Synthesis of these complexes would be followed by evaluation of their O₂ reactivity both in the presence and absence of H₂O. Special attention would be paid to the formation of benzoylformic acid, to determine the role of ligand bulkiness, coordination number and metal ion identity in allowing cleavage of only the C(1)-C(2) bond of the acireductone. It is possible that the redox flexibility of a ferrous center is absolutely required for such chemistry, but that has not yet been definitively demonstrated.

The ease of oxidation of the bulky acireductone substrate exhibited in complexes **1** and **2** also provides another interesting potential area of investigation. Recently, the Farmer group reported that a manganese-containing form of quercetin dioxygenase promoted the facile cleavage of its quercetin substrate in the presence of nitroxyl (HNO) in a regioselective manner (Scheme 6-8 (top)).²⁴ This “nitroxigenase” reactivity is



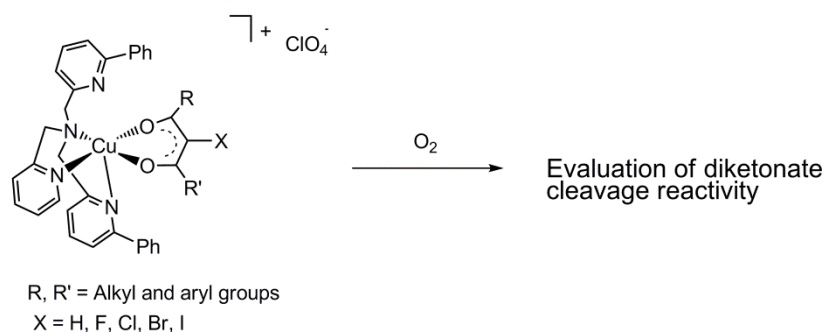
Scheme 6-8. The nitroxygenase reaction catalyzed by the manganese-containing form of QDO proceeds in a regiospecific manner (top). A proposed reaction of acireductone complexes with the nitroxyl donor Piloty's acid (bottom).

interesting for several reasons. Nitroxyl is related to the potent signaling molecule nitric oxide by one electron reduction and protonation, and its biological role is still poorly understood.²⁵ Thus, the observation of substrate cleavage by nitroxyl is very interesting as most prior investigations had focused on its interaction with metal centers as the deprotonated NO^- anion. Also, while NO^- is isoelectronic with $^3\text{O}_2$, protonation to form HNO splits the degeneracy of the π^* orbitals and leads to a singlet ground state – making nitroxyl isoelectronic with $^1\text{O}_2$.²⁶ HNO could therefore be used as a replacement for singlet oxygen in mechanistic investigations. Unfortunately, the application of HNO for nitroxygenase reactivity in model systems of the quercetin dioxygenases is hindered by the slow thermal reactivity of these complexes, requiring elevated temperatures greater than 80 °C.²¹ By contrast, our acireductone dioxygenase models (**1** and **2**) undergo facile reactivity at room temperature, and provide an ideal system for investigating the regioselectivity effects of utilizing HNO rather than O_2 as a terminal oxidant. We envision a regime in which nitroxyl is introduced to the reaction in a solution buffered at pH ~9 by the decomposition of the nitroxyl donor Piloty's acid (Scheme 6-8 (bottom)).²⁷

Chapter 3. The synthetic methodology we have developed for acetylated C(1)H acireductone precursors will allow the rapid synthesis of a series of *para*-substituted phenyl reductones. This series would vary the electron density within the acireductone π system, allowing us to evaluate the effect of this on the regioselectivity of the cleavage reaction.²⁸ Another important question that has not yet been answered is whether the C(1)H acireductone complexes (**3** and **4**) that we have been investigating undergo their cleavage via the formation of a vicinal tricarbonyl intermediate, as occurred for the related complexes **1** and **2** that utilized a bulky acireductone substrate. This tricarbonyl

intermediate is formed by the two-electron oxidation of the acireductone with the concomitant formation of hydroperoxide. Unlike in the reactions of **1** and **2**, in which the diphenylpropantrione intermediate “trapped” itself, via a Lewis acid mediated benzoyl migration to form benzil, no equivalent byproduct has yet been observed in the reactions of **3** and **4**. An important test would be whether the tricarbonyl intermediate, 2,3-dioxo-3-phenylpropanal can react with hydroperoxide in the presence of a Ni(II) or Fe(II) center to lead to oxidative C-C cleavage. The regioselectivity of this process as a function of metal ion would be a good indicator as to whether the tricarbonyl compound is a viable intermediate in C(1)H acireductone oxidation. Recent advances in the synthesis of vicinal tricarbonyls provide a viable synthetic route to 2,3-dioxo-3-phenylpropanal.²⁹

Chapter 5. The facile oxidative cleavage of a α -chloro diketonate mediated by a Cu(II) complex at room temperature is very interesting. However, much remains to be determined both about the mechanism of the reaction and its scope in terms of substrates. With this in mind, there are several important questions that remain to be answered. First and foremost, the role of the α -substituent is not entirely clear. Therefore, we propose the synthesis of a series of α -substituted diketonate Cu(II) complexes, where the α -



Scheme 6-9. Proposed variations of substituents of the diketonate moiety from **7** to investigate the scope of substrate cleavage by O₂.

substituent contains a series of halides and a hydrogen atom, and evaluating their O₂ reactivity (Scheme 6-9). Addition of electron-rich substituents, such as a hydroxyl group, is unlikely to be beneficial, as the anions of these compounds are known to undergo dioxygenolysis even in the absence of a metal center. The scope of substitution at the aryl groups of the substrate is also a potential area of investigation. While varying the *para*-substituent on the phenyl rings would allow a Hammett analysis of the nature of the rate-determining step of the reaction, replacing the aryl groups with alkyl chains would open up this chemistry to much broader applications. Another important question involves the role of the copper center, which currently remains unclear. In contrast to complex **7**, the related Ni(II) complexes **6** were found to be thermally stable and only reacted during photoirradiation, and thus we are interested in understanding how varying the metal center across the first-row transition metals may influence the cleavage of the substrate.

Perspective

Overall, the work presented in this dissertation encompasses an important body of original research and investigation that adds to our understanding of the chemistry of carbon-carbon bond cleavage. We have made important experimental contributions to understanding the role of a metal center in the regioselectivity of the acireductone dioxygenases – work that is now supported by advanced computational investigations. We have also investigated some new ways to utilize divalent late first-row transition metals for the activation of dioxygen, an approach that may hold great promise for application to diverse substrates. The merit of this work is apparent, not just in the raw science itself, but also in its acknowledgement in peer-reviewed literature and at presentations at scientific meetings.³⁰

Most importantly, however, even though we have answered a number of important questions, both about how carbon-carbon bonds are activated to react with dioxygen, and about how the selectivity of the subsequent reaction is determined, at the end of this body of research we are left more questions than we began and with a better appreciation of how much more yet remains to be understood.

References

- [1] Allpress, C. J.; Berreau, L. M. *Coord. Chem. Rev.* **2013**, *257*, 3005-3029.
- [2] Pochapsky, T. C.; Ju, T.; Dang, M.; Beaulieu, R.; Pagani, G. M.; OuYang, B. In *Metal Ions in Life Sciences*; Sigel, A., Sigel, H., Sigel, R. K. O., Eds.; Wiley-VCH: Weinheim, Germany, 2007; Vol. 2, pp 473-500.
- [3] Day, Y.; Wensink, P.C.; Abeles, R. H. *J. Biol. Chem.* **1999**, *274*, 1193-1195.
- [4] Szajna, E.; Arif, A. M.; Berreau, L. M. *J. Am. Chem. Soc.* **2005**, *127*, 17186-17187.
- [5] Dai, Y.; Pochapsky, T. C.; Abeles, R. H. *Biochemistry*, **2001**, *40*, 6379-6387.
- [6] Zhang, Y.; Heinsen, M. H.; Kostic, M.; Pagani, G. M.; Riera, T. V.; Perovic, I.; Hedstrom, L.; Snider, B. B.; Pochapsky, T. C. *Bioorg. Med. Chem.* **2004**, *12*, 3847-3855.
- [7] (a) Rudzka, K.; Arif, A. M.; Berreau, L. M. *Inorg. Chem.* **2008**, *47*, 10832-10840.
(b) Rudzka, K.; Grubel, K.; Arif, A. M.; Berreau, L. M. *Inorg. Chem.* **2010**, *49*, 7623-7625.
- [8] Straganz, G. D.; Nidetzky, B. *J. Am. Chem. Soc.* **2005**, *127*, 12306-12314.
- [9] (a) Siewert, I.; Limberg, C. *Angew. Chem. Int. Ed., Engl.* **2008**, *47*, 7953-7956.
(b) Diebold, A. R.; Straganz, G. D.; Solomon, E. I. *J. Am. Chem. Soc.* **2011**, *133*, 15979-15991.

- [10] (a) Crabtree, R. H. *Nature*, **2000**, *408*, 415–416. (b) Jun, C.-H. *Chem. Soc. Rev.*, **2004**, *33*, 610–618.
- [11] (a) Gettys, N. S. *J. Chem. Ed.* **1998**, *75*, 665-668. (b) National Research Council (US) Chemical Sciences Roundtable. Bioinspired Chemistry for Energy: A Workshop Summary to the Chemical Sciences Roundtable. Washington (DC): National Academies Press (US); 2008. (c) National Research Council (US). Health and Medicine: Challenges for the Chemical Sciences in the 21st Century. Washington (DC): National Academies Press (US); 2004.
- [12] Anastas, P. T.; Warner, J. C. *Green Chemistry: Theory and Practice*; Oxford University Press, Oxford, England, 1998.
- [13] Sparta, M.; Valdez, C. E.; Alexandrova, A. N. *J. Mol. Biol.* **2013**, *425*, 3007-3018.
- [14] Albers, E. *IUBMB Life* **2009**, *61*, 1132-1142.
- [15] (a) Sekowska, A.; Dénervaud, C.; Ashida, H.; Michoud, K.; Haas, D.; Yokota, A.; Danchin, A. *BMC Microbiol.* **2004**, *4*, 9. (b) Imker, H. J.; Fedorov, A. A.; Fedorov, E. V.; Almo, S. C.; Gerlt, J. A. *Biochemistry*, **2007**, *46*, 4077-4089. (c) Singh, J.; Tabita, F. R. *J. Bacteriol.* **2010**, *192*, 1324-1331.
- [16] Suzuki, M. *Acc. Chem. Res.* **2007**, *40*, 609-617.
- [17] Kieber-Emmons, M. T.; Riordan, C. G. *Acc. Chem. Res.* **2007**, *40*, 618-625.
- [18] Company, A.; Yao, S.; Ray, K.; Driess, M. *Chem. Eur. J.* **2010**, *16*, 9669-9675.
- [19] (a) Fujita, K.; Rheingold, A. L.; Riordan, C. G. *Dalton Trans.* **2003**, 2004-2008. (b) Bai, G.; Wei, P.; Stephan, D. W. *Organometallics*, **2005**, *24*, 5901-5908.

- [20] (a) Lewis, E. A.; Tolman, W. B. *Chem. Rev.* **2004**, *104*, 1047-1076. (b) Mirica, L. M.; Ottenwaelder, X.; Stack, T. D. P. *Chem. Rev.* **2004**, *104*, 1013-1045. (c) Allen, S. E.; Walvoord, R. R.; Padilla-Salinas, R.; Kozlowski, M. C. *Chem. Rev.* **2013**, *113*, 6234-6458.
- [21] (a) Kaizer, J.; Pap, J. S.; Speier, G. In *Copper-Oxygen Chemistry*; Karlin, K.D.; Itoh, S., Eds.; John Wiley & Sons Inc., Hoboken, NJ, 2011; pp 23-52. (b) Pap, J. S.; Kaizer, J.; Speier, G. *Coord. Chem. Rev.* **2010**, *254*, 781-793.
- [22] (a) Atlamsani, A.; Brégeault, J. –M. *Synthesis*, **1993**, 79-81. (b) Cossy, J.; Belotti, D.; Brocca, B. D.; *Tet. Lett.* **1994**, *35*, 6089-6092.
- [23] Grubel, K.; Ingle, G. K.; Fuller, A. L.; Arif, A. M.; Berreau, L. M. *Dalton Trans.* **2011**, *40*, 10609-10620.
- [24] Kumar, M. R.; Zapata, A.; Ramirez, A. J.; Bowen, S. K.; Francisco, W. A.; Farmer, P. J. *Proc. Natl. Acad. Sci.* **2011**, *108*, 18926-18931.
- [25] Fukuto, J.M.; Cisneros, C.J.; Kinkade, R.L. *J. Inorg. Biochem.* **2013**, *118*, 201-208.
- [26] Doctorovich, F.; Farmer, P. J. *J. Inorg. Biochem.* **2013**, *118*, 107.
- [27] Hughes, M. N.; Cammack, R. *Methods in Enzymology*, **1999**, *301*, 279-287.
- [28] A wide range of *para*-substituted analogues of 3-phenylprop-2-yn-1-ol are commercially available.
- [29] Goswami, S.; Maity, A. C.; Fun, H.-K.; Chantrapromma, S. *Eur. J. Org. Chem.* **2009**, 1417-1426.
- [30] The work presented in this dissertation has thus far resulted in 5 peer-reviewed publications and 5 poster and oral presentations at national conferences. Additionally, the

work presented in Chapter 2 has been highlighted in the ACS virtual issue “Models of Metalloenzymes.”

APPENDIX

ELSEVIER LICENSE
TERMS AND CONDITIONS
Nov 05, 2013

This is a License Agreement between Caleb J Allpress ("You") and Elsevier ("Elsevier") provided by Copyright Clearance Center ("CCC"). The license consists of your order details, the terms and conditions provided by Elsevier, and the payment terms and conditions.

All payments must be made in full to CCC. For payment instructions, please see information listed at the bottom of this form.

Supplier	Elsevier Limited The Boulevard, Langford Lane Kidlington, Oxford, OX5 1GB, UK
Registered Company Number	1982084
Customer name	Caleb J Allpress
Customer address	339 E 600 N LOGAN, UT 84321
License number	3262301191939
License date	Nov 04, 2013
Licensed content publisher	Elsevier
Licensed content publication	Coordination Chemistry Reviews
Licensed content title	Oxidative aliphatic carbon-carbon bond cleavage reactions
Licensed content author	Caleb J. Allpress, Lisa M. Berreau
Licensed content date	November 2013
Licensed content volume number	257
Licensed content issue number	21-22
Number of pages	25
Start Page	3005
End Page	3029
Type of Use	reuse in a thesis/dissertation
Portion	full article
Format	print
Are you the author of this Elsevier article?	Yes
Will you be translating?	No
Order reference number	
Title of your thesis/dissertation	OXIDATIVE ALIPHATIC CARBON-CARBON BOND CLEAVAGE REACTIONS
Expected completion date	Dec 2013
Estimated size (number of pages)	
Elsevier VAT number	GB 494 6272 12
Permissions price	0.00 USD
VAT/Local Sales Tax	0.00 USD / GBP
Total	0.00 USD

INTRODUCTION

1. The publisher for this copyrighted material is Elsevier. By clicking "accept" in connection with completing this licensing transaction, you agree that the following terms and conditions apply to this transaction (along with the Billing and Payment terms and conditions established by Copyright Clearance Center, Inc. ("CCC"), at the time that you opened your Rightslink account and that are available at any time at <http://myaccount.copyright.com>).

GENERAL TERMS

2. Elsevier hereby grants you permission to reproduce the aforementioned material subject to the terms and conditions indicated.

3. Acknowledgement: If any part of the material to be used (for example, figures) has appeared in our publication with credit or acknowledgement to another source, permission must also be sought from that source. If such permission is not obtained then that material may not be included in your publication/copies. Suitable acknowledgement to the source must be made, either as a footnote or in a reference list at the end of your publication, as follows:

“Reprinted from Publication title, Vol /edition number, Author(s), Title of article / title of chapter, Pages No., Copyright (Year), with permission from Elsevier [OR APPLICABLE SOCIETY COPYRIGHT OWNER].” Also Lancet special credit - “Reprinted from The Lancet, Vol. number, Author(s), Title of article, Pages No., Copyright (Year), with permission from Elsevier.”

4. Reproduction of this material is confined to the purpose and/or media for which permission is hereby given.

5. Altering/Modifying Material: Not Permitted. However figures and illustrations may be altered/adapted minimally to serve your work. Any other abbreviations, additions, deletions and/or any other alterations shall be made only with prior written authorization of Elsevier Ltd. (Please contact Elsevier at permissions@elsevier.com)

6. If the permission fee for the requested use of our material is waived in this instance, please be advised that your future requests for Elsevier materials may attract a fee.

7. Reservation of Rights: Publisher reserves all rights not specifically granted in the combination of (i) the license details provided by you and accepted in the course of this licensing transaction, (ii) these terms and conditions and (iii) CCC's Billing and Payment terms and conditions.

8. License Contingent Upon Payment: While you may exercise the rights licensed immediately upon issuance of the license at the end of the licensing process for the transaction, provided that you have disclosed complete and accurate details of your proposed use, no license is finally effective unless and until full payment is received from you (either by publisher or by CCC) as provided in CCC's Billing and Payment terms and conditions. If full payment is not received on a timely basis, then any license preliminarily granted shall be deemed automatically revoked and shall be void as if never granted. Further, in the event that you breach any of these terms and conditions or any of CCC's Billing and Payment terms and conditions, the license is automatically revoked and shall be void as if never granted. Use of materials as described in a revoked license, as well as any use of the materials beyond the scope of an unrevoked license, may constitute copyright infringement and publisher reserves the right to take any and all action to protect its copyright in the materials.

9. **Warranties:** Publisher makes no representations or warranties with respect to the licensed material.
10. **Indemnity:** You hereby indemnify and agree to hold harmless publisher and CCC, and their respective officers, directors, employees and agents, from and against any and all claims arising out of your use of the licensed material other than as specifically authorized pursuant to this license.
11. **No Transfer of License:** This license is personal to you and may not be sublicensed, assigned, or transferred by you to any other person without publisher's written permission.
12. **No Amendment Except in Writing:** This license may not be amended except in a writing signed by both parties (or, in the case of publisher, by CCC on publisher's behalf).
13. **Objection to Contrary Terms:** Publisher hereby objects to any terms contained in any purchase order, acknowledgment, check endorsement or other writing prepared by you, which terms are inconsistent with these terms and conditions or CCC's Billing and Payment terms and conditions. These terms and conditions, together with CCC's Billing and Payment terms and conditions (which are incorporated herein), comprise the entire agreement between you and publisher (and CCC) concerning this licensing transaction. In the event of any conflict between your obligations established by these terms and conditions and those established by CCC's Billing and Payment terms and conditions, these terms and conditions shall control.
14. **Revocation:** Elsevier or Copyright Clearance Center may deny the permissions described in this License at their sole discretion, for any reason or no reason, with a full refund payable to you. Notice of such denial will be made using the contact information provided by you. Failure to receive such notice will not alter or invalidate the denial. In no event will Elsevier or Copyright Clearance Center be responsible or liable for any costs, expenses or damage incurred by you as a result of a denial of your permission request, other than a refund of the amount(s) paid by you to Elsevier and/or Copyright Clearance Center for denied permissions.

LIMITED LICENSE

The following terms and conditions apply only to specific license types:

15. **Translation:** This permission is granted for non-exclusive world **English** rights only unless your license was granted for translation rights. If you licensed translation rights you may only translate this content into the languages you requested. A professional translator must perform all translations and reproduce the content word for word preserving the integrity of the article. If this license is to re-use 1 or 2 figures then permission is granted for non-exclusive world rights in all languages.
16. **Website:** The following terms and conditions apply to electronic reserve and author websites:
Electronic reserve: If licensed material is to be posted to website, the web site is to be password-protected and made available only to bona fide students registered on a relevant course if:
 This license was made in connection with a course,
 This permission is granted for 1 year only. You may obtain a license for future website posting,
 All content posted to the web site must maintain the copyright information line on the bottom of each image,
 A hyper-text must be included to the Homepage of the journal from which you are licensing at <http://www.sciencedirect.com/science/journal/xxxxx> or the Elsevier homepage for books at <http://www.elsevier.com> , and
Central Storage: This license does not include permission for a scanned version of the material to be stored in a central repository such as that provided by Heron/XanEdu.

17. **Author website** for journals with the following additional clauses:

All content posted to the web site must maintain the copyright information line on the bottom of each image, and the permission granted is limited to the personal version of your paper. You are not allowed to download and post the published electronic version of your article (whether PDF or HTML, proof or final version), nor may you scan the printed edition to create an electronic version. A hyper-text must be included to the Homepage of the journal from which you are licensing at <http://www.sciencedirect.com/science/journal/xxxxx> . As part of our normal production process, you will receive an e-mail notice when your article appears on Elsevier's online service ScienceDirect (www.sciencedirect.com). That e-mail will include the article's Digital Object Identifier (DOI). This number provides the electronic link to the published article and should be included in the posting of your personal version. We ask that you wait until you receive this e-mail and have the DOI to do any posting.

Central Storage: This license does not include permission for a scanned version of the material to be stored in a central repository such as that provided by Heron/XanEdu.

18. **Author website** for books with the following additional clauses:

Authors are permitted to place a brief summary of their work online only.

A hyper-text must be included to the Elsevier homepage at <http://www.elsevier.com> . All content posted to the web site must maintain the copyright information line on the bottom of each image. You are not allowed to download and post the published electronic version of your chapter, nor may you scan the printed edition to create an electronic version.

Central Storage: This license does not include permission for a scanned version of the material to be stored in a central repository such as that provided by Heron/XanEdu.

19. **Website** (regular and for author): A hyper-text must be included to the Homepage of the journal from which you are licensing at <http://www.sciencedirect.com/science/journal/xxxxx>. or for books to the Elsevier homepage at <http://www.elsevier.com>

20. **Thesis/Dissertation**: If your license is for use in a thesis/dissertation your thesis may be submitted to your institution in either print or electronic form. Should your thesis be published commercially, please reapply for permission. These requirements include permission for the Library and Archives of Canada to supply single copies, on demand, of the complete thesis and include permission for UMI to supply single copies, on demand, of the complete thesis. Should your thesis be published commercially, please reapply for permission.

21. **Other Conditions**: Permission is not required from Elsevier in future to reuse author's own work in thesis/dissertation in print format.

American Chemical Society's Policy on Theses and Dissertations

If your university requires you to obtain permission, you must use the RightsLink permission system.
See RightsLink instructions at <http://pubs.acs.org/page/copyright/permissions.html>.

This is regarding request for permission to include **your** paper(s) or portions of text from **your** paper(s) in your thesis. Permission is now automatically granted; please pay special attention to the **implications** paragraph below. The Copyright Subcommittee of the Joint Board/Council Committees on Publications approved the following:

Copyright permission for published and submitted material from theses and dissertations

ACS extends blanket permission to students to include in their theses and dissertations their own articles, or portions thereof, that have been published in ACS journals or submitted to ACS journals for publication, provided that the ACS copyright credit line is noted on the appropriate page(s).

Publishing implications of electronic publication of theses and dissertation material

Students and their mentors should be aware that posting of theses and dissertation material on the Web prior to submission of material from that thesis or dissertation to an ACS journal may affect publication in that journal. Whether Web posting is considered prior publication may be evaluated on a case-by-case basis by the journal's editor. If an ACS journal editor considers Web posting to be "prior publication", the paper will not be accepted for publication in that journal. If you intend to submit your unpublished paper to ACS for publication, check with the appropriate editor prior to posting your manuscript electronically.

Reuse/Republication of the Entire Work in Theses or Collections: Authors may reuse all or part of the Submitted, Accepted or Published Work in a thesis or dissertation that the author writes and is required to submit to satisfy the criteria of degree-granting institutions. Such reuse is permitted subject to the ACS' "Ethical Guidelines to Publication of Chemical Research" (<http://pubs.acs.org/page/policy/ethics/index.html>); the author should secure written confirmation (via letter or email) from the respective ACS journal editor(s) to avoid potential conflicts with journal prior publication*/embargo policies. Appropriate citation of the Published Work must be made. If the thesis or dissertation to be published is in electronic format, a direct link to the Published Work must also be included using the ACS Articles on Request author-directed link – see <http://pubs.acs.org/page/policy/articlesonrequest/index.html>

* Prior publication policies of ACS journals are posted on the ACS website at <http://pubs.acs.org/page/policy/prior/index.html>

If your paper has **not** yet been published by ACS, please print the following credit line on the first page of your article: "Reproduced (or 'Reproduced in part') with permission from [JOURNAL NAME], in press (or 'submitted for publication'). Unpublished work copyright [CURRENT YEAR] American Chemical Society." Include appropriate information.

If your paper has already been published by ACS and you want to include the text or portions of the text in your thesis/dissertation, please print the ACS copyright credit line on the first page of your article: "Reproduced (or 'Reproduced in part') with permission from [FULL REFERENCE CITATION.] Copyright [YEAR] American Chemical Society." Include appropriate information.

Submission to a Dissertation Distributor: If you plan to submit your thesis to UMI or to another dissertation distributor, you should not include the unpublished ACS paper in your thesis if the thesis will be disseminated electronically, until ACS has published your paper. After publication of the paper by ACS, you may release the entire thesis (**not the individual ACS article by itself**) for electronic dissemination through the distributor; ACS's copyright credit line should be printed on the first page of the ACS paper.

JOHN WILEY AND SONS LICENSE
TERMS AND CONDITIONS

Nov 05, 2013

This is a License Agreement between Caleb J Allpress ("You") and John Wiley and Sons ("John Wiley and Sons") provided by Copyright Clearance Center ("CCC"). The license consists of your order details, the terms and conditions provided by John Wiley and Sons, and the payment terms and conditions.

All payments must be made in full to CCC. For payment instructions, please see information listed at the bottom of this form.

License Number	3261760486507
License date	Nov 04, 2013
Licensed content publisher	John Wiley and Sons
Licensed content publication	Chemistry - A European Journal
Licensed content title	Photochemically Initiated Oxidative Carbon–Carbon Bond-Cleavage Reactivity in Chlorodiketonate NiII Complexes
Licensed copyright line	Copyright © 2011 WILEY-VCH Verlag GmbH & Co. KGaA, Weinheim
Licensed content author	Caleb J. Allpress, Atta M. Arif, Dylan T. Houghton, Lisa M. Berreau
Licensed content date	Dec 8, 2011
Start page	14962
End page	14973
Type of use	Dissertation/Thesis
Requestor type	Author of this Wiley article
Format	Print and electronic
Portion	Full article
Will you be translating?	No
Total	0.00 USD
Terms and Conditions	

TERMS AND CONDITIONS

This copyrighted material is owned by or exclusively licensed to John Wiley & Sons, Inc. or one of its group companies (each a "Wiley Company") or a society for whom a Wiley Company has exclusive publishing rights in relation to a particular journal (collectively "WILEY"). By clicking "accept" in connection with completing this licensing transaction, you agree that the following terms and conditions apply to this transaction (along with the billing and payment terms and conditions established by the Copyright Clearance Center Inc., ("CCC's Billing and Payment terms and conditions"), at the time that you opened your RightsLink account (these are available at any time at <http://myaccount.copyright.com>).

Terms and Conditions

1. The materials you have requested permission to reproduce (the "Materials") are protected by copyright.

2. You are hereby granted a personal, non-exclusive, non-sublicensable, non-transferable, worldwide, limited license to reproduce the Materials for the purpose specified in the licensing process. This license is for a one-time use only with a maximum distribution equal to the number that you identified in the licensing process. Any form of republication granted by this license must be completed within two years of the date of the grant of this license (although copies prepared before may be distributed thereafter). The Materials shall not be used in any other manner or for any other purpose. Permission is granted subject to an appropriate acknowledgement given to the author, title of the material/book/journal and the publisher. You shall also duplicate the copyright notice that appears in the Wiley publication in your use of the Material. Permission is also granted on the understanding that nowhere in the text is a previously published source acknowledged for all or part of this Material. Any third party material is expressly excluded from this permission.

3. With respect to the Materials, all rights are reserved. Except as expressly granted by the terms of the license, no part of the Materials may be copied, modified, adapted (except for minor reformatting required by the new Publication), translated, reproduced, transferred or distributed, in any form or by any means, and no derivative works may be made based on the Materials without the prior permission of the respective copyright owner. You may not alter, remove or suppress in any manner any copyright, trademark or other notices displayed by the Materials. You may not license, rent, sell, loan, lease, pledge, offer as security, transfer or assign the Materials, or any of the rights granted to you hereunder to any other person.

4. The Materials and all of the intellectual property rights therein shall at all times remain the exclusive property of John Wiley & Sons Inc or one of its related companies (WILEY) or their respective licensors, and your interest therein is only that of having possession of and the right to reproduce the Materials pursuant to Section 2 herein during the continuance of this Agreement. You agree that you own no right, title or interest in or to the Materials or any of the intellectual property rights therein. You shall have no rights hereunder other than the license as provided for above in Section 2. No right, license or interest to any trademark, trade name, service mark or other branding ("Marks") of WILEY or its licensors is granted hereunder, and you agree that you shall not assert any such right, license or interest with respect thereto.

5. NEITHER WILEY NOR ITS LICENSORS MAKES ANY WARRANTY OR REPRESENTATION OF ANY KIND TO YOU OR ANY THIRD PARTY, EXPRESS, IMPLIED OR STATUTORY, WITH RESPECT TO THE MATERIALS OR THE ACCURACY OF ANY INFORMATION CONTAINED IN THE MATERIALS, INCLUDING, WITHOUT LIMITATION, ANY IMPLIED WARRANTY OF MERCHANTABILITY, ACCURACY, SATISFACTORY QUALITY, FITNESS FOR A PARTICULAR PURPOSE, USABILITY, INTEGRATION OR NON-INFRINGEMENT AND ALL SUCH WARRANTIES ARE HEREBY EXCLUDED BY WILEY AND ITS LICENSORS AND WAIVED BY YOU.

6. WILEY shall have the right to terminate this Agreement immediately upon breach of this Agreement by you.

7. You shall indemnify, defend and hold harmless WILEY, its Licensors and their respective directors, officers, agents and employees, from and against any actual or threatened claims, demands, causes of action or proceedings arising from any breach of this Agreement by you.

8. IN NO EVENT SHALL WILEY OR ITS LICENSORS BE LIABLE TO YOU OR ANY OTHER PARTY OR ANY OTHER PERSON OR ENTITY FOR ANY SPECIAL, CONSEQUENTIAL, INCIDENTAL, INDIRECT, EXEMPLARY OR PUNITIVE DAMAGES, HOWEVER CAUSED, ARISING OUT OF OR IN CONNECTION WITH THE DOWNLOADING, PROVISIONING, VIEWING OR USE OF THE MATERIALS REGARDLESS OF THE FORM OF ACTION, WHETHER FOR BREACH OF CONTRACT, BREACH OF WARRANTY, TORT, NEGLIGENCE, INFRINGEMENT OR OTHERWISE (INCLUDING, WITHOUT LIMITATION, DAMAGES BASED ON LOSS OF PROFITS, DATA, FILES, USE, BUSINESS OPPORTUNITY OR CLAIMS OF THIRD PARTIES), AND

WHETHER OR NOT THE PARTY HAS BEEN ADVISED OF THE POSSIBILITY OF SUCH DAMAGES. THIS LIMITATION SHALL APPLY NOTWITHSTANDING ANY FAILURE OF ESSENTIAL PURPOSE OF ANY LIMITED REMEDY PROVIDED HEREIN.

9. Should any provision of this Agreement be held by a court of competent jurisdiction to be illegal, invalid, or unenforceable, that provision shall be deemed amended to achieve as nearly as possible the same economic effect as the original provision, and the legality, validity and enforceability of the remaining provisions of this Agreement shall not be affected or impaired thereby.

10. The failure of either party to enforce any term or condition of this Agreement shall not constitute a waiver of either party's right to enforce each and every term and condition of this Agreement. No breach under this agreement shall be deemed waived or excused by either party unless such waiver or consent is in writing signed by the party granting such waiver or consent. The waiver by or consent of a party to a breach of any provision of this Agreement shall not operate or be construed as a waiver of or consent to any other or subsequent breach by such other party.

11. This Agreement may not be assigned (including by operation of law or otherwise) by you without WILEY's prior written consent.

12. Any fee required for this permission shall be non-refundable after thirty (30) days from receipt

13. These terms and conditions together with CCC's Billing and Payment terms and conditions (which are incorporated herein) form the entire agreement between you and WILEY concerning this licensing transaction and (in the absence of fraud) supersedes all prior agreements and representations of the parties, oral or written. This Agreement may not be amended except in writing signed by both parties. This Agreement shall be binding upon and inure to the benefit of the parties' successors, legal representatives, and authorized assigns.

14. In the event of any conflict between your obligations established by these terms and conditions and those established by CCC's Billing and Payment terms and conditions, these terms and conditions shall prevail.

15. WILEY expressly reserves all rights not specifically granted in the combination of (i) the license details provided by you and accepted in the course of this licensing transaction, (ii) these terms and conditions and (iii) CCC's Billing and Payment terms and conditions.

16. This Agreement will be void if the Type of Use, Format, Circulation, or Requestor Type was misrepresented during the licensing process.

17. This Agreement shall be governed by and construed in accordance with the laws of the State of New York, USA, without regards to such state's conflict of law rules. Any legal action, suit or proceeding arising out of or relating to these Terms and Conditions or the breach thereof shall be instituted in a court of competent jurisdiction in New York County in the State of New York in the United States of America and each party hereby consents and submits to the personal jurisdiction of such court, waives any objection to venue in such court and consents to service of process by registered or certified mail, return receipt requested, at the last known address of such party.

Wiley Open Access Terms and Conditions

Wiley publishes Open Access articles in both its Wiley Open Access Journals program [<http://www.wileyopenaccess.com/view/index.html>] and as Online Open articles in its subscription journals. The majority of Wiley Open Access Journals have adopted the [Creative Commons Attribution](#)

[License](#) (CC BY) which permits the unrestricted use, distribution, reproduction, adaptation and commercial exploitation of the article in any medium. No permission is required to use the article in this way provided that the article is properly cited and other license terms are observed. A small number of Wiley Open Access journals have retained the [Creative Commons Attribution Non Commercial License](#) (CC BY-NC), which permits use, distribution and reproduction in any medium, provided the original work is properly cited and is not used for commercial purposes.

Online Open articles - Authors selecting Online Open are, unless particular exceptions apply, offered a choice of Creative Commons licenses. They may therefore select from the CC BY, the CC BY-NC and the [Attribution-NoDerivatives](#) (CC BY-NC-ND). The CC BY-NC-ND is more restrictive than the CC BY-NC as it does not permit adaptations or modifications without rights holder consent.

Wiley Open Access articles are protected by copyright and are posted to repositories and websites in accordance with the terms of the applicable Creative Commons license referenced on the article. At the time of deposit, Wiley Open Access articles include all changes made during peer review, copyediting, and publishing. Repositories and websites that host the article are responsible for incorporating any publisher-supplied amendments or retractions issued subsequently.

Wiley Open Access articles are also available without charge on Wiley's publishing platform, **Wiley Online Library** or any successor sites.

Conditions applicable to all Wiley Open Access articles:

- The authors' moral rights must not be compromised. These rights include the right of "paternity" (also known as "attribution" - the right for the author to be identified as such) and "integrity" (the right for the author not to have the work altered in such a way that the author's reputation or integrity may be damaged).
- Where content in the article is identified as belonging to a third party, it is the obligation of the user to ensure that any reuse complies with the copyright policies of the owner of that content.
- If article content is copied, downloaded or otherwise reused for research and other purposes as permitted, a link to the appropriate bibliographic citation (authors, journal, article title, volume, issue, page numbers, DOI and the link to the definitive published version on Wiley Online Library) should be maintained. Copyright notices and disclaimers must not be deleted.
 - Creative Commons licenses are copyright licenses and do not confer any other rights, including but not limited to trademark or patent rights.
- Any translations, for which a prior translation agreement with Wiley has not been agreed, must prominently display the statement: "This is an unofficial translation of an article that appeared in a Wiley publication. The publisher has not endorsed this translation."

Conditions applicable to non-commercial licenses (CC BY-NC and CC BY-NC-ND)

For non-commercial and non-promotional purposes individual non-commercial users may access, download, copy, display and redistribute to colleagues Wiley Open Access articles. In addition, articles adopting the CC BY-NC may be adapted, translated, and text- and data-mined subject to the conditions above.

Use by commercial "for-profit" organizations

Use of non-commercial Wiley Open Access articles for commercial, promotional, or marketing purposes requires further explicit permission from Wiley and will be subject to a fee. Commercial purposes include:

- Copying or downloading of articles, or linking to such articles for further redistribution, sale or licensing;
- Copying, downloading or posting by a site or service that incorporates advertising with such content;
- The inclusion or incorporation of article content in other works or services (other than normal quotations with an appropriate citation) that is then available for sale or licensing, for a fee (for example, a compilation produced for marketing purposes, inclusion in a sales pack)
- Use of article content (other than normal quotations with appropriate citation) by for-profit organizations for promotional purposes
- Linking to article content in e-mails redistributed for promotional, marketing or educational purposes;
- Use for the purposes of monetary reward by means of sale, resale, license, loan, transfer or other form of commercial exploitation such as marketing products
- Print reprints of Wiley Open Access articles can be purchased from: corporatesales@wiley.com

The modification or adaptation for any purpose of an article referencing the CC BY-NC-ND License requires consent which can be requested from RightsLink@wiley.com .

v1.8

30 October 2013

Dr. Katarzyna Grubel
Department of Chemistry
Yale University
225 Prospect Street
New Haven CT 06520 8107

Caleb Allpress
Dept. of Chemistry and Biochemistry
Utah State University
0300 Old Main Hill
Logan, UT 84322-0300
Phone (435) 797-0365
Fax (435) 797-3390

Dear Dr. Grubel,

I am in the process of preparing my dissertation in Chemistry and Biochemistry Department at Utah State University.

I am requesting your permission to include the following manuscript in their entirety as a chapter in my dissertation:

Allpress, C. J.; Grubel, K.; Szajna-Fuller, E.; Arif, A. M.; Berreau, L. M. *J. Am. Chem. Soc.* **2013**, *135*, 659-668.

I will acknowledge your contribution to this part of my dissertation by the inclusion of a footnote on the title page for that chapter. Additionally, a copy of this letter will become an Appendix to the dissertation. Please, advise me of any changes you require.

Please, indicate your approval of this request by signing the endorsement below. If you have any questions, please call me at the number above.

If possible, please provide your reply immediately. Thank you very much for your consideration.

Caleb Allpress

I hereby give permission to Caleb Allpress to reprint the manuscripts listed above in his dissertation.

Signed Grubel Date 31st Oct. 2013

03 November 2013

Dr. Ewa Szajna-Fuller

Caleb Allpress
Dept. of Chemistry and Biochemistry
Utah State University
0300 Old Main Hill
Logan, UT 84322-0300
Phone (435) 797-0365
Fax (435) 797-3390

Dear Dr. Szajna-Fuller,

I am in the process of preparing my dissertation in Chemistry and Biochemistry Department at Utah State University.

I am requesting your permission to include the following manuscript in its entirety as a chapter in my dissertation:

Allpress, C. J.; Grubel, K.; Szajna-Fuller, E.; Arif, A. M.; Berreau, L. M. *J. Am. Chem. Soc.* **2013**, *135*, 659-668.

I will acknowledge your contribution to this part of my dissertation by the inclusion of a footnote on the title page for that chapter. Additionally, a copy of this letter will become an Appendix to the dissertation. Please, advise me of any changes you require.

Please, indicate your approval of this request by signing the endorsement below. If you have any questions, please call me at the number above.

If possible, please provide your reply immediately. Thank you very much for your consideration.

Caleb Allpress

I hereby give permission to Caleb Allpress to reprint the manuscripts listed above in his dissertation.

Signed Ewa Szajna-Fuller Date 11/8/2013

03 November 2013

Dr. Atta M. Arif
Department of Chemistry
University of Utah
Salt Lake City, UT

Caleb Allpress
Dept. of Chemistry and Biochemistry
Utah State University
0300 Old Main Hill
Logan, UT 84322-0300
Phone (435) 797-0365
Fax (435) 797-3390

Dear Dr. Arif,

I am in the process of preparing my dissertation in Chemistry and Biochemistry Department at Utah State University.

I am requesting your permission to include the following manuscripts in their entirety as a chapter in my dissertation:

Allpress, C. J.; Grubel, K.; Szajna-Fuller, E.; Arif, A. M.; Berreau, L. M. *J. Am. Chem. Soc.* **2013**, *135*, 659-668.

Allpress, C. J.; Arif, A. M.; Houghton, D. T.; Berreau, L. M. *Chem. Eur. J.* **2011**, *17*, 14972-14973.

I will acknowledge your contribution to this part of my dissertation by the inclusion of a footnote on the title page for that chapter. Additionally, a copy of this letter will become an Appendix to the dissertation. Please, advise me of any changes you require.

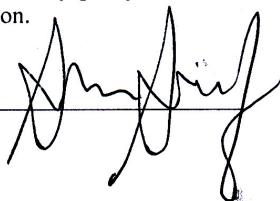
Please, indicate your approval of this request by signing the endorsement below. If you have any questions, please call me at the number above.

If possible, please provide your reply immediately. Thank you very much for your consideration.

Caleb Allpress

I hereby give permission to Caleb Allpress to reprint the manuscripts listed above in his dissertation.

Signed



Date

11/4/2013

CURRICULUM VITAE

Caleb Allpress

Department of Chemistry and Biochemistry
Utah State University
Logan, UT 84322-0300
(435) 770-1949
c.allpress@aggiemail.usu.edu
Permanent resident of USA

Education

- 2009-present PhD, Inorganic Chemistry (anticipated December 2013)
Utah State University, Logan UT
Department of Chemistry and Biochemistry
Advisor: Dr Lisa M. Berreau
Dissertation: "Oxidative Aliphatic Carbon-carbon Bond Cleavage
Reactivity."
- 2006-2008 BSc in Chemistry
University of Canterbury, Christchurch New Zealand

Publications

6. Allpress, C.J.; Borowski, T.; Tierney, D.L.; Arif, A.M.; Berreau, L.M. "Oxidative Carbon-Carbon Bond Cleavage in a Chlorodiketonate Cu^{II} complex" (Manuscript in Preparation).
5. Allpress, C.J. and Berreau L.M. "Oxidative Aliphatic Carbon-Carbon Bond Cleavage Reactions" *Coord. Chem. Rev.* **2013**, *257*, 3005-3029.
4. Allpress, C.J.; Grubel, K.; Szajna-Fuller, E.; Arif, A.M.; Berreau, L.M. "Regioselective Aliphatic Carbon-Carbon Bond Cleavage by a Model System of Relevance to Iron-Containing Acireductone-Dioxygenase." *J. Am. Chem. Soc.* **2013**, *135*, 659-668. (Highlighted in the ACS virtual issue "Models of Metalloenzymes", <http://pubs.acs.org/page/vi/2013/models-of-metalloenzymes.html>).
3. Grubel, K.; Marts, A.R.; Greer, S.M.; Tierney, D.L.; Allpress, C.J.; Anderson, S.N.; Laughlin, B.J.; Smith, R.C.; Arif, A.M.; Berreau, L.M. "Photoinitiated Dioxygenase-Type Reactivity of Open-Shell 3d Divalent Metal Flavonolato Complexes" *Eur. J. Inorg. Chem.* **2012**, *29*, 4750-4757.

2. Allpress, C.J.; Arif, A.M.; Houghton, D.T.; Berreau, L.M., "Photochemically Initiated Oxidative Carbon-Carbon Bond Cleavage Reactivity in Chlorodiketonate Ni^{II} Complexes" *Chem. Eur. J.* **2011**, *17*, 14962-14973.
1. Berreau, L.M.; Borowski, T.; Grubel, K.; Allpress, C.J.; Wikstrom, J.P.; Germain, M.E.; Rybak-Akimova, E.V.; Tierney, D.L., "Mechanistic Studies of the O₂-dependent Aliphatic Carbon-carbon Bond Cleavage Reaction of a Nickel Enolate Complex" *Inorg. Chem.* **2011**, *50*, 1047-1057.

Presentations

5. Allpress, C.J.; Grubel, K.; Szajna-Fuller, E.; Arif, A.M.; Berreau, L.M. "Regioselective aliphatic carbon-carbon bond cleavage by a model system of relevance to iron-containing acireductone dioxygenase (Fe-ARD)" Presented at the 245th American Chemical Society National Meeting and Exposition, New Orleans LA, April 7-11 2013. (Oral presentation)
4. Allpress, C.J.; Grubel, K.; Szajna-Fuller, E.; Arif, A.M.; Berreau, L.M. "Iron-promoted Aliphatic Carbon-carbon Bond Cleavage of Relevance to Fe-ARD" Presented at the 2nd Penn State University Bioinorganic Workshop Seminar, State College, PA, May 31-June 9 2012. (Poster)
3. Allpress, C.J.; Arif, A.M.; Houghton, D.T.; Berreau, L.M., "Photochemically Initiated Oxidative Carbon-Carbon Bond Cleavage Reactivity in Chlorodiketonate Ni^{II} Complexes" Presented at Bioinorganic Chemistry Gordon Research Seminar, Ventura CA, January 26-29 2012. (Poster)
2. Allpress, C.J.; Grubel, K.; Arif, A.M.; Berreau, L.M., "Studies Toward Modeling the Active Site Chemistry of Fe-ARD" Presented at 242nd American Chemical Society National Meeting and Exposition, Denver CO, August 28 – September 1 2011. (Poster)
1. Allpress, C.J.; Arif, A.M.; Berreau, L.M. "The Photoreactivity of Chlorodiketonate Ni(II) Complexes" Presented at Inorganic Reaction Mechanisms Gordon Research Conference, Galveston TX, March 6-11 2011. (Poster)

Technical Skills

Synthesis: Experienced in synthesis of multi-dentate ligands, novel organic compounds and first-row transition metal coordination complexes, including air-sensitive materials

Spectroscopy and characterization: FTIR, UV-vis, fluorescence, NMR (of paramagnetic and diamagnetic compounds, including the use of variable temperature and two-dimensional methods), magnetic measurements, cyclic voltammetry, GC-TCD and GC-MS

Photochemistry: Developed protocols for quantum yield measurements

Other Techniques: Extensive use of Schlenk line and glove-box techniques for the handling of air-sensitive and hazardous chemicals

Writing: Heavily involved in writing all published papers as well as aiding in the preparation of multiple NSF and NIH proposals, including a recently funded NSF grant.

Awards

- College of Science Graduate Student Researcher of the Year (2013)
- Department of Chemistry Graduate Student of the Year (2013)
- Marjorie H. Gardner Teaching Award (2011)
- Zobell Graduate Scholarship (2011)
- Haydon Prize in Chemistry (2008)
- Carlisle Trust Scholarship (2008)
- New Zealand Institute of Chemistry Prize (2007)
- University of Canterbury Emerging Leaders Scholarship (2006)

Research and Travel Funding

- American Chemical Society Division of Inorganic Chemistry Travel Award (2013)
- Utah State University Graduate Research and Project Grant (2013)
- Travel Awards for conference presentations from the Department of Chemistry, School of Graduate Studies and College of Science at Utah State University (2011-2013)

Teaching Experience

As a Teaching Assistant (Utah State University, 2009-present):

- CHEM1215 General Chemistry Laboratory I
- CHEM1220 General Chemistry II
- CHEM1225 General Chemistry Laboratory II
- CHEM3005 Quantitative Analysis Lab
- CHEM3510 Intermediate Inorganic Chemistry Lab

- CHEM5650 Instrumental Analysis Lab

Guest Lectures (Utah State University)

- CHEM1210 General Chemistry I
- CHEM1220 General Chemistry II
- CHEM5530 Advanced Synthesis Lab

Involved in training seven undergraduate and two graduate students in the research laboratory

Professional Affiliations

American Chemical Society (Division of Inorganic Chemistry)

Updated November 2013